

Response to Anonymous Referee #1

(Note: Reviewer comments are listed in grey, and responses to reviewer comments are in black. Pasted text from the new version of the paper is in italics.)

Yi et al. investigate the response of surface ozone concentrations due to changes in sea surface temperature (SST) in three different ocean basins (North Pacific –NP, North Atlantic – NA, and North Indian Ocean, NIO). The authors use an Earth System Model (CESM) and perform a set of sensitivity studies in which they alter in turn the climatological SSTs of $\pm 1^\circ\text{C}$ over the NP, NA and NIO. The imposed variation in SST leads to changes in surface ozone up to 5 ppbv. The authors focused on the summer season and they show that changes in transport associated to the SSTs anomalies are important in driving ozone anomaly at the surface. In general, increased SST reduces the intercontinental transport of O₃. Overall the manuscript is relatively well written and logically organized. However, in the introduction several references to previous work are missing, several parts of the manuscript need to be clarified and the authors should try to be consistent when displaying the results (see comments below). Overall, the study presents interesting new aspects and fits well with the scope of the journal. However, before publication large improvements are needed.

We really appreciate the reviewer's thoughtful and valuable comments. Following the reviewer's suggestion, we have extended the introduction and discussion based on these important references in the revised manuscript. The IPR analysis used in our study has been described more thoroughly to make it easier to understand. Based on the reviewer's comments, we have further clarified the text and improved the quality of relevant figures: high-resolution plots are provided in the revised manuscript, which are more distinguishable and understandable. We believe it substantially helps to improve our manuscript by addressing these issues. Please see our response to each comment below.

Major comments:

1) I suggest including a sensitivity test in which the SSTs in all 3 basins is increased. It will be interesting to see the effect of a generalized warming. I would also recommend to include a discussion of the results for winter season (see specific comments below)

Good suggestion. Following the reviewer's suggestion, we conducted two sensitivity tests with 1°C SST warming and 1°C SST cooling superimposed onto all three ocean basins (i.e., the North Pacific, North Atlantic and North Indian Ocean), denoted as "All-W" and "All-C", respectively. Their effects on surface O₃ distributions are

compared with the sum of results from three individual warming or cooling cases during boreal summer (see Figure S5 or S6 below) and winter (see Figure S7 or S8 below). It shows that the responses of surface O_3 to a generalized SST anomaly over all three ocean basins generally resemble the sum of results from individual oceans. Slight differences are observed over the extratropical North Pacific for the warming cases in boreal summer.

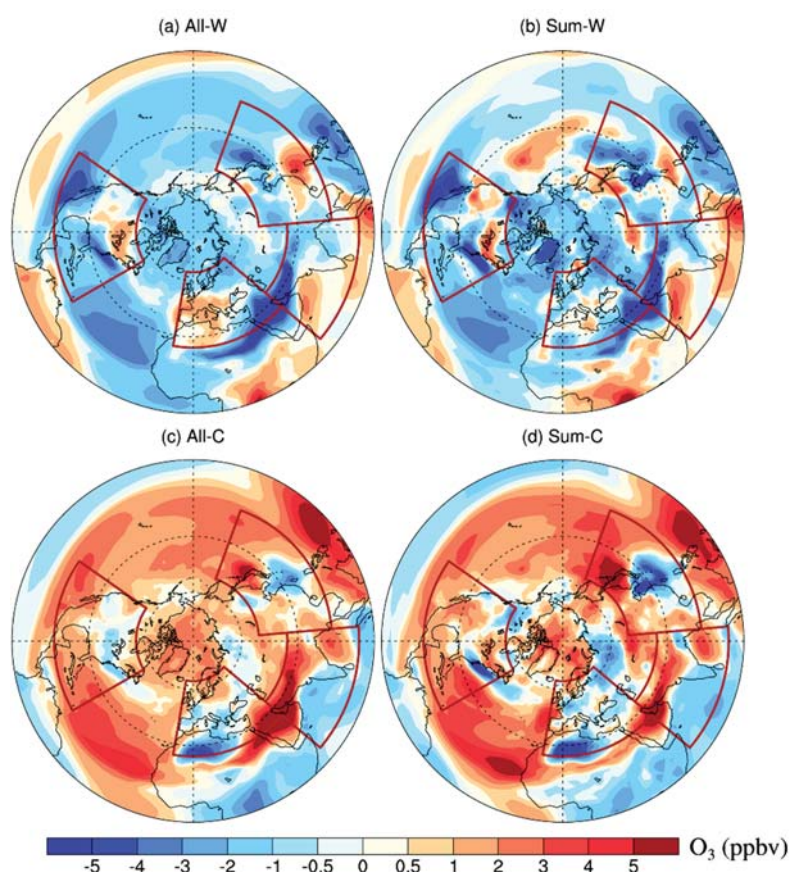


Figure S5. Left column: Changes in the summertime (June-August) surface O_3 concentrations (ppbv) in the Northern Hemisphere induced by 1°C warming (a) and 1°C cooling (b) in all three ocean basins (i.e., the North Pacific, North Atlantic and North Indian Ocean) relative to the CTRL. Right column: Sum of changes in the summertime (June-August) surface O_3 concentrations (ppbv) from the three warming cases (i.e., Pacific-W, Atlantic-W and Indian-W) and three cooling cases (i.e., Pacific-C, Atlantic-C and Indian-C) relative to the CTRL, denoted as (b) Sum-W and (d) Sum-C, respectively. The four major regions of interest (i.e., NA, EU, EA and SA) are marked with polygons.

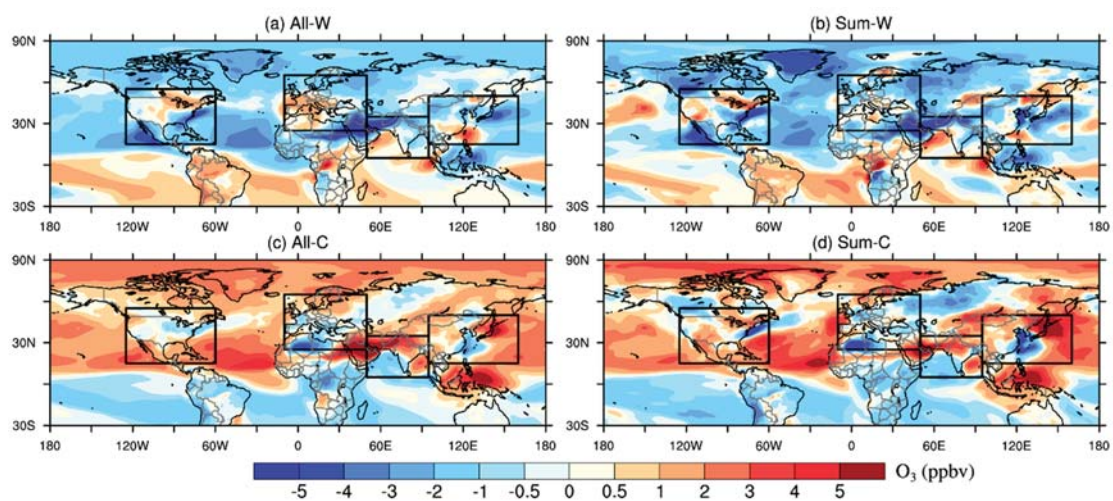


Figure S6. As in Figure S5 but using the Mercator projection.

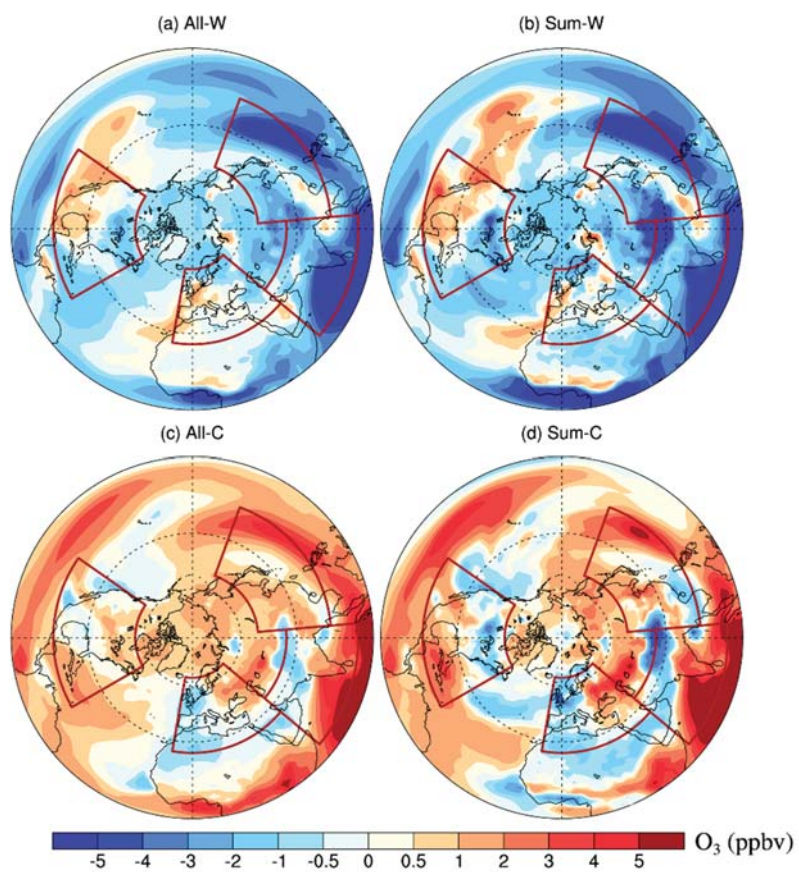


Figure S7. Same as Figure S5 but for the wintertime (December-February).

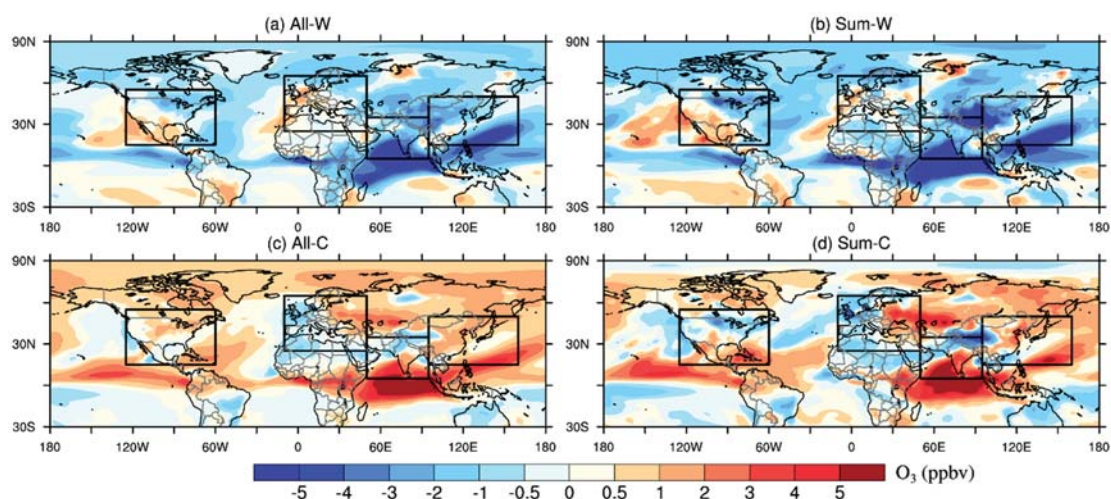


Figure S8. As in Figure S7 but using the Mercator projection.

Considering nonlinear relationships existed in the climate system and O₃ formation processes, the response of surface O₃ to a generalized SST anomaly over all three oceans can not perfectly match the sum of individual results. Regardless those slight difference, our results indicate that the effect of a generalized SST warming on surface O₃ can be decomposed into individual regional ocean forcings. This may help to interpret the responses of surface O₃ to a global-wide warming documented in previous studies (Doherty et al., 2013; Jacob and Winner, 2009; Wu et al., 2008). In the revised manuscript, we made the following revisions in Section 3 (Page 10, Lines 283-291):

“...We further conduct two sensitivity tests with 1 °C SST warming and 1 °C SST cooling superimposed onto all three ocean basins (i.e., the North Pacific, North Atlantic and North Indian Ocean) in the Northern Hemisphere, denoted as “All-W” and “All-C”, respectively. The effects of these combined warming and cooling cases on surface O₃ distributions are respectively compared with the sum of the three individual warming cases (i.e., Pacific-W, Atlantic-W and Indian-W) and three individual cooling cases (i.e., Pacific-C, Atlantic-C and Indian-C). The responses of surface O₃ to a hemispheric SST anomaly generally resemble the sum of responses to different regional SST changes (see Figures S5 and S7 in the supplementary material).”

We also diagnosed the results for winter season, it shows that the responses of surface O₃ and other relevant variables are generally insignificant over land, especially over the four continental regions of interest (i.e., NA, EU, EA and SA). Therefore, we decided to focus mainly on boreal summers. More detailed discussion is provided in our reply to specific comments below.

2) I had major problems in understanding several figures: sometimes the figures are too “crowded” and it is not possible to distinguish the continents (e.g. figures. 4, 6, 9); the panels are often very small in particular in figures 1, 3, 4, 6, 9. The few figures that are clear are the one using the Mercator (or equirectangular) type of projection (e.g., Figures 5, 7, 8, S4, S5). I recommend the authors to be consistent and use the Mercator projection for all figures.

Furthermore, the authors should also be consistent with the use of colorbars: sometimes they use white for values that are not significant (e.g. figure 1), other times for small values (e.g. figure 3), other times they don't use it at all (e.g. figure 4). I recommend not using white color bins for small values, especially if they are significant as in figure 3. See specific comments. I struggle to understand the lack of consistency in making the plots (type of projections, type of colorbar, choice of significant levels, choice of how to display the significant values, etc) that makes it harder for the reader to follow.

Thanks for this really helpful suggestions. We agree that the quality of some figures are low. In our revised manuscript, high-resolution figures are provided that are more distinguishable. We also improved these figures (Figures 6 and 9) that look too “crowded” by removing unnecessary information. The continental outlines in all figures were thicker and darker than the old version. As for the type of projections, we compared the performance of different projections and decided to consistently use polar projection to exhibit our results in hemispheric scale (e.g., Figures 1, 3 and 4 as well as other figures in the supplementary material) while use Mercator projection for regional analysis (e.g., Figures 5-8). The polar projection looks better than Mercator projection when showing the continuous cross-regional relationship along the hemispheric-scale general circulation. Figures using the Mercator projection are also provided in the supplementary material. Please see Figures S2, S14 and S15 below for some examples. Following the reviewer's suggestions, we also enhanced the consistency of these figures. We have removed white color bins for small values (e.g., Figure 3) and consistently used the same symbols to mark results that are significant at the 0.05 level (e.g., Figure 1). We also substantially increased the quality of figures which contain smaller plots. Now these figures can be read more easily and clearly. Following figures show you some examples about these improvements. Please see the revised manuscript for all figures.

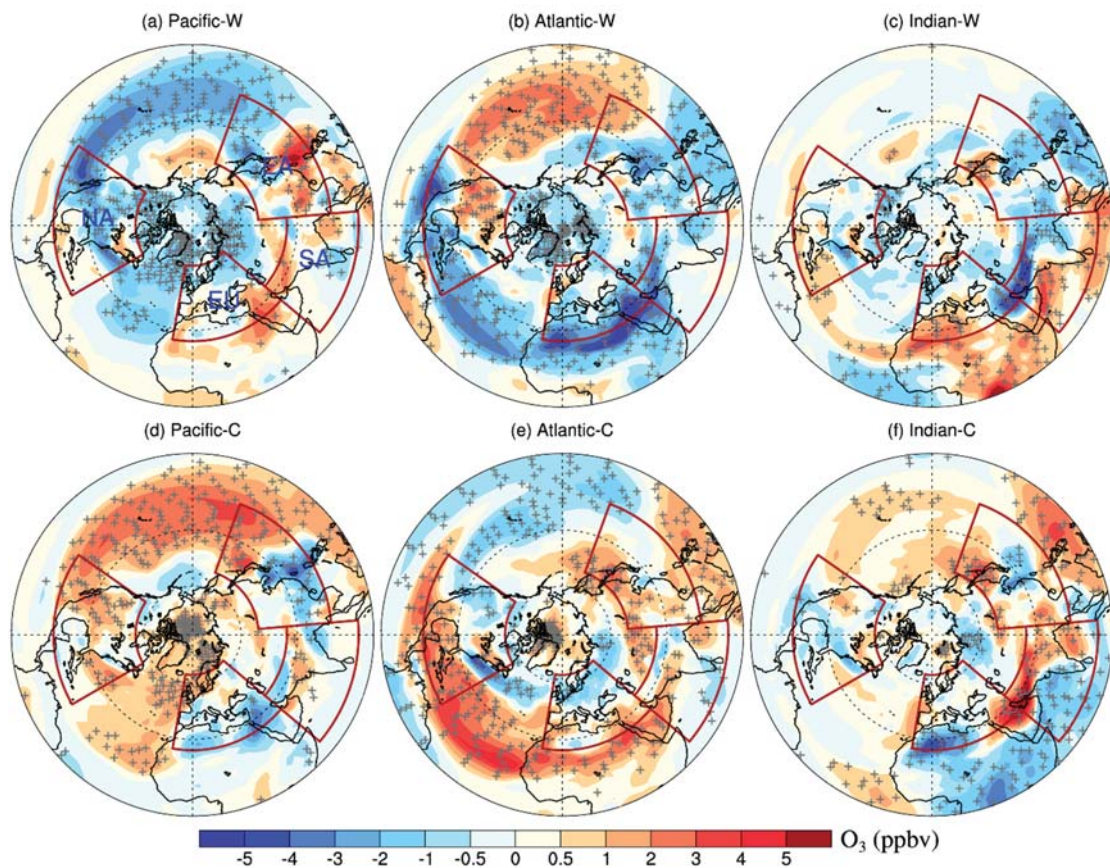


Figure 1. Changes in the summertime (June-August) surface O₃ concentrations (ppbv) in the Northern Hemisphere induced by 1°C warming (top) and 1°C cooling (bottom) in the North Pacific Ocean (left), North Atlantic Ocean (center), and North Indian Ocean (right) relative to the CTRL. The four major regions of interest (i.e., NA (15°N–55 °N; 60°W–125°W), EU (25°N–65 °N; 10°W-50 °E), EA (15 °N–50 °N; 95°E–160 °E) and SA (5 °N–35 °N; 50 °E–95°E)) are marked with red polygons. The + symbols denote areas where results are significant at the 0.05 level, evaluated by Student’s t-test using 20 years of data (plots using the Mercator projection are shown in Figure S2 in the supplementary material).

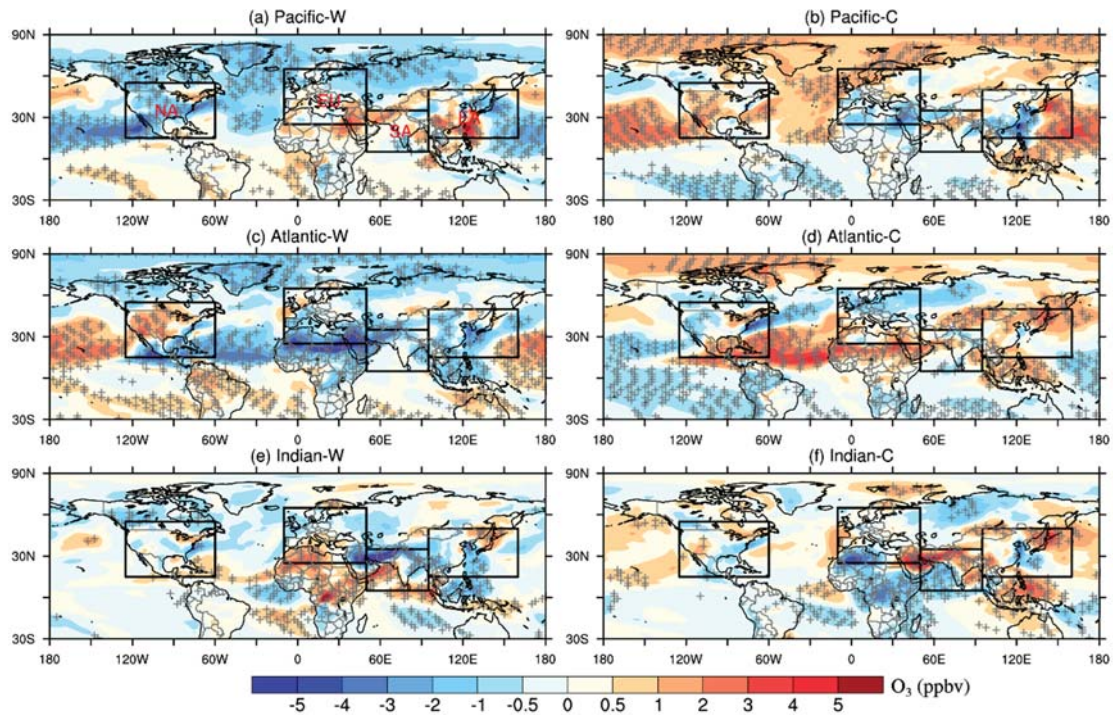


Figure S2. Changes in the summertime (June–August) surface O_3 concentrations (ppbv) in the Northern Hemisphere induced by 1°C warming (top) and 1°C cooling (bottom) in the North Pacific Ocean (left), North Atlantic Ocean (center), and North Indian Ocean (right) relative to the CTRL. The four major regions of interest (i.e., NA (15°N – 55°N ; 60°W – 125°W), EU (25°N – 65°N ; 10°W – 50°E), EA (15°N – 50°N ; 95°E – 160°E) and SA (5°N – 35°N ; 50°E – 95°E)) are marked with polygons. The + symbols denote areas where the results are significant at the 0.05 level, evaluated by Student’s t-test using 20 years of data.

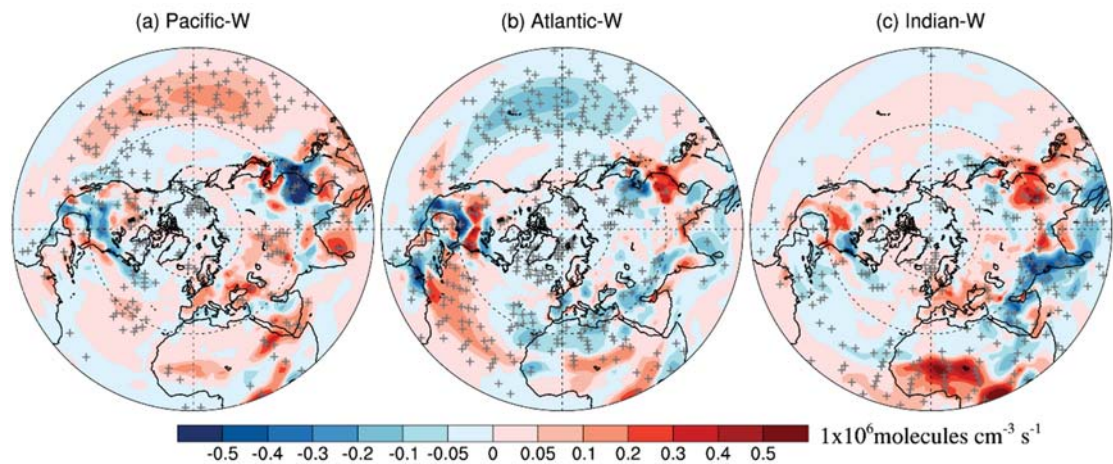


Figure 3. Perturbations of the surface net O_3 production rate ($1 \times 10^6 \text{ molecules cm}^{-3} \text{ s}^{-1}$)

¹⁾ for (a) Pacific-W, (b) Atlantic-W, and (c) Indian-W relative to the CTRL in the boreal summer. The + symbols denote areas where the results are significant at the 0.05 level, evaluated by Student's t-test using 20 years of data (plots using the Mercator projection are shown in Figure S14 in the supplementary material).

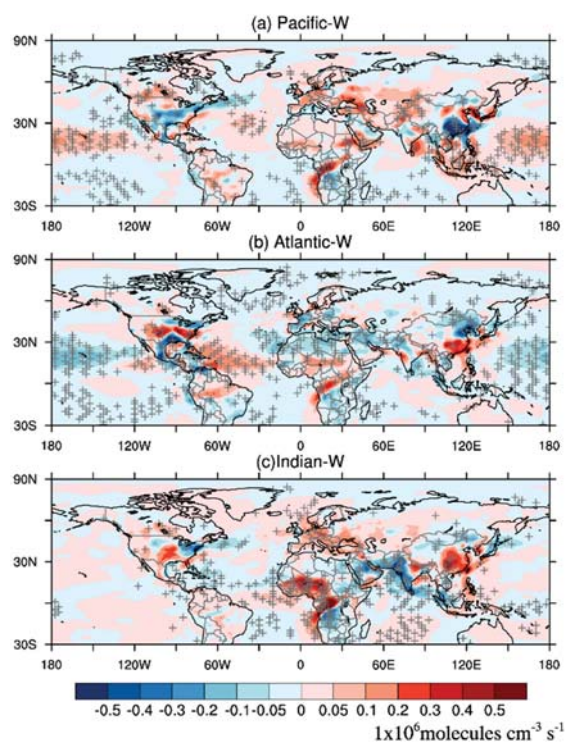


Figure S14. Perturbations of the surface net O₃ production rate ($1 \times 10^6 \text{ molecules cm}^{-3} \text{ s}^{-1}$) for (a) Pacific-W, (b) Atlantic-W, and (c) Indian-W relative to the CTRL in the boreal summer. The + symbols denote areas where the results are significant at the 0.05 level, evaluated by Student's t-test using 20 years of data.

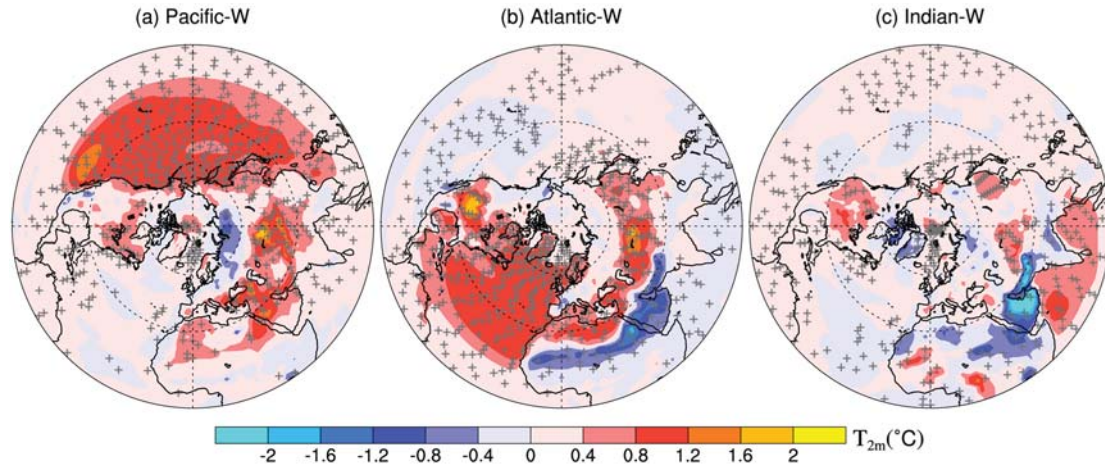


Figure 4. Changes in the surface air temperature ($^{\circ}\text{C}$) for (a) Pacific-W, (b) Atlantic-W, and (c) Indian-W relative to CTRL in the Northern Hemisphere in the boreal summer. The + symbols denote areas where the results are significant at the 0.05 level, evaluated by Student's t-test using 20 years of data (plots using the Mercator projection are shown in Figure S15 in the supplementary material).

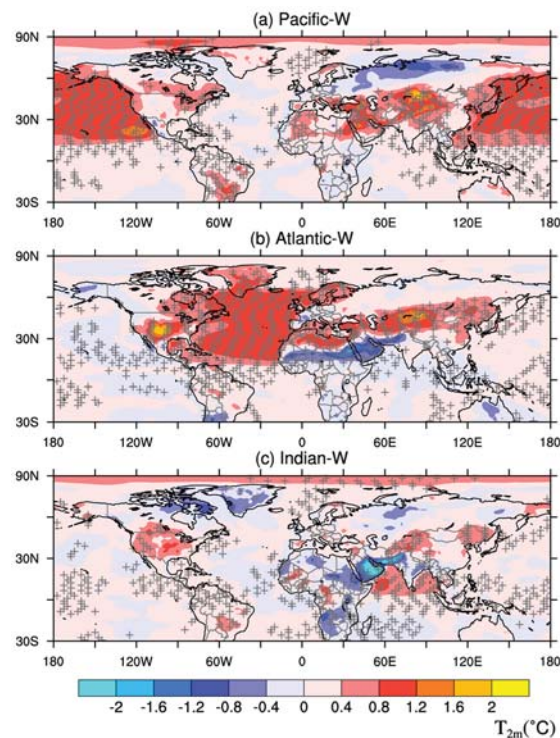


Figure S15. Changes in the surface air temperature ($^{\circ}\text{C}$) for (a) Pacific-W, (b) Atlantic-W, and (c) Indian-W relative to the CTRL in the boreal summer. The + symbols denote areas where the results are significant at the 0.05 level, evaluated by Student's t-test using 20 years of data.

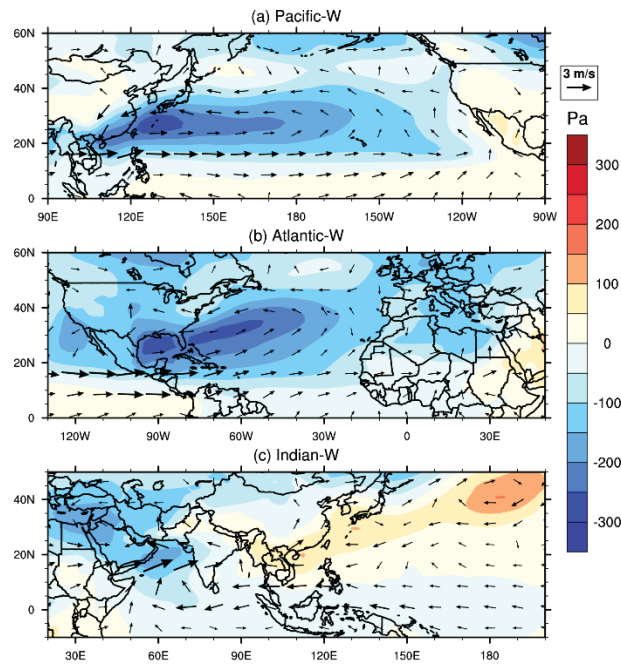


Figure 5. Changes in the surface pressure (color contours, Pa) and 850-hPa wind (arrows, m s^{-1}) for (a) Pacific-W, (b) Atlantic-W, and (c) Indian-W relative to the CTRL in the boreal summer.

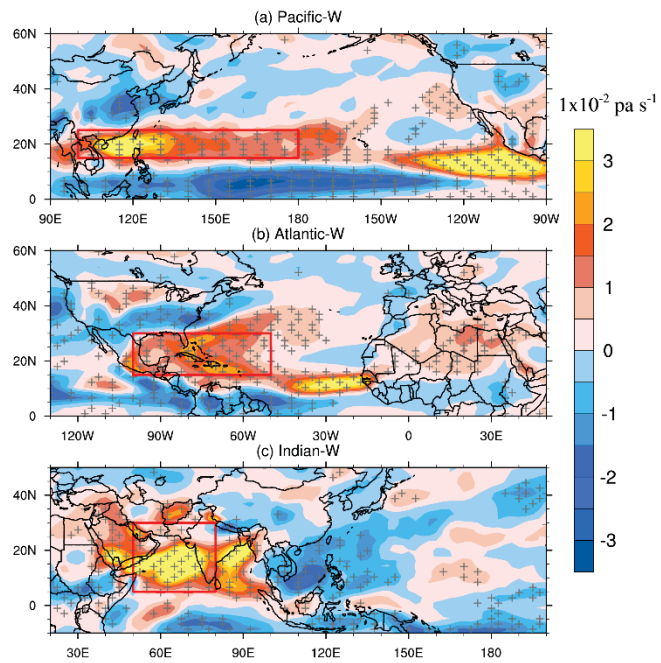


Figure 6. Spatial pattern of vertical velocity changes at 500 hPa (color contours, $1 \times 10^{-2} \text{ Pa s}^{-1}$) for (a) Pacific-W, (b) Atlantic-W, and (c) Indian-W relative to the CTRL in the boreal summer. Positive values indicate upward motion. Red polygons denote the

regions where the surface pressure responses to SST anomalies are significant (see Figure 5 a-c). The + symbols indicate areas where the results are significant at the 0.05 level, evaluated by Student's t-test using 20 years of data.

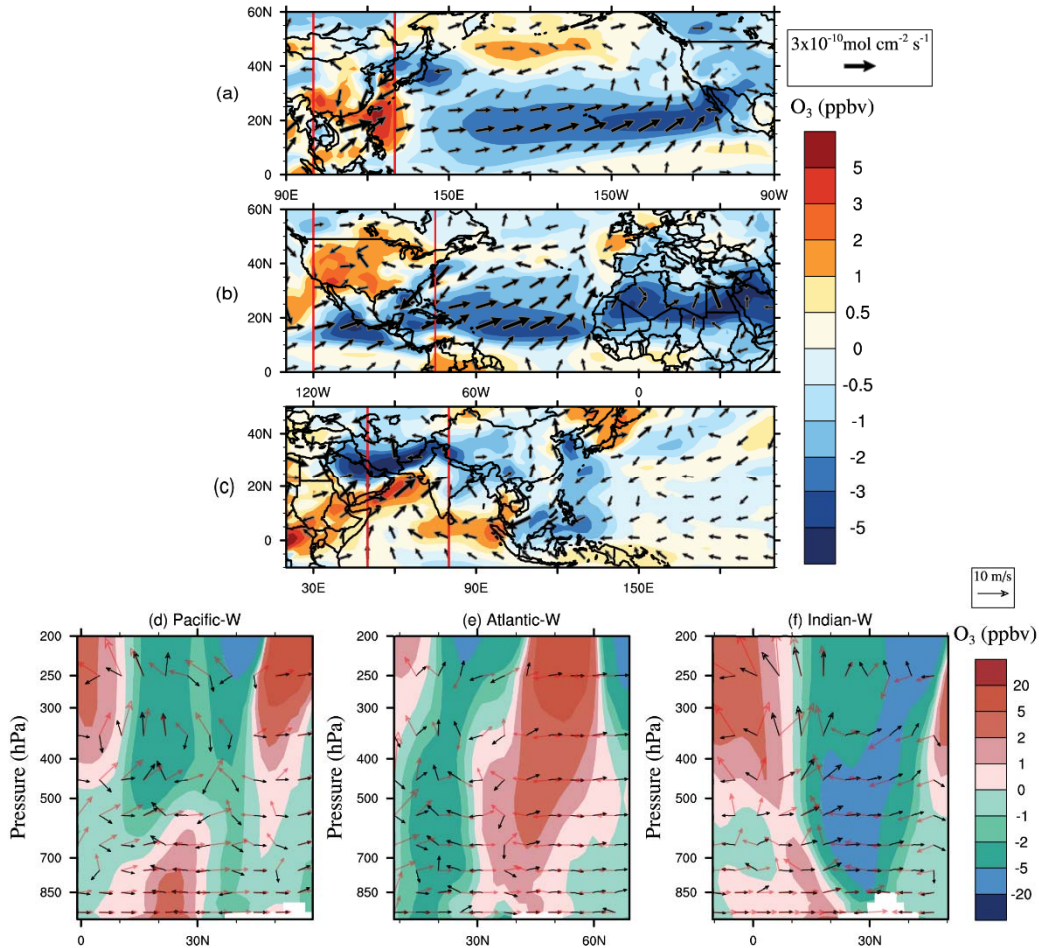


Figure 7. Top three rows: Changes in O₃ concentrations (color contours, ppbv) and horizontal fluxes (arrows, mol cm⁻² s⁻¹) at the surface level for (a) Pacific-W, (b) Atlantic-W, (c) Indian-W relative to the CTRL in the boreal summer. Last row: zonal average of the tropospheric O₃ changes (color contours, ppbv), wind fluxes in CTRL (red arrows, m s⁻¹) and the wind flux perturbation (black arrows, m s⁻¹) in (d) Pacific-W, (e) Atlantic-W, (f) Indian-W relative to the CTRL in the boreal summer. The red rectangles in (a), (b) and (c) denote the longitudinal range used for the zonal averages in (d), (e) and (f), respectively. The vertical wind velocity is amplified 1000 times to make it comparable to the horizontal wind velocity.

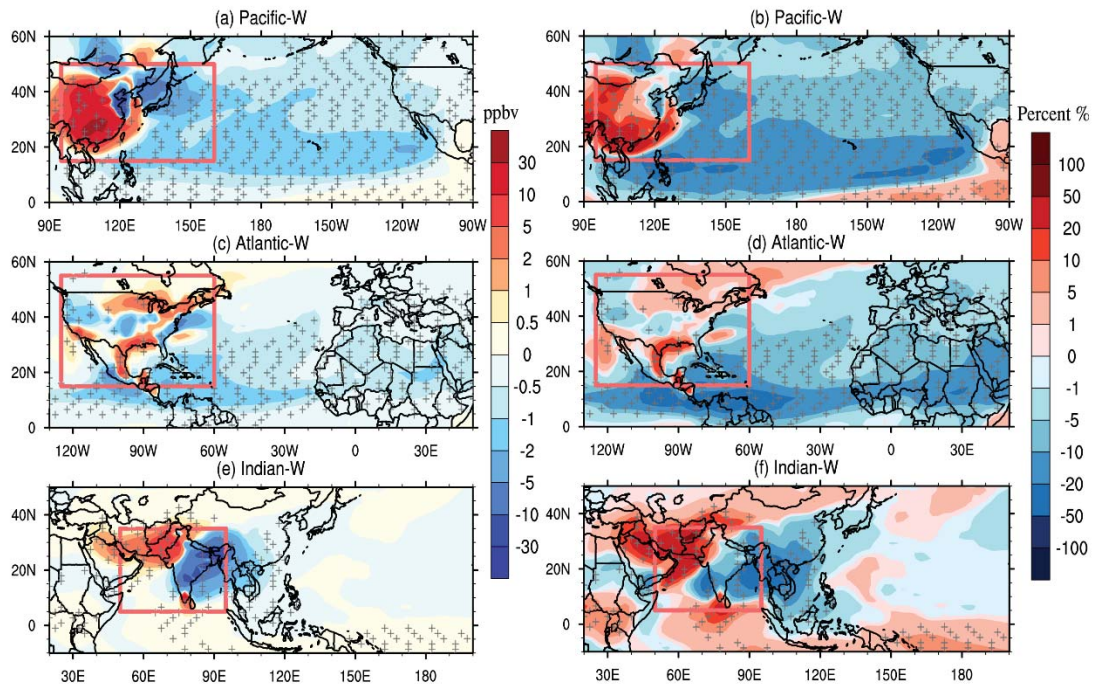


Figure 8. Left-hand panel: Difference in the surface concentration (ppbv) of a CO-like tracer emitted from (a) East Asia for Pacific-W, (c) North America for Atlantic-W and (e) the South Asia for Indian-W relative to the CTRL in the boreal summer. Right-hand panel: The percentage changes in the surface concentration of a CO-like tracer emitted from (b) East Asia for Pacific-W, (d) North America for Atlantic-W and (f) South Asia for Indian-W relative to the CTRL in the boreal summer. Red polygons denote the region where the CO-like tracer is emitted from. The + symbol denotes areas where the results are significant at the 0.05 level, evaluated by Student's t-test using 20 years of data.

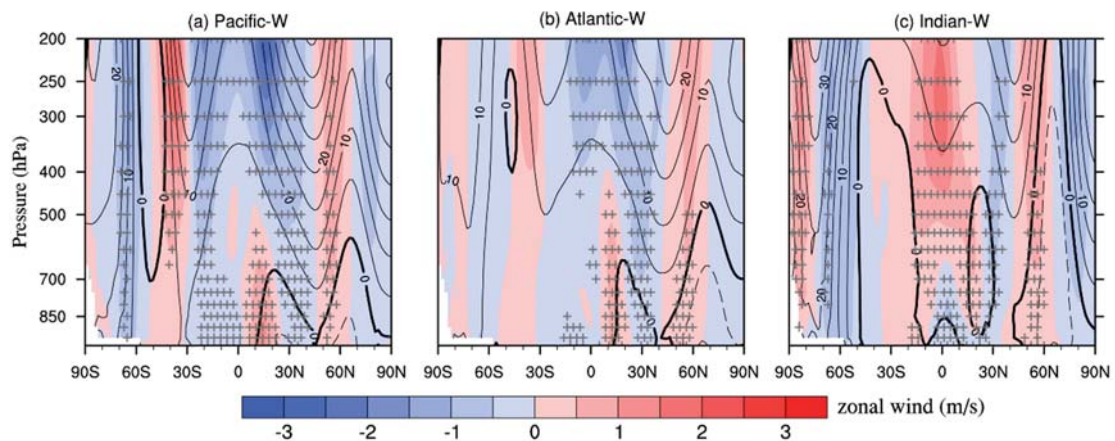


Figure 9. Zonally averaged changes in zonal wind (color contour, m/s) and geopotential

height (contour, m) for (a) Pacific-W, (b) Atlantic-W and (c) Indian-W relative to the CTRL in the boreal summer. Black solid and dashed lines in the contours indicate positive and negative geopotential height anomalies, respectively (contour interval: 5 m). The + symbol denotes areas where the zonal wind changes are significant at the 0.05 level, evaluated by Student's t-test using 20 years of data .

3) In the introduction the authors do not cite several works done previously on the intercontinental transport of O₃ and the meteorological factors affecting it, citing only 4 papers, which are not even the first to address these issues. Please make sure to include the references suggested in “specific comments” and possibly also extend the introduction/discussion.

Good suggestion! We have cited the references following the reviewer's suggestion and expanded our introduction and discussion accordingly. Please see the improved text below and refer to our response to specific comments for more details.

In the Introduction section (see P3, L62-67 and L72-83):

“...The long-range transport of O₃ and its precursors has been extensively studied, and their inter-continental impacts have been evaluated using measurements and model simulations (Parrish et al., 1993;Fehsenfeld et al., 1996;Wild and Akimoto, 2001;Creilson et al., 2003;Simmonds et al., 2004;Fiore et al., 2009;Brown-Steiner and Hess, 2011;Lin et al., 2012a;Lin et al., 2014).”

...

“Atmospheric circulation considerably determines the timescale and pathway of O₃ transport (Bronnimann et al., 2000;Auvray and Bey, 2005;Hess and Mahowald, 2009). The efficiency of O₃ transport varies coherently with atmospheric circulations on different scales. Knowland et al. (2015) demonstrated the important role of mid-latitude storms in redistributing O₃ concentrations during springtime. The North Atlantic Oscillation (NAO) significantly affects surface and tropospheric O₃ concentrations over most of Europe by influencing the intercontinental transport of air masses (Creilson et al., 2003;Christoudias et al., 2012;Pausata et al., 2012). Lamarque and Hess (2004) indicated that the Arctic Oscillation (AO) can modulate springtime tropospheric O₃ burdens over North America. The shift in the position of the jet stream associated with climate change was found to strongly affect summertime surface O₃ variability over eastern North America (Barnes and Fiore, 2013).”

General Minor comments:

- Why do the authors pick 11 years? Is 11 years enough to capture interannual O₃ variability? The SSTs are fixed and in general 15-20 years should be enough to capture interannual atmospheric variability. I'm not sure about 11 though.

Good question. We originally performed 11-year simulations referring to previous studies. For example, Doherty et al. (2013) conducted a 2000-year long unforced simulation to provide a comprehensive measure of model internal variability. They concluded that 5 years is long enough to capture the climate change signal with fixed SSTs. Given that the SST anomaly prescribed in our simulations (i.e., $\pm 1^\circ\text{C}$) is comparable to the climate change effects of a specific ocean, we originally thought that 11 years are enough to capture the relevant signal in our study (see Figure 1 and Figure R1 for example). However, following the reviewer's suggestion, we extended our simulations to 21 years with the first year used for model spin-up. It shows that the 20-year averaged results are generally consistent with the 11-year averaged results except for a few minor differences (e.g., see Figure 1 and Figure R1 below). In our revised manuscript, we redo our calculation and regenerate all plots based on the 20-year averaged results.

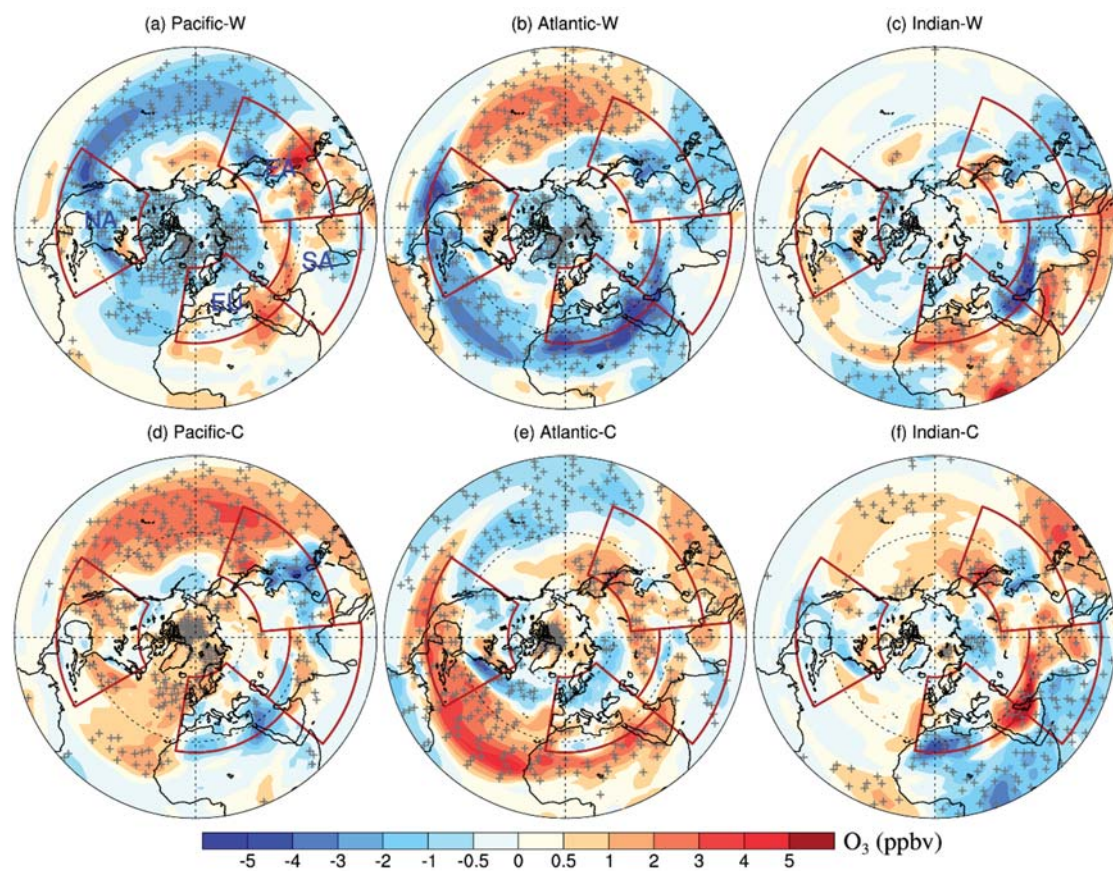


Figure 1. Changes in the summertime (June-August) surface O₃ concentrations (ppbv)

in the Northern Hemisphere induced by 1°C warming (top) and 1°C cooling (bottom) in the North Pacific Ocean (left), North Atlantic Ocean (center), and North Indian Ocean (right) relative to the CTRL. The four major regions of interest (i.e., NA (15°N–55 °N; 60°W–125°W), EU (25°N–65 °N; 10°W–50 °E), EA (15 °N–50 °N; 95°E–160 °E) and SA (5 °N–35 °N; 50 °E–95°E)) are marked with red polygons. The + symbols denote areas where results are significant at the 0.05 level, evaluated by Student’s t-test using 20 years of data (plots using the Mercator projection are shown in Figure S2 in the supplementary material).

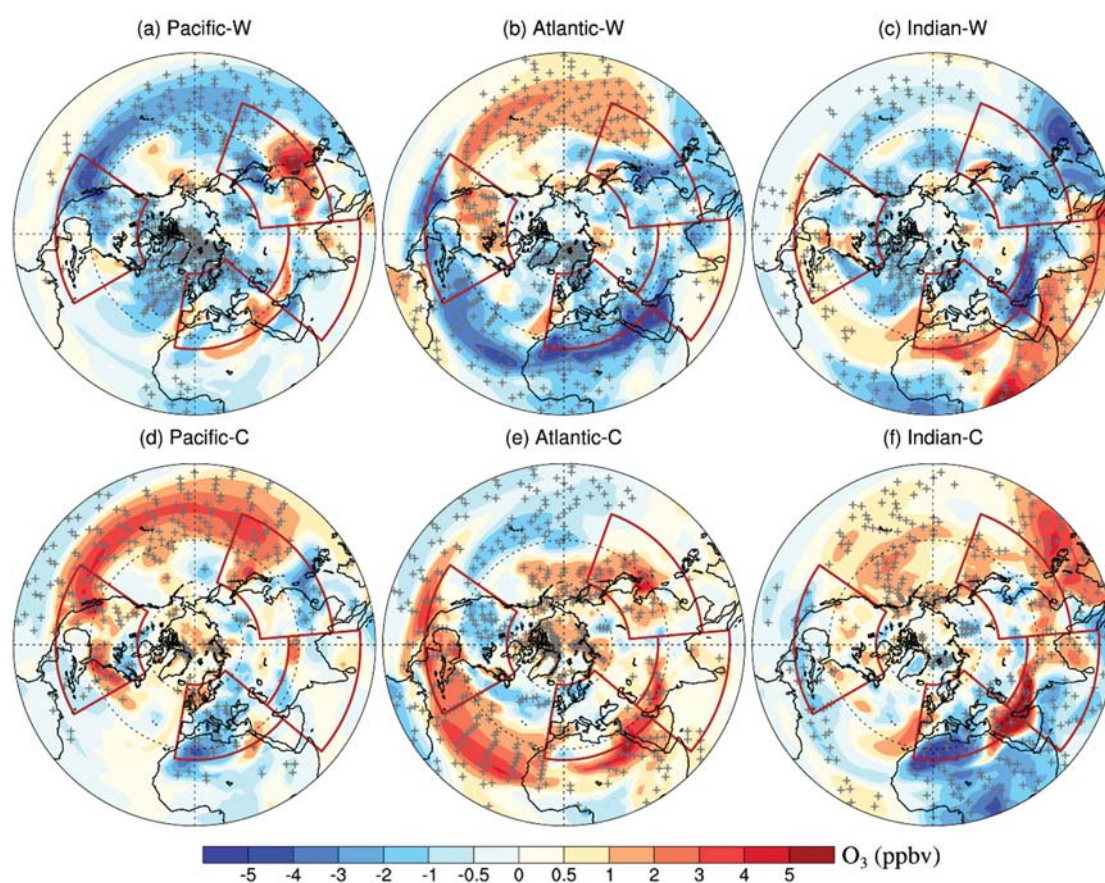


Figure R1. As in Figure 1 but for 11-year simulations

- The authors use different significance levels throughout the manuscript (0.01 or 0.05). Please, pick one and use that for all the analysis.

Good suggestion. We pick the significant level of 0.05 to be consistent in our revised manuscript.

- I suggest not overusing sentences in which part of the text is in parenthesis in order to avoid writing another sentence (e.g.: LL24-25 Increasing 25 (**decreasing**) SST by 1 °C in one of the regions of focus induces decreases (**increases**)). It makes it hard to follow. I think adding another sentence makes it much more easy to read (especially in the main text where there is no word limits).

We follow reviewer's suggestion and revised the relevant texts to avoid the overuse of parenthesis.

In the Abstract (P1, L24-27):

“...The responses of surface O₃ associated with basin-scale SST warming and cooling have similar magnitude but are opposite in sign. Increasing the SST by 1 °C in one of the oceans generally decreases the surface O₃ concentrations from 1 to 5 ppbv.”

In Section 3 (P9-10, L264-280):

“...Surface O₃ changes in response to positive and negative SST anomalies generally pronounce a consistent spatial pattern but are opposite in sign, suggesting robust relationships between surface O₃ levels and SST anomalies (Figure 1). An increase in summertime SST over a specific ocean basin tends to increase the surface O₃ concentration over the upwind regions but reduce this concentration over downwind continents. For instance, a 1 °C warming over the North Pacific leads to a widespread decrease in surface O₃ over the North Pacific, North America and the North Atlantic of approximately 1 ppbv (Table S1) but may enhance the surface O₃ by nearly 3 ppbv over South China. Similarly, in the “Atlantic-W” case, the surface O₃ levels decrease by 1~2 ppbv over the North Atlantic and Europe but increase (~1 ppbv) over North America and the North Pacific. For the North Indian Ocean, positive SST anomalies tend to increase the surface O₃ over the Indian Ocean and Africa but decrease the surface O₃ over South and East Asia (Figure 1). During the boreal winter, a widespread decrease in surface O₃ associated with the warming of different oceans is observed. Significant changes (e.g., up to 5 ppbv) mainly occur over remote ocean areas. Over populated continents, the response of the surface O₃ to basin-scale SST changes is typically insignificant. Details are shown in Figure S3 in the supplementary material.”

- It is not necessary to include the figure captions in the text. Sentences like “Figure 2 shows ...” belong to figure captions not the main text, and make it hard to follow. Please, discuss directly the results and point to the figure that shows them in the running text, e.g. *Larger anomalies (i.e., up to 5ppbv) are simulated in locations including the east*

coast of China, the Indian subcontinent, and remote oceans (Figure 1 and Figure S2).

We have changed the text accordingly in our revised manuscript (e.g., P11, L305-308):

“...In this study, the SST-induced, process-level O₃ changes are spatially averaged over four populated continental regions (i.e., NA, EU, EA and SA, Figure 2) and three ocean basins (i.e., the North Pacific, North Atlantic and North Indian Oceans, Figure S9).”

Specific comments:

LL59-61 Beside the missing reference pointed out in the short comment by Dr. Meiyun Lin there are several other key references missing that are related to the O₃ long-range transport: Parrish et al., 1993; Fehsenfeld et al., 1996; Wild and Akimoto, 2001; Creilson et al., 2003; Simmonds et al., 2004.

Good suggestion. We have added these important references related to the O₃ long-range transport in our revised manuscript (P3, L62-67):

“...The long-range transport of O₃ and its precursors has been extensively studied, and their inter-continental impacts have been evaluated using measurements and model simulations (Parrish et al., 1993;Fehsenfeld et al., 1996;Wild and Akimoto, 2001;Creilson et al., 2003;Simmonds et al., 2004;Fiore et al., 2009;Brown-Steiner and Hess, 2011;Lin et al., 2012a;Lin et al., 2014).”

LL66 Here as well, the authors do not cite several studies on the topic (e.g., Bronnimann et al. 2000; Hess and Mahowald, 2009; Pausata et al. 2012).

We have cited these valuable studies and expanded our introduction (see P3, L72-83):

“...Atmospheric circulation considerably determines the timescale and pathway of O₃ transport (Bronnimann et al., 2000;Auvray and Bey, 2005;Hess and Mahowald, 2009). The efficiency of O₃ transport varies coherently with atmospheric circulations on different scales. Knowland et al. (2015) demonstrated the important role of mid-latitude storms in redistributing O₃ concentrations during springtime. The North Atlantic Oscillation (NAO) significantly affects surface and tropospheric O₃ concentrations over most of Europe by influencing the intercontinental transport of air masses (Creilson et al., 2003;Christoudias et al., 2012;Pausata et al., 2012). Lamarque and Hess (2004) indicated that the Arctic Oscillation (AO) can modulate springtime tropospheric O₃ burdens over North America. The shift in the position of the jet stream associated with climate change was found to strongly affect summertime surface O₃

variability over eastern North America (Barnes and Fiore, 2013)."

L104 remove spaces before and after comma.

We removed these spaces (P4, L119-121).

"...The mechanisms responsible for SST variability includes ocean circulation variability, wind stress, and ocean-atmosphere feedbacks (Frankignoul, 1985;Deser et al., 2010)."

L113 remove the hyphen after impacts.

We removed this mistake in our revised manuscript (P5, L135-136):

"...Except for the ENSO impacts, very few studies to date have directly addressed the linkage between SST and O₃."

L114 ENSO is an oscillation; hence "ENSO spring" does not mean anything. Please specify the ENSO phase the authors are referring to.

We changed "ENSO spring" to "strong La Niña spring" for clear clarification (P5, L128-131):

"...Lin et al. (2015) found that more frequent deep stratospheric intrusions appear over the western US during strong La Niña springs because of the meandering of the polar jet towards this region. This process can remarkably increase surface O₃ levels in the western US."

LL114-115 indulge a bit more and provide the explanation of how ENSO affects stratospheric intrusions in western US. Otherwise the reader is forced to look it up.

Good suggestion. We revised this sentence in the introduction section to briefly explain the impacts of ENSO on stratospheric intrusions in western US (P5, L128-131):

"...Lin et al. (2015) found that more frequent deep stratospheric intrusions appear over the western US during strong La Niña springs because of the meandering of the polar jet towards this region. This process can remarkably increase surface O₃ levels in the western US."

L194 mention also here at least some of the individual processes accounted for.

We revised this sentence in Section 2.3 (P8, L222-226) to give some examples of the individual processes:

“...This method calculates the accumulated contributions of individual processes (e.g., chemical production and loss, advection, vertical diffusion, dry deposition, etc.) to O₃ predictions during the model simulation and has been widely used for air pollution diagnostics (Li et al., 2012; Zhang and Wu, 2013; Tao et al., 2015).”

LL233-234 the sentence is unclear.

Here we means the responses of surface O₃ to SST changes in different cases behave differently in terms of spatial distribution. Different oceans warming can impact the surface O₃ at specific regions. In our revised manuscript, we changed this sentence in Section 3 (P10, L282-283) for clarification:

“Our simulations reveal that different oceans can exert distinct region-specific effects on the O₃ distribution.”

LL253-254 It's not clear to me how the authors can conclude that the change in CHEM is “therefore” causing the increase in ozone at the surface over NA due to warmer Atlantic SSTs. See also comment on figure 2.

Good question. The integrated process rate (IPR) method can decompose the contribution of different physical and chemical processes to O₃ evolution. Typically a positive change in IPR is responsible for the increase of surface O₃ due to the change of SST, which is sometimes balanced by certain negative IPR changes. For instance, the increase in VDIF is always accompanied with a commensurate decrease in DRYD, resulting in an insignificant net change in TURB (here TURB=VDIF+DRYD). We redraw these plots and merge VDIF and DRYD into TURB and DEEP and SHAL into CONV (see Figure 2). Now it shows that the increase of CHEM tends to play the dominate role in enhancing the surface O₃ concentrations over North America.

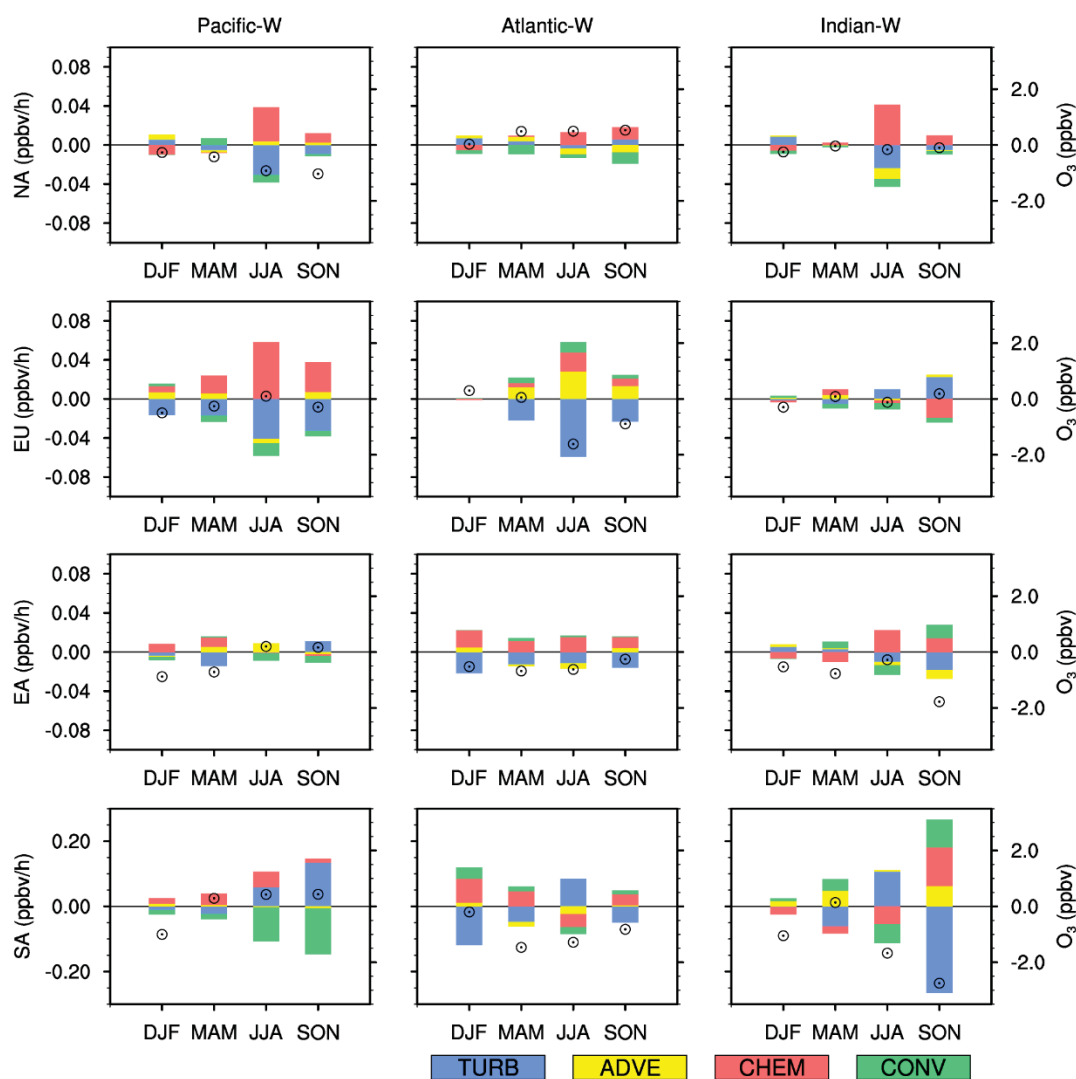


Figure 2. Seasonally averaged changes in the IPR contributions (bars, ppbv/h, left scale) and surface O₃ concentrations (hollow circles, ppbv, right scale) for Pacific-W (left), Atlantic-W (middle) and Indian-W (right) relative to the CTRL. Values are regionally averaged over NA (first row), EU (second row), EA (third row) and SA (last row). TURB is defined as the sum of VDIF and DRYD. CONV is the sum of DEEP and SHAL. IPR contributions from the four processes (i.e., TURB, ADVE, CHEM and CONV) are represented by different colors. A more detailed IPR result is shown in Figure S10 in the supplementary material.

To clarify our analysis, we added more descriptions on the IPR analysis in both Section 2.3 and Section 4.1 in the revised manuscript:

In Section 2.3 (*P8-9, L226-241*):

“In this study, we added the IPR scheme to the CESM framework to track the contribution of six physicochemical processes (i.e., gas-phase chemistry (CHEM), advection (ADVE), vertical diffusion (VDIF), dry deposition (DRYD), shallow convection (SHAL) and deep convection (DEEP)) to O₃ concentrations in every grid box. Wet deposition and aqueous-phase chemistry are ignored here due to the low solubility and negligible chemical production of O₃ in water (Jacob, 1999). Therefore, CHEM represents the net production (production minus loss) rate of O₃ due to gas-phase photochemistry. DRYD represents the dry deposition fluxes of O₃, which is an important sink for O₃. The other IPR terms (i.e., ADVE, VDIF, SHAL and DEEP) represent contributions from different transport processes. The IPR scheme tracks and archives the O₃ flux in each grid from every process during each model time step. The sum of the O₃ fluxes from these six processes matches the change in the O₃ concentration. The IPR performance is verified by comparing the predicted hourly O₃ changes with the sum of the individual fluxes from the six processes. As shown in Figure S1, the hourly surface O₃ changes are well represented by the sum of these fluxes in the model.”

In Section 4.1 (P10-II, L296-316):

“IPR analysis is used to evaluate the contribution of different physicochemical processes to O₃ evolution. This type of analysis has been widely used in air quality studies to examine the cause of pollution episodes (Wang et al., 2010; Li et al., 2012). When applied in climate sensitivity analysis (usually measuring the difference between two equilibriums), the net change of all IPRs approaches zero. Typically, the positive changes in IPRs are mainly responsible for the increase in surface O₃, which may further induce O₃ removal to balance this forcing in a new equilibrium. Therefore, here, the IPR analysis is used not to budget the SST-induced O₃ concentration changes but rather to help examine the relative importance of different transport and chemical processes in driving the sensitivity of O₃ to SST forcing. In this study, the SST-induced, process-level O₃ changes are spatially averaged over four populated continental regions (i.e., NA, EU, EA and SA, Figure 2) and three ocean basins (i.e., the North Pacific, North Atlantic and North Indian Oceans, Figure S9). In most cases, VDIF and DRYD are the key processes controlling the O₃ variation. The downward transport of O₃ through diffusion is an important source of surface O₃, while DRYD acts as a sink.

Both processes are simultaneously determined by the strength of turbulence. Here, we define a new term TURB as the sum of DRYD and VDIF, which can capture the overall effect of turbulence changes on surface O₃ concentrations. In addition, we merge SHAL and DEEP as CONV to represent the total contribution of convective transport to surface O₃ (Figures 2 and S9). More detailed IPR results are shown in Figures S10 and S11 in the supplementary material.”

L264 “inconsistent surface O₃ response”: do the authors mean “opposite surface O₃ response”?

We replaced “inconsistent” with “distinct” (see P12, L340-342):

“These opposite changes in VDIF over upwind and downwind regions lead to distinct surface O₃ responses.”

L270 I understand the authors’ point on investigating only summer since it’s the seasons with higher O₃ concentration at the surface. However, during winter and spring the ozone at the surface is mainly affect by changes in long-range transport and stratosphere-troposphere exchange. Hence, it is important to understand how the warming in the SST in different basins can affect long range and stratosphere-troposphere exchange. I would suggest expanding the analysis to also winter.

Thanks for this helpful suggestion. In this study, we had investigated both the SST-O₃ relationship in both summer and winter seasons (see Figure 1 and Figure S3). It shows that in boreal winter, the warming of different oceans generally induces a widespread decrease of surface O₃. However, significant changes (up to 5 ppbv) mainly happen over remote oceanic regions. Over land, the O₃ response to SST changes is generally insignificant (see Figure S3). Besides surface O₃, the responses of meteorological fields to SST changes are also significant only over remote oceans (see Figure R3). Similar to the summer case, physical transport is the key process modulating surface O₃ during winters. As shown in Figure R2 and R3, these vertical and horizontal wind field changes are more robust over oceans than the polluted continents. Since the main focus of this study is to examine how O₃ air pollution in a populated continent is affected by regional SST changes, we therefore pay most attention to boreal summers than other seasons.

In the revised manuscript, we follow the reviewer’s suggestions and add a brief discussion in Section 3 (see P10, L276-280) for wintertime response:

“...During the boreal winter, a widespread decrease in surface O_3 associated with the warming of different oceans is observed. Significant changes (e.g., up to 5 ppbv) mainly occur over remote ocean areas. Over populated continents, the response of the surface O_3 to basin-scale SST changes is typically insignificant. Details are shown in Figure S3 in the supplementary material.”

We further clarified why we only focus on summertime in Section 4.1 (P12, L344-347) :

“In the following subsections, the mechanisms of the SST- O_3 relationship for the four polluted continents are further explored. Here we focus on boreal summers since the surface O_3 response to SST changes is more robust during this period than other seasons.”

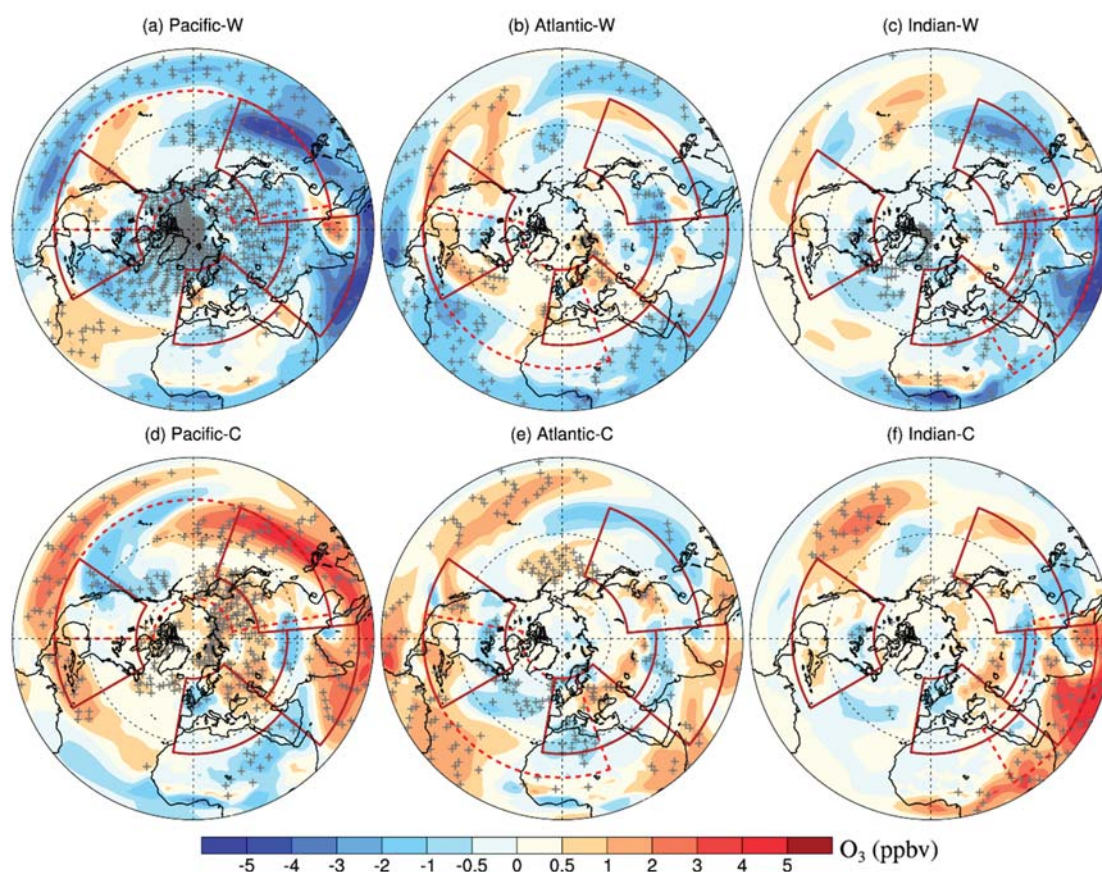


Figure S3. Changes in the wintertime (December-February) surface O_3 concentrations (ppbv) in the Northern Hemisphere for (a) Pacific-W, (b) Atlantic-W, (c) Indian-W, (d) Pacific-C, (e) Atlantic-C and (f) Indian-C relative to the CTRL. The four major regions of interest (i.e., NA, EU, EA and SA) are marked with solid polygons. Red dashed lines mark the regions where the SST has been changed. The + symbols denote areas where the results are significant at the 0.05 level, evaluated by Student’s t-test using 20

years of data.

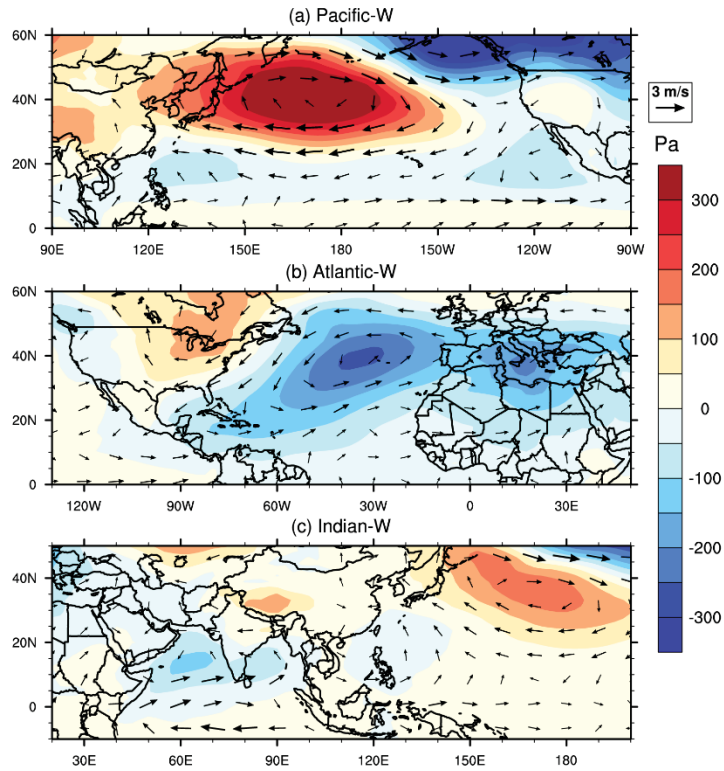


Figure R2. Changes in the surface pressure (color contours, Pa) and 850-hPa wind (arrows, m s^{-1}) for (a) Pacific-W, (b) Atlantic-W, and (c) Indian-W relative to the CTRL in the boreal winter.

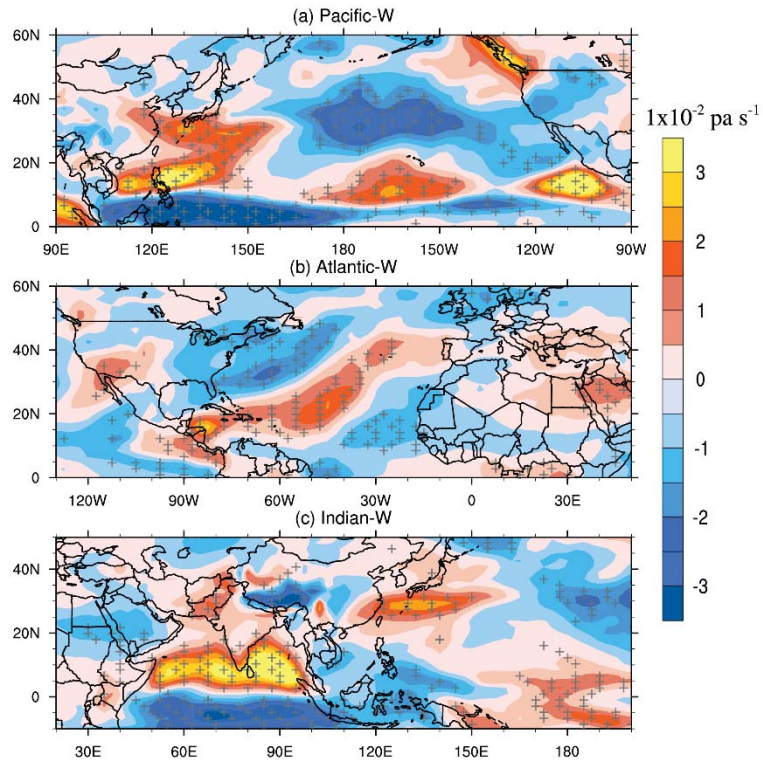


Figure R3. Spatial pattern of vertical velocity changes at 500 hPa (color contours, 1×10^{-2} Pa s⁻¹) for (a) Pacific-W, (b) Atlantic-W, and (c) Indian-W relative to the CTRL in the boreal winter. Positive values indicate upward motion. Red polygons denote the regions where the surface pressure responses to SST anomalies are significant (see Figure 5 a-c). The + symbols indicate areas where the results are significant at the 0.05 level, evaluated by Student's t-test using 20 years of data.

L291 “is believed”: Beliefs do not belong to science. Please rephrase it and provide references to support the *belief*.

The effect of the North Indian Ocean warming on cloud formation has been well-documented in previous studies (Chaudhari et al., 2016; Roxy et al., 2015; Xi et al., 2015). We have rephrased this sentence in Section 4.2 (P13, L367-372) as below:

“...Previous studies have indicated that moist convection is more sensitive to the SST changes in the tropical oceans than in mid- or high- latitude oceans (Lau and Nath, 1994; Lau et al., 1997; Hartmann, 2015). The SST increase over the North Indian Ocean tends to strengthen the moist convection that eventually facilitates cloud formation in the upper troposphere (Roxy et al., 2015; Xi et al., 2015; Chaudhari et al., 2016)...”

LL356-357 The authors stated that the O₃ changes at the surface over North America (Fig. 7 “b”, which is actually c) are negligible. However, they look quite large (regionally) to me: over the Great Lakes, California and Baja California peninsula; also along the east coast of United States the changes are not that small. Furthermore, the changes aloft (that the authors define “large”) are of the same order of magnitude that the changes seen at the surface.

Good question. We agree that the surface O₃ changes over NA (~1-2 ppbv) are large and significant for regional air quality management. In the revised manuscript, we have revised this description in Section 4.3 (P16, L447-448):

“...O₃ changes are observed to be larger in the upper troposphere than at the surface (Figure 7e)...”

We also reordered the plots in Figure 7:

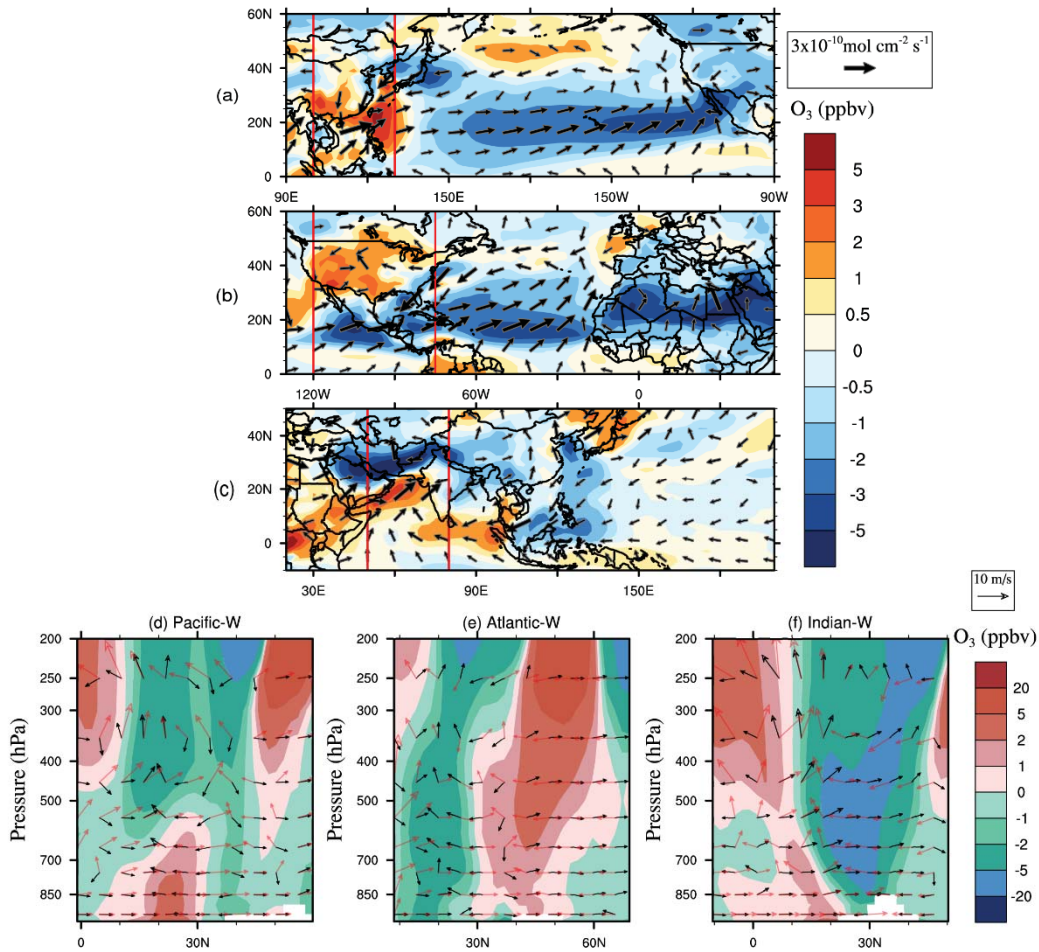


Figure 7. Top three rows: Changes in O₃ concentrations (color contours, ppbv) and horizontal fluxes (arrows, mol cm⁻² s⁻¹) at the surface level for (a) Pacific-W, (b) Atlantic-W, (c) Indian-W relative to the CTRL in the boreal summer. Last row: zonal average of the tropospheric O₃ changes (color contours, ppbv), wind fluxes in CTRL (red arrows, m s⁻¹) and the wind flux perturbation (black arrows, m s⁻¹) in (d) Pacific-W, (e) Atlantic-W, (f) Indian-W relative to the CTRL in the boreal summer. The red rectangles in (a), (b) and (c) denote the longitudinal range used for the zonal averages in (d), (e) and (f), respectively. The vertical wind velocity is amplified 1000 times to make it comparable to the horizontal wind velocity.

L357-359 Given the above-mentioned comments, I am not sure how the authors could state that the changes seen in figure 7c are mostly due to enhanced photochemical production. This comment is also related to my previous comments on LL253-254.

Good question. Following our detailed response to the previous comments on L253-

254, the IPR analysis helps to identify the key processes associated to the SST induced O₃ evolution. For example, the warming of the North Atlantic Ocean leads to 1~2 ppbv increase in surface O₃ over North America. Ignoring VDIF and DRYD (they tend to offset each other in most cases, resulting in an insignificant net change in TURB, see Figure 2). Therefore, the change of CHEM is the dominant factor leading to the surface O₃ increase over North America. Please refer to our response to previous comments on L253-254 for more detail. Figure 7, on the other hand, further indicates that changes in the horizontal fluxes of O₃ over North America show no significant effect on the corresponding increase of surface O₃ levels.

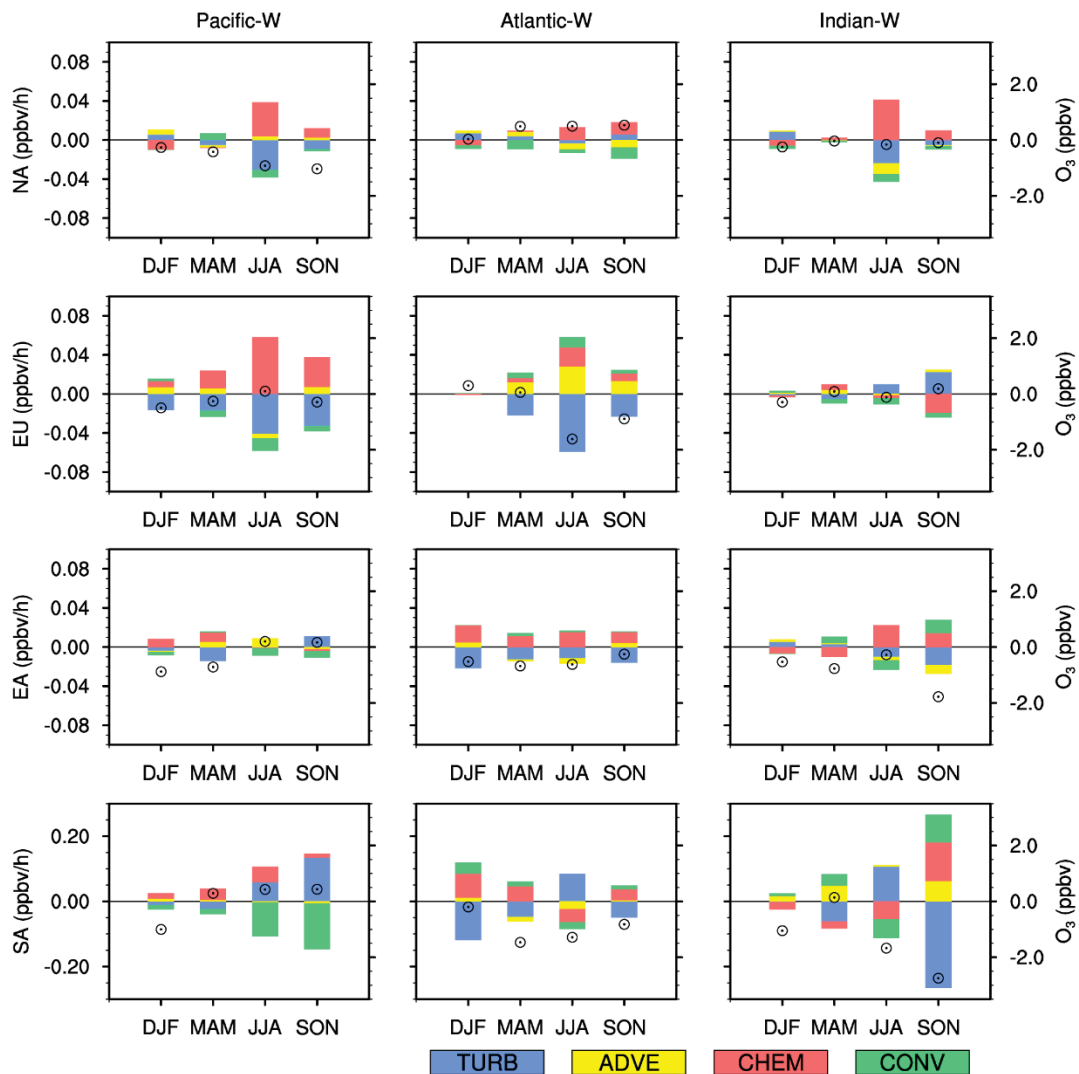


Figure 2. Seasonally averaged changes in the IPR contributions (bars, ppbv/h, left scale) and surface O₃ concentrations (hollow circles, ppbv, right scale) for Pacific-W (left), Atlantic-W (middle) and Indian-W (right) relative to the CTRL. Values are regionally averaged over NA (first row), EU (second row), EA (third row) and SA (last row). TURB is defined as the sum of VDIF and DRYD. CONV is the sum of DEEP and

SHAL. IPR contributions from the four processes (i.e., TURB, ADVE, CHEM and CONV) are represented by different colors. A more detailed IPR result is shown in Figure S10 in the supplementary material.

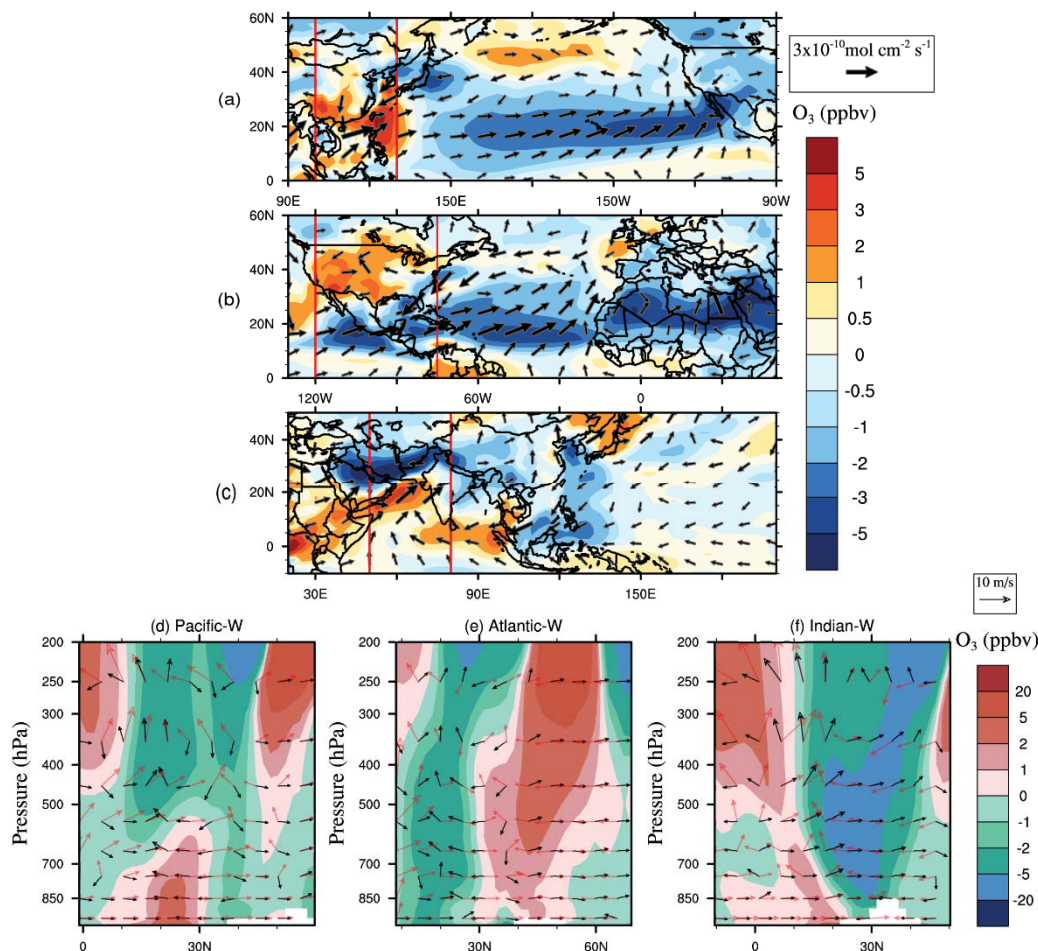


Figure 7. Top three rows: Changes in O₃ concentrations (color contours, ppbv) and horizontal fluxes (arrows, $\text{mol cm}^{-2} \text{ s}^{-1}$) at the surface level for (a) Pacific-W, (b) Atlantic-W, (c) Indian-W relative to the CTRL in the boreal summer. Last row: zonal average of the tropospheric O₃ changes (color contours, ppbv), wind fluxes in CTRL (red arrows, m s^{-1}) and the wind flux perturbation (black arrows, m s^{-1}) in (d) Pacific-W, (e) Atlantic-W, (f) Indian-W relative to the CTRL in the boreal summer. The red rectangles in (a), (b) and (c) denote the longitudinal range used for the zonal averages in (d), (e) and (f), respectively. The vertical wind velocity is amplified 1000 times to make it comparable to the horizontal wind velocity.

In the revised manuscript, we rephrased this analysis to clarify our statement (P15-16, L444-450):

“In the “Atlantic-W” case, the SST warming-induced surface pressure anomalies lead to substantial O₃ redistribution, especially over the North Atlantic Ocean (Figure 7b). For North America, the changes in horizontal O₃ fluxes have no significant effect on the O₃ concentration increase. In addition, O₃ changes are observed to be larger in the upper troposphere than at the surface (Figure 7e). As demonstrated in Section 4.1, the response of lower-altitude O₃ over North America to the North Atlantic warming is mainly caused by enhanced chemical production, rather than physical transport.”

LL366-368 please refer to figure 2 as well.

Thanks, referred (see P16, L456-460).

“According to the IPR analysis, the surface O₃ increase over the Indian Ocean is mainly caused by the enhanced vertical transport of O₃ to the surface through deep convection and vertical diffusion processes (Figure S11). However, over the nearby Indian subcontinent, the suppressed convection tends to decrease surface O₃ in that region (Figure 2).”

L369 The IPR analysis show suppressed deep-convection. However, the warming of the Indian Ocean strengthens the Indian Summer Monsoon, as also stated by the authors (e.g. LL290-292), hence I wonder why the deep-convection is weakened. Please comment on that.

Good question. Changes in DEEP in the IPR analysis indicates that a warming of Indian Ocean tends to reduce surface O₃ over South Asia (Figure S10), but increase surface O₃ over North Indian Ocean (Figure S11). This is because that the warming of the North Indian Ocean enhances the deep convection above it while suppress the deep-convection over the Indian subcontinent. According to previous studies (e.g., Hartmann, 2015;Lau et al., 1997;Lau and Nath, 1994), the SST increase over the Indian Ocean strengthens deep-convection above it. A low-pressure anomaly is observed centered over the Arabian Sea (Figure 5). It consequently strengthens the southwesterly flow towards the Indian subcontinent, as a part of the Indian Summer Monsoon. On the other

hand, the enhanced upward movement of moist air above the Indian Ocean enhances cloud formation. This tends to block solar radiation reaching the earth surface and cools the surface air over the Indian subcontinent. A remarkable reduction of surface solar radiation and air temperature are shown in Figure S17 and Figure 4, respectively. This decrease in surface temperature over the Indian subcontinent may suppress the development of deep-convection there.

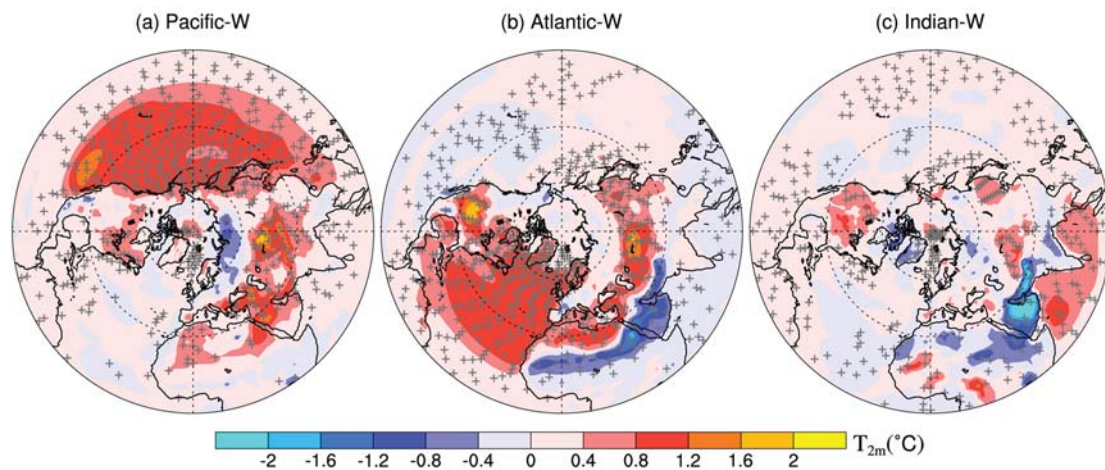


Figure 4. Changes in the surface air temperature ($^{\circ}\text{C}$) for (a) Pacific-W, (b) Atlantic-W, and (c) Indian-W relative to CTRL in the Northern Hemisphere in the boreal summer. The + symbols denote areas where the results are significant at the 0.05 level, evaluated by Student's t-test using 20 years of data (plots using the Mercator projection are shown in Figure S15 in the supplementary material).

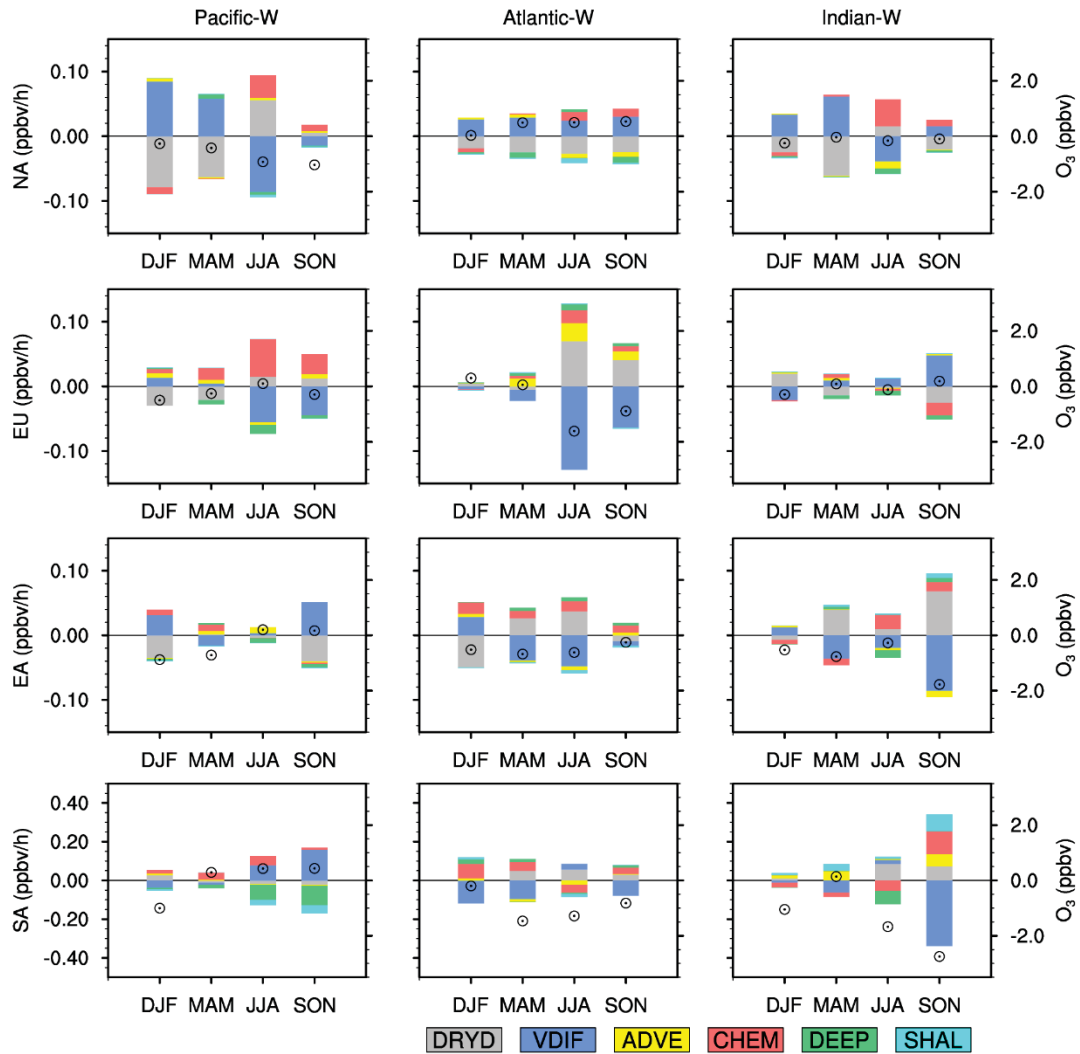


Figure S10. Seasonally averaged changes in the IPR contributions (bars, ppbv h⁻¹, left scale) and surface O₃ concentrations (hollow circles, ppbv, right scale) for Pacific-W (left), Atlantic-W (middle) and Indian-W (right) relative to the CTRL. Values are regionally averaged over NA (first row), EU (second row), EA (third row) and SA (last row). IPR contributions from the six processes (i.e., DRYD, VDIF, ADVE, CHEM, DEEP and SHAL) are represented by different colors.

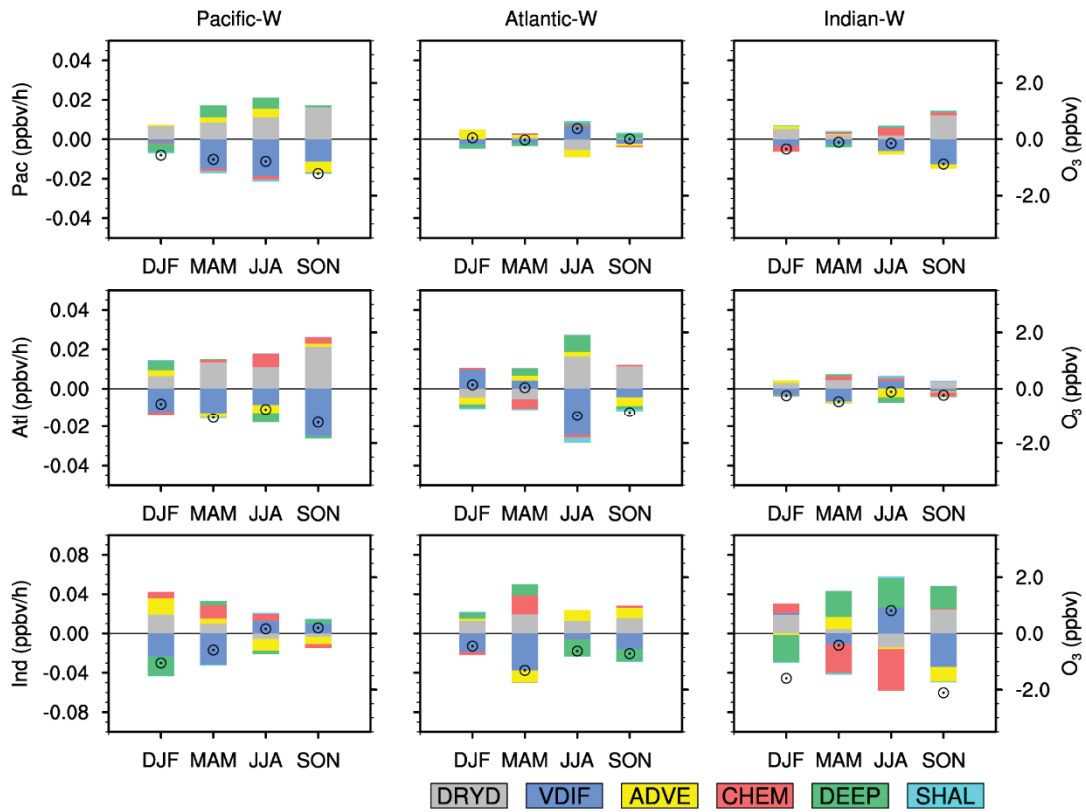


Figure S11. Same as Figure S6 but for three ocean basins defined in our study.

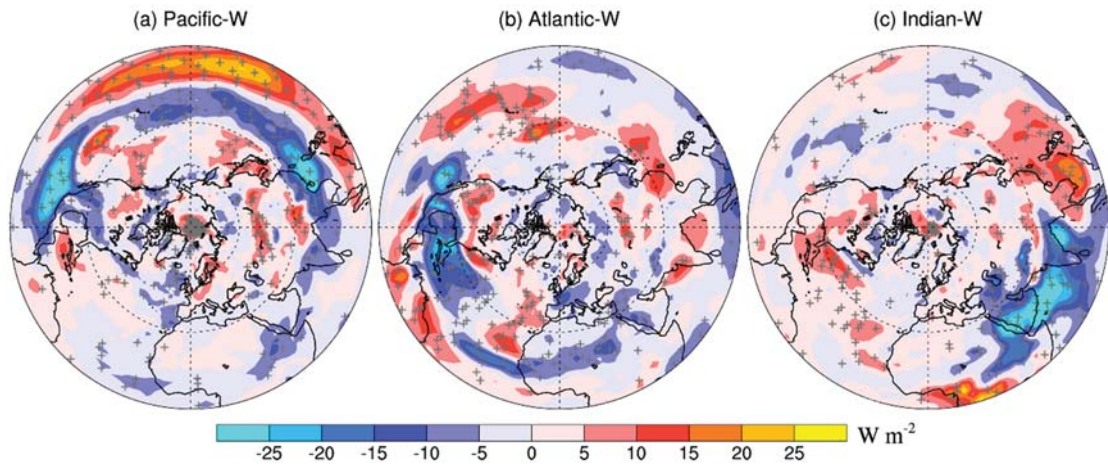


Figure S17. Perturbations of the surface solar radiations (W m^{-2}) for (a) Pacific-W, (b) Atlantic-W, and (c) Indian-W relative to the CTRL in the boreal summer. The + symbols denote areas where the results are significant at the 0.05 level, evaluated by Student's t-test.

We have clarified the corresponding text in Section 4.2 (see *P13*, *L361-380*):

“An increase in SST of 1 °C in any ocean basin leads to a widespread enhancement of the surface air temperature (i.e., the air temperature at 2 m) over most continental areas (Figure 4). An exception is the North Indian Ocean, where an increase in SST tends to cool the Indian subcontinent by 1-2 °C. This temperature decrease is not only limited to the surface but also spreads to 600 hPa (Figure S16). Associated with this temperature decrease is a remarkable reduction in the solar radiation received at the continent below (more than 15 W/m², Figure S17). Previous studies have indicated that moist convection is more sensitive to the SST changes in the tropical oceans than in mid- or high- latitude oceans (Lau and Nath, 1994; Lau et al., 1997; Hartmann, 2015). The SST increase over the North Indian Ocean tends to strengthen the moist convection that eventually facilitates cloud formation in the upper troposphere (Roxy et al., 2015; Xi et al., 2015; Chaudhari et al., 2016). The latent heat released from convective activities significantly warms the air temperature over the upper troposphere (Sabeerli et al., 2012; Xi et al., 2015). Meanwhile, the corresponding increase in cloud cover blocks the solar radiation reaching the surface of the Indian subcontinent and reduce the air temperature of lower troposphere in that region. These processes lead to opposite air temperature changes between upper and lower troposphere over South Asia in response to the North Indian warming (as shown in Figure S16), which may further suppress the development of deep convection over the Indian subcontinent.”

LL396-400 Beside the fact that Figure 9 is difficult to read. The reduction in geopotential height over the Arabian Sea seems actually to increase the southwesterly flow towards the Indian subcontinent. Furthermore, the land sea contrast may play a very small role in enhancing or weakening the strength of the Indian Summer Monsoon (Molnar et al. 2010). Hence, an in depth analysis should be done before claiming that the change in land-sea contrast is what weakens the “thermal wind”. Furthermore, the changes in temperature does not show a clear decrease in land-sea contrast, since there is a warming of SST, a cooling of the Tibert Plateau and northwestern Indian subcontinent, and a warming north of that cooling. Hence I really don't see the authors' point.

In any case, the sentence is not very clear and should be reformulated: “This nonuniform increase in air temperature (i.e., more significant at mid-latitudes) weakens the meridional temperature gradient, resulting in a reduction of thermal winds.” What is more significant at mid-latitudes? The nonuniform increase in temperature? Or the fact that the temperature increases more there than the ocean? Or what?

Good question. The original Figure 9 contains many variables (i.e., air temperature, wind pattern and geopotential height at 500 hPa) that make it difficult to read. The changes of westerly wind are also hard to distinguish in Figure 9. In the revised

manuscript, we illustrated our result in a more clear way. The zonal averaged changes in zonal wind and geopotential height are now shown in Figure 9, which is more distinguishable.

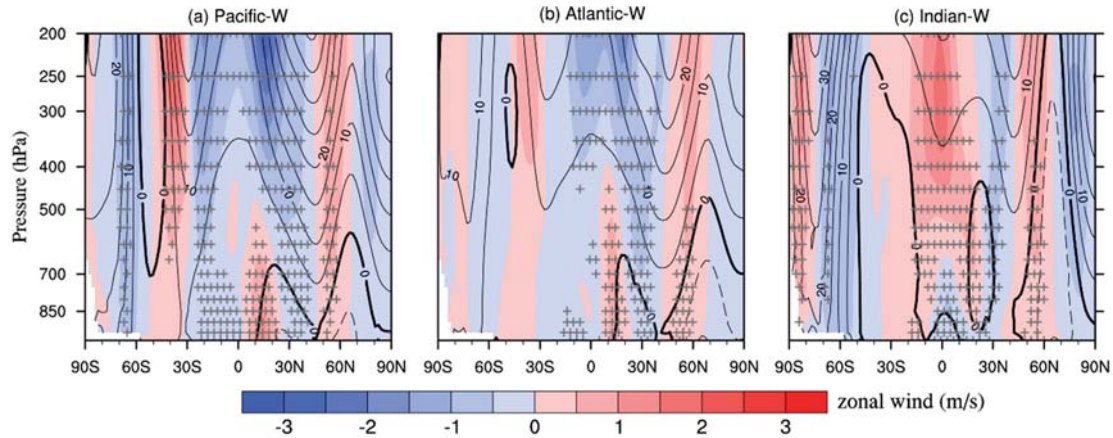


Figure 9. Zonally averaged changes in zonal wind (color contour, m/s) and geopotential height (contour, m) for (a) Pacific-W, (b) Atlantic-W and (c) Indian-W relative to the CTRL in the boreal summer. Black solid and dashed lines in the contours indicate positive and negative geopotential height anomalies, respectively (contour interval: 5 m). The + symbol denotes areas where the zonal wind changes are significant at the 0.05 level, evaluated by Student’s t-test using 20 years of data.

We agree that the increase in southwesterly flow towards the Indian subcontinent could not be simply explained by the changes in land-sea thermal contrast. According to our analysis, the warming of the North Indian Ocean creates a warm-core cyclonic anomaly centered over the Arabian Sea, which is responsible for the enhancement of the southwesterly flow towards the Indian subcontinent. A detail description is provided in our response to the comments on L369. The “thermal wind” theory here was used to explain the weakening of the westerly wind at mid-latitudes associated with the basin-scale SST warming. We find that a basin-scale SST warming, especially for the North Pacific and North Atlantic, tends to increase the air temperature (Figure S16) and geopotential height (Figure 9) more significantly at mid-latitudes than elsewhere. Consequently, the meridional temperature and geopotential height gradients are decreasing in the tropical-to-mid-latitude troposphere while increasing at higher latitudes. It tends to decrease the zonal westerly wind at lower-middle latitudes (25°N - 45 °N) in the Northern Hemisphere while increase it at higher latitudes (Figure 9).

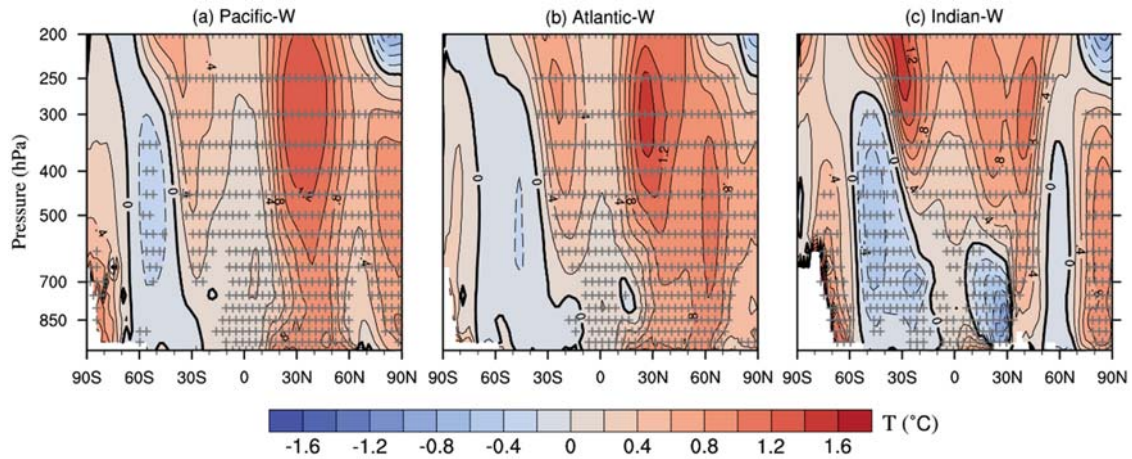


Figure S16. Vertical-meridional distributions of changes in the air temperature (contours, °C) for (a) Pacific_W (zonal averaged from 100°E-90°W), (b) Atlantic_W (zonal averaged from 100°W-180°W) and (c) Indian_W (zonal averaged from 30°E-100°E) relative to the CTRL in boreal summer. Black solid and dashed lines in the contours indicate positive and negative air temperature anomalies, respectively (contour interval: 0.2 °C). The + symbol denotes areas where the changes of air temperature are significant at the 0.05 level, evaluated by Student's t-test.

In the revised manuscript, we clarified our analysis in Section 5 (P17, L489-498):

“...Further investigations of zonal wind suggest that an increase in SST over different oceans consistently decreases the westerly winds at lower mid-latitudes (25°N-45 °N) in the Northern Hemisphere but increases these winds at higher latitudes (Figure 9). In general, increases in the geopotential height induced by basin-scale SST warming are more significant at mid-latitudes than at other latitudes, which is consistent with the air temperature changes. Consequently, the meridional geopotential height gradient is decreasing at lower latitudes but increasing at higher latitudes, leading to corresponding changes in the westerly winds. The latitude band at 25°N - 45 °N covers many polluted regions (i.e., North America and East Asia). A weakened westerly wind may reduce long-rang O₃ transport.”

LL383-385 Referring to figure 8b, the authors state: “Similarly, for the North American tracer, a warming of North Atlantic SSTs by 1°C slightly increases (~2%) concentrations in North America but decreases (3-4 %) concentrations over downwind Europe”. To me it looks like a slight decrease over Europe and quite an increase over large areas of North America. Please correct/clarify.

We previously showed absolute change. If switching to the percentage change (see the Figure 8 below), the pattern would be different. To avoid confusion, we decide to show both absolute and percentage changes in Figure 8 and remove the word “slightly” in this sentence in Section 5 (P16, L471-474):

“...Similarly, for the North American tracer, a warming of North Atlantic SSTs by 1°C increases (~1%) the concentrations in North America but decreases (3-4 %) the concentrations over downwind Europe (Figure 8d).”

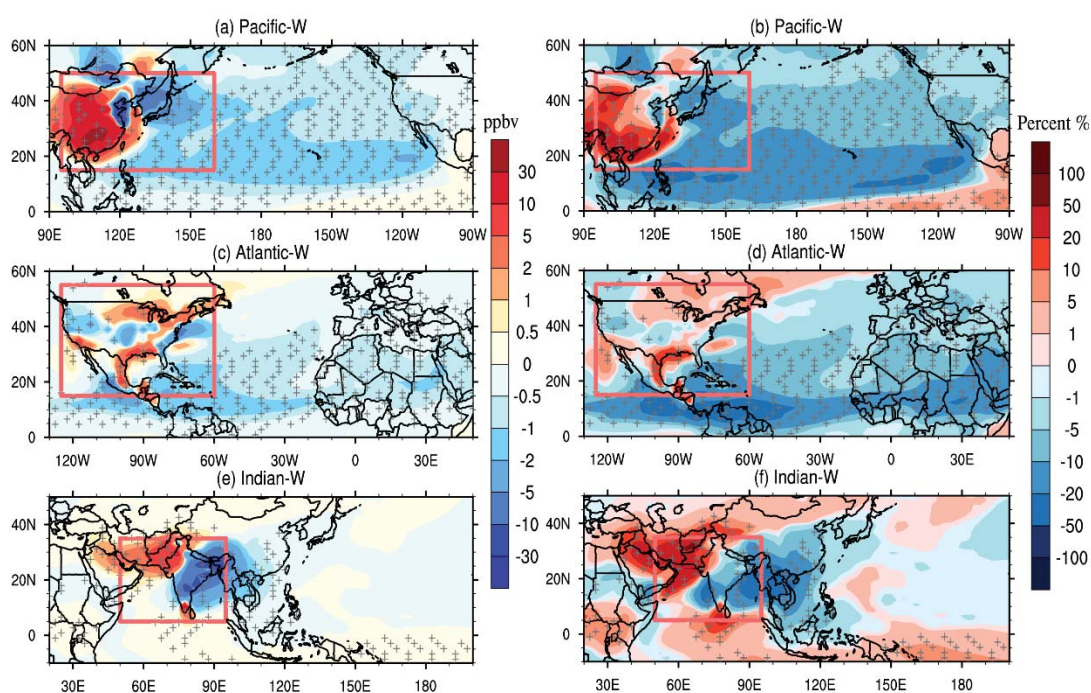


Figure 8. Left-hand panel: Difference in the surface concentration (ppbv) of a CO-like tracer emitted from (a) East Asia for Pacific-W, (c) North America for Atlantic-W and (e) the South Asia for Indian-W relative to the CTRL in the boreal summer. Right-hand panel: The percentage changes in the surface concentration of a CO-like tracer emitted from (b) East Asia for Pacific-W, (d) North America for Atlantic-W and (f) South Asia for Indian-W relative to the CTRL in the boreal summer. Red polygons denote the region where the CO-like tracer is emitted from. The + symbol denotes areas where the results are significant at the 0.05 level, evaluated by Student’s t-test using 20 years of data.

L443 I suggest to replace “reveal” with “show”

We have rephrased this sentence in Section 6 (P19, L551-552) following the reviewer's suggestion:

"...We further show that air temperature is an important factor controlling the surface O₃ responses to SST anomalies."

Figure 2: It is not clear to me how one can get the changes in O₃ from the IPR analysis. It seems that the positive anomalies counterbalance the negative ones (if so this should be made clear, readers may not be familiar with the IPR analysis you are presenting). Therefore I wonder how can the total O₃ anomalies be negative or positive (the circle)? It's not clear to me how to read the figure. Please clarify.

Why don't the authors plot in figure2 only the CONV and the TURB and instead place the figure with the full analysis in the supplementary?

Good suggestion. The IPR analysis helps to identify the key processes that cause O₃ changes. Since some processes always offset the others (e.g., VERD and DRYD), we follow the reviewer's suggestion and merge those processes and show the CONV and the TURB instead (see the new Figure 2 below), and put the more detailed decomposition in the supporting information. In addition, we added more descriptions in the revised Section 2.3 and Section 4.1:

In Section 2.3 (P8-9, L221-241)

"To provide a process-level explanation for the response of surface O₃ to regional SST changes, the IPR method is applied. This method calculates the accumulated contributions of individual processes (e.g., chemical production and loss, advection, vertical diffusion, dry deposition, etc.) to O₃ predictions during the model simulation and has been widely used for air pollution diagnostics (Li et al., 2012; Zhang and Wu, 2013; Tao et al., 2015). In this study, we added the IPR scheme to the CESM framework to track the contribution of six physicochemical processes (i.e., gas-phase chemistry (CHEM), advection (ADVE), vertical diffusion (VDIF), dry deposition (DRYD), shallow convection (SHAL) and deep convection (DEEP)) to O₃ concentrations in every grid box. Wet deposition and aqueous-phase chemistry are ignored here due to the low solubility and negligible chemical production of O₃ in water (Jacob, 1999). Therefore,

CHEM represents the net production (production minus loss) rate of O₃ due to gas-phase photochemistry. DRYD represents the dry deposition fluxes of O₃, which is an important sink for O₃. The other IPR terms (i.e., ADVE, VDIF, SHAL and DEEP) represent contributions from different transport processes. The IPR scheme tracks and archives the O₃ flux in each grid from every process during each model time step. The sum of the O₃ fluxes from these six processes matches the change in the O₃ concentration. The IPR performance is verified by comparing the predicted hourly O₃ changes with the sum of the individual fluxes from the six processes. As shown in Figure S1, the hourly surface O₃ changes are well represented by the sum of these fluxes in the model.”

In Section 4.1 (P10-II, L296-316), we have:

“IPR analysis is used to evaluate the contribution of different physicochemical processes to O₃ evolution. This type of analysis has been widely used in air quality studies to examine the cause of pollution episodes (Wang et al., 2010; Li et al., 2012). When applied in climate sensitivity analysis (usually measuring the difference between two equilibriums), the net change of all IPRs approaches zero. Typically, the positive changes in IPRs are mainly responsible for the increase in surface O₃, which may further induce O₃ removal to balance this forcing in a new equilibrium. Therefore, here, the IPR analysis is used not to budget the SST-induced O₃ concentration changes but rather to help examine the relative importance of different transport and chemical processes in driving the sensitivity of O₃ to SST forcing. In this study, the SST-induced, process-level O₃ changes are spatially averaged over four populated continental regions (i.e., NA, EU, EA and SA, Figure 2) and three ocean basins (i.e., the North Pacific, North Atlantic and North Indian Oceans, Figure S9). In most cases, VDIF and DRYD are the key processes controlling the O₃ variation. The downward transport of O₃ through diffusion is an important source of surface O₃, while DRYD acts as a sink. Both processes are simultaneously determined by the strength of turbulence. Here, we define a new term TURB as the sum of DRYD and VDIF, which can capture the overall effect of turbulence changes on surface O₃ concentrations. In addition, we merge SHAL and DEEP as CONV to represent the total contribution of convective transport to surface O₃ (Figures 2 and S9).”

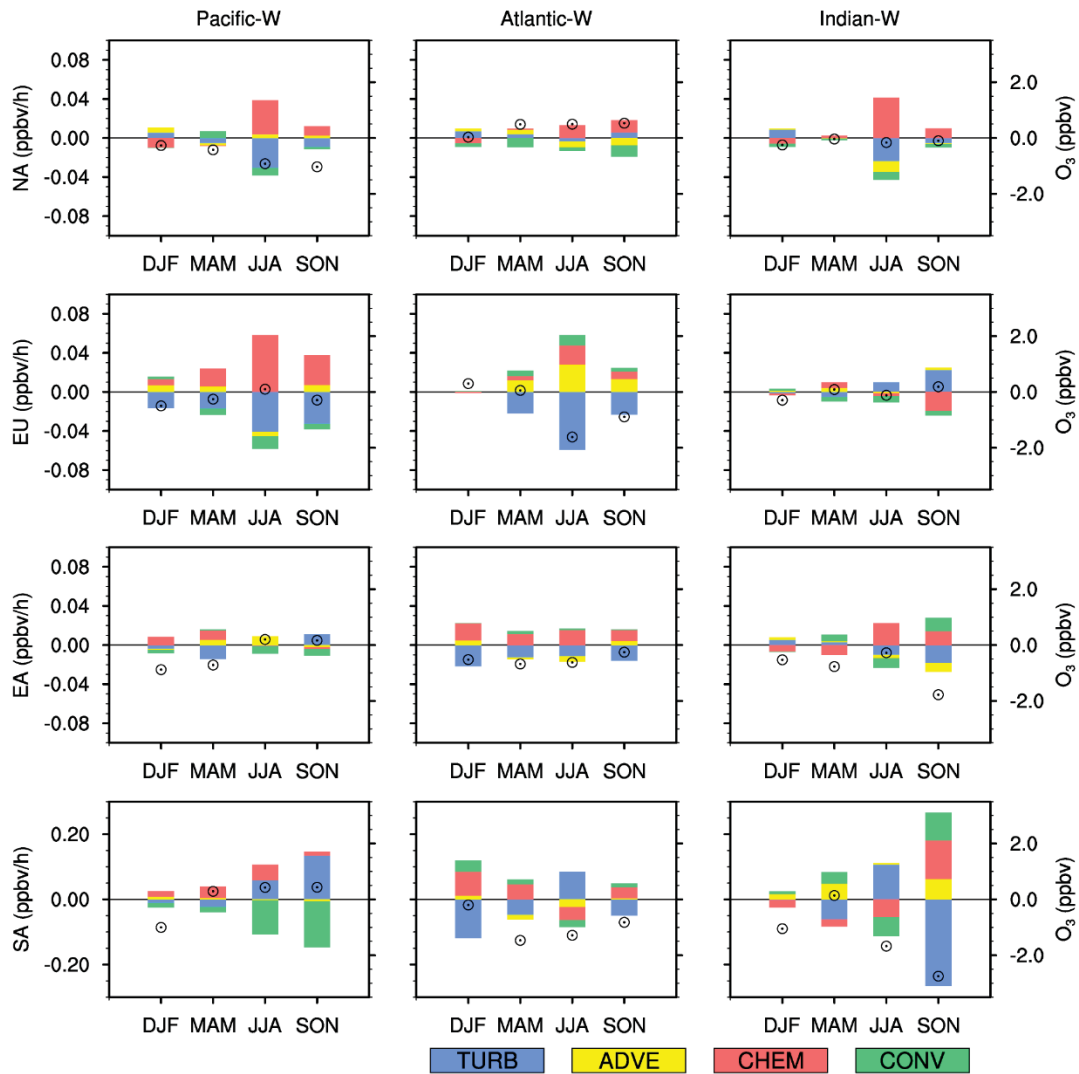


Figure 2. Seasonally averaged changes in the IPR contributions (bars, ppbv/h, left scale) and surface O₃ concentrations (hollow circles, ppbv, right scale) for Pacific-W (left), Atlantic-W (middle) and Indian-W (right) relative to the CTRL. Values are regionally averaged over NA (first row), EU (second row), EA (third row) and SA (last row). TURB is defined as the sum of VDIF and DRYD. CONV is the sum of DEEP and SHAL. IPR contributions from the four processes (i.e., TURB, ADVE, CHEM and CONV) are represented by different colors. A more detailed IPR result is shown in Figure S10 in the supplementary material.

Figure 3: the authors use 0.05 as significance level while in figure 1 was 0.01. Please pick one level. In figure 1 white colors were used for non-significant values, please be consistent. Furthermore, in figure 3 sometime white areas present significant changes.

Good suggestion. We used 0.05 as the significance level for all relevant figures. We have also removed white color bins used for small values and non-significant values. Please see the revised Figure 3 below for an example.

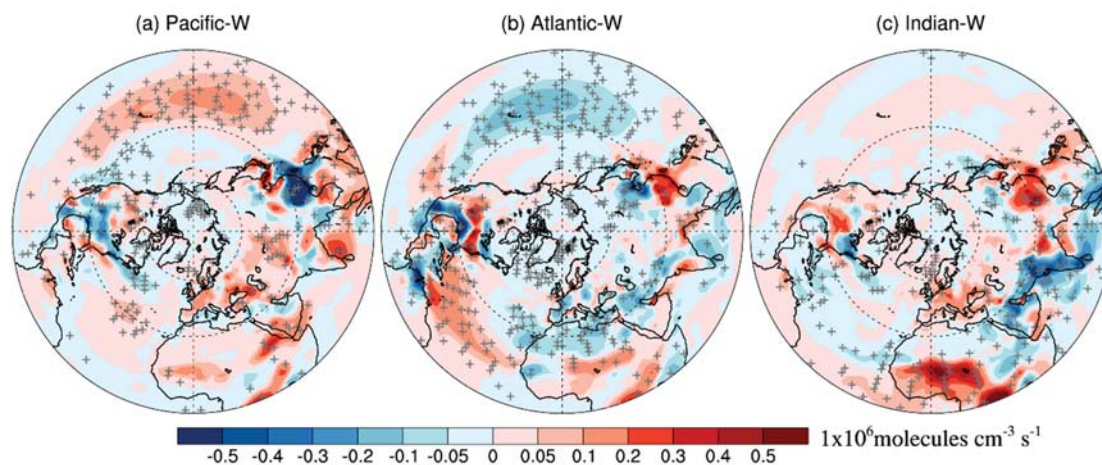


Figure 3. Perturbations of the surface net O₃ production rate (1×10^6 molecules $\text{cm}^{-3} \text{s}^{-1}$) for (a) Pacific-W, (b) Atlantic-W, and (c) Indian-W relative to the CTRL in the boreal summer. The + symbols denote areas where the results are significant at the 0.05 level, evaluated by Student's t-test using 20 years of data (plots using the Mercator projection are shown in Figure S14 in the supplementary material).

Figure 4: The panels are small and it's hard to see the continents. Please use Mercator projection.

Thanks for this suggestion. As we discussed previously (see our response to major comment 2), we compared the performance of different projections and decided to consistently use polar projection since it is easier to interpret the hemispheric flow patterns although it is true that it's hard to see continents. We realized that the difficulty of reading the original Figure 4 were mainly caused by the low figure quality and blurry continental outlines. In the revised version, high-resolution figure is provided. In addition, the continental outlines are thicker and darker than before. Please see the revised Figure 4 below:

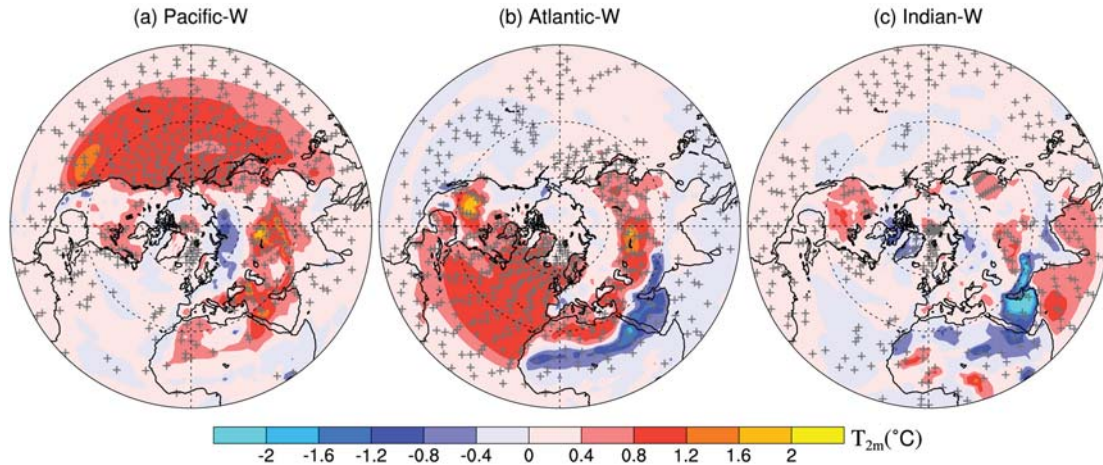


Figure 4. Changes in the surface air temperature ($^{\circ}\text{C}$) for (a) Pacific-W, (b) Atlantic-W, and (c) Indian-W relative to CTRL in the Northern Hemisphere in the boreal summer. The + symbols denote areas where the results are significant at the 0.05 level, evaluated by Student's t-test using 20 years of data (plots using the Mercator projection are shown in Figure S15 in the supplementary material).

On the other hand, plots using the Mercator projection are also provided in the supplementary material. Please see Figure S15 below:

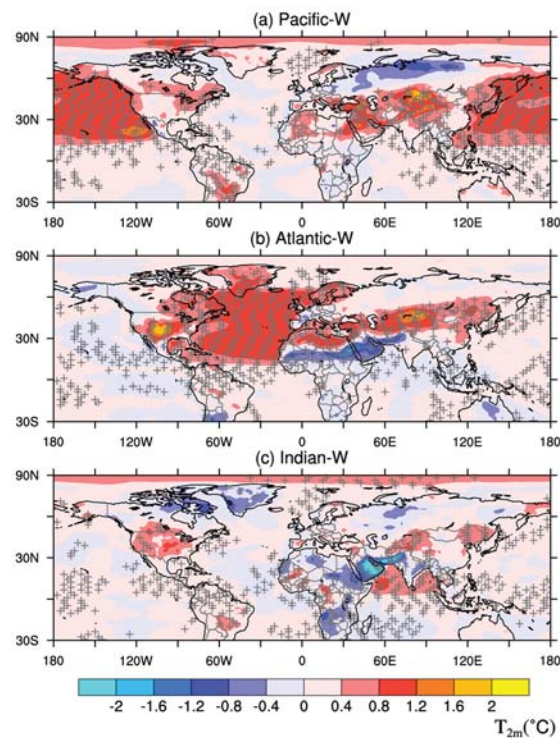


Figure S15. Changes in the surface air temperature ($^{\circ}\text{C}$) for (a) Pacific-W, (b) Atlantic-

W, and (c) Indian-W relative to the CTRL in the boreal summer. The + symbols denote areas where the results are significant at the 0.05 level, evaluated by Student's t-test using 20 years of data.

Figure 5: I think it would be better to show both the upwind and downwind area around the basin, i.e. in panel a) please show also the western coast of North and Central America; in panel b) please show the European coast. Finally, the authors plot the wind pattern but do not specify the level: is it at the surface or 850 hPa, ...? Please clarify it. Furthermore, I would suggest not to use the surface level but rather a low-middle atmosphere level (850 or 700 hPa).

Good suggestion. We have used the same map projection for Figure 5-8 that shows both the upwind and downwind area around the basin. Please refer to our response to major comment 2 for more details. The wind pattern at 850 hPa is depicted in Figure 5.

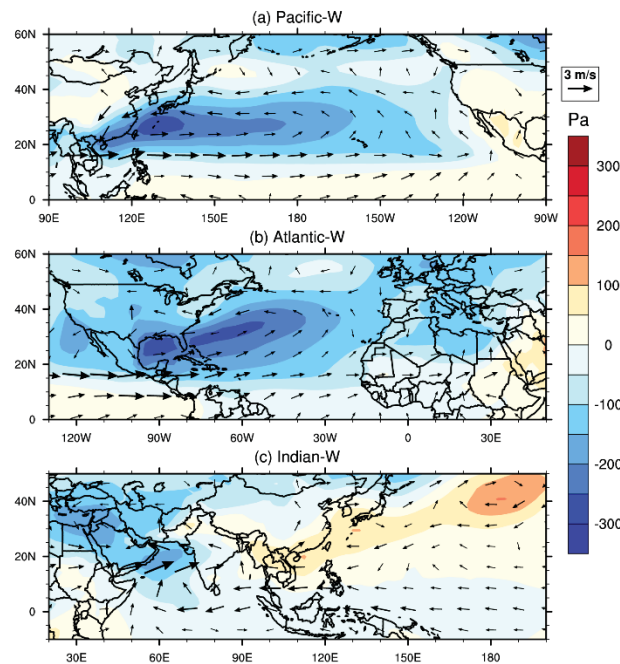


Figure 5. Changes in the surface pressure (color contours, Pa) and 850-hPa wind (arrows, m s^{-1}) for (a) Pacific-W, (b) Atlantic-W, and (c) Indian-W relative to the CTRL in the boreal summer.

Figure 6: Impossible to understand it without major efforts.

Thanks for bringing this problem up. Figure 6 shows the spatial pattern of vertical velocity changes at 500 hPa. We agree that the old version was hard to read because of

the low figure quality. We have optimized this figure with large improvement. We also changed the map projection of Figure 6 to make it comparable with Figures 5, 7 and 8. Please see the revised Figure 6 below:

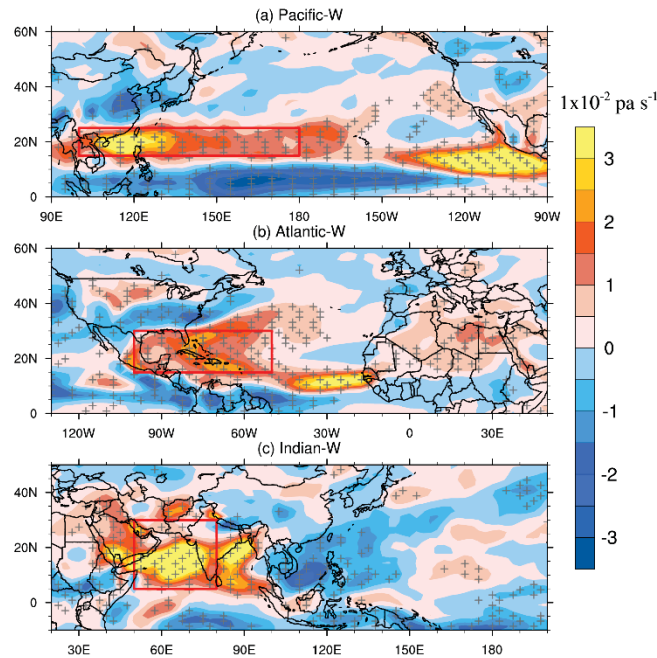


Figure 6. Spatial pattern of vertical velocity changes at 500 hPa (color contours, $1 \times 10^{-2} \text{ Pa s}^{-1}$) for (a) Pacific-W, (b) Atlantic-W, and (c) Indian-W relative to the CTRL in the boreal summer. Positive values indicate upward motion. Red polygons denote the regions where the surface pressure responses to SST anomalies are significant (see Figure 5 a-c). The + symbols indicate areas where the results are significant at the 0.05 level, evaluated by Student's t-test using 20 years of data.

Figure 7: as for figure 5 I don't understand the choice of the domain shown for each of the sensitivity experiment. Furthermore, panel b) should be switched with panel c). Furthermore, the authors should also here be consistent with the choice of the domain to show. I would advice to adopt the domain (or a similar one) used in figure 8.

Good suggestion! We have used the same map projection for Figures 5-8 that shows both the upwind and downwind areas around the ocean basin and revised mistakes in the original figure panel:

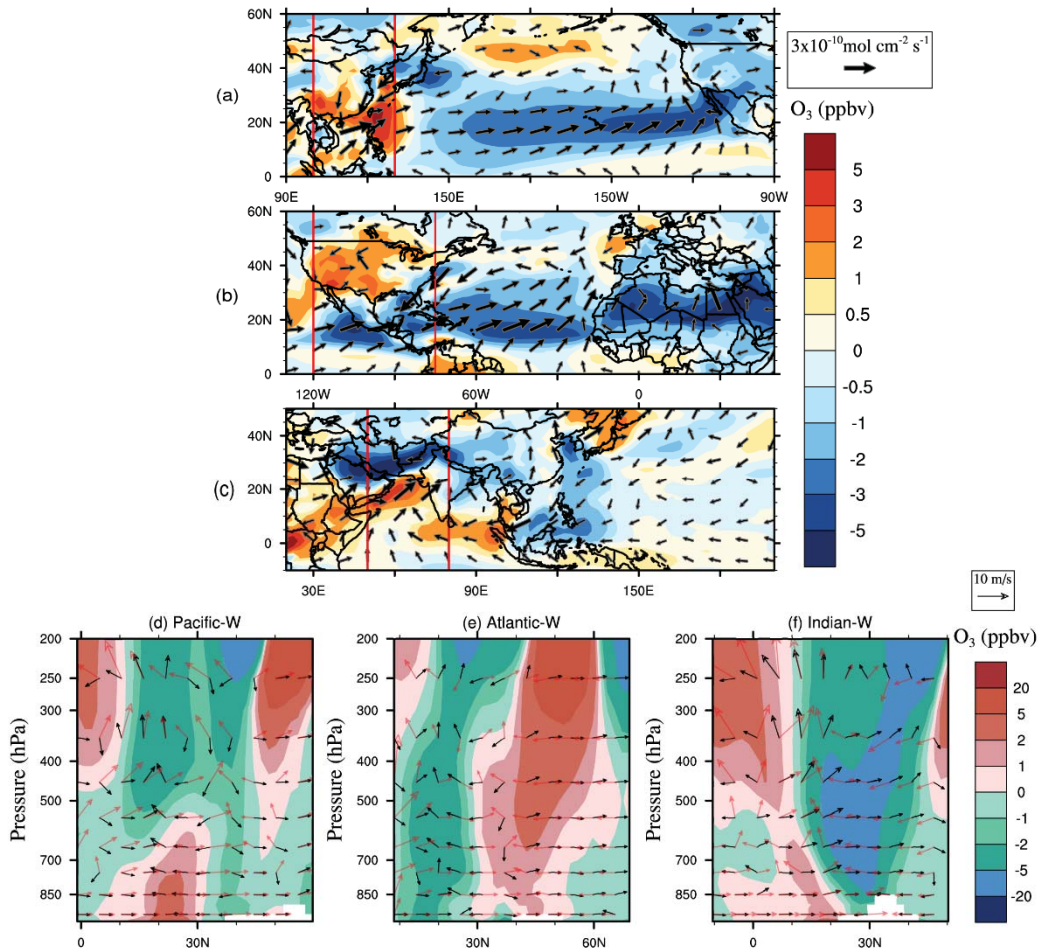


Figure 7. Top three rows: Changes in O₃ concentrations (color contours, ppbv) and horizontal fluxes (arrows, mol cm⁻² s⁻¹) at the surface level for (a) Pacific-W, (b) Atlantic-W, (c) Indian-W relative to the CTRL in the boreal summer. Last row: zonal average of the tropospheric O₃ changes (color contours, ppbv), wind fluxes in CTRL (red arrows, m s⁻¹) and the wind flux perturbation (black arrows, m s⁻¹) in (d) Pacific-W, (e) Atlantic-W, (f) Indian-W relative to the CTRL in the boreal summer. The red rectangles in (a), (b) and (c) denote the longitudinal range used for the zonal averages in (d), (e) and (f), respectively. The vertical wind velocity is amplified 1000 times to make it comparable to the horizontal wind velocity.

Figure S3: which season?

This Figure is referring to the boreal summer. We have revised the caption of Figure S16 (i.e., the Figure S3 in old version) and clearly clarified the relevant season.

“Figure S16. Vertical-meridional distributions of changes in the air temperature (contours, °C) for (a) Pacific_W (zonal averaged from 100°E-90°W), (b) Atlantic_W (zonal averaged from 100°W-180°W) and (c) Indian_W (zonal averaged from 30°E-100°E) relative to the CTRL in boreal summer. Black solid and dashed lines in the contours indicate positive and negative air temperature anomalies, respectively (contour interval: 0.2 °C). The + symbol denotes areas where the changes of air temperature are significant at the 0.05 level, evaluated by Student’s t-test using 20 years of data.”

References:

- Bronnimann, S., Luterbacher, J., Schmutz, C., Wanner, H., and Staehelin, J.: Variability of total ozone at Arosa, Switzerland, since 1931 related to atmospheric circulation indices, *Geophys. Res. Lett.*, 27, 2213–2216, 2000.
- Creilson, J. K., Fishman, J., and Wozniak, A. E.: Intercontinental transport of tropospheric ozone: a study of its seasonal variability across the North Atlantic utilizing tropospheric ozone residuals and its relationship to the North Atlantic Oscillation, *Atmos. Chem. Phys.*, 3, 2053–2066, doi:10.5194/acp-3-2053-2003, 2003.
- Fehsenfeld, F. C., Daum, P., Leitch, W. R., Trainer, M., Parrish, D. D., and Hubler, G.: Transport and processing of O₃ and O₃ precursors over the North Atlantic: An overview of the 1993 North Atlantic Regional Experiment (NARE) summer intensive, *J. Geophys. Res.-Atmos.*, 101, 28877–28891, 1996.
- Hess, P. and Mahowald, N.: Interannual variability in hindcasts of atmospheric chemistry: the role of meteorology, *Atmos. Chem. Phys.*, 9, 5261–5280, doi:10.5194/acp-9-5261-2009, 2009.
- Lamarque, J. F. and Hess, P. G.: Arctic Oscillation modulation of the Northern Hemisphere spring tropospheric ozone, *Geophys. Res. Lett.*, 31, 2246–2269, 2004.
- Parrish, D. D., Ryerson, T. B., Holloway, J. S., Frost, G. J., and Fehsenfeld, F. C.: Export of North American ozone pollution to the North Atlantic Ocean, *Science*, 259, 1436–1439, 1993.
- Pausata, F. S. R., L. Pozzoli, E. Vignati, and F. J. Dentener (2012), North Atlantic Oscillation and tropospheric ozone variability in Europe: Model analysis and measurements intercomparison, *Atmos. Chem. Phys.*, 12, 6357–6376.
- Simmonds, P. G., Derwent, R. G., Manning, A. L., and Spain, G.: Significant growth in surface ozone at Mace Head, Ireland, 1987–2003, *Atmos. Environ.*, 38, 4769–4778, 2004.
- Wild, O. and Akimoto, H.: Intercontinental transport of ozone and its precursors in a three-dimensional global CTM, *J. Geophys. Res.-Atmos.*, 106, 27729–27744, 2001.
- Molnar, Peter, William R. Boos, and David S. Battisti. "Orographic controls on climate and

- paleoclimate of Asia: thermal and mechanical roles for the Tibetan Plateau." *Annual Review of Earth and Planetary Sciences* 38.1 (2010): 77.
- Auvray, M., and Bey, I.: Long - range transport to Europe: Seasonal variations and implications for the European ozone budget, *Journal of Geophysical Research: Atmospheres* (1984–2012), 110, 2005.
- Barnes, E. A., and Fiore, A. M.: Surface ozone variability and the jet position: Implications for projecting future air quality, *Geophys Res Lett*, 40, 2839-2844, 2013.
- Bronnimann, S., Luterbacher, J., Schmutz, C., Wanner, H., and Staehelin, J.: Variability of total ozone at Arosa, Switzerland, since 1931 related to atmospheric circulation indices, *Geophys Res Lett*, 27, 2213-2216, 2000.
- Chaudhari, H. S., Pokhrel, S., Kulkarni, A., Hazra, A., and Saha, S. K.: Clouds–SST relationship and interannual variability modes of Indian summer monsoon in the context of clouds and SSTs: observational and modelling aspects, *Int J Climatol*, 36, 4723-4740, 2016.
- Christoudias, T., Pozzer, A., and Lelieveld, J.: Influence of the North Atlantic Oscillation on air pollution transport, *Atmos Chem Phys*, 12, 869-877, 2012.
- Creilson, J., Fishman, J., and Wozniak, A.: Intercontinental transport of tropospheric ozone: a study of its seasonal variability across the North Atlantic utilizing tropospheric ozone residuals and its relationship to the North Atlantic Oscillation, *Atmos Chem Phys*, 3, 2053-2066, 2003.
- Deser, C., Alexander, M. A., Xie, S.-P., and Phillips, A. S.: Sea surface temperature variability: Patterns and mechanisms, *Annual Review of Marine Science*, 2, 115-143, 2010.
- Doherty, R. M., Wild, O., Shindell, D. T., Zeng, G., MacKenzie, I. A., Collins, W. J., Fiore, A. M., Stevenson, D. S., Dentener, F. J., Schultz, M. G., Hess, P., Derwent, R. G., and Keating, T. J.: Impacts of climate change on surface ozone and intercontinental ozone pollution: A multi-model study, *J Geophys Res-Atmos*, 118, 3744-3763, 10.1002/jgrd.50266, 2013.
- Frankignoul, C.: Sea surface temperature anomalies, planetary waves, and air - sea feedback in the middle latitudes, *Reviews of geophysics*, 23, 357-390, 1985.
- Hartmann, D. L.: Pacific sea surface temperature and the winter of 2014, *Geophys Res Lett*, 42, 1894-1902, 2015.
- Hess, P., and Mahowald, N.: Interannual variability in hindcasts of atmospheric chemistry: the role of meteorology, *Atmos. Chem. Phys*, 9, 5261-5280, 2009.
- Jacob, D.: *Introduction to atmospheric chemistry*, Princeton University Press, 1999.
- Jacob, D. J., and Winner, D. A.: Effect of climate change on air quality, *Atmos Environ*, 43, 51-63, 2009.
- Knowland, K., Doherty, R., and Hodges, K. I.: The effects of springtime mid-latitude storms on trace gas composition determined from the MACC reanalysis, *Atmos Chem Phys*, 15, 3605-3628, 2015.
- Lamarque, J. F., and Hess, P. G.: Arctic Oscillation modulation of the Northern Hemisphere spring tropospheric ozone, *Geophys Res Lett*, 31, 2004.
- Lau, K., Wu, H., and Bony, S.: The role of large-scale atmospheric circulation in the relationship

- between tropical convection and sea surface temperature, *J Climate*, 10, 381-392, 1997.
- Lau, N.-C., and Nath, M. J.: A modeling study of the relative roles of tropical and extratropical SST anomalies in the variability of the global atmosphere-ocean system, *J Climate*, 7, 1184-1207, 1994.
- Li, L., Chen, C., Huang, C., Huang, H., Zhang, G., Wang, Y., Wang, H., Lou, S., Qiao, L., and Zhou, M.: Process analysis of regional ozone formation over the Yangtze River Delta, China using the Community Multi-scale Air Quality modeling system, *Atmos Chem Phys*, 12, 10971-10987, 2012.
- Lin, M., Fiore, A. M., Horowitz, L. W., Langford, A. O., Oltmans, S. J., Tarasick, D., and Rieder, H. E.: Climate variability modulates western US ozone air quality in spring via deep stratospheric intrusions, *Nat Commun*, 6, 2015.
- Pausata, F. S., Pozzoli, L., Vignati, E., and Dentener, F. J.: North Atlantic Oscillation and tropospheric ozone variability in Europe: model analysis and measurements intercomparison, *Atmos Chem Phys*, 12, 6357-6376, 2012.
- Roxy, M. K., Ritika, K., Terray, P., Murtugudde, R., Ashok, K., and Goswami, B.: Drying of Indian subcontinent by rapid Indian Ocean warming and a weakening land-sea thermal gradient, *Nat Commun*, 6, 2015.
- Sabeerali, C., Rao, S. A., Ajayamohan, R., and Murtugudde, R.: On the relationship between Indian summer monsoon withdrawal and Indo-Pacific SST anomalies before and after 1976/1977 climate shift, *Clim Dynam*, 39, 841-859, 2012.
- Tao, W., Liu, J., Ban-Weiss, G., Hauglustaine, D., Zhang, L., Zhang, Q., Cheng, Y., Yu, Y., and Tao, S.: Effects of urban land expansion on the regional meteorology and air quality of eastern China, *Atmos Chem Phys*, 15, 8597-8614, 2015.
- Wu, S., Mickley, L. J., Leibensperger, E. M., Jacob, D. J., Rind, D., and Streets, D. G.: Effects of 2000–2050 global change on ozone air quality in the United States, *Journal of Geophysical Research: Atmospheres*, 113, 2008.
- Xi, J., Zhou, L., Murtugudde, R., and Jiang, L.: Impacts of intraseasonal sst anomalies on precipitation during Indian summer monsoon, *J Climate*, 28, 4561-4575, 2015.
- Zhang, Y., and Wu, S.-Y.: Understanding of the Fate of Atmospheric Pollutants Using a Process Analysis Tool in a 3-D Regional Air Quality Model at a Fine Grid Scale, *Atmospheric and Climate Sciences*, 3, 18, 2013.

Response to Anonymous Referee #2

(Note: Reviewer comments are listed in grey, and responses to reviewer comments are in black. Pasted text from the new version of the paper is in italics.)

This paper presents a very detailed description of changes in ozone due to basin wide changes in SST. Changes can be up to 5 ppbv. The authors have provided great detail for the mechanisms behind the changes. The previous reviewers have commented on many aspects of this paper. Here I will restrict my comments to the overall methodology.

In short, for reasons explained in more detail below I am having difficulty interpreting the paper's results. The authors need to justify their methodology in detail, expand on some of the sensitivities of the solution to the methodology chosen and possibly run some additional simulations to put the results in context.

The authors set rectangular patches of ocean temperature warmer (or colder) by 1 degree within very large ocean-basin domains. The reasons for this setup are not well explained. How did they choose the size of the patch? How did they choose the southern and northern boundaries? The various patches are not similar in latitude or longitude nor do they apparently align with the edge of the ocean basins. We know the resulting circulation changes are sensitive to where the SST is perturbed. In particular there are large differences between the impact of SST perturbations in mid-latitudes and those in the tropics. Teleconnections stemming from tropical ocean SST perturbations can have long-range impacts depending very much on the location of the perturbation. Changes in ocean temperature gradients are also likely to be important for the transport. We note that the simulations in this paper rather dramatically modify the ocean temperature gradients along all boundaries of the perturbation. While the authors smooth out the gradients I am not sure of the resulting impact. I would like to understand the impact of the details of their methodology on the solutions. As it stands I don't really see a strong justification to how they perturbed the ocean temperatures.

I am also having a difficult time interpreting the results. If the authors are interested in understanding the importance of SST perturbations on present day transport it would make sense to perturb the SST using realistic SST variability – perhaps an EOF analysis would be helpful here. This is because the result is sensitive to how the SST is perturbed. If the authors are interested in the importance of climate change it is also difficult to interpret the results. Perturbing the SST in one ocean basin is likely to alter the land-sea pressure gradients and transport in a different way than changes under

CO₂ influenced climate change. It may be possible to parse the impact of transport changes from climate change in terms of the perturbation simulations carried out by the authors but they have not done this.

So, I'm not sure what I ultimately have learned from the paper. The authors do a great job in providing details of transport changes due to SST modification: changes in stability, in clouds, in overall transport and other processes are important. It is not surprising that whole-scale changes in SST modify the transport and ozone chemistry. However, it is unclear to what extent these details are an artifact of their simulation setup and how they apply to the real world (either to interannual variations in SST or to climate induced variations). Specific details of the solution are likely to depend on how the SST has been changed. Thus I'm left with a very detailed analysis but I'm not sure what I have really learned.

We appreciate the reviewer's thoughtful comments. In this study, we mainly focus on exploring the sensitivity of surface O₃ distributions to SST anomalies in different ocean basins and investigating the mechanisms that govern this SST-O₃ relationship. Therefore, we used the Community Earth System Model (CESM) to investigate the response of surface O₃ concentrations at different continents to the basin-scale warming and cooling of individual Northern Hemispheric oceans. In our model experiments, idealized uniform sea surface temperature (SST) anomalies of +/- 1°C are superimposed onto the North Pacific (15°N-65°N; 100°E-90°W), North Atlantic (15°N-65°N; 100°W-20°E) and North Indian Oceans (5°N-30°N; 30°E-100°E), individually. The rectangular patches of SST changes in different cases can not be consistent in latitudinal and longitudinal ranges due to geographical differences in various ocean basins. We defined the latitudinal and longitudinal ranges of these oceans basin mainly based on their geographical features. The boundaries of prescribed SST anomalies generally align with the edge of the ocean basins that constrained by the continental line except for the southern side. The southern boundary of each ocean is relatively difficult to define since there is no apparent geographical boundary in the south. To constrain our prescribed SST anomalies in the Northern Hemisphere, we defined a southern boundary of 15°N for the North Pacific and North Atlantic oceans to be consistent. As for the North Indian Ocean, which is mainly located in the tropical regions, a lower southern boundary (i.e., 5°N) is chosen. If using 15°N as the southern boundary, the size of North Indian Ocean is too small. In each perturbation simulation, we further linearly smoothed the southern boundaries of these SST anomalies toward the equator to remove the sharp SST anomaly gradients at the edge.

To examine the sensitivity of the solution to the methodology we chosen to perturb the SST, we conducted an additional simulation based on the North Pacific warming case, in which no smoothness toward the equator is used, denoted as “Nosmooth”. The corresponding changes of summertime surface O_3 in both perturbation simulations (i.e., with and without smoothing) are depicted in Figure R1. It shows that the responses of surface O_3 to these SST perturbations are broadly consistent in spatial patterns, though small differences do exist at specific places. According to previous studies (e.g., Lau et al., 1997; Li et al., 2015; Zhou et al., 2017 and references therein), the atmospheric response to SST changes over the tropical oceans are mainly locally driven and thermally direct owing to deep convection. There is no doubt that if we extend the southern boundary southward to the equatorial line, the atmospheric responses would be much larger, especially over the tropics. Since this study focuses more on qualitative understanding how the mid-latitude air quality is affected by the fluctuation of basin-scale SST changes in individual Northern Hemisphere oceans, the idealized SST anomaly employed here is a relatively straightforward way. In addition, smoothing out the gradient of prescribed SST anomalies is widely used in previous studies (e.g., Hu and Veres, 2016; Seager and Henderson, 2016; Sutton and Hodson, 2007; Taschetto et al., 2016).

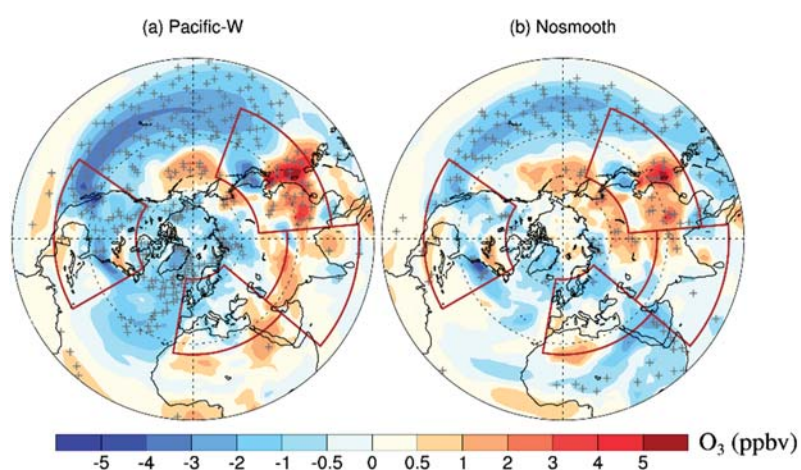


Figure R1. Changes in the summertime (June-August) surface ozone concentrations (ppbv) in the Northern Hemisphere for (a) Pacific-W and (b) Nosmooth relative to the CTRL. The four major regions of interest (i.e., NA (15°N–55 °N; 60°W–125°W), EU (25°N–65 °N; 10°W–50 °E), EA (15 °N–50 °N; 95°E–160 °E) and SA (5 °N–35 °N; 50 °E–95°E)) are marked with red solid polygons. The + symbols denote areas where the results are significant at the 0.05 level, evaluated by Student’s t-test using 20 years of data.

As we have mentioned in our Introduction section, the realistic SST is undergoing a variety of changes in different spatial and temporal scales. The relevant anomalies picked up from observation dataset are closely depended on the timescale we choose. SST anomalies over different oceans are often inter-correlated and difficult to separate from each other. The pattern of SST anomaly decomposed statistically (e.g., EOF analysis) is also largely depended on the duration of observation used. What's more, the prediction of future SST variability also remains great uncertainty. Hence, it is very difficult to define a representative SST anomaly pattern for each ocean basin. Since we are mainly interested in investigating the sensitivity of surface O₃ distributions to the SST changes in different ocean basins and the mechanisms governing the SST-O₃ relationships, this idealized SST anomaly setup are sufficient to address our questions. In previous studies, idealized, uniform SST anomalies have been widely used to explore the ocean-atmosphere relationships in the climate systems (e.g., Taschetto et al., 2016, Fan et al., 2016, Hu and Veres, 2016, Kushnir et al., 2002 and so on), which could simplify the interpretation and are easier for theoretical analysis.

In our revised manuscript, we further conducted two sensitivity tests with 1°C SST warming and cooling superimposed onto all three ocean basins (i.e., the North Pacific, North Atlantic and North Indian Ocean), denoted as All-W and All-C, respectively. Their effects on surface O₃ distributions are found to be comparable to the sum of the effects from individual oceans during boreal summers (see Figure S5 or S6 below) and winters (see Figure S7 or S8 below). This indicates that the SST forcing on O₃ distribution is geographically additive. Local environmental policymakers may pay more attention to the SST variability over specific oceans. A lot of studies have used decomposed SST anomalies for different regions to identify their relevant roles in a particular climate response (Camargo et al., 2013; Sutton and Hodson, 2005; Ueda et al., 2015). A linear assumption that the influence of large SST anomaly pattern on the atmosphere can be generally constructed by the linear combination of the influences of individual SST patches have been verified by previous studies, especially for the tropical regions where the signal-to-noise is higher (Fan et al., 2016; Seager and Henderson, 2016).

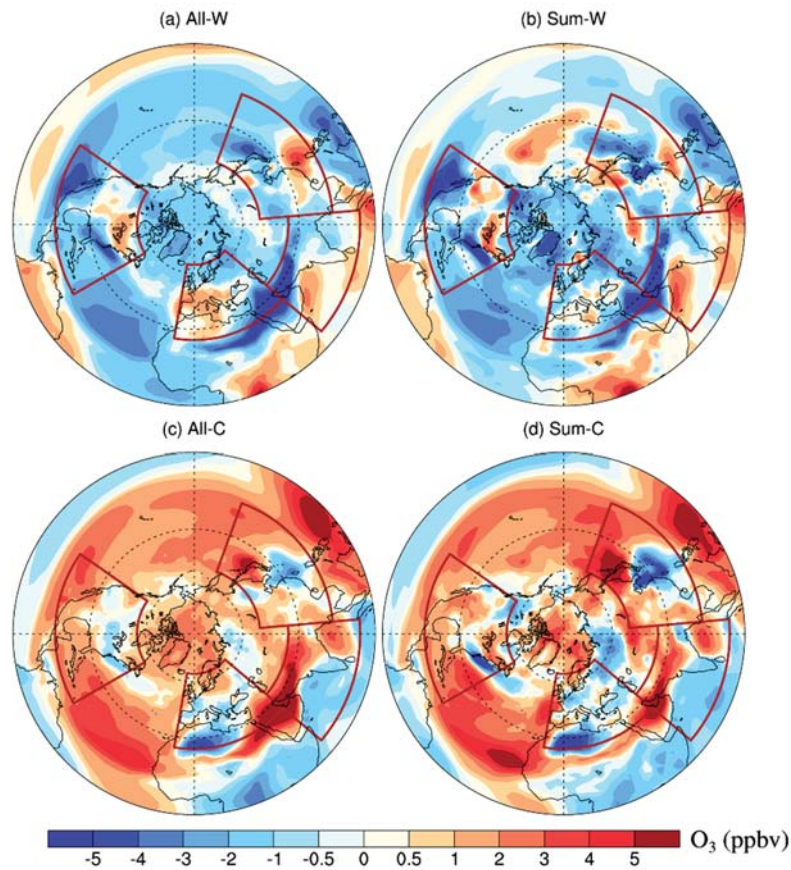


Figure S5. Left column: Changes in the summertime (June-August) surface O₃ concentrations (ppbv) in the Northern Hemisphere induced by 1°C warming (a) and 1°C cooling (b) in all three ocean basins (i.e., the North Pacific, North Atlantic and North Indian Ocean) relative to the CTRL. Right column: Sum of changes in the summertime (June-August) surface O₃ concentrations (ppbv) from the three warming cases (i.e., Pacific-W, Atlantic-W and Indian-W) and three cooling cases (i.e., Pacific-C, Atlantic-C and Indian-C) relative to the CTRL, denoted as (b) Sum-W and (d) Sum-C, respectively. The four major regions of interest (i.e., NA, EU, EA and SA) are marked with polygons.

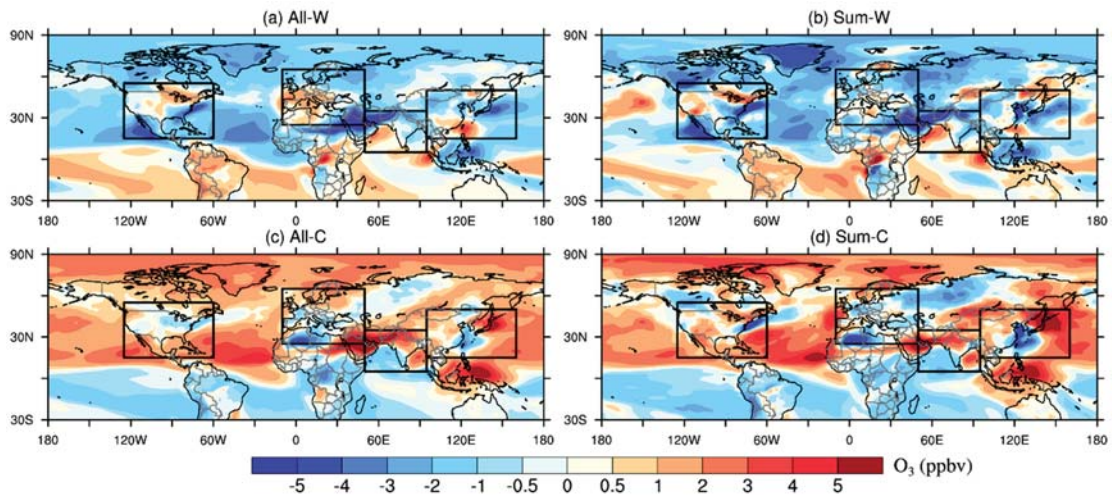


Figure S6. As in Figure S5 but using the Mercator projection.

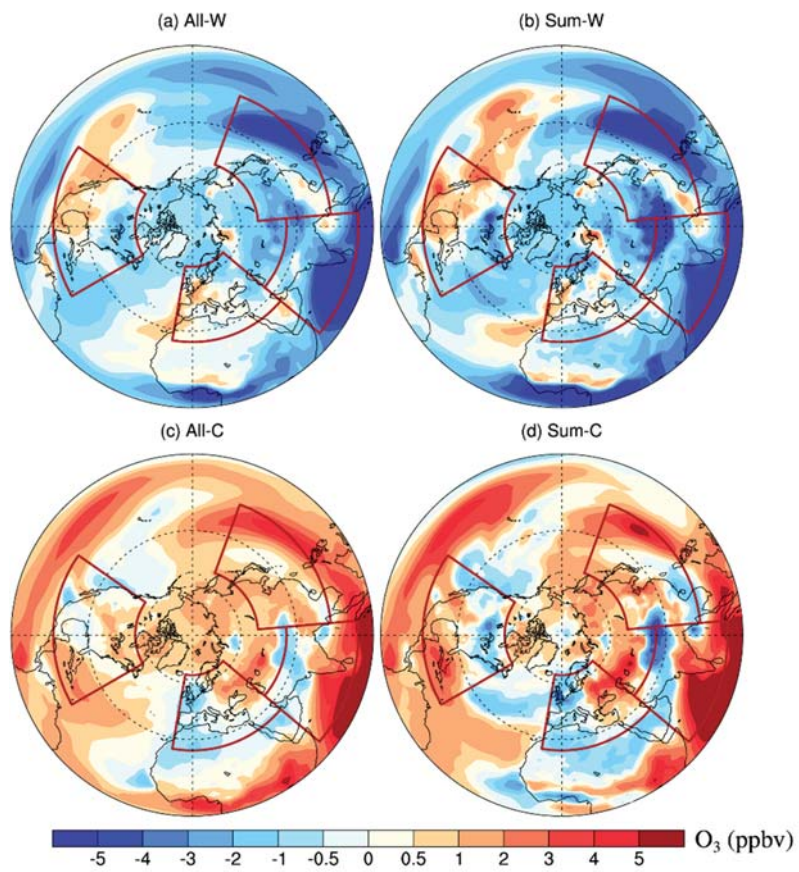


Figure S7. Same as Figure S5 but for the wintertime (December-February).

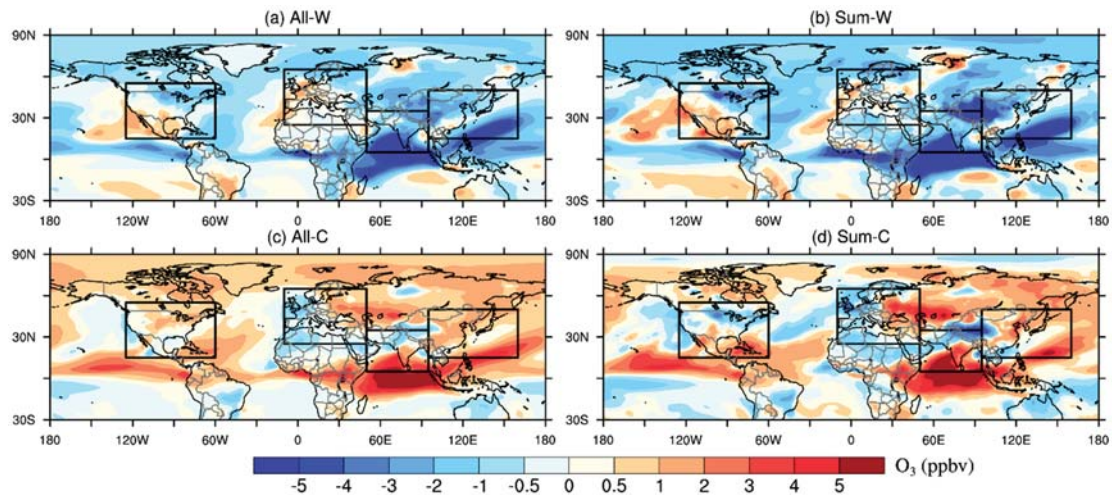


Figure S8. As in Figure S7 but using the Mercator projection.

Even through the response of atmosphere to SST changes in different scales have been extensively studied in the last several decades, their corresponding effects on air quality are rarely investigated directly. There are many important questions need to be addressed to provide a comprehensive understanding of the SST-O₃ relationship. In this study, we explored the responses of surface O₃ to idealized SST changes imposed in different ocean basins. The ultimate objective of this study is to differentiate roles of each Northern Hemispheric ocean played on the surface O₃ evolution over these highly populated regions (e.g., NA, EU, EA and IN). We provided a detailed analysis about the mechanisms modulating the SST-O₃ relationships at the process level. An opposite response pattern is observed between the upwind and downwind regions of an ocean. This though can not exactly match the real world conditions, but can provides useful implications for environmental management. Since the basin-scale warming or cooling has been frequently observed in different oceans, conducting idealized model experiments can capture the large-scale features of the observed anomaly patterns while ignores the local noisy variability. On the other hand, given the near-linear relationships existed in the ocean-atmosphere interactions, our analysis also illustrates the spatial extent of different oceans that modulate the surface O₃ in a changing climate system. In the revised manuscript, we have clarified our objectives as well as the ways how we perturb the SST in different oceans.

In the Introduction section (*P5, L135-138 and L140-144*):

“...Except for the ENSO impacts, very few studies to date have directly addressed the linkage between SST and O₃. Therefore, a comprehensive understanding of the response of surface O₃ to SST changes in individual ocean basins is lacking and necessary.

To fill this gap, this study focuses on examining the sensitivity of O₃ evolution over four polluted continental regions in the Northern Hemisphere (i.e., North America (NA, 15°N–55°N; 60°W–125°W), Europe (EU, 25°N–65°N; 10°W–50°E), East Asia (EA, 15°N–50°N; 95°E–160°E) and South Asia (SA, 5°N–35°N; 50°E–95°E), defined in Fiore et al. (2009)) with respect to nearby basin-scale SST changes.”

In Section 2.2 (P7, L192-206), we have:

“We first conduct a control simulation, hereafter referred to as CTRL, with prescribed climatological SSTs averaged from 1981 to 2010 (see Hurrell et al. (2008)). We then conduct six perturbation simulations with monthly SSTs that are uniformly increased or decreased by 1°C in three ocean basins in the Northern Hemisphere: the North Pacific (15°N–65°N; 100°E–90°W), North Atlantic (15°N–65°N; 100°W–20°E) and North Indian Oceans (5°N–30°N, 30°E–100°E; here 5°N is used to attain a relatively larger domain size). The simulations are denoted as “Pacific-W”, “Atlantic-W” and “Indian-W” for the three warming cases and “Pacific-C”, “Atlantic-C” and “Indian-C” for the three cooling cases. We defined the latitudinal and longitudinal ranges of these ocean basins mainly based on their geographical features. The boundaries of the prescribed SST anomalies generally align with the edge of the ocean basins, except along the southern side. In each perturbation simulation, we further linearly smooth the southern boundaries of these SST anomalies towards the equator to remove the sharp SST anomaly gradients at the edge, following a previous approach (e.g., Taschetto et al., 2016; Seager and Henderson, 2016).”

In Section 3 (P10, L282-291):

“Our simulations reveal that different oceans can exert distinct region-specific effects on the O₃ distribution. We further conduct two sensitivity tests with 1 °C SST warming and 1 °C SST cooling superimposed onto all three ocean basins (i.e., the North Pacific, North Atlantic and North Indian Ocean) in the Northern Hemisphere, denoted as “All-W” and “All-C”, respectively. The effects of these combined warming and cooling cases on surface O₃ distributions are respectively compared with the sum of the three individual warming cases (i.e., Pacific-W, Atlantic-W and Indian-W) and three individual cooling cases (i.e., Pacific-C, Atlantic-C and Indian-C). The responses of surface O₃ to a hemispheric SST anomaly generally resemble the sum of responses to different regional SST changes (see Figures S5 and S7 in the supplementary material).”

In the Summary section (P20, L569-574), we have:

“Overall, our study highlights the sensitivity of O₃ evolution to basin-wide SST changes in the Northern Hemisphere and identifies the key chemical or dynamical factors that control this evolution. However, to provide a more comprehensive understanding of the SST-O₃ relationship, further studies using realistic SST variability are necessary. This study may aid in the management of O₃ pollution by considering the influence of specific SST variability.”

References:

- Camargo, S. J., Ting, M., and Kushnir, Y.: Influence of local and remote SST on North Atlantic tropical cyclone potential intensity, *Clim Dynam*, 40, 1515-1529, 2013.
- Fan, L., Shin, S.-I., Liu, Z., and Liu, Q.: Sensitivity of Asian Summer Monsoon precipitation to tropical sea surface temperature anomalies, *Clim Dynam*, 47, 2501-2514, 2016.
- Fiore, A., Dentener, F., Wild, O., Cuvelier, C., Schultz, M., Hess, P., Textor, C., Schulz, M., Doherty, R., and Horowitz, L.: Multimodel estimates of intercontinental source - receptor relationships for ozone pollution, *Journal of Geophysical Research: Atmospheres* (1984–2012), 114, 2009.
- Hu, Q., and Veres, M. C.: Atmospheric responses to North Atlantic SST anomalies in idealized experiments. Part II: North American precipitation, *J Climate*, 29, 659-671, 2016.
- Hurrell, J. W., Hack, J. J., Shea, D., Caron, J. M., and Rosinski, J.: A new sea surface temperature and sea ice boundary dataset for the Community Atmosphere Model, *J Climate*, 21, 5145-5153, 2008.
- Kushnir, Y., Robinson, W., Bladé, I., Hall, N., Peng, S., and Sutton, R.: Atmospheric GCM response to extratropical SST anomalies: Synthesis and evaluation, *J Climate*, 15, 2233-2256, 2002.
- Lau, K., Wu, H., and Bony, S.: The role of large-scale atmospheric circulation in the relationship between tropical convection and sea surface temperature, *J Climate*, 10, 381-392, 1997.
- Li, X., Xie, S.-P., Gille, S. T., and Yoo, C.: Atlantic-induced pan-tropical climate change over the past three decades, *Nat Clim Change*, 2015.
- Seager, R., and Henderson, N.: On the Role of Tropical Ocean Forcing of the Persistent North American West Coast Ridge of Winter 2013/14 a, *J Climate*, 29, 8027-8049, 2016.
- Sutton, R. T., and Hodson, D. L.: Atlantic Ocean forcing of North American and European summer climate, *science*, 309, 115-118, 2005.
- Sutton, R. T., and Hodson, D. L.: Climate response to basin-scale warming and cooling of the North Atlantic Ocean, *J Climate*, 20, 891-907, 2007.
- Taschetto, A., Rodrigues, R., Meehl, G., McGregor, S., and England, M.: How sensitive are the Pacific–tropical North Atlantic teleconnections to the position and intensity of El Niño-related warming?, *Clim Dynam*, 46, 1841-1860, 2016.
- Ueda, H., Kamae, Y., Hayasaki, M., Kitoh, A., Watanabe, S., Miki, Y., and Kumai, A.: Combined effects of recent Pacific cooling and Indian Ocean warming on the Asian monsoon, *Nat Commun*, 6, 2015.
- Zhou, G., Latif, M., Greatbatch, R. J., and Park, W.: State Dependence of Atmospheric Response to Extratropical North Pacific SST Anomalies, *J Climate*, 30, 509-525, 2017.

Response to Anonymous Referee #3

(Note: Reviewer comments are listed in grey, and responses to reviewer comments are in black. Pasted text from the new version of the paper is in italics.)

This is an interesting modelling study that examines how surface ozone is influenced by warmer SSTs over the Pacific, Atlantic and Indian oceans. With a one degree warming across these basins, the changes in seasonal-mean ozone in the oceanic basin and its surrounding continents are rather large at 1-5 ppb. An increase in SST leads to lower surface ozone over the Pacific and Atlantic oceans but a more mixed response over the Indian ocean. The authors probe the contribution of chemistry and transport processes to these ozone changes. The paper is mostly well written but a number conclusions lack clarity and are not well-substantiated for reasons relating to poor and inconsistent figure quality and interpretation as outlined below. Hence the manuscript, needs much improvement before publication.

We greatly appreciate the reviewer for these detailed and valuable comments. In our revised manuscript, we have significantly improved the quality and consistency of the figures. The IPR analysis in this study has been described more clearly and all the relevant text has been clarified. We have also expanded our explanation and discussion by adding more sensitivity tests. By addressing the reviewer's comments, we believe our manuscript has considerably improved. Please see our response to each comment below:

Major comments:

1) (i) As noted by the other reviewer, the map projections used vary by figure in a non- logical fashion, hence it is extremely difficult to compare results across different figures and hence verify the conclusions in the text. For example, the vertical velocity changes in Figure 6 versus the surface pressure pattern changes in Figure 5 versus the changes in ozone concentrations in Figure 7 (See specific comments also). (ii) In addition, the continental outlines and hence oceanic basins are too difficult to distinguish if they are visible at all. (iii) Finally, most figure panels are too small to be legible- except for Figures S2-S5 which are hugely improved on the other figures (although the continental outlines are still hard to see in Figure S2).

Thanks for pointing out this. In our revised manuscript, we have fixed these problems and consistently used map projection. Specifically, we use Polar projection to show hemispheric scale results (e.g., Figures 1-4) and the Mercator projection to show basin-scale results (e.g., Figures 5-8). To make it more comparable, we also redraw Figures 1-4 using the Mercator projection and put them into the supplementary material (e.g., Figures S2, S14 and S15). Please see some examples of the improved figures below:

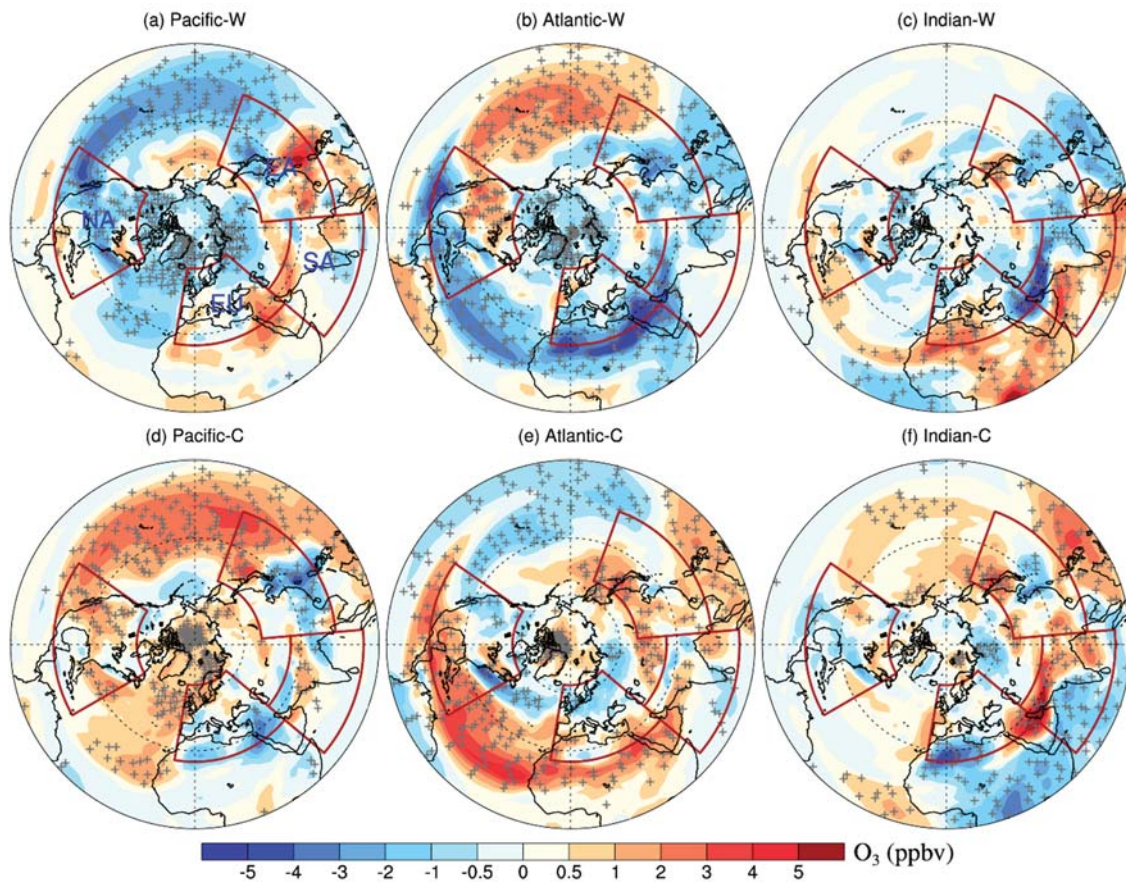


Figure 1. Changes in the summertime (June-August) surface O₃ concentrations (ppbv) in the Northern Hemisphere induced by 1°C warming (top) and 1°C cooling (bottom) in the North Pacific Ocean (left), North Atlantic Ocean (center), and North Indian Ocean (right) relative to the CTRL. The four major regions of interest (i.e., NA (15°N–55 °N; 60°W–125°W), EU (25°N–65 °N; 10°W–50 °E), EA (15 °N–50 °N; 95°E–160 °E) and SA (5 °N–35 °N; 50 °E–95°E)) are marked with red polygons. The + symbols denote areas where results are significant at the 0.05 level, evaluated by Student’s t-test using 20 years of data (plots using the Mercator projection are shown in Figure S2 in the supplementary material).

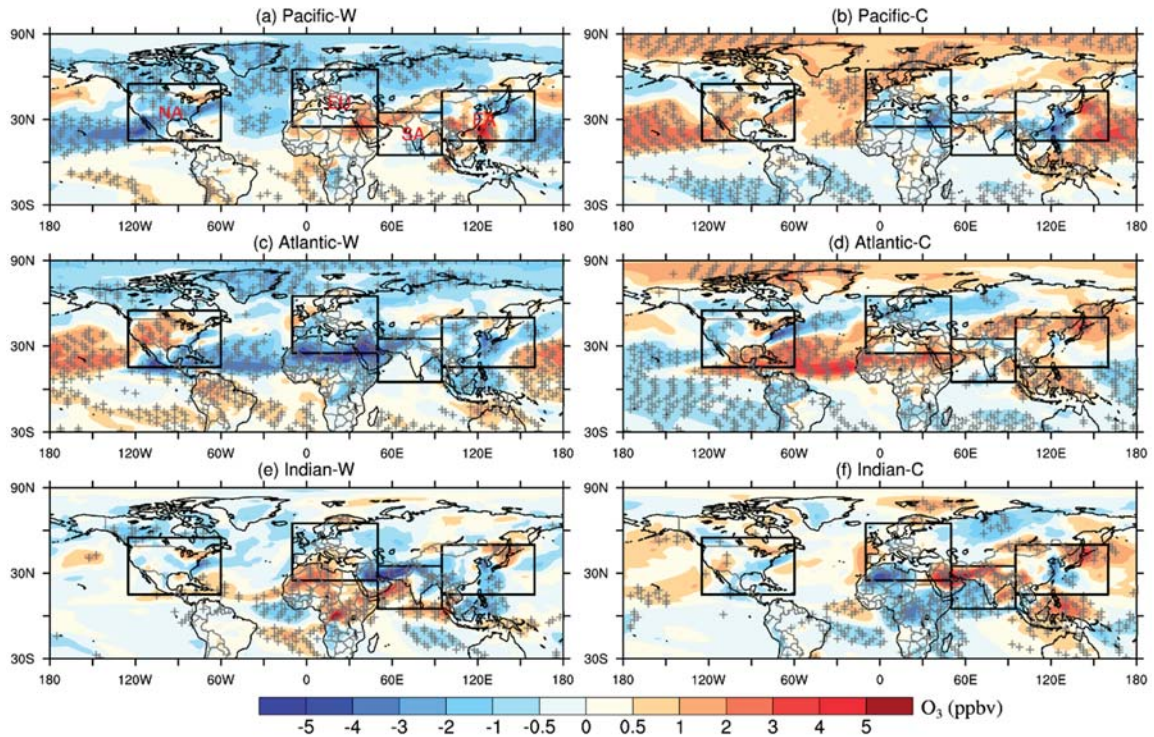


Figure S2. Changes in the summertime (June–August) surface O_3 concentrations (ppbv) in the Northern Hemisphere induced by 1°C warming (top) and 1°C cooling (bottom) in the North Pacific Ocean (left), North Atlantic Ocean (center), and North Indian Ocean (right) relative to the CTRL. The four major regions of interest (i.e., NA (15°N – 55°N ; 60°W – 125°W), EU (25°N – 65°N ; 10°W – 50°E), EA (15°N – 50°N ; 95°E – 160°E) and SA (5°N – 35°N ; 50°E – 95°E)) are marked with polygons. The + symbols denote areas where the results are significant at the 0.05 level, evaluated by Student’s t-test using 20 years of data.

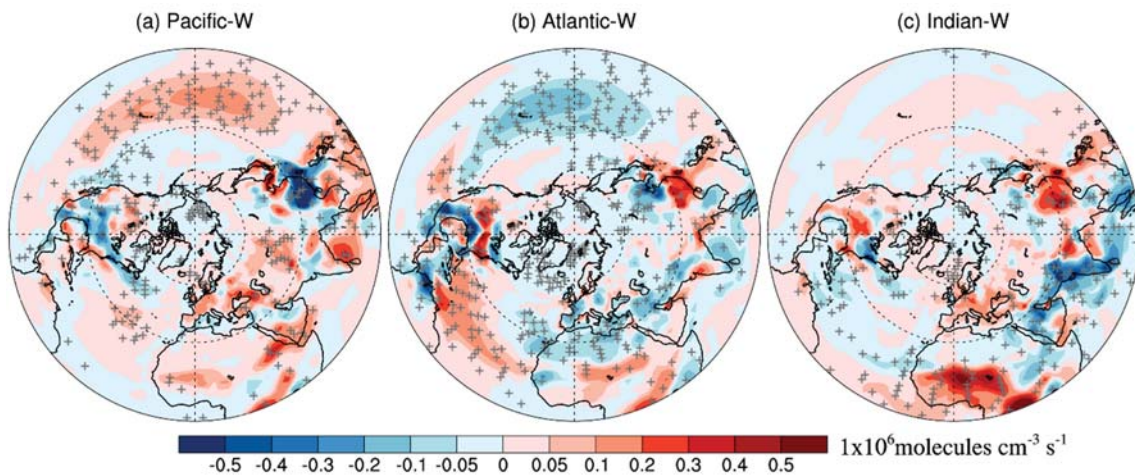


Figure 3. Perturbations of the surface net O_3 production rate ($1 \times 10^6 \text{ molecules cm}^{-3} \text{ s}^{-1}$) for (a) Pacific-W, (b) Atlantic-W, and (c) Indian-W relative to the CTRL in the boreal summer. The +

symbols denote areas where the results are significant at the 0.05 level, evaluated by Student's t-test using 20 years of data (plots using the Mercator projection are shown in Figure S14 in the supplementary material).

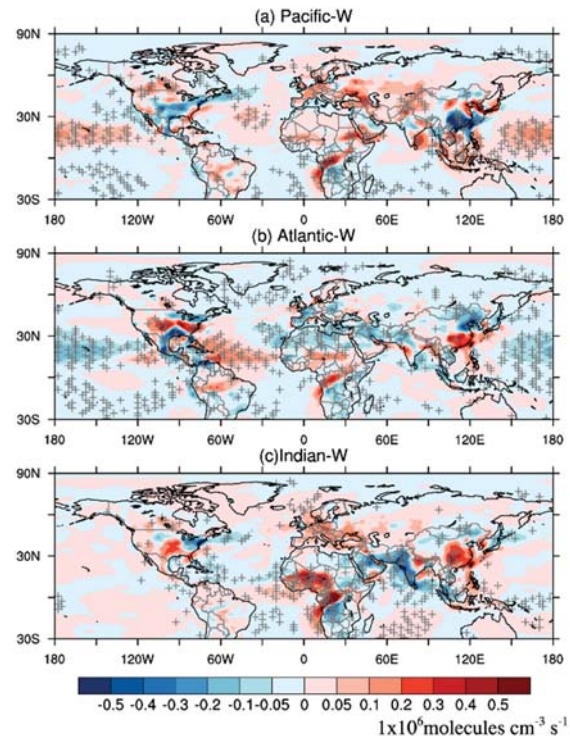


Figure S14. Perturbations of the surface net O₃ production rate (1×10^6 molecules $\text{cm}^{-3} \text{s}^{-1}$) for (a) Pacific-W, (b) Atlantic-W, and (c) Indian-W relative to the CTRL in the boreal summer. The + symbols denote areas where the results are significant at the 0.05 level, evaluated by Student's t-test using 20 years of data.

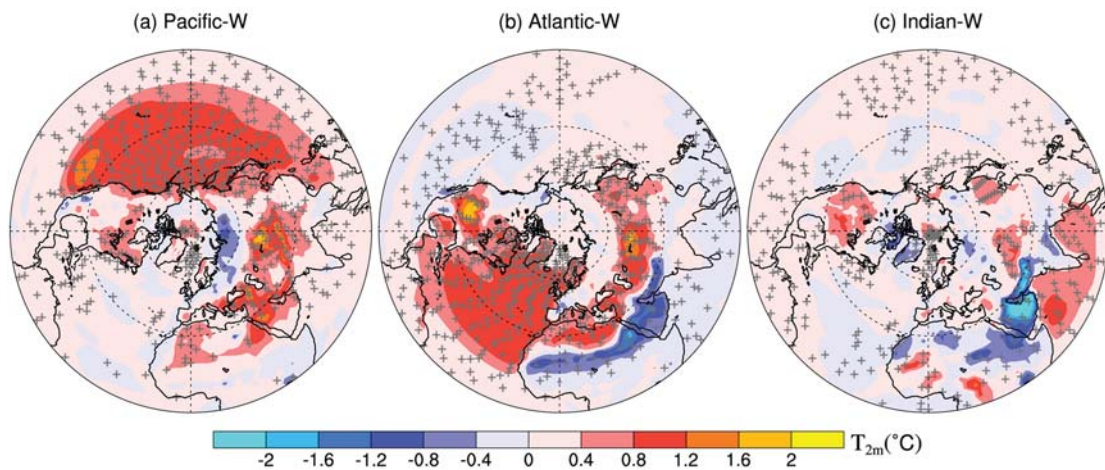


Figure 4. Changes in the surface air temperature ($^{\circ}\text{C}$) for (a) Pacific-W, (b) Atlantic-W, and (c) Indian-W relative to CTRL in the Northern Hemisphere in the boreal summer. The + symbols denote areas where the results are significant at the 0.05 level, evaluated by Student's t-test using 20 years of data (plots using the Mercator projection are shown in Figure S15 in the supplementary material).

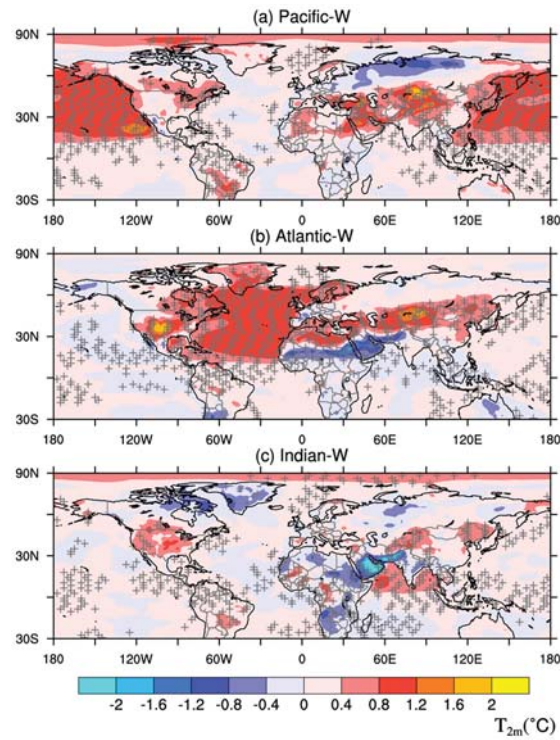


Figure S15. Changes in the surface air temperature ($^{\circ}\text{C}$) for (a) Pacific-W, (b) Atlantic-W, and (c) Indian-W relative to the CTRL in the boreal summer. The + symbols denote areas where the results are significant at the 0.05 level, evaluated by Student's t-test using 20 years of data.

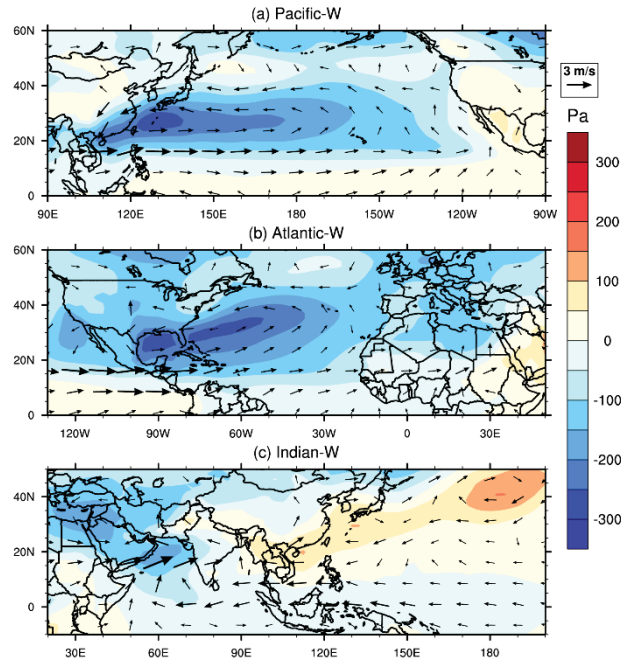


Figure 5. Changes in the surface pressure (color contours, Pa) and 850-hPa wind (arrows, m s^{-1}) for (a) Pacific-W, (b) Atlantic-W, and (c) Indian-W relative to the CTRL in the boreal summer.

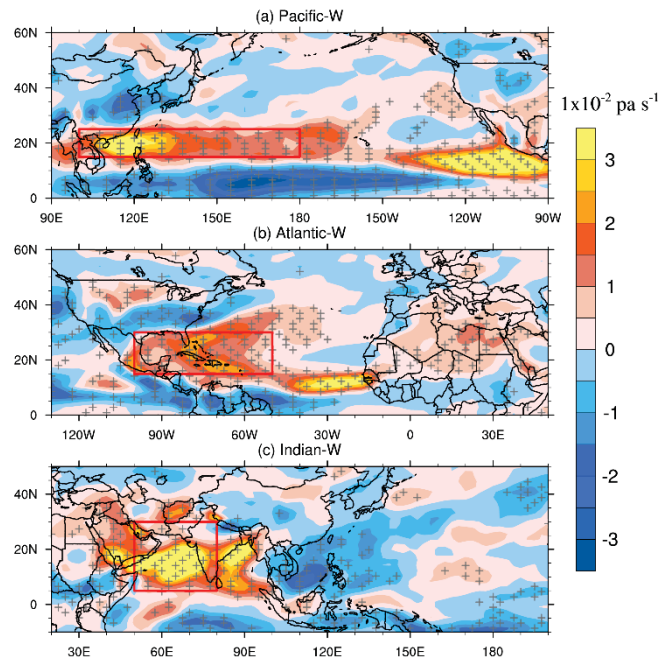


Figure 6. Spatial pattern of vertical velocity changes at 500 hPa (color contours, $1 \times 10^{-2} \text{ Pa s}^{-1}$) for (a) Pacific-W, (b) Atlantic-W, and (c) Indian-W relative to the CTRL in the boreal summer. Positive values indicate upward motion. Red polygons denote the regions where the surface pressure responses to SST anomalies are significant (see Figure 5 a-c). The + symbols indicate areas where the results are significant at the 0.05 level, evaluated by Student's t-test using 20 years of data.

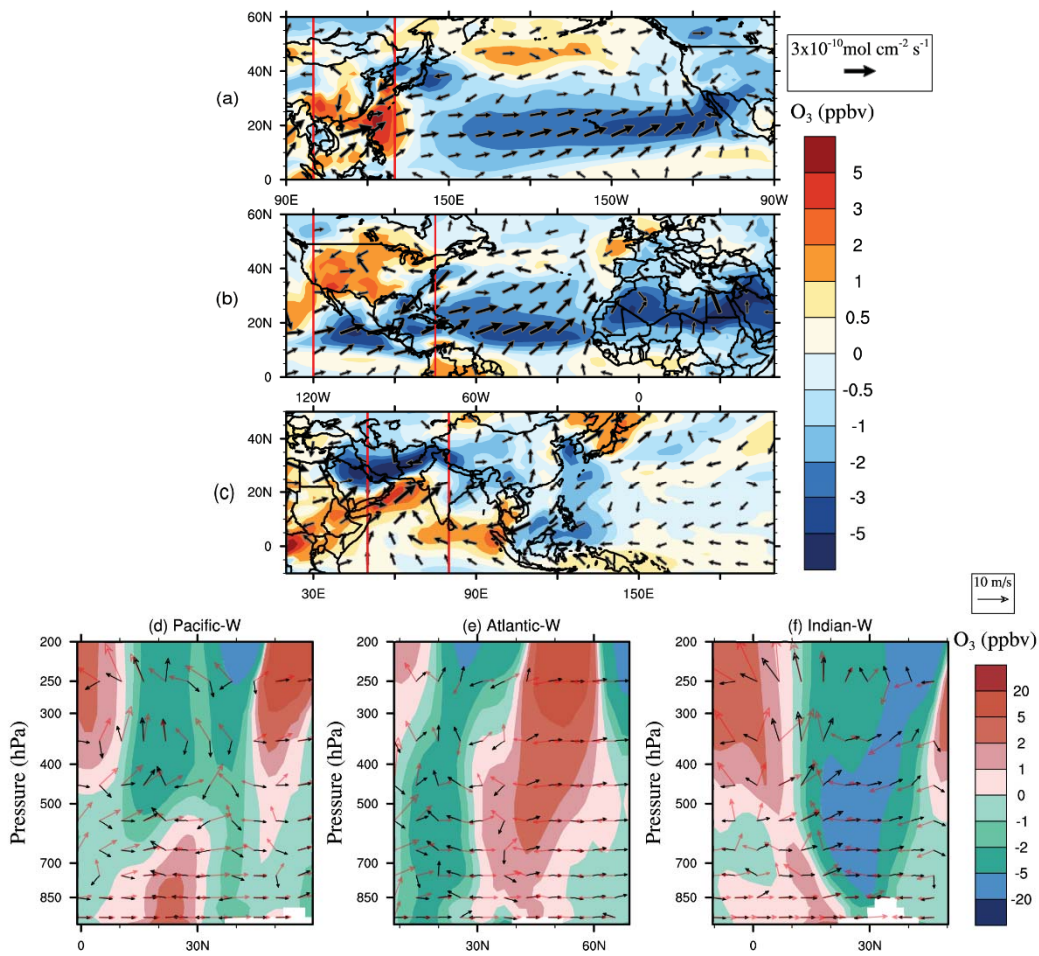


Figure 7. Top three rows: Changes in O_3 concentrations (color contours, ppbv) and horizontal fluxes (arrows, $\text{mol cm}^{-2} \text{s}^{-1}$) at the surface level for (a) Pacific-W, (b) Atlantic-W, (c) Indian-W relative to the CTRL in the boreal summer. Last row: zonal average of the tropospheric O_3 changes (color contours, ppbv), wind fluxes in CTRL (red arrows, m s^{-1}) and the wind flux perturbation (black arrows, m s^{-1}) in (d) Pacific-W, (e) Atlantic-W, (f) Indian-W relative to the CTRL in the boreal summer. The red rectangles in (a), (b) and (c) denote the longitudinal range used for the zonal averages in (d), (e) and (f), respectively. The vertical wind velocity is amplified 1000 times to make it comparable to the horizontal wind velocity.

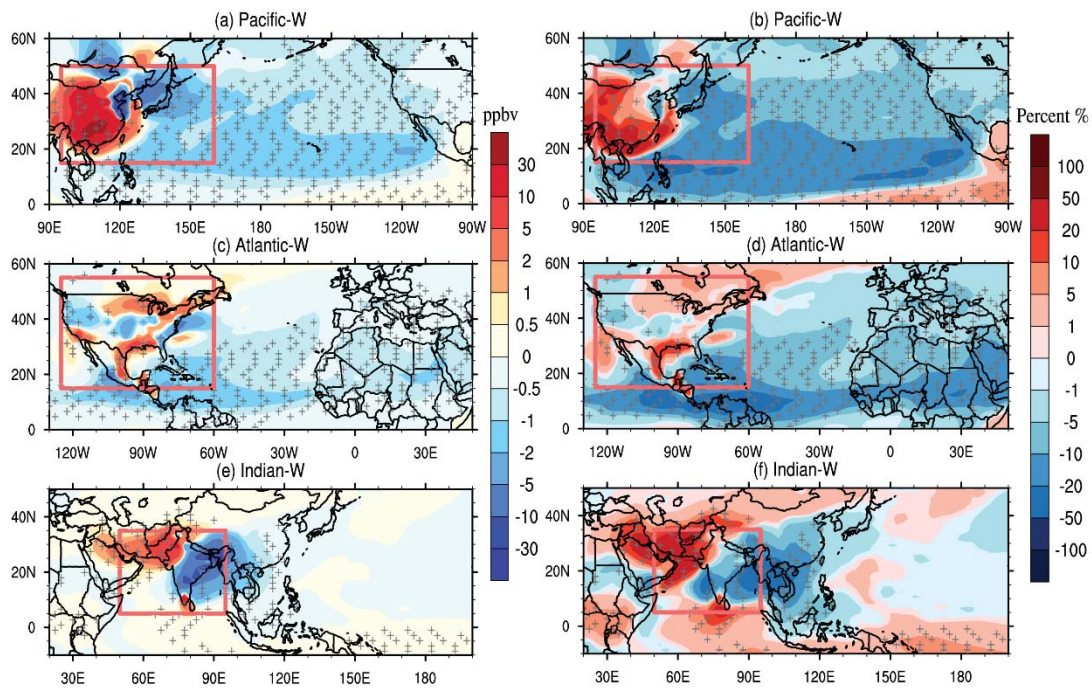


Figure 8. Left-hand panel: Difference in the surface concentration (ppbv) of a CO-like tracer emitted from (a) East Asia for Pacific-W, (c) North America for Atlantic-W and (e) the South Asia for Indian-W relative to the CTRL in the boreal summer. Right-hand panel: The percentage changes in the surface concentration of a CO-like tracer emitted from (b) East Asia for Pacific-W, (d) North America for Atlantic-W and (f) South Asia for Indian-W relative to the CTRL in the boreal summer. Red polygons denote the region where the CO-like tracer is emitted from. The + symbol denotes areas where the results are significant at the 0.05 level, evaluated by Student's t-test using 20 years of data.

The continental outlines in all figures are now thicker and darker than previous ones. Please see Figure 4 above as an example and refer to the revised manuscript for more details.

Some figures have a set of small plots. In the previous version, we uploaded low-quality PDF plots. In this revised version, we have significantly improved the figure quality. Please see Figure 9 below for example:

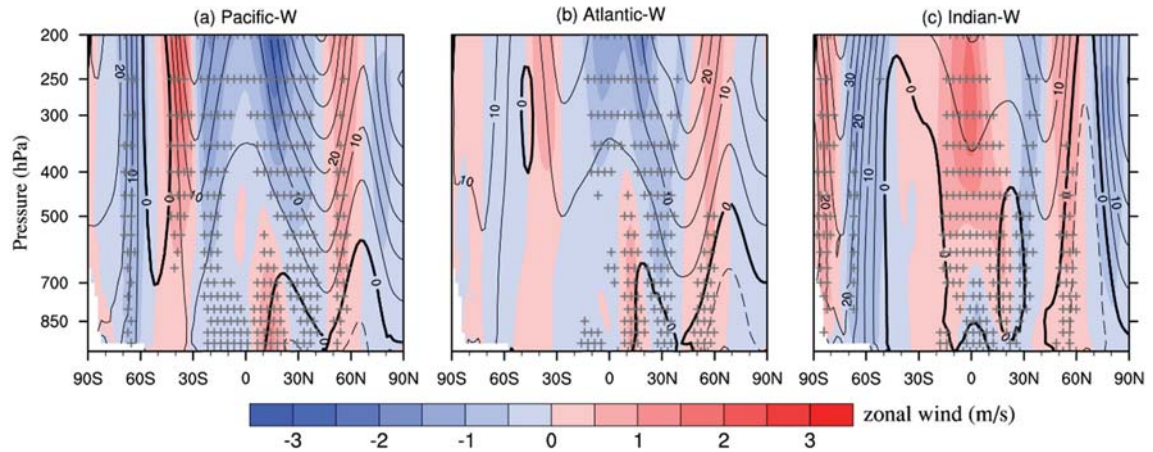


Figure 9. Zonally averaged changes in zonal wind (color contour, m/s) and geopotential height (contour, m) for (a) Pacific-W, (b) Atlantic-W and (c) Indian-W relative to the CTRL in the boreal summer. Black solid and dashed lines in the contours indicate positive and negative geopotential height anomalies, respectively (contour interval: 5 m). The + symbol denotes areas where the zonal wind changes are significant at the 0.05 level, evaluated by Student's t-test using 20 years of data.

2) The seasonal mean surface ozone changes are quite large. This message could be brought out much more clearly. It would be beneficial to see some discussion of the magnitude of these surface ozone responses through comparison with previous papers even if these only relate to the effects of changes in air temperature or climate on surface ozone, as the further impacts of atmospheric circulation changes can be outlined.

Good suggestion. We add some discussion about the magnitude of these surface ozone responses in our revised manuscript, and compare our results with previous works (see P9, L248-260):

“The responses of surface O_3 concentrations to basin-scale SST changes (i.e., ± 1 °C) are mainly within 3 ppbv in the Northern Hemisphere (Table 1 and Table S1), though large anomalies (i.e., up to 5ppbv) are also observed over the east coast of China, the Indian subcontinent, and certain oceanic areas (Figure 1 and Figure S2). This SST- O_3 sensitivity is comparable to previous findings. For instance, Bloomer et al. (2009) reported a positive O_3 -temperature relationship of 2.2~3.2 ppbv/°C across the rural eastern United States. Wu et al. (2008) found that summertime surface O_3 may increase by 2-5 ppbv over the northeastern United States in the 2050s. Additionally, Fiore et al. (2009) demonstrated an intercontinental decrease of surface O_3 by no more than 1 ppbv in response to 20% reductions in anthropogenic emissions within a continental

region. Our study indicates that basin-scale SST change alone may exert significant effects on the surface O₃ above specific ocean basin and its surrounding continents.”

3) (i) The IPR analysis needs to be described more thoroughly and the processes selected would benefit with expanded definitions. In particular, gas-phase chemistry (CHEM) should be defined more clearly as later in the manuscript various other terms are used: net chemical production (Figure 3); photochemistry (line 265). Also vertical diffusion (VDIF) and dry deposition (DRYD) are combined into one term TURB- but these terms act in opposite directions in Figure 2. It would be useful to provide a brief outline as to why these terms are expected to act in opposite directions. (ii) All IPR related figures- Figures 2/S1 are very difficult to read. In addition the relationship between the fluxes and concentrations as plotted on figure 2 is unclear, and appears sensitive to the scaling's used on the right and left hand y-axes. See specific comments 3-8 below. (iii) The text discussing IPR results in section 4.1 is generally confusing and not well substantiated: often the season being referred to is not provided and general statements are sometimes given that only seem applicable to results in boreal summer. The text in section 4.3 also needs to be clarified and tightened in a good number of places- see specific comments. iv) For Figure 2/Table 1, it would be highly beneficial to also have results for the direct effect of a change in SSTs on regional surface ozone in that surface basin before any discussion of upwind or downwind continents. This would aid with interpretation as to the dilution of the ozone response with regional averaging.

(i) Good suggestion. The IPR analysis calculates the accumulated contributions of individual processes (e.g., net chemical production (production minus loss), advection, vertical diffusion, dry deposition, etc.) to the changes of O₃ concentrations. It is a widely used tool for air pollution diagnostics (Li et al., 2012; Zhang and Wu, 2013; Tao et al., 2015). In this study, we implemented the IPR scheme in the model to examine the O₃ flux in individual processes, including gas-phase chemistry, advection, vertical diffusion, dry deposition, shallow convection and deep convection. The wet deposition and aqueous-phase chemistry are ignored because of the low solubility and production rate of O₃ in water (Jacob, 1999). The sum of the IPR archived fluxes in CHEM, ADVE, VDIF, DRYD, SHAL and DEEP matches well the changes of O₃ concentration (Figure S1). Here the CHEM represents the net production (or production minus loss) flux of O₃ from gas-phase chemistry, which is consistent with the net production rate shown in Figure 3. DRYD represents the removal rate of O₃ by dry deposition. VDIF represents the transport of O₃ to the surface due to vertical diffusion. Both DRYD and VDIF are closely dependent on turbulent mixing. The efficiencies of O₃ vertical diffusion and the corresponding dry deposition are all positively related to the strength of turbulence, but with opposite sign. We therefore define a new term TURB to represent the sum of DRYD and VDIF, which can represent the overall effect of

turbulence change on surface O_3 . In the revised manuscript, we added more descriptions about the IPR method in Section 2.3 and Section 4.1. Please also refer to our reply to the specific comments for more details.

In Section 2.3 (P8, L226-238):

“...In this study, we added the IPR scheme to the CESM framework to track the contribution of six physicochemical processes (i.e., gas-phase chemistry (CHEM), advection (ADVE), vertical diffusion (VDIF), dry deposition (DRYD), shallow convection (SHAL) and deep convection (DEEP)) to O_3 concentrations in every grid box. Wet deposition and aqueous-phase chemistry are ignored here due to the low solubility and negligible chemical production of O_3 in water (Jacob, 1999). Therefore, CHEM represents the net production (production minus loss) rate of O_3 due to gas-phase photochemistry. DRYD represents the dry deposition fluxes of O_3 , which is an important sink for O_3 . The other IPR terms (i.e., ADVE, VDIF, SHAL and DEEP) represent contributions from different transport processes. The IPR scheme tracks and archives the O_3 flux in each grid from every process during each model time step. The sum of the O_3 fluxes from these six processes matches the change in the O_3 concentration. The IPR performance is verified by comparing the predicted hourly O_3 changes with the sum of the individual fluxes from the six processes. As shown in Figure S1, the hourly surface O_3 changes are well represented by the sum of these fluxes in the model.”

In Section 4.1 (P10-11, L296-316), we also add more explanations about the IPR results:

“IPR analysis is used to evaluate the contribution of different physicochemical processes to O_3 evolution. This type of analysis has been widely used in air quality studies to examine the cause of pollution episodes (Wang et al., 2010; Li et al., 2012). When applied in climate sensitivity analysis (usually measuring the difference between two equilibriums), the net change of all IPRs approaches zero. Typically, the positive changes in IPRs are mainly responsible for the increase in surface O_3 , which may further induce O_3 removal to balance this forcing in a new equilibrium. Therefore, here, the IPR analysis is used not to budget the SST-induced O_3 concentration changes but rather to help examine the relative importance of different transport and chemical processes in driving the sensitivity of O_3 to SST forcing. In this study, the SST-induced, process-level O_3 changes are spatially averaged over four populated continental regions (i.e., NA, EU, EA and SA, Figure 2) and three

ocean basins (i.e., the North Pacific, North Atlantic and North Indian Oceans, Figure S9). In most cases, VDIF and DRYD are the key processes controlling the O_3 variation. The downward transport of O_3 through diffusion is an important source of surface O_3 , while DRYD acts as a sink. Both processes are simultaneously determined by the strength of turbulence. Here, we define a new term TURB as the sum of DRYD and VDIF, which can capture the overall effect of turbulence changes on surface O_3 concentrations. In addition, we merge SHAL and DEEP as CONV to represent the total contribution of convective transport to surface O_3 (Figures 2 and S9). More detailed IPR results are shown in Figures S10 and S11 in the supplementary material.”

(ii) As we have mentioned above, each of the IPR processes (i.e., CHEM, ADVE, VDIF, DRYD, SHAL and DEEP) archived hourly and the sum of them matches well the time-varying O_3 concentration changes. Figure S1 in the supporting materials (see below) demonstrates the performance of the IPR scheme.

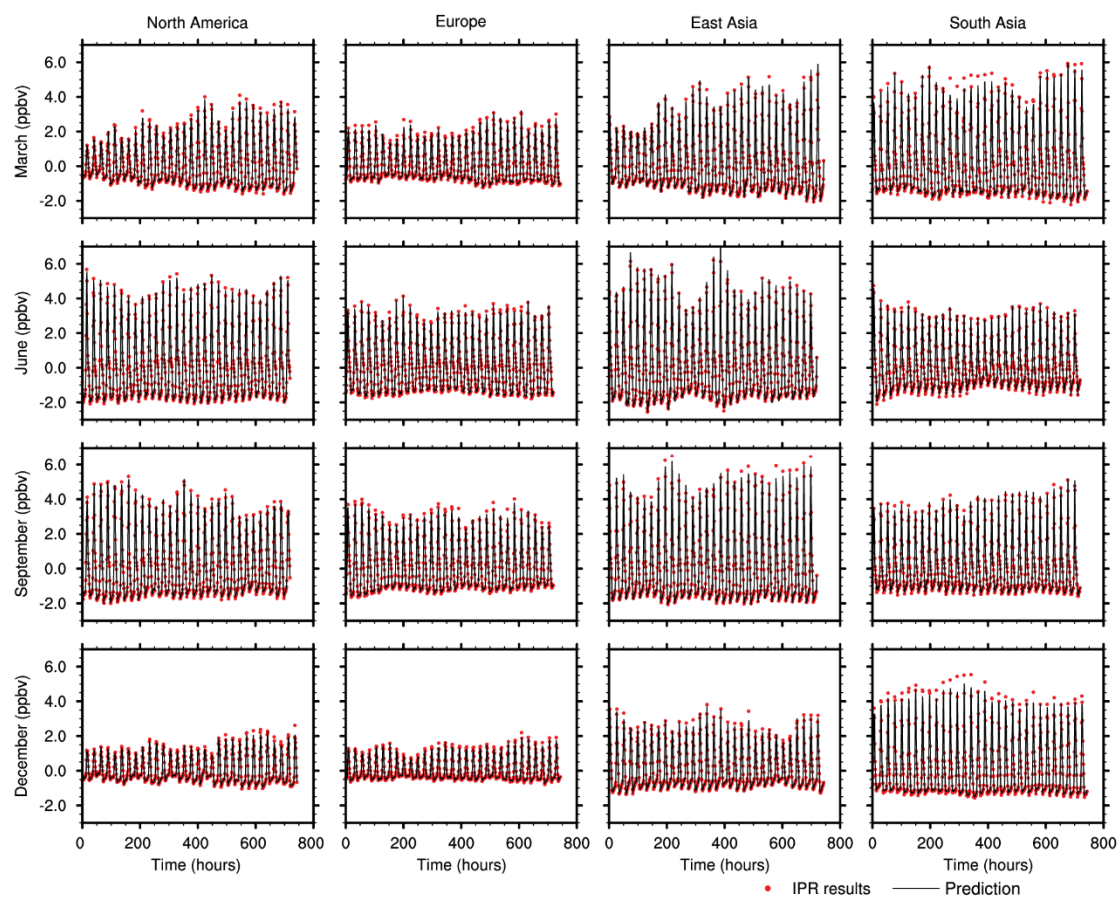


Figure S1. Hourly time-series of predicted O_3 changes (black lines) and the sum of IPR results (red dots) averaged over the four major regions of interest (i.e., America (15°N – 55°N ; 60°W – 125°W), Europe (25°N – 65°N ; 10°W – 50°E), East Asia (15°N – 50°N ; 95°E – 160°E) and South Asia (5°N – 35°N ; 50°E – 95°E)) during March (first row), June (second row), September (third row) and

December (last row) of random modeling years in the CTRL.

Figure 2, on the other hand, demonstrates the seasonally averaged results rather than the time-series shown in Figure S1. Positive changes of fluxes are generally counterbalanced by the negative ones because the climatological O₃ concentrations reside in an equilibrium when averaged over a long period of time. Therefore, the net flux changes could not be directly compared with surface O₃ changes between two climatological cases. Here we compared these IPR fluxes individually to identify the impact of basin-scale SST changes on each O₃ evolution process. Typically, the positive change of a particular IPR process is mainly responsible for the increase of surface O₃, which may further induces O₃ loss process to counteract these factors. With this information, we can explore the relative importance of different processes closely linked to the SST changes, which helps to explain the variability of surface O₃ over different regions.

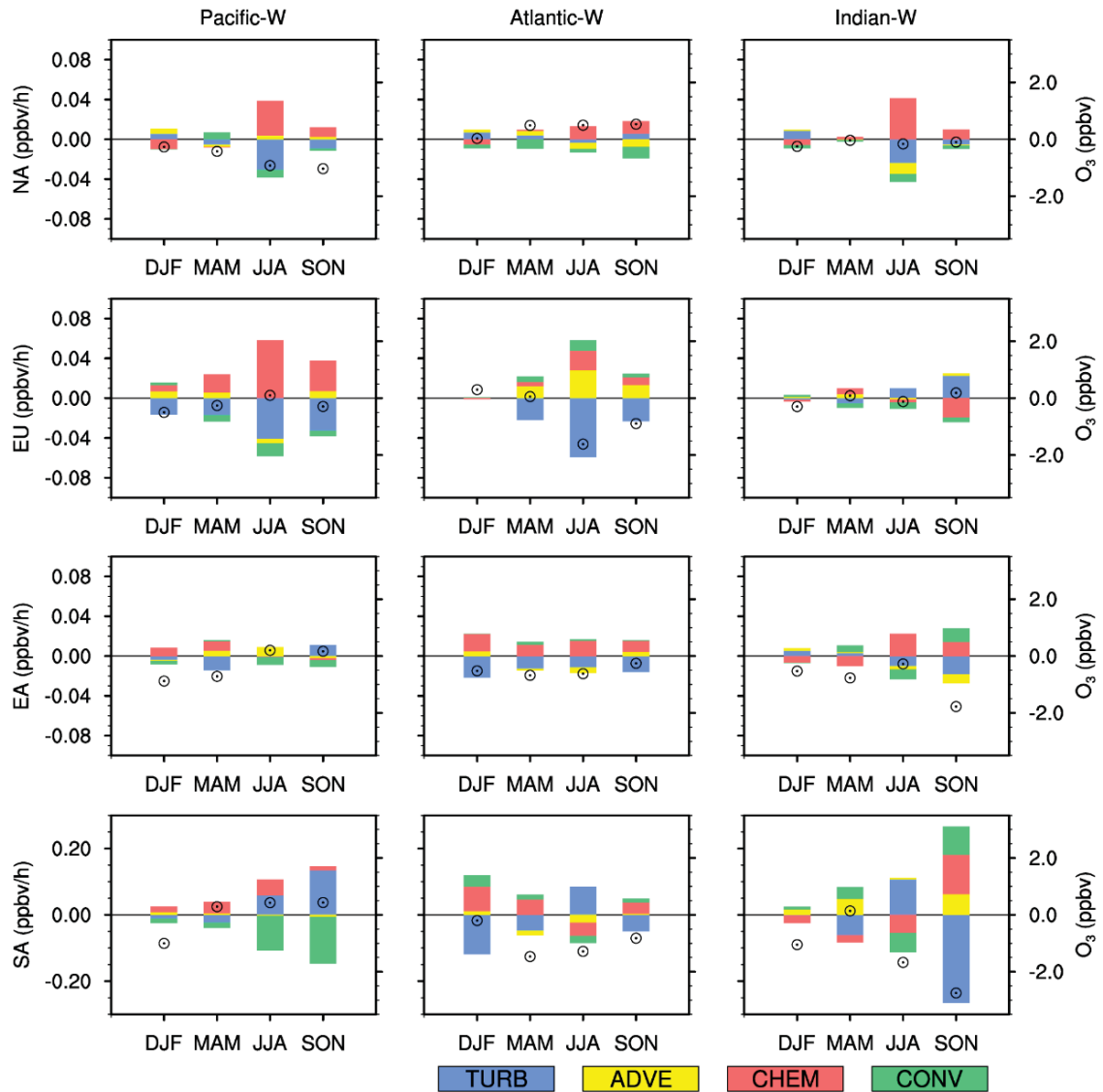


Figure 2. Seasonally averaged changes in the IPR contributions (bars, ppbv/h, left scale) and surface O₃ concentrations (hollow circles, ppbv, right scale) for Pacific-W (left), Atlantic-W (middle) and Indian-W (right) relative to the CTRL. Values are regionally averaged over NA (first row), EU (second row), EA (third row) and SA (last row). TURB is defined as the sum of VDIF and DRYD. CONV is the sum of DEEP and SHAL. IPR contributions from the four processes (i.e., TURB, ADVE, CHEM and CONV) are represented by different colors. A more detailed IPR result is shown in Figure S10 in the supplementary material.

(iii) We agree that some text needs more clarification. This study focuses mainly on summertime since both surface O₃ levels and their response to SST changes are highest during this period. We also find that an increase in SST in the North Pacific or North Atlantic tends to elevate the VDIF

of O₃ over upwind regions (i.e., East Asia and North America, respectively) but suppress it over downwind regions during JJA. In the revised manuscript, we have clarified the seasons we discussed and improved the consistency of the analysis. Please see our response to specific comments below.

iv) Good suggestion! We have added a similar table (Table S1) and figure (Figure S9) to examine the effect of SST changes on O₃ distribution over different ocean basins.

Table S1. Regionally and seasonally averaged (only ocean grid boxes are included) changes in surface O₃ concentrations (ppbv) over three ocean basins in the Northern Hemisphere (i.e., the North Pacific Ocean (15°N-65°N; 100°E-90°W), the North Atlantic Ocean (15°N-65°N; 100°W-20°E) and the North Indian Ocean (5°N-30°N; 30°E-100°E)) for basin-scale SST perturbation cases relative to the control simulation. Positive (negative) changes that are significant at the 0.05 level evaluated by Student's t-test are marked in red (blue).

Ozone (ppbv)			DJF	MAM	JJA	SON
North Pacific	+1°C	North Pacific	-0.56*	-0.71*	-0.78*	-1.22*
		North Atlantic	-0.55*	-1.08*	-0.74*	-1.25*
		North India	-1.05*	-0.59	0.16	0.20
	-1°C	North Pacific	0.32	0.55*	1.04*	1.00*
		North Atlantic	0.43*	0.53*	0.75*	0.80*
		North India	0.77*	-0.06	-0.03	0.16
North Atlantic	+1°C	North Pacific	0.05	-0.02	0.38*	0.01
		North Atlantic	0.14	0.04	-1.00*	-0.86*
		North India	-0.45*	-1.31*	-0.63*	-0.72*
	-1°C	North Pacific	0.11	0.32	0.11	-0.30
		North Atlantic	-0.02	-0.14	0.76*	0.43*
		North India	0.39	0.59	0.38*	0.48
North India	+1°C	North Pacific	-0.34	-0.11	-0.14	-0.88*
		North Atlantic	-0.25	-0.46	-0.11	-0.23
		North India	-1.59*	-0.42	0.81*	-2.11*
	-1°C	North Pacific	0.32	0.32	0.50*	0.52*
		North Atlantic	-0.07	-0.42	0.11	-0.37*
		North India	1.32*	0.89*	-0.38*	1.84*

*Significant at the 0.05 level from Student's t-test using 20 years of model results.

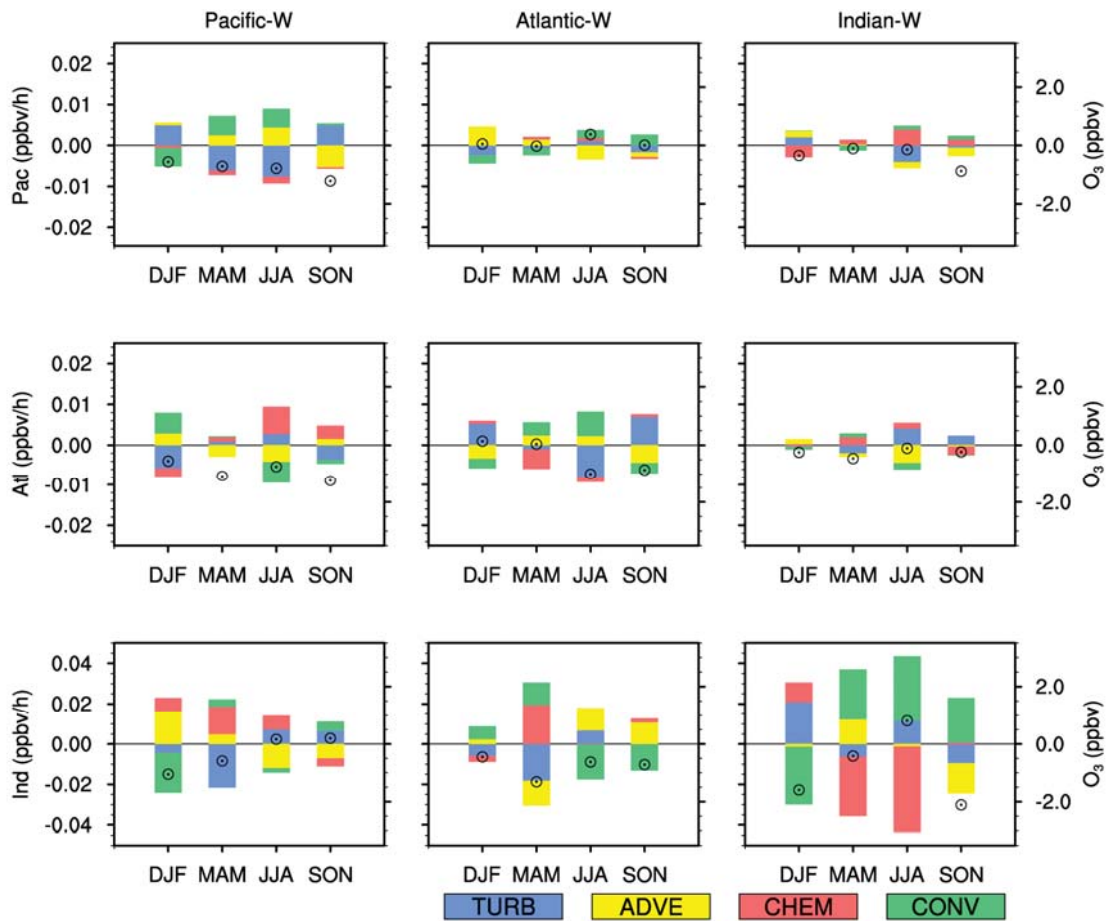


Figure S9. Seasonally averaged changes in the IPR contributions (bars, ppbv h^{-1} , left scale) and surface O_3 concentrations (hollow circles, ppbv , right scale) for Pacific-W (left), Atlantic-W (middle) and Indian-W (right) relative to the CTRL. Values are regionally averaged over North Pacific (15°N - 65°N ; 100°E - 90°W , demoted as “Pac”, first row), North Atlantic (15°N - 65°N ; 100°W - 20°E , demoted as “Atl”, second row) and North Indian Ocean (5°N - 30°N ; 30°E - 100°E , demoted as “Ind”, third row). IPR contributions from the four processes (i.e., TURB, ADVE, CHEM and CONV) are represented by different colors.

It shows that during boreal summers, the warming of North Pacific or North Atlantic leads to a widespread decrease of surface O_3 , while the warming of North Indian Ocean increases local surface O_3 . The IPR results indicate that the warming of the North Pacific or North Atlantic induce a reduction of TURB (mainly caused by the decrease of VDIF) and CHEM, which are responsible for the significant decrease of surface O_3 in JJA (Figure S19). The North Indian Ocean warming, on the other hand, enhances the CONV and TURB locally, leading to an increase of local surface O_3 in JJA. In the revised manuscript, more discussions on these effects are given:

In Section 3 (P9-10, L266-276):

“An increase in summertime SST over a specific ocean basin tends to increase the surface O₃ concentration over the upwind regions but reduce this concentration over downwind continents. For instance, a 1 °C warming over the North Pacific leads to a widespread decrease in surface O₃ over the North Pacific, North America and the North Atlantic of approximately 1 ppbv (Table S1) but may enhance the surface O₃ by nearly 3 ppbv over South China. Similarly, in the “Atlantic-W” case, the surface O₃ levels decrease by 1~2 ppbv over the North Atlantic and Europe but increase (~1 ppbv) over North America and the North Pacific. For the North Indian Ocean, positive SST anomalies tend to increase the surface O₃ over the Indian Ocean and Africa but decrease the surface O₃ over South and East Asia (Figure 1).”

In Section 4.1 (P12, L331-335 and L337-340):

“...The IPR analysis over the ocean basins shows that the warming of the North Pacific or North Atlantic induces reductions in VDIF and CHEM, which are responsible for the significant decrease in surface O₃ above these regions in JJA (Figure S11). The North Indian Ocean warming, on the other hand, enhances DEEP and VDIF, leading to a local increase in surface O₃ in JJA.”

...

“The IPR analysis indicates that, in general, an SST increase in the North Pacific or North Atlantic is more likely to enhance the vertical diffusion of O₃ over upwind regions (i.e., East Asia or North America, respectively) but suppress this diffusion over the ocean basin as well as downwind continents in JJA (Figure S12).”

4) As noted above for the IPR results, but also in general, the text on the various contributions or roles of intercontinental transport versus that of chemistry is difficult to follow in a number of places and some conclusions appear over-stated. For example, the abstract discusses “suppression of O₃ intercontinental transport due to increased stagnation at mid-latitudes induced by SST changes”. Stagnation is a localised process largely determined by boundary layer processes and entrainment. Hence, the authors should be cautious in their interpretation based on large-scale changes in wind vectors and vertical velocity to infer changes in stagnation/ventilation. Perhaps clear definitions of what is meant by these terms would be useful. See specific comments below.

Thanks for bringing this issue up. We agree that stagnation/ventilation were improperly used here. Throughout the analysis, we find that the basin-scale SST increase not only strengthens upward motions over the low-latitudes oceans, but also lead to decreases of upward velocity over mid-latitudes (Figure S23). Previous studies have revealed that strengthened deep convection will

trigger large-scale subsidence over the nearby regions through modulating large-scale circulations, which may suppress convective air movement there (Lau et al., 1997;Roxy et al., 2015;Ueda et al., 2015). Here we also demonstrate a weaker vertical temperature gradient associated with regional SST warming (Figure S16). Both factors (i.e., large-scale subsidence and weaker vertical temperature gradient) tend to stabilize the atmosphere that may inhibit vertical air transport. In our revised manuscript, we further examine the vertical transport of O₃ based on the IPR analysis (shown in Figure S12). It shows a widespread reduction of vertical diffusion transport of O₃ to the surface (i.e. VDIF) except for the upwind regions. We also find that SST increases of a specific ocean in the Northern Hemisphere, especially for the North Pacific and North Atlantic oceans, tend to increase the air temperature (Figure S16) and geopotential height (Figure 9) more significantly at mid-latitudes than other latitudes. Consequently, the meridional geopotential height gradient is decreasing in the tropical-to-mid-latitude troposphere while increasing at higher latitudes. It tends to decrease the westerly wind at lower-middle latitudes (25°N - 45 °N) in the Northern Hemisphere (Figure 9). Based on these facts, the warming of SST over a specific ocean may stabilize the troposphere at mid-latitudes that suppress the O₃ intercontinental transport. This effect is also supported by the CO-tracer analysis, which shows a significant reduction of intercontinental transport (Figure 8). We have discussed these processes in detail in the revised manuscript.

Here we revised the texts as below:

In Abstract (P2, L35-37):

“...This process, as confirmed by tagged CO-like tracers, indicates a considerable suppression of intercontinental O₃ transport due to increased tropospheric stability at lower mid-latitudes induced by SST changes.”

In Section 4.3 (P15, L422-427), we have:

“...Meanwhile, the air temperature increase in response to regional SST warming is more significant above the lower troposphere, which leads to a decrease in the vertical temperature gradient (Figure S16). These factors tend to restrain the vertical exchange of air pollutants at mid-latitudes, which facilitates surface O₃ accumulation over polluted continental regions in JJA but may weaken the intrusion of O₃ from the upper troposphere to the surface in most unpolluted areas.”

In the summary section (P19-20, L563-567):

“...The basin-scale SST increases in the Northern Hemisphere reduce the tropospheric temperature gradient at mid-latitudes that restrains vertical transport of O₃ over continents and

weakens the westerlies at lower mid-latitudes. The response of the CO-tracer also suggests that these factors may jointly exert a negative effect on the intercontinental transport of O₃.

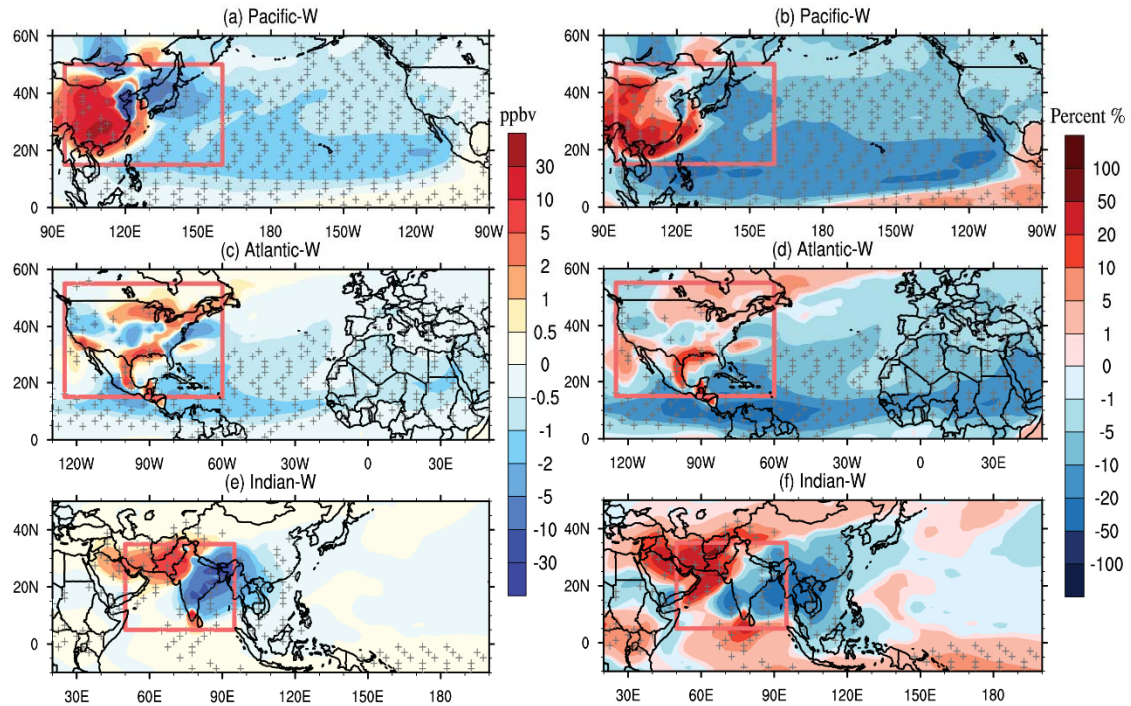


Figure 8. Left-hand panel: Difference in the surface concentration (ppbv) of a CO-like tracer emitted from (a) East Asia for Pacific-W, (c) North America for Atlantic-W and (e) the South Asia for Indian-W relative to the CTRL in the boreal summer. Right-hand panel: The percentage changes in the surface concentration of a CO-like tracer emitted from (b) East Asia for Pacific-W, (d) North America for Atlantic-W and (f) South Asia for Indian-W relative to the CTRL in the boreal summer. Red polygons denote the region where the CO-like tracer is emitted from. The + symbol denotes areas where the results are significant at the 0.05 level, evaluated by Student’s t-test using 20 years of data.

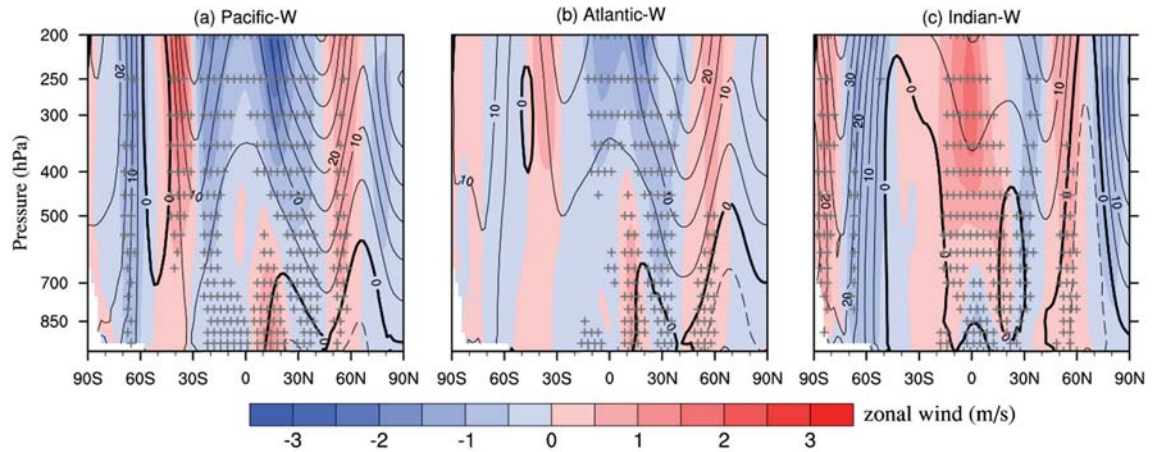


Figure 9. Zonally averaged changes in zonal wind (color contour, m/s) and geopotential height (contour, m) for (a) Pacific-W, (b) Atlantic-W and (c) Indian-W relative to the CTRL in the boreal summer. Black solid and dashed lines in the contours indicate positive and negative geopotential height anomalies, respectively (contour interval: 5 m). The + symbol denotes areas where the zonal wind changes are significant at the 0.05 level, evaluated by Student's t-test using 20 years of data.

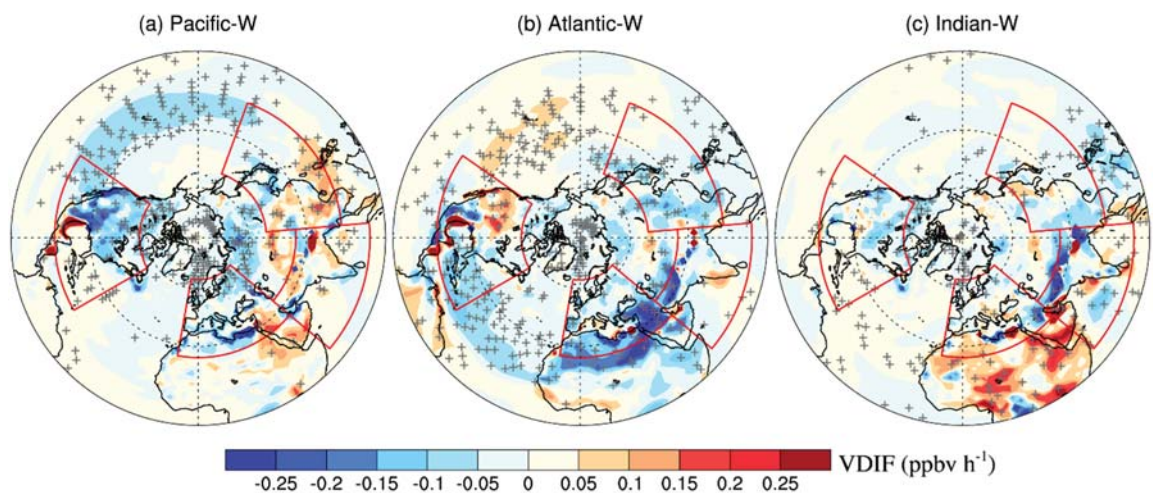


Figure S12. Changes in VDIF (ppbv h⁻¹) for (a) Pacific-W, (b) Atlantic-W and (c) Indian-W relative to the CTRL in the boreal summer. The four major regions of interest (i.e., NA, EU, EA and SA) are marked by red solid lines. The + symbols denote areas where the results are significant at the 0.05 level, evaluated by Student's t-test using 20 years of data.

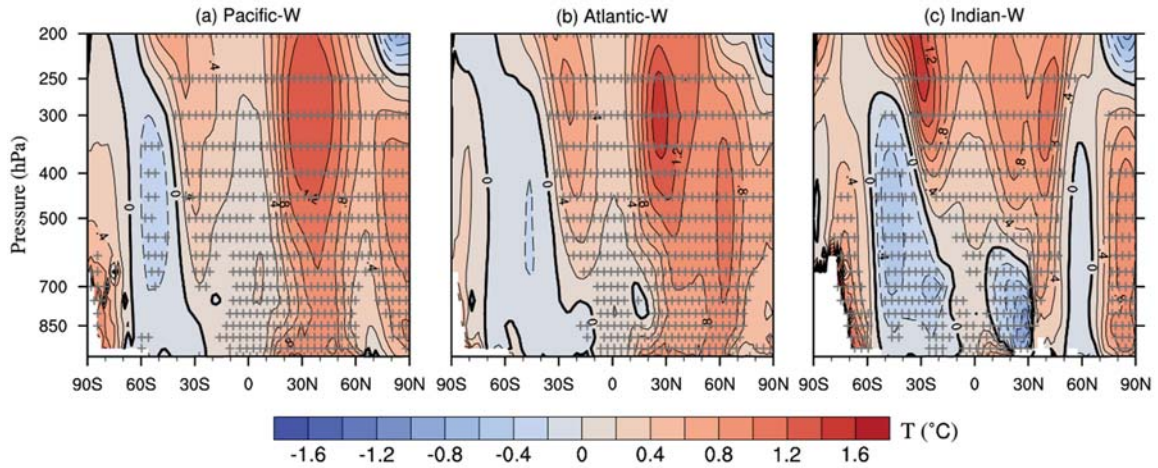


Figure S16. Vertical-meridional distributions of changes in the air temperature (contours, °C) for (a) Pacific_W (zonal averaged from 100°E-90°W), (b) Atlantic_W (zonal averaged from 100°W-180°W) and (c) Indian_W (zonal averaged from 30°E-100°E) relative to the CTRL in boreal summer. Black solid and dashed lines in the contours indicate positive and negative air temperature anomalies, respectively (contour interval: 0.2 °C). The + symbol denotes areas where the changes of air temperature are significant at the 0.05 level, evaluated by Student's t-test using 20 years of data.

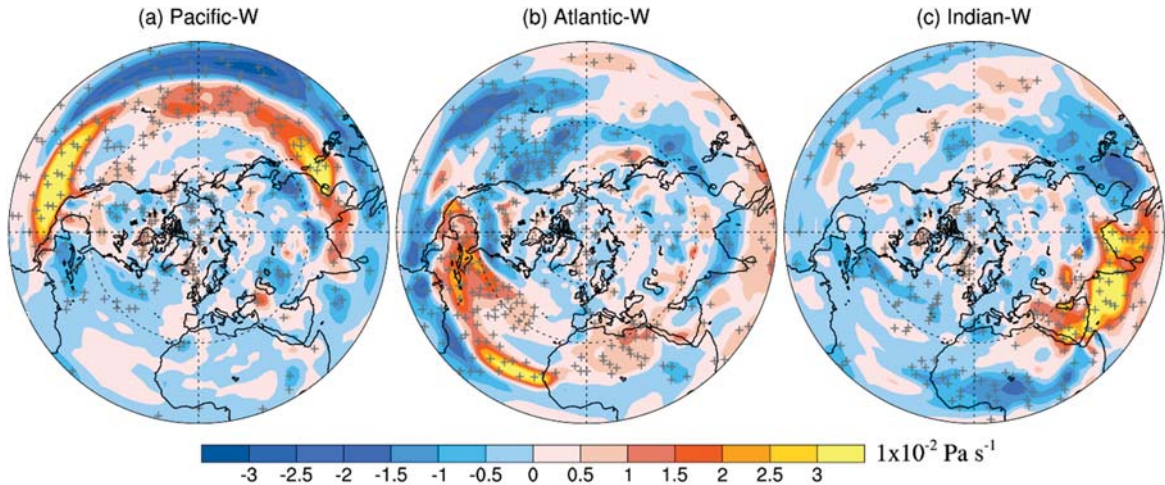


Figure S23. Spatial pattern of vertical velocity changes at 500 hPa (color contours, $1 \times 10^{-2} \text{ Pa s}^{-1}$) for (a) Pacific-W, (b) Atlantic-W, and (c) Indian-W relative to the CTRL in the boreal summer. Positive values indicate upward motion. The + symbols indicate areas where results are significant at the 0.05 level, evaluated by Student's t-test using 20 years of data.

5) A number of references in the text are rather old, and some updated references would be highly beneficial. See specific comments below. Also with multi-references the logical order is unclear-chronological order is most commonly used.

Good suggestion! We have updated our references by citing more recent studies. Please see our response to specific comments below. We have also reordered references chronologically.

Specific comments:

1) As also noted by the other reviewer the frequent use of parenthesis to state a key result dilutes the message of the sentence and makes for a confusing read. Please rephrase when key points are being made in the abstract and main text (lines 223-230).

Good suggestion. We rephrased these key results following the reviewer's suggestions, see below or the revised abstract and text:

In Abstract (PI, L24-27):

“...The responses of surface O₃ associated with basin-scale SST warming and cooling have similar magnitude but are opposite in sign. Increasing the SST by 1 °C in one of the oceans generally decreases the surface O₃ concentrations from 1 to 5 ppbv.”

In Section 3 (P9-10, L264-280):

“...Surface O₃ changes in response to positive and negative SST anomalies generally pronounce a consistent spatial pattern but are opposite in sign, suggesting robust relationships between surface O₃ levels and SST anomalies (Figure 1). An increase in summertime SST over a specific ocean basin tends to increase the surface O₃ concentration over the upwind regions but reduce this concentration over downwind continents. For instance, a 1 °C warming over the North Pacific leads to a widespread decrease in surface O₃ over the North Pacific, North America and the North Atlantic of approximately 1 ppbv (Table S1) but may enhance the surface O₃ by nearly 3 ppbv over South China. Similarly, in the “Atlantic-W” case, the surface O₃ levels decrease by 1–2 ppbv over the North Atlantic and Europe but increase (~1 ppbv) over North America and the North Pacific. For the North Indian Ocean, positive SST anomalies tend to increase the surface O₃ over the Indian Ocean and Africa but decrease the surface O₃ over South and East Asia (Figure 1). During the boreal winter, a widespread decrease in surface O₃ associated with the warming of different oceans is observed. Significant changes (e.g., up to 5 ppbv) mainly occur over remote ocean areas. Over populated continents, the response of the surface O₃ to basin-scale SST changes is typically insignificant. Details are shown in Figure S3 in the supplementary material.”

2) Line 207/Table 1 – as noted above it would be beneficial to first show a similar table that examines the effect of SST changes within each basin and on other ocean basins.

Good suggestion. We add such a table in the supplementary material, see Table S1 below.

Table S1. Regionally and seasonally averaged (only ocean grid boxes are included) changes in surface O₃ concentrations (ppbv) over three ocean basins in the Northern Hemisphere (i.e., the North Pacific Ocean (15°N-65°N; 100°E-90°W), North Atlantic Ocean (15°N-65°N; 100°W-20°E) and North Indian Ocean (5°N-30°N; 30°E-100°E)) for basin-scale SST perturbation cases relative to the control simulation. Positive (negative) changes that are significant at the 0.05 level evaluated by Student’s t-test are marked in red (blue).

Ozone (ppbv)			DJF	MAM	JJA	SON
North Pacific	+1°C	North Pacific	-0.56*	-0.71*	-0.78*	-1.22*
		North Atlantic	-0.55*	-1.08*	-0.74*	-1.25*
		North India	-1.05*	-0.59	0.16	0.20
	-1°C	North Pacific	0.32	0.55*	1.04*	1.00*
		North Atlantic	0.43*	0.53*	0.75*	0.80*
		North India	0.77*	-0.06	-0.03	0.16
North Atlantic	+1°C	North Pacific	0.05	-0.02	0.38*	0.01
		North Atlantic	0.14	0.04	-1.00*	-0.86*
		North India	-0.45*	-1.31*	-0.63*	-0.72*
	-1°C	North Pacific	0.11	0.32	0.11	-0.30
		North Atlantic	-0.02	-0.14	0.76*	0.43*
		North India	0.39	0.59	0.38*	0.48
North India	+1°C	North Pacific	-0.34	-0.11	-0.14	-0.88*
		North Atlantic	-0.25	-0.46	-0.11	-0.23
		North India	-1.59*	-0.42	0.81*	-2.11*
	-1°C	North Pacific	0.32	0.32	0.50*	0.52*
		North Atlantic	-0.07	-0.42	0.11	-0.37*
		North India	1.32*	0.89*	-0.38*	1.84*

*Significant at the 0.05 level from Student’s t-test using 20 years of model results.

We also revised the text accordingly, see Section 3 (P9-10, L264-276) or below:

“...Surface O₃ changes in response to positive and negative SST anomalies generally pronounce a consistent spatial pattern but are opposite in sign, suggesting robust relationships between surface O₃ levels and SST anomalies (Figure 1). An increase in summertime SST over a specific ocean basin tends to increase the surface O₃ concentration over the upwind regions but reduce this concentration over downwind continents. For instance, a 1 °C warming over the North Pacific leads to a widespread decrease in surface O₃ over the North Pacific, North America and the North Atlantic of approximately 1 ppbv (Table S1) but may enhance the surface O₃ by nearly 3 ppbv over South China. Similarly, in the “Atlantic-W” case, the surface O₃ levels decrease by 1~2 ppbv over the North Atlantic and Europe but increase (~1 ppbv) over North America and the North Pacific. For the North Indian Ocean, positive SST anomalies tend to increase the surface O₃ over the Indian Ocean and Africa but decrease the surface O₃ over South and East Asia (Figure 1).”

3) Line 242- what is meant by atmospheric turbulence intensity and explain to the reader how this relates to VDIF and DRYD.

Good question. Both VDIF and DRYD processes are dynamically determined by the strength of turbulence. Stronger turbulence enhances the downward transport of O₃ to the ground level, which also induces more O₃ dry deposition. Therefore, DRYD tends to behave concurrently with VDIF, but with an opposite sign. We have clarified this in our revised manuscript (see P11, L308-313):

“...In most cases, VDIF and DRYD are the key processes controlling the O₃ variation. The downward transport of O₃ through diffusion is an important source of surface O₃, while DRYD acts as a sink. Both processes are simultaneously determined by the strength of turbulence. Here, we define a new term TURB as the sum of DRYD and VDIF, which can capture the overall effect of turbulence changes on surface O₃ concentrations.”

4) Line 248 “reducing it over North America. For the Pacific W panels in Figure 2 a reduction in VDIF is only seen in in summer in North America; VDIF increases just as strongly in North America in winter and spring.

This sentence only refers to summers. We have clarified this in Section 4.1 of the revised manuscript (P11, L323-325).

“...In the “Atlantic-W” case, increases in VDIF are also observed over the upwind regions (i.e., North America) in JJA.”

5) Line 248- “similar increases in VDIF are simulated over North America. Similar to ?

We state the increases in VDIF over North America in JJA is a “similar increase” because it also happens over upwind regions associated with the North Atlantic warming that is similar to the East Asia in the “Pacific-W” case. We realize that the word “similar” may induce confusion and we delete it in the revised manuscript (*P11, L323-325*).

“...In the “Atlantic-W” case, increases in VDIF are also observed over the upwind regions (i.e., North America) in JJA.”

6) Line 253- “the increase of CHEM tends to dominate the surface O₃ increase over North America.” This is not obvious from Figure 2 (and it is unclear which season/s are being discussed), and is unintuitive without a clearer definition of CHEM, and how fluxes relate to concentrations in Figure 2.

Here we show the key processes enhancing the surface O₃ over North America in JJA in the Atlantic_W case. CHEM tracks the surface O₃ flux due to net chemical production (i.e., production minus loss). In the revised Figure 2, we replaced VDIF and DRYD by TURB, and DEEP and SHAL by CONV. Now it is easier to see that a warmer SST over the Atlantic enhances O₃ chemical production, which positively contributes to the surface O₃ increase over North America. Please see the revised Figure 2 below:

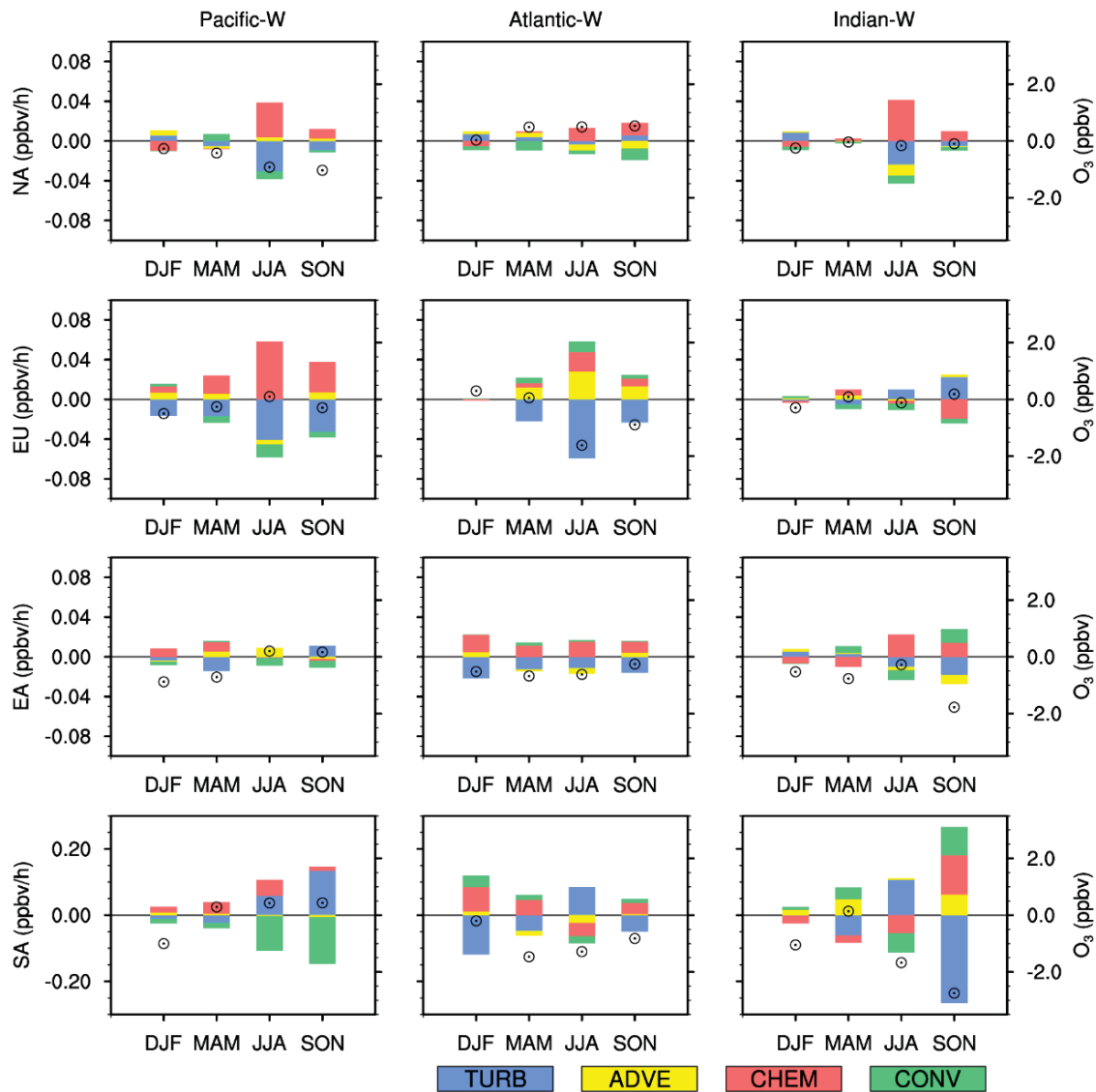


Figure 2. Seasonally averaged changes in the IPR contributions (bars, ppbv/h, left scale) and surface O₃ concentrations (hollow circles, ppbv, right scale) for Pacific-W (left), Atlantic-W (middle) and Indian-W (right) relative to the CTRL. Values are regionally averaged over NA (first row), EU (second row), EA (third row) and SA (last row). TURB is defined as the sum of VDIF and DRYD. CONV is the sum of DEEP and SHAL. IPR contributions from the four processes (i.e., TURB, ADVE, CHEM and CONV) are represented by different colors. A more detailed IPR result is shown in Figure S10 in the supplementary material.

In the revised manuscript, we have rephrased this sentence (see *P11, L323-328*):

“...In the “Atlantic-W” case, increases in VDIF are also observed over the upwind regions (i.e., North America) in JJA. However, these increases are accompanied by commensurate decreases in

DRYD, resulting in an insignificant overall change in TURB (Figure 2). Therefore, the increase in CHEM is mainly responsible for the surface O₃ increase over North America in JJA.”

7) Line 254- “TURB is more important ... leading to reduced surface O₃ concentrations.” Again the positive and negative fluxes in JJA and SON look to balance so why are there reduced ozone concentrations. Line 257- as above the fluxes look as though they balance (especially in JJA) but ozone concentrations are reduced.

As mentioned in our reply to comment (3), the IPR scheme in our study tracks all processes that are related to the O₃ formation. It has been widely used in air quality studies to examine the cause of pollution episodes (Wang et al., 2010; Li et al., 2012). When applied in climate sensitivity relevant analysis (usually measuring the difference between two equilibrium states), the net change of all IPRs approaches zero. The multi-year seasonally averaged positive and negative fluxes are balanced with each other after model spin-up. Typically, the positive change of a particular IPR process is mainly responsible for the increase of surface O₃, which may further induce O₃ removal to counteract this forcing. Therefore, here the IPR analysis is not used to budget SST induced O₃ concentration changes. Instead, it helps to screen out the key processes driving the sensitivity of O₃ to a SST forcing. In the revised manuscript, we have clarified this issue and focused mainly on the individual process-level responses to SST changes. Please see our revised text in Section 4.1 (see *P10-11, L296-316 and L318-335*) or below:

“IPR analysis is used to evaluate the contribution of different physicochemical processes to O₃ evolution. This type of analysis has been widely used in air quality studies to examine the cause of pollution episodes (Wang et al., 2010; Li et al., 2012). When applied in climate sensitivity analysis (usually measuring the difference between two equilibriums), the net change of all IPRs approaches zero. Typically, the positive changes in IPRs are mainly responsible for the increase in surface O₃, which may further induce O₃ removal to balance this forcing in a new equilibrium. Therefore, here, the IPR analysis is used not to budget the SST-induced O₃ concentration changes but rather to help examine the relative importance of different transport and chemical processes in driving the sensitivity of O₃ to SST forcing. In this study, the SST-induced, process-level O₃ changes are spatially averaged over four populated continental regions (i.e., NA, EU, EA and SA, Figure 2) and three ocean basins (i.e., the North Pacific, North Atlantic and North Indian Oceans, Figure S9). In most cases, VDIF and DRYD are the key processes controlling the O₃ variation. The downward transport of O₃ through diffusion is an important source of surface O₃, while DRYD acts as a sink. Both processes are simultaneously determined by the strength of turbulence. Here, we define a new term TURB as the sum of DRYD and VDIF, which can capture the overall effect of turbulence changes on surface O₃ concentrations. In addition, we merge SHAL and DEEP as CONV to represent the

total contribution of convective transport to surface O_3 (Figures 2 and S9). More detailed IPR results are shown in Figures S10 and S11 in the supplementary material.”

“In the ‘Pacific-W’ case, a 1 °C SST warming over the North Pacific increases VDIF over eastern China in JJA (Figure S12), which is insignificant if averaged over the whole East Asia region. Meanwhile, this Pacific warming considerably reduces VDIF over North America (Figure S10). The corresponding decrease in TURB over North America mainly determines the surface O_3 reduction in JJA and SON, while the reduction in CONV exerts an additional negative impact (Figure 2). In the ‘Atlantic-W’ case, increases in VDIF are also observed over the upwind regions (i.e., North America) in JJA. However, these increases are accompanied by commensurate decreases in DRYD, resulting in an insignificant overall change in TURB (Figure 2). Therefore, the increase in CHEM is mainly responsible for the surface O_3 increase over North America in JJA. TURB is more relatively important over Europe (only in JJA and SON), leading to reduced surface O_3 abundance. In the ‘Indian-W’ case, both CHEM and CONV are reduced over South Asia in JJA, leading to overall reductions in surface O_3 over the Indian subcontinent (Figure 2). The IPR analysis over the ocean basins shows that the warming of the North Pacific or North Atlantic induces reductions in VDIF and CHEM, which are responsible for the significant decrease in surface O_3 above these regions in JJA (Figure S11). The North Indian Ocean warming, on the other hand, enhances DEEP and VDIF, leading to a local increase in surface O_3 in JJA.”

8) Lines 260-263- It would be helpful to define remote versus downwind. Remote is used in this sentence and downwind in the following sentence. If North America is the remote continent in the Pacific W simulation then VDIF is only suppressed in summer, but not in winter and spring.

Good suggestion. To avoid confusion, we have replaced “remote” with “downwind” for consistency (P12, L337-342):

“The IPR analysis indicates that, in general, an SST increase in the North Pacific or North Atlantic is more likely to enhance the vertical diffusion of O_3 over upwind regions (i.e., East Asia or North America, respectively) but suppress this diffusion over the ocean basin as well as downwind continents in JJA (Figure S12). These opposite changes in VDIF over upwind and downwind regions lead to distinct surface O_3 responses.”

9) Line 266- “change in photochemistry. . . advection . . . dominates the feedbacks of Indian Ocean warming- CHEM appears as a substantial component in the lowermost right hand panel of Figure 2.

Good question! As shown in Figure 2, the North Indian warming leads to substantial decreases of CHEM and CONV, which are responsible for the reduction of surface O_3 over South Asia. We have clarified this sentence in Section 3 of the revised manuscript (P12, L329-331):

“...In the “Indian-W” case, both CHEM and CONV are reduced over South Asia in JJA, leading to overall reductions in surface O_3 over the Indian subcontinent (Figure 2).”

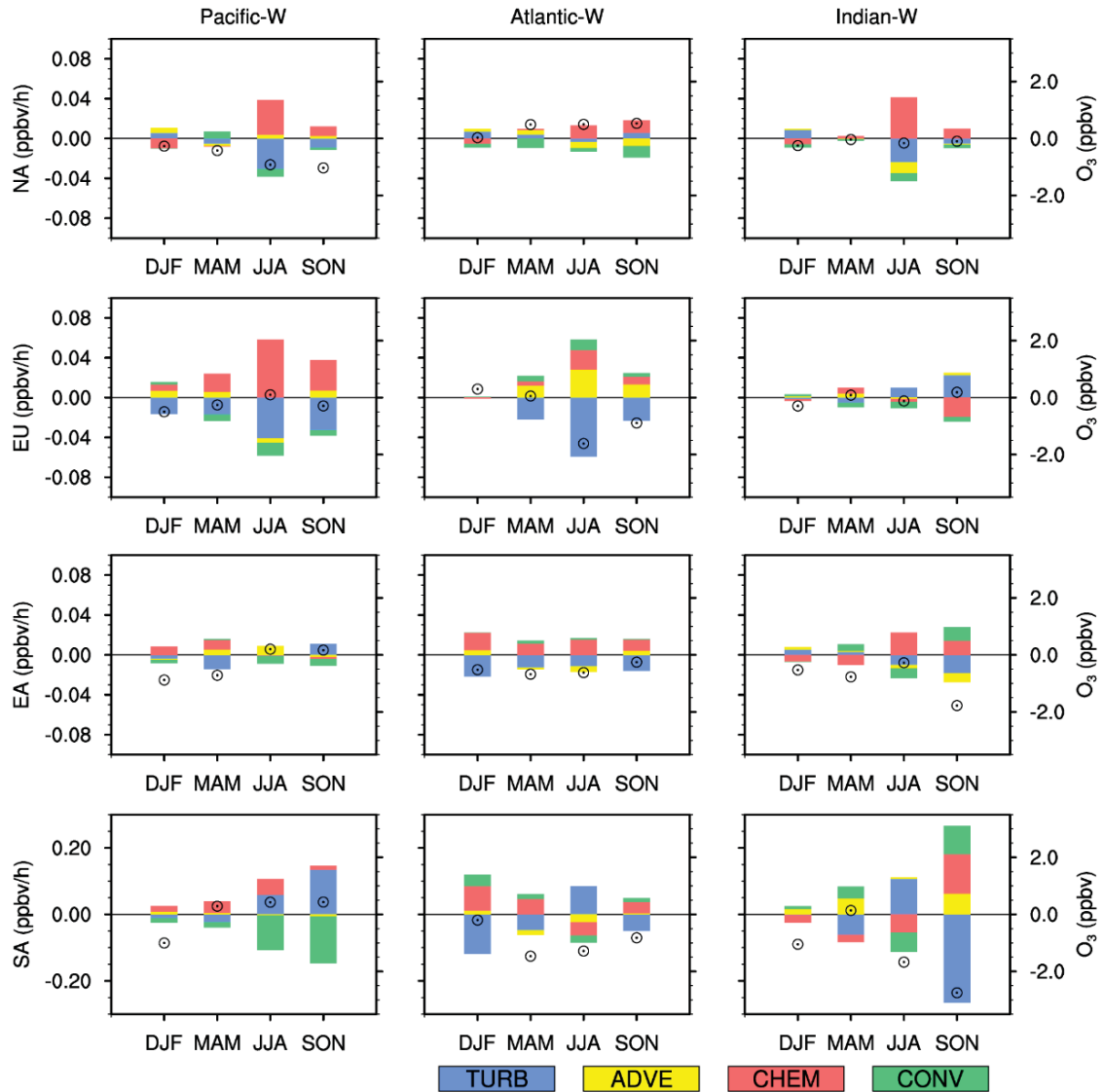


Figure 2. Seasonally averaged changes in the IPR contributions (bars, ppbv/h, left scale) and surface O_3 concentrations (hollow circles, ppbv, right scale) for Pacific-W (left), Atlantic-W (middle) and Indian-W (right) relative to the CTRL. Values are regionally averaged over NA (first row), EU (second row), EA (third row) and SA (last row). TURB is defined as the sum of VDIF and DRYD. CONV is the sum of DEEP and SHAL. IPR contributions from the four processes (i.e., TURB, ADVE, CHEM and CONV) are represented by different colors. A more detailed IPR result is shown

in Figure S10 in the supplementary material.

10) Line 275- “Peak changes are confined to the polluted region because of their high precursor emissions”. This is not obviously related. Please explain this statement more clearly. The examples that follow to the end of the paragraph referring to Figure 3 (the regions discussed are hard to see) do not clearly substantiate this.

As shown in Figure 3, changes of O₃ net production rate are generally highest over North America, East and South Asia where O₃ precursors’ emissions are high. In addition, significant change also happens in tropical Africa, when North Indian SST is warmer. Therefore, we agree with the reviewer that our original explanation is not clear. Please see our revised text in Section 4.2 (P12, L350-357) or below:

“Changes in the net production rate (i.e., chemical production rate minus loss rate) of O₃ at the surface in JJA associated with basin-scale SST increases are shown in Figure 3. The peak changes are mainly confined to regions where O₃ precursors are abundant (e.g., South and East Asia and North America). For example, a warmer North Pacific SST exerts a positive (negative) impact on net O₃ production in the northern (southern) regions of East Asia. Similarly, the warming of the North Atlantic promotes a dipole impact on the surface O₃ production over North America, while the warming of the North Indian Ocean significantly decreases the net O₃ production rate over South Asia.”

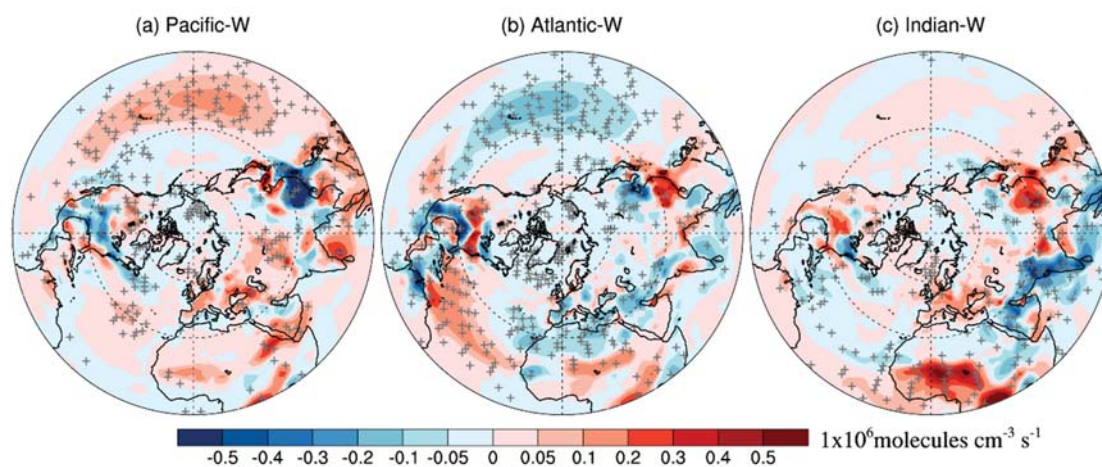


Figure 3. Perturbations of the surface net O₃ production rate ($1 \times 10^6 \text{ molecules cm}^{-3} \text{ s}^{-1}$) for (a) Pacific-W, (b) Atlantic-W, and (c) Indian-W relative to the CTRL in the boreal summer. The +

symbols denote areas where the results are significant at the 0.05 level, evaluated by Student's t-test using 20 years of data (plots using the Mercator projection are shown in Figure S14 in the supplementary material).

11) Lines 290 to end of paragraph- "Increase in SST facilitates moist convection... Lau. . .1997)"- Figure 2 for summer for the Indian W influence on SA suggests a decrease in deep convection. Please clarify? Here the references used are rather old. This is an interesting find, an increase in SST would be normally accompanied by an increase in surface air temperature directly above the ocean, but yet figure S3 shows cooling but with warming above. Hence it would be beneficial to provide an expanded interpretation of this finding, compare the results with those from more recent papers on how elevated SSTs in the Indian Ocean region or tropics affect surface air temperature and convection.

Good suggestion. Figure S11 shows that a warmer North Indian Ocean increases the DEEP (i.e., the contribution of deep convection to surface O₃) while Figure S10 suggests a decrease in the DEEP over South Asia. Actually, this SST increase facilitates deep convection over the North Indian Ocean while suppresses deep convection over the Indian subcontinent. Generally, an increase in SST for tropical oceans are more likely to enhance evaporation and vertical movement of warm moist air above its surface (Lau and Nath, 1994;Lau et al., 1997;Hartmann, 2015). However, its effects on convection over nearby and remote regions are rather complicated. In this case, the SST increase over the Indian Ocean strengthens deep-convection above it according to our analysis as well as previous studies (Roxy, 2014;Xi et al., 2015;Chaudhari et al., 2016). The enhanced upward movement of warm moist air above the Indian Ocean promotes cloud formation in the upper troposphere. As demonstrated in our study, there is a remarkable reduction of solar radiation received at the surface (Figure S17) and a significant decrease of surface air temperature (Figure 4) over Indian subcontinent. This decrease of surface temperature over the Indian subcontinent suppresses the development of deep-convection above. Additionally, the latent heat release from convective activity warms the air temperature in upper troposphere significantly (Sabeerali et al., 2012;Xi et al., 2015), leading to opposite changes of air temperature between upper and lower troposphere over South Asia. We have discussed these processes with some most recent references in Section 4.2 of the revised manuscript (P13, L363-380).

"...An exception is the North Indian Ocean, where an increase in SST tends to cool the Indian subcontinent by 1-2 °C. This temperature decrease is not only limited to the surface but also spreads to 600 hPa (Figure S16). Associated with this temperature decrease is a remarkable reduction in the solar radiation received at the continent below (more than 15 W/m², Figure S17). Previous

studies have indicated that moist convection is more sensitive to the SST changes in the tropical oceans than in mid- or high- latitude oceans (Lau and Nath, 1994; Lau et al., 1997; Hartmann, 2015). The SST increase over the North Indian Ocean tends to strengthen the moist convection that eventually facilitates cloud formation in the upper troposphere (Roxy et al., 2015; Xi et al., 2015; Chaudhari et al., 2016). The latent heat released from convective activities significantly warms the air temperature over the upper troposphere (Sabeerali et al., 2012; Xi et al., 2015). Meanwhile, the corresponding increase in cloud cover blocks the solar radiation reaching the surface of the Indian subcontinent and reduce the air temperature of lower troposphere in that region. These processes lead to opposite air temperature changes between upper and lower troposphere over South Asia in response to the North Indian warming (as shown in Figure S16), which may further suppress the development of deep convection over the Indian subcontinent.”

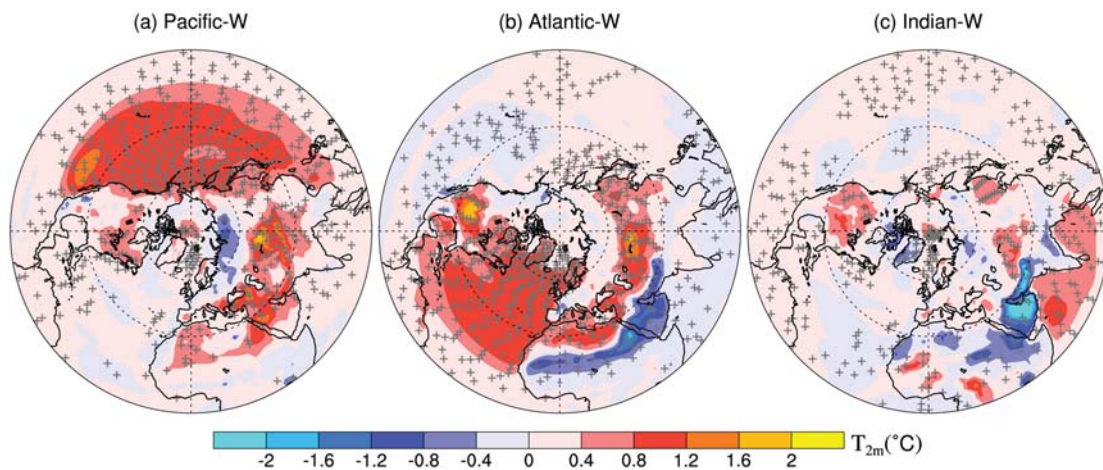


Figure 4. Changes in the surface air temperature (°C) for (a) Pacific-W, (b) Atlantic-W, and (c) Indian-W relative to CTRL in the Northern Hemisphere in the boreal summer. The + symbols denote areas where the results are significant at the 0.05 level, evaluated by Student’s t-test using 20 years of data (plots using the Mercator projection are shown in Figure S15 in the supplementary material).

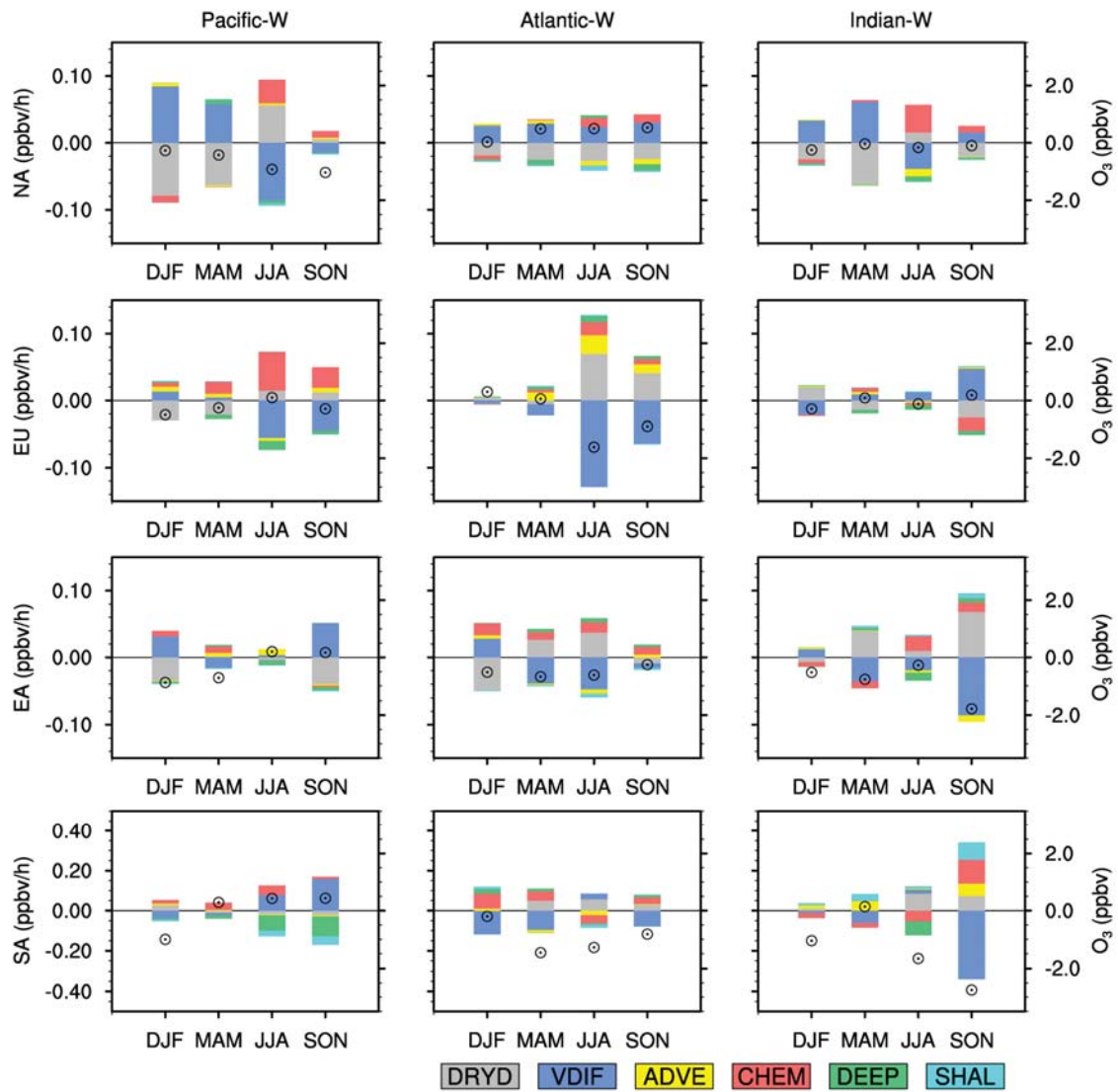


Figure S10. Seasonally averaged changes in the IPR contributions (bars, ppbv h⁻¹, left scale) and surface O₃ concentrations (hollow circles, ppbv, right scale) for Pacific-W (left), Atlantic-W (middle) and Indian-W (right) relative to the CTRL. Values are regionally averaged over NA (first row), EU (second row), EA (third row) and SA (last row). IPR contributions from the six processes (i.e., DRYD, VDIF, ADVE, CHEM, DEEP and SHAL) are represented by different colors.

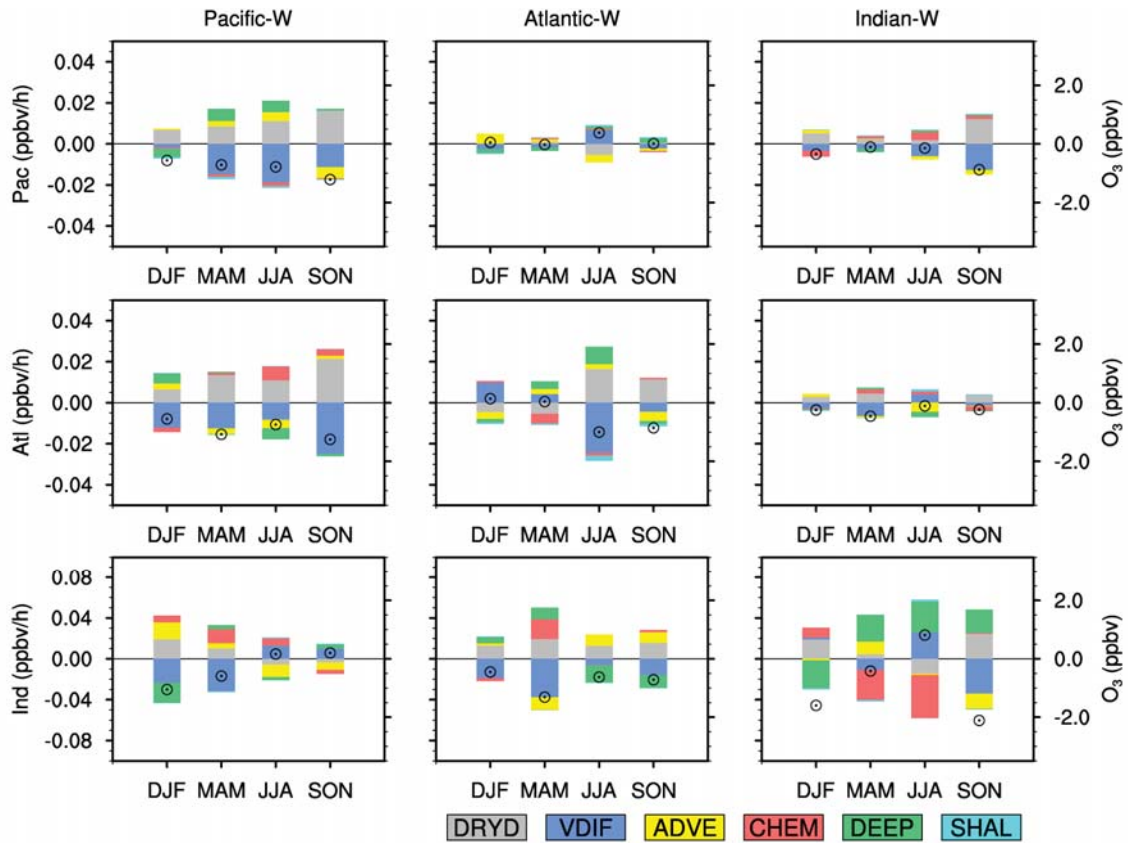


Figure S11. Same as Figure S10 but for the three ocean basins defined in our study.

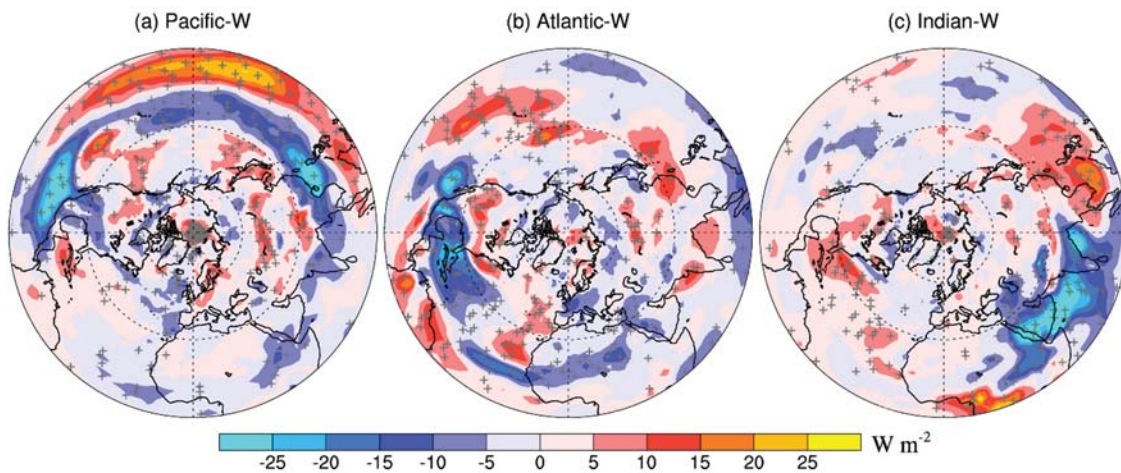


Figure S17. Perturbations of the surface solar radiations (W m^{-2}) for (a) Pacific-W, (b) Atlantic-W, and (c) Indian-W relative to the CTRL in the boreal summer. The + symbols denote areas where the results are significant at the 0.05 level, evaluated by Student's t-test.

12) Line 297- The text relating ozone production -temperature relationships to net surface ozone production relationships with temperature should be clarified: it is the ozone not the ozone

production that is related to temperature in the references cited, and as the authors note both ozone production and destruction rates will increase with temperature (directly and indirectly through higher humidity).

Good suggestion. Figure S19 compares the O₃ chemical production rate and destruction rate. The former usually dominates the net chemical production over continental regions, whereas the latter is relatively important over oceans. This indicates that although both ozone production and destruction rates increase with temperature, the response of O₃ is more relevant to the changes of O₃ production rate over continental regions. In contrast, the effects of humidity on O₃ destruction and concentrations are more important over coastal and oceanic areas. Please see the revised text in Section 4.2 (P13-14, L382-389) or below:

“Previous studies have indicated that air temperature positively affects both O₃ production and destruction rates (Zeng et al., 2008; Pusede et al., 2015). As shown in Figure S19, changes in the net O₃ production rate are mainly dominated by O₃ production over continents but by O₃ destruction over oceans. An increase in SST leads to a widespread enhancement of the air temperature, resulting in a positive change in the net O₃ production over most continental regions (Figure 3). However, a warmer SST also increases the air humidity (Figure S21), which enhances O₃ destruction over most coastal and oceanic areas.”

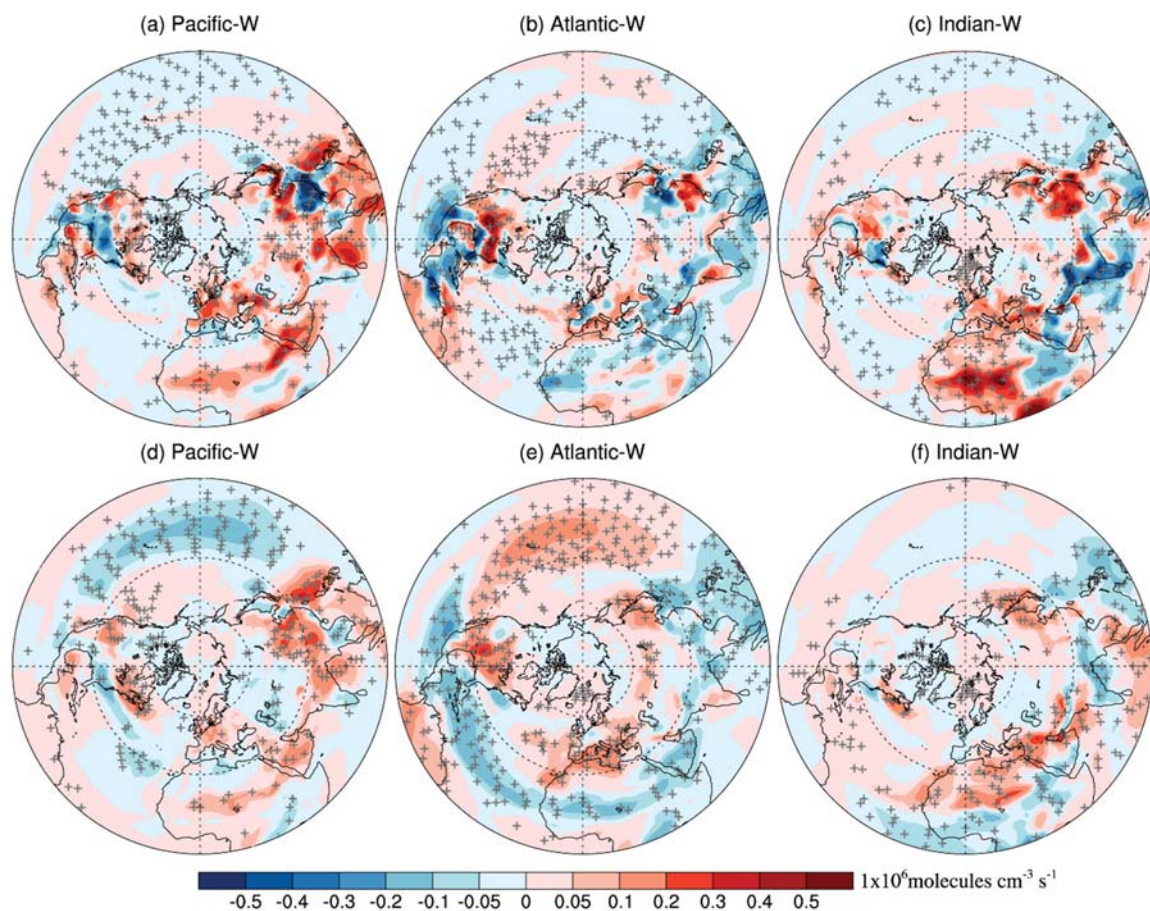


Figure S19. Top row: Perturbations of the surface chemical O₃ production rate (1×10^6 molecules $\text{cm}^{-3} \text{s}^{-1}$) for (a) Pacific-W, (b) Atlantic-W, and (c) Indian-W relative to the CTRL in the boreal summer. Bottom row: Perturbations of surface chemical O₃ loss rate (1×10^6 molecules $\text{cm}^{-3} \text{s}^{-1}$) for (d) Pacific-W, (e) Atlantic-W, and (f) Indian-W relative to the CTRL in the boreal summer. The + symbols denote areas where the results are significant at the 0.05 level, evaluated by Student's t-test using 20 years of data.

13) Line 318- As shown in Figure 6. . . surface pressure reduction is closely associated with enhanced upward motion. Please use the same map in Figures 5 and 6 in order to see this association.

Good suggestion. Now we use the same map for Figures 5 and 6 (see below), and put the original Figure 6 (using polar projection) into the supporting information (i.e., Figure S23):

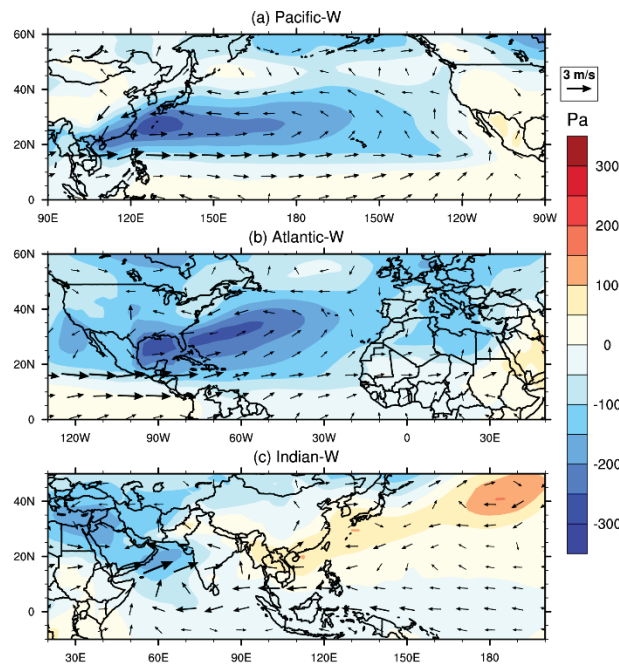


Figure 5. Changes in the surface pressure (color contours, Pa) and 850-hPa wind (arrows, m s^{-1}) for (a) Pacific-W, (b) Atlantic-W, and (c) Indian-W relative to the CTRL in the boreal summer.

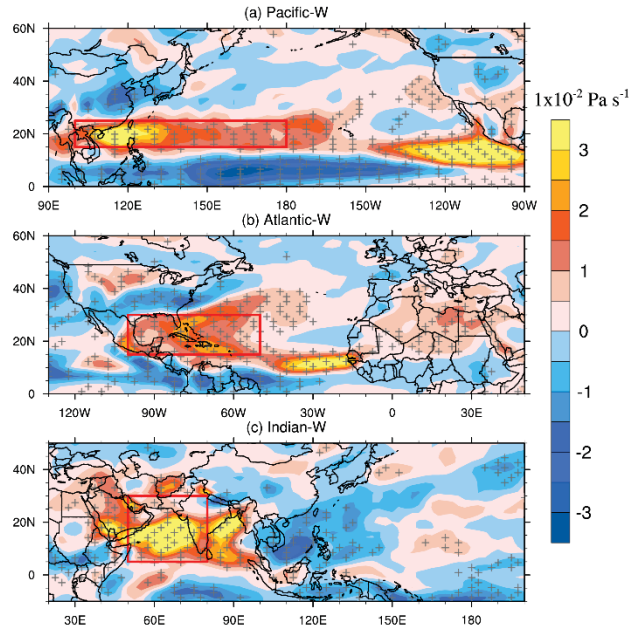


Figure 6. Spatial pattern of vertical velocity changes at 500 hPa (color contours, $1 \times 10^{-2} \text{ Pa s}^{-1}$) for (a) Pacific-W, (b) Atlantic-W, and (c) Indian-W relative to the CTRL in the boreal summer. Positive values indicate upward motion. Red polygons denote the regions where the surface pressure responses to SST anomalies are significant (see Figure 5 a-c). The + symbols indicate areas where the results are significant at the 0.05 level, evaluated by Student's t-test using 20 years of data.

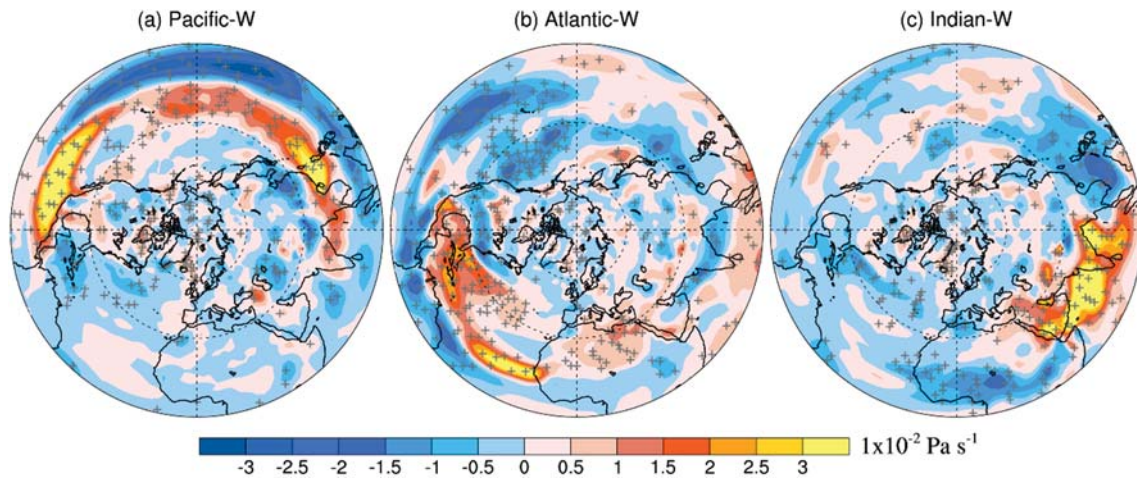


Figure S23. Spatial pattern of vertical velocity changes at 500 hPa (color contours, $1 \times 10^{-2} \text{ Pa s}^{-1}$) for (a) Pacific-W, (b) Atlantic-W, and (c) Indian-W relative to the CTRL in the boreal summer. Positive values indicate upward motion. The + symbols indicate areas where results are significant at the 0.05 level, evaluated by Student's t-test using 20 years of data.

14) Line 329- “This effect is confirmed by widespread decreases of upward vertical velocity”. Again it is hard to see if vertical velocity reductions are occurring only over the adjacent regions to the regions where the authors suggest enhanced convection may occur.

As shown in Figure 6, a basin-scale SST increase strengthens the upward motions locally. Adjacent to these anomalous upward motion, significant decreases of upward velocity are observed. For example, decreases of upward velocity are shown over East Asia associated with the North Pacific warming, and similarly the changes over North America associated with the North Atlantic warming. Additionally, decreases of upward vertical velocity are also demonstrated over higher latitudes and remote regions (shown in Figure S23). For example, the warming of the North Atlantic may induces a decrease of upward vertical velocity over the North Pacific. These effects have been reported in previous studies (Lau et al., 1997;Roxy et al., 2015;Ueda et al., 2015). We have optimized the relevant figures to verify our conclusion, please refer to our response to the former comment for the relevant figures (Figure 6 and Figure S23). We also modified the text below in Section 4.3 (P14-15, L416-422) for clarification:

“...Strengthened deep convection will trigger large-scale subsidence over nearby regions through the modulation of large-scale circulation patterns, which may suppress convective transport (Lau et al., 1997;Roxy et al., 2015;Ueda et al., 2015). This effect is verified by the decreases in upward velocity at 500 hPa. As depicted in Figure 6, significant decreases in upward velocity occur over regions adjacent to the strengthened deep convection. Similar effects are also observed over higher latitudes or remote oceans (Figure S23).”

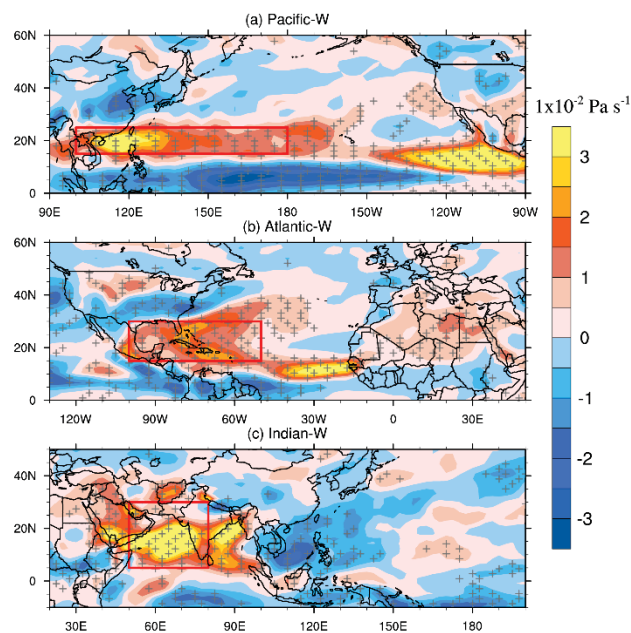


Figure 6. Spatial pattern of vertical velocity changes at 500 hPa (color contours, $1 \times 10^{-2} \text{ Pa s}^{-1}$) for (a) Pacific-W, (b) Atlantic-W, and (c) Indian-W relative to the CTRL in the boreal summer. Positive

values indicate upward motion. Red polygons denote the regions where the surface pressure responses to SST anomalies are significant (see Figure 5 a-c). The + symbols indicate areas where the results are significant at the 0.05 level, evaluated by Student's t-test using 20 years of data.

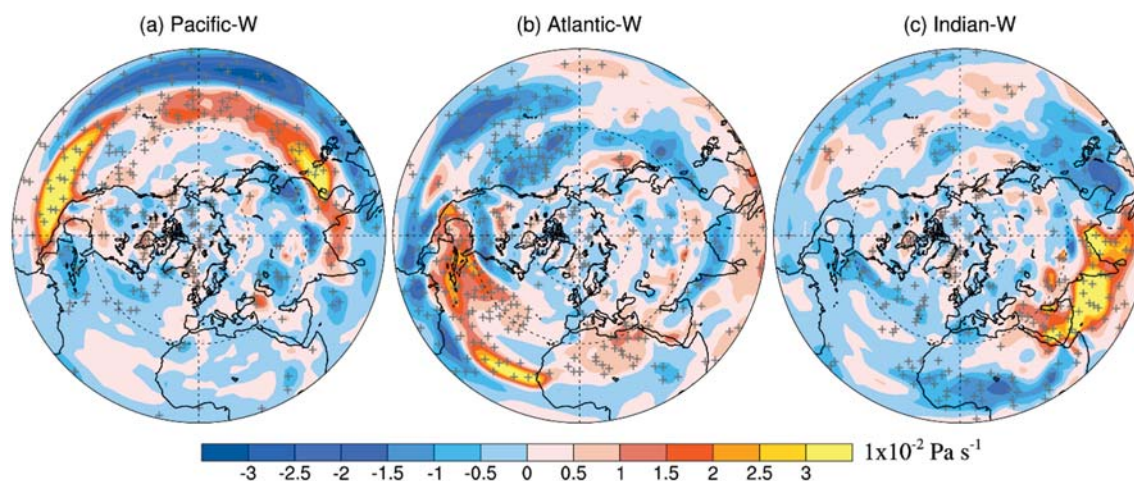


Figure S23. Spatial pattern of vertical velocity changes at 500 hPa (color contours, $1 \times 10^{-2} \text{ Pa s}^{-1}$) for (a) Pacific-W, (b) Atlantic-W, and (c) Indian-W relative to the CTRL in the boreal summer. Positive values indicate upward motion. The + symbols indicate areas where results are significant at the 0.05 level, evaluated by Student's t-test using 20 years of data.

15) Line 333-end of paragraph. This first sentence of the paragraph discusses atmospheric stability based on zonal mean large-scale temperatures changes between the upper and lower troposphere (a weaker vertical temperature gradient; Figure S3) and stagnation/ventilation which are local processes often related to surface winds. Hence these processes may not be as simply related as suggested. In addition, a differential ozone response over clean and polluted regions seem unlikely to be associated with change in atmospheric stability associated with large-scale increases in upper tropospheric temperature. The final sentence of the paragraph needs substantiated especially given the link proposed in the previous section between clean regions with reduced net ozone production due to greater destruction.

Referring to our response to major comment 4, we agree that stagnation/ventilation were improperly used here and have rephrased our explanation in the revised manuscript. The basin-scale SST increase not only strengthens upward motions over the low-latitudes of the specific ocean, but also leads to the decrease of upward velocity over mid-latitudes (Figure S23). Previous studies have revealed that strengthened deep convection will trigger large-scale subsidence over other regions through modulating large-scale circulations, which may suppress convective air movement there (Lau et al., 1997; Roxy et al., 2015; Ueda et al., 2015). Here we also demonstrate a

weaker vertical temperature gradient associated with regional SST warming (Figure S16). Both factors (i.e., large-scale subsidence and weaker vertical temperature gradient) tend to slow down vertical air movement. In the revised manuscript, we further examined the vertical transport of O_3 based on the IPR analysis (shown in Figure S12). It shows a wide-spread reduction of transport of O_3 by vertical diffusion to the surface (i.e. VDIF). Considering that the responses of O_3 destructions to SST anomalies are more important over oceans than land (referring to our reply to previous comment 12), it is reasonable for us to infer that this reduced vertical transport may also exert a negative effect on surface O_3 over clean continents. Please see the relevant figures below. A detail explanation is provided in Section 4.3 of our revised manuscript (P14-15, L416-430):

“Strengthened deep convection will trigger large-scale subsidence over nearby regions through the modulation of large-scale circulation patterns, which may suppress convective transport (Lau et al., 1997; Roxy et al., 2015; Ueda et al., 2015). This effect is verified by the decreases in upward velocity at 500 hPa. As depicted in Figure 6, significant decreases in upward velocity occur over regions adjacent to the strengthened deep convection. Similar effects are also observed over higher latitudes or remote oceans (Figure S23). Meanwhile, the air temperature increase in response to regional SST warming is more significant above the lower troposphere, which leads to a decrease in the vertical temperature gradient (Figure S16). These factors tend to restrain the vertical exchange of air pollutants at mid-latitudes, which facilitates surface O_3 accumulation over polluted continental regions in JJA but may weaken the intrusion of O_3 from the upper troposphere to the surface in most unpolluted areas. This process helps to explain the widespread decrease in surface O_3 over unpolluted regions associated with an SST increase, as described in Section 3, and can be further verified by the wide-spread reduction in VDIF shown in Figure S12.”

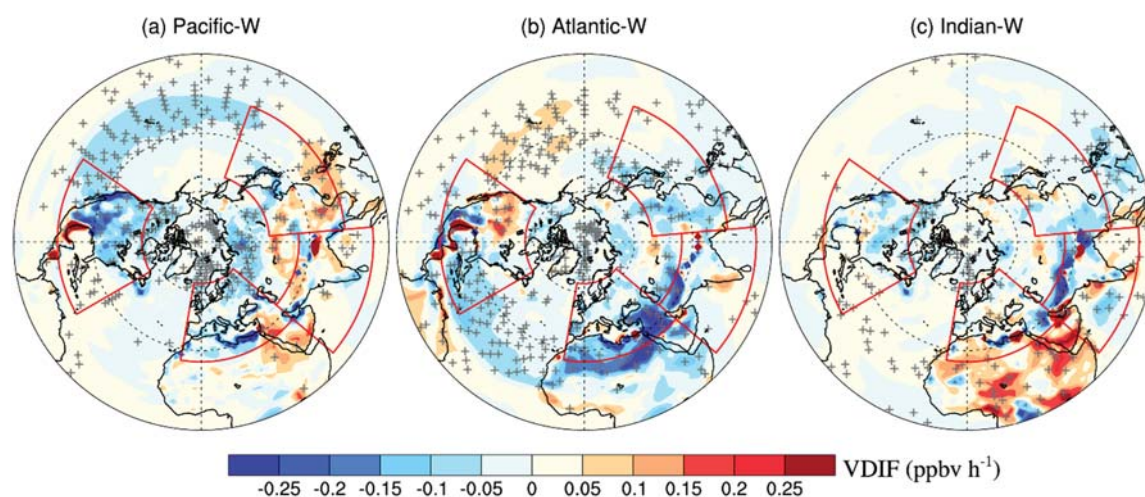


Figure S12. Changes in VDIF (ppbv h^{-1}) for (a) Pacific-W, (b) Atlantic-W and (c) Indian-W relative to the CTRL in the boreal summer. The four major regions of interest (i.e., NA, EU, EA and SA) are marked by red solid lines. The + symbols denote areas where the results are significant at the 0.05 level, evaluated by Student's t-test using 20 years of data.

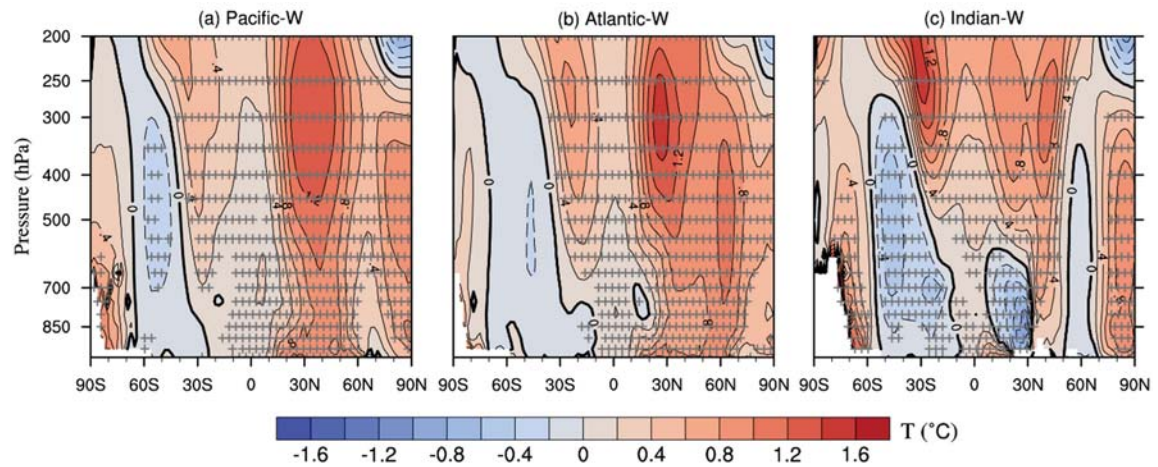


Figure S16. Vertical-meridional distributions of changes in the air temperature (contours, $^{\circ}\text{C}$) for (a) Pacific_W (zonal averaged from 100°E - 90°W), (b) Atlantic_W (zonal averaged from 100°W - 180°W) and (c) Indian_W (zonal averaged from 30°E - 100°E) relative to the CTRL in boreal summer. Black solid and dashed lines in the contours indicate positive and negative air temperature anomalies, respectively (contour interval: 0.2°C). The + symbol denotes areas where the changes of air temperature are significant at the 0.05 level, evaluated by Student's t-test using 20 years of data.

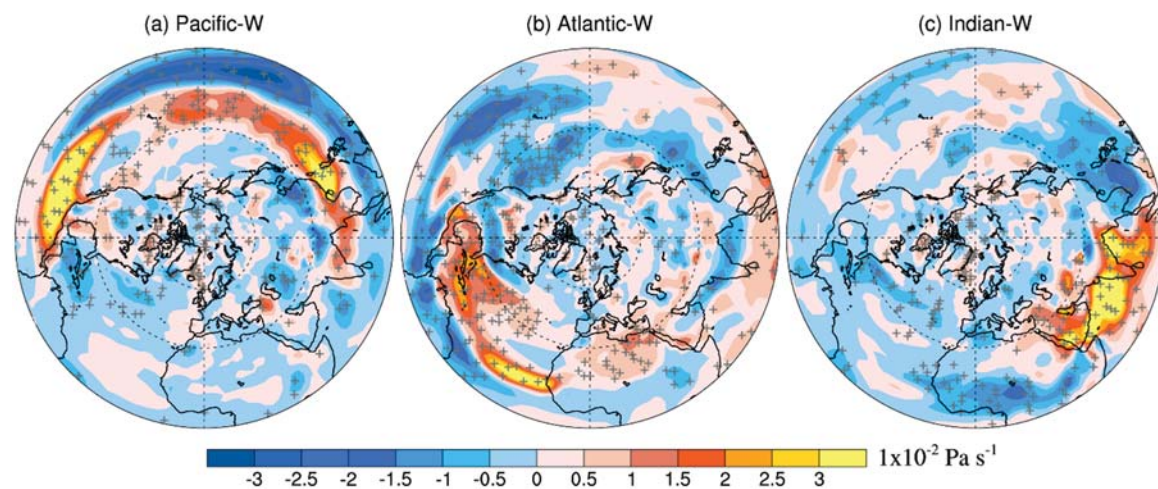


Figure S23. Spatial pattern of vertical velocity changes at 500 hPa (color contours, $1 \times 10^{-2} \text{ Pa s}^{-1}$) for (a) Pacific-W, (b) Atlantic-W, and (c) Indian-W relative to the CTRL in the boreal summer.

Positive values indicate upward motion. The + symbols indicate areas where results are significant at the 0.05 level, evaluated by Student's t-test using 20 years of data.

16) Line 341- please explain how a reduction in low pressure weakens the East Asian monsoon?

Good question. As shown in Figure 5, this low pressure induces a cyclonic anomaly in the lower troposphere over the subtropical northwestern Pacific. This weakens southwesterly winds to East China and thus the East Asian summer monsoon. However, East Asian summer monsoon is a rather complicated phenomenon when considering its onset, withdrawal, and relationship with precipitation. These factors are beyond the focus of this study. We therefore removed this discussion in Section 4.3. Now we have (see *P15, L433-437*):

“...For example, the low-pressure anomaly centered over the subtropical northwestern Pacific in the “Pacific-W” case causes the convergence of wind in the lower troposphere (Figure 5a). Consequently, surface O₃ pollution is enhanced in southern China due to an increase in O₃ transport from more polluted northern China (Figure 7a).”

17) Line 349/Line 357- if the IPR analysis refers to Figure 2 there seem to be a few inconsistencies – the influence of Pacific W on EA then VDIF appears to have the strongest role, yet advective transport is discussed here? The influence of the Atlantic W on NA then CHEM seems only to have a small contribution in Figure 2 and not be the main contribution discussed here. Furthermore, the logic of the argument that physical transport is not important because of large changes in the upper troposphere but small changes at the surface is unclear.

Thanks for pointing out this. The IPR analysis here does not refer to Figure 2. In Figure 2, we averaged IPR changes over East Asia. In this sentence, the IPR analysis only focus on southern China. The warming of the North Pacific increases the surface O₃ over upwind region in JJA, but this effect is insignificant when averaging over the whole East Asia (shown in Table 1). Correspondingly, the increase of VDIF over EA is also insignificant in JJA based on the IPR analysis. As shown in Figure 1, the increases of surface O₃ are highest over southern China while accompanied with a slight decrease over the North China. We find that the wind pattern anomaly induced by the warming of the North Pacific may be responsible for this dipole changes through modulating surface O₃ transport. The IPR analysis indicates that the increase in advective transport is mainly responsible for the surface O₃ increase in southern China. These results are not shown in the manuscript.

As for the cases of “Atlantic-W”, we find that the VDIF and DRYD are two processes that changes significantly over NA (Figure S10). However, they tend to offset each other in most places, resulting in an insignificant overall change in TURB (please see our revised Figure 2). Therefore, the change of CHEM are higher than TURB and dominates the surface O₃ increase over NA in “Atlantic-W” (as discussed in Section 4.1). Please refer to our response to specific comment 6 for more details. Here we further demonstrated the changes in horizontal fluxes of O₃ over NA in “Atlantic-W”, which shows no significant effect on the increase of surface O₃ (Figure 7b). Therefore, we conclude that the response of ground-level O₃ over North America to the North Atlantic warming is mainly caused by the enhanced chemical production, rather than physical transport. The discussion of the difference in O₃ changes between upper troposphere and surface is not a supporting argument. It only indicates that O₃ transport maybe more important over upper troposphere.

We have clarified our descriptions in Section 4.3 (P15, L432-442 and L444-450) as follows:

“The surface pressure anomalies induced by SST changes can play a dominant role in modulating surface O₃ transport at specific locations. For example, the low-pressure anomaly centered over the subtropical northwestern Pacific in the “Pacific-W” case causes the convergence of wind in the lower troposphere (Figure 5a). Consequently, surface O₃ pollution is enhanced in southern China due to an increase in O₃ transport from more polluted northern China (Figure 7a). The vertical distribution of the corresponding O₃ changes also shows that the increase in O₃ over southern China occurs below 700hPa, accompanied by noticeable decreases above 700hPa as well as over nearby northern China (Figure 7d). The IPR analysis also indicates that the increases in advective transport and downward turbulent transport are mainly responsible for the surface O₃ increase in southern China.”

“In the “Atlantic-W” case, the SST warming-induced surface pressure anomalies lead to substantial O₃ redistribution, especially over the North Atlantic Ocean (Figure 7b). For North America, the changes in horizontal O₃ fluxes have no significant effect on the O₃ concentration increase. In addition, O₃ changes are observed to be larger in the upper troposphere than at the surface (Figure 7e). As demonstrated in Section 4.1, the response of lower-altitude O₃ over North America to the North Atlantic warming is mainly caused by enhanced chemical production, rather than physical transport.”

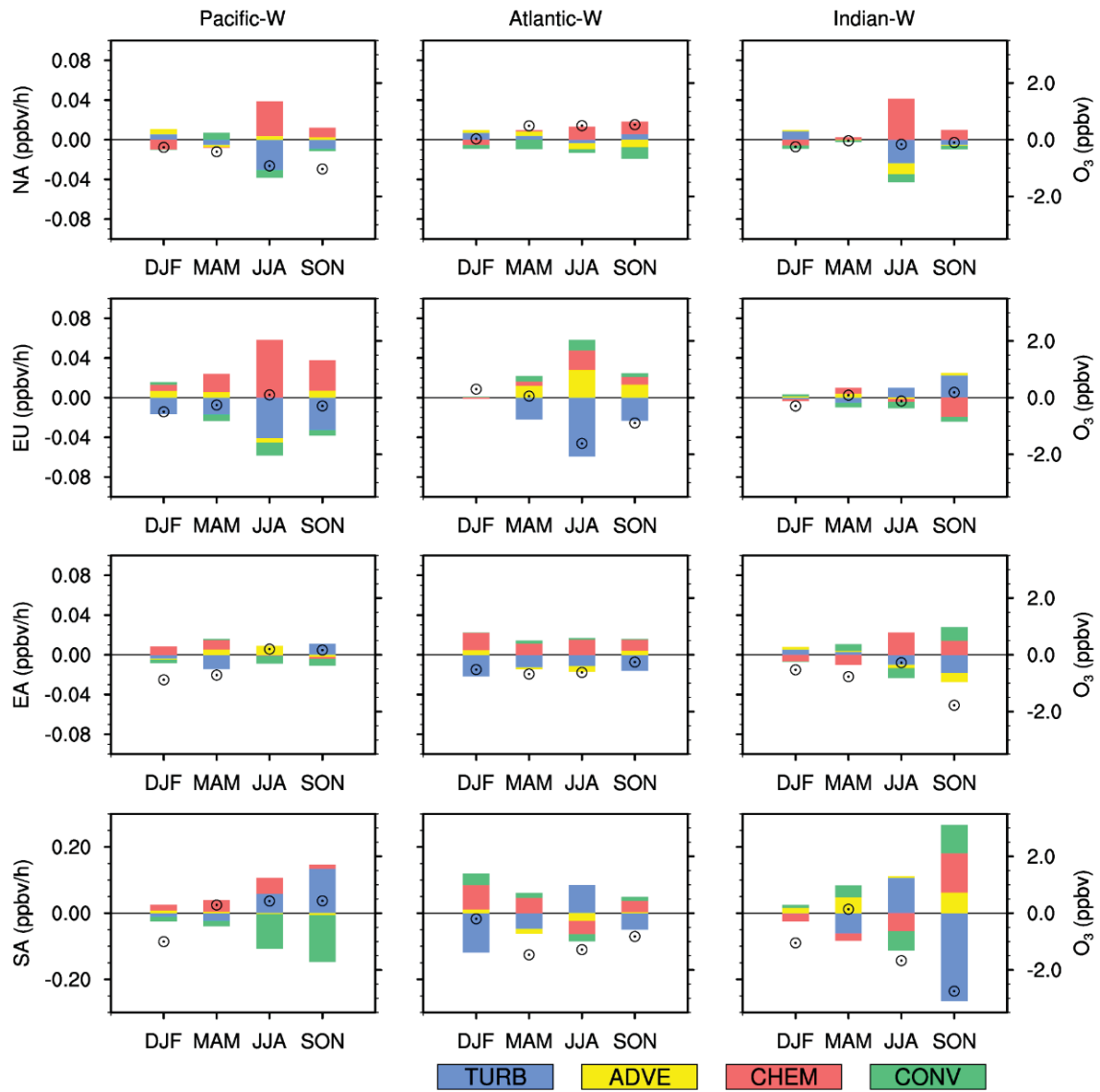


Figure 2. Seasonally averaged changes in the IPR contributions (bars, ppbv/h, left scale) and surface O₃ concentrations (hollow circles, ppbv, right scale) for Pacific-W (left), Atlantic-W (middle) and Indian-W (right) relative to the CTRL. Values are regionally averaged over NA (first row), EU (second row), EA (third row) and SA (last row). TURB is defined as the sum of VDIF and DRYD. CONV is the sum of DEEP and SHAL. IPR contributions from the four processes (i.e., TURB, ADVE, CHEM and CONV) are represented by different colors. A more detailed IPR result is shown in Figure S10 in the supplementary material.

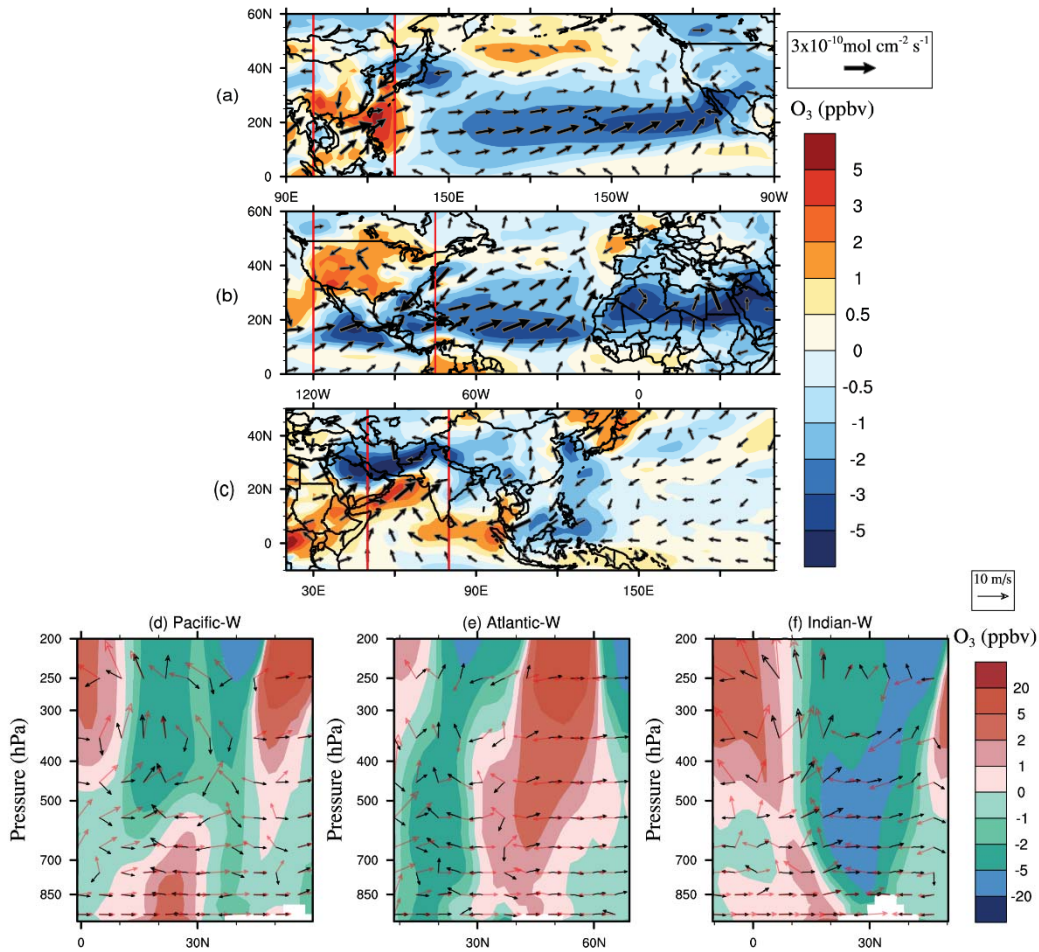


Figure 7. Top three rows: Changes in O₃ concentrations (color contours, ppbv) and horizontal fluxes (arrows, mol cm⁻² s⁻¹) at the surface level for (a) Pacific-W, (b) Atlantic-W, (c) Indian-W relative to the CTRL in the boreal summer. Last row: zonal average of the tropospheric O₃ changes (color contours, ppbv), wind fluxes in CTRL (red arrows, m s⁻¹) and the wind flux perturbation (black arrows, m s⁻¹) in (d) Pacific-W, (e) Atlantic-W, (f) Indian-W relative to the CTRL in the boreal summer. The red rectangles in (a), (b) and (c) denote the longitudinal range used for the zonal averages in (d), (e) and (f), respectively. The vertical wind velocity is amplified 1000 times to make it comparable to the horizontal wind velocity.

18) Line 380 to end of paragraph- The results in figures 8 (CO tracer) and 7 (ozone concentrations) look similar and reinforce each other except over the Indian Ocean. Please comment on this.

Good suggestion! Given that the CO-like tracers added in our simulation are idealized with fixed decay lifetime, their concentration changes associated with SST anomalies can be completely

attributed to the corresponding changes of air mass. As shown in Figure 8a, changes in surface concentrations of CO-like tracer emitted from EA resembles that of surface O₃ depicted in Figure 7a. This indicates that changes in transport associated with North Pacific warming play an important role in redistributing the surface O₃ over East Asia. As for the CO-like tracer emitted from NA in the “Atlantic-W” case, it shows a slight increase at the surface over the NA source. However, the spatial pattern of its concentration change (Figure 8c) is not consistent with that of O₃ (Figure 7b). This is because the increase of surface O₃ over NA is mainly caused by the enhanced chemical production, which deviates it substantially from the CO-like transport pattern. The response of the South Asia CO tracer to North Indian Ocean warming also shows an inconsistent spatial pattern with that of surface O₃ concentrations, suggesting the importance of chemistry on surface O₃. Therefore, the diagnosis of CO-like tracers not only infers the response of O₃ long-range transport to SST anomalies, but can also help to verify our previous arguments. We have improved this text and added more discussions in the revised manuscript (P17, L477-487).

“...Because the CO-like tracers added in the simulation have a fixed decay lifetime, their concentration changes are completely caused by the SST-induced transport anomalies. The decrease in CO tracer concentrations over downwind regions suggests that the warming of basin-scale SST tends to suppress the long-range transport of air pollutants. Additionally, in the “Pacific-W” case, changes in the East Asian CO tracer (Figure 8a) generally resemble the changes in surface O₃ over East Asia (Figure 7a), indicating the dominant effect of physical transport on the O₃ distribution over East Asia. Regarding the North American CO tracer in response to the North Atlantic warming or the South Asian CO tracer in response to the North Indian Ocean warming, their concentration changes are spatially inconsistent with those of O₃ (see Figures 7 and 8). This further indicates the distinct roles that different basin-scale SSTs play in nearby air quality.”

19) Line 395 to end of paragraph- Is significance plotted in figure 9? The text cannot be followed well here with the current figure quality. The conclusion on vertical diffusion is hard to follow, given text in previous sections discussing areas of both enhanced convection and subsidence in the ocean basin and downwind.

Thanks for pointing this problem out. We have improved the quality of Figure 9. The changes of zonal wind depicted in Figure 9 have been verified to be significant at 0.05 level with the Student t-test using 20 years of data.

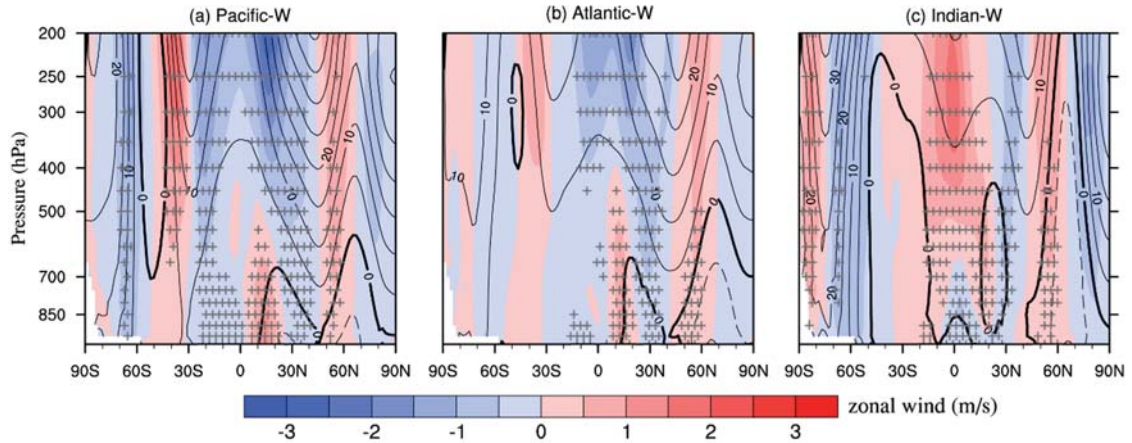


Figure 9. Zonally averaged changes in zonal wind (color contour, m/s) and geopotential height (contour, m) for (a) Pacific-W, (b) Atlantic-W and (c) Indian-W relative to the CTRL in the boreal summer. Black solid and dashed lines in the contours indicate positive and negative geopotential height anomalies, respectively (contour interval: 5 m). The + symbol denotes areas where the zonal wind changes are significant at the 0.05 level, evaluated by Student’s t-test using 20 years of data.

This discussion here mainly focuses on the circulation pattern changes induced by basin-scale SST changes. Our result shows that the response of air temperature to a warmer North Pacific or North Atlantic mainly happens in the mid-latitudes (Figure 9). Thus, the associated meridional temperature gradient is decreasing at lower latitudes while increasing at higher latitudes. Consequently, it weakens the westerly wind at lower mid-latitudes ($25^{\circ}\text{N} - 45^{\circ}\text{N}$) while intensifies it at higher latitudes. As for vertical transport (mainly discussed in Section 4.3), a warmer basin-scale SST facilitates the deep convection over tropical regions while suppresses the upward transport at higher latitudes. The decreases of upward velocity at mid-latitudes are also demonstrated in Figure 6 and Figure S6. A detail description is provided in Section 4.3 (see our response to specific comments 13 and 15). Therefore, here we attribute the decreases in CO tracer transport to remote regions (Figure 8a and 8c) to the suppressed vertical transport and weakened westerlies at mid-latitudes. We have clarified this text in our revised manuscript (see *PI7, L489-502*).

“Further investigations of zonal wind suggest that an increase in SST over different oceans consistently decreases the westerly winds at lower mid-latitudes ($25^{\circ}\text{N} - 45^{\circ}\text{N}$) in the Northern Hemisphere but increases these winds at higher latitudes (Figure 9). In general, increases in the geopotential height induced by basin-scale SST warming are more significant at mid-latitudes than at other latitudes, which is consistent with the air temperature changes. Consequently, the meridional geopotential height gradient is decreasing at lower latitudes but increasing at higher latitudes, leading to corresponding changes in the westerly winds. The latitude band at $25^{\circ}\text{N} -$

45 °N covers many polluted regions (i.e., North America and East Asia). A weakened westerly wind may reduce long-rang O₃ transport. As demonstrated in Section 4.3, the basin-scale SST increases also exert negative effects on the upward transport of air masses at mid-latitudes. Therefore, the decreases in CO tracer concentrations over downwind regions (Figure 8a and 8c) can be explained by both suppressed vertical transport and weakened westerly winds.”

20) Line 435- “90% of surface O₃”- first mention of this in the text.

Thanks for pointing out this. We have rephrased this in the revised manuscript (P19, L542-545).

“...Specifically, the chemical production changes are mainly responsible for the surface O₃ increases over North America in response to the North Atlantic SST warming but exert a negative effect on South Asia in response to the North Indian SST warming.”

Minor comments:

1) Line 49- it would be useful to state why ground-level ozone affects food security. Also it would be useful to provide a more up to date reference than 2006 for WHO.

Good suggestion! We have specified the ground-level ozone effects on human health and food security. We have also provided more recent references (see P2, L50-52):

“High ground-level ozone (O₃) concentrations adversely impact human health by inducing respiratory diseases and threaten food security by lowering crop yields (Brown and Bowman, 2013;Organization, 2013;Chuwah et al., 2015).”

2) Line 54- again can the authors use a more recent reference than Vingarzan et al. 2004.

We have added several more recent references here (P2, L57-58)

“These precursors originate from both natural and anthropogenic sources (Vingarzan, 2004;Simon et al., 2014; Jiang et al., 2016).”

3) Line 66- an enhanced description of what is meant by atmospheric circulations would be useful e.g. Barnes and Fiore (2013) specifically discuss the effect of the Jetstream in the northern midlatitudes at 500 hPa. Other processes to mention are mid-latitude cyclones and the North

Atlantic Oscillation for the N. Atlantic. Some further useful references include: Creilson et al. 2003; Christoudias et al. 2012; Knowland et al. 2014. Line et al. (2012/14) and references therein are useful for circulations relating to atmospheric circulations in the N. Pacific.

Creilson, J. K., Fishman, J., and Wozniak, A. E.: Intercontinental transport of tropospheric ozone: a study of its seasonal variability across the North Atlantic utilizing tropospheric ozone residuals and its relationship to the North Atlantic Oscillation, *Atmos. Chem. Phys.*, 3, 2053–2066, doi:10.5194/acp-3-2053-2003, 2003

Christoudias, T., Pozzer, A., and Lelieveld, J.: Influence of the North Atlantic Oscillation on air pollution transport, *Atmos. Chem. Phys.*, 12, 869–877, doi:10.5194/acp-12-869-2012, 2012
Knowland, K. E., Doherty, R. M., and Hodges, K. I.: The effects of spring-time mid-latitude storms on trace gas composition determined from the MACC reanalysis, *Atmos. Chem. Phys.*, 15, 3605–3628, doi:10.5194/acp-15-3605-2015, 2015.

Good suggestion. These references are valuable and closely related to our work. We have cited them and expanded our introduction with more detailed descriptions (see *P3, L72-83*).

“...Atmospheric circulation considerably determines the timescale and pathway of O₃ transport (Bronnimann et al., 2000; Auvray and Bey, 2005; Hess and Mahowald, 2009). The efficiency of O₃ transport varies coherently with atmospheric circulations on different scales. Knowland et al. (2015) demonstrated the important role of mid-latitude storms in redistributing O₃ concentrations during springtime. The North Atlantic Oscillation (NAO) significantly affects surface and tropospheric O₃ concentrations over most of Europe by influencing the intercontinental transport of air masses (Creilson et al., 2003; Christoudias et al., 2012; Pausata et al., 2012). Lamarque and Hess (2004) indicated that the Arctic Oscillation (AO) can modulate springtime tropospheric O₃ burdens over North America. The shift in the position of the jet stream associated with climate change was found to strongly affect summertime surface O₃ variability over eastern North America (Barnes and Fiore, 2013).”

4) Line 79- what is meant by “SST is an indicator for both marine and terrestrial meteorology”?

Here we want to emphasize the important role of SST played in the climate system. The SST anomalies have been widely used to indicate the climate variability and have great implications for climate predictions. We have rephrased this in the revised manuscript (*P4, L95-96*):

“Sea surface temperature (SST) is an important indicator that characterizes the state of the climate system.”

5) Line 83- perhaps the reference to the text book is unnecessary.

We agree that the reference to the text book is unnecessary here and have removed it.

6) Line 87- some recent references from the IPCC AR5 report will be relevant here.

We have updated our references with more recent studies (P4, L101-104).

“...Numerous studies have shown that SST changes over different oceans and at different latitudes lead to significantly different meteorological sensitivities and climate responses (Webster, 1981; Lau and Nath, 1994; Lau, 1997; Sutton and Hodson, 2007; Sabeerali et al., 2012; Ueda et al., 2015).”

7) Line 92- it would be more useful to the reader to refer to the specific chapter in IPCC AR5- the science of climate change that discusses SST changes rather than broadly reference the IPCC synthesis report.

Good suggestion! We have changed our reference to the Chapter 2 in IPCC AR5 (P4, L107-108):

“SSTs are generally increasing due to the impacts of anthropogenic forcings on global climate change (IPCC, 2013, Chapter 2).”

8) Line 102- is “according to observations” needed?

We agree that it is an unnecessary description here and has removed it in our revised manuscript (P4, L117-119).

“The North Atlantic Ocean pronounces various modes of low-frequency SST variability (Kushnir, 1994; Wu and Liu, 2005; Fan and Schneider, 2012; Taboada and Anadon, 2012).”

9) Line 105 “Emissions of aerosols.. complicate regional SST variability because of their climate effects”- this sentence is unclear.

Here we state that regional SST can be significantly influenced by the aerosol and GHGs emitted from anthropogenic and natural sources through modulating the solar radiation at an oceanic surface. These processes may contribute to the SST variability, especially in the regional scale. For example, the responses of SST to volcanic eruptions have been identified to vary between regions. We have clarified these sentences in the revised manuscript (P4-5, L121-124).

“...Aerosols and greenhouse gases (GHGs) emitted from anthropogenic and natural sources also contribute to regional SST variability through modulation of the solar radiation received by the ocean surface (Rotstayn and Lohmann, 2002; Wu and Kinter, 2011; Hsieh et al., 2013; Ding et al., 2014; Meehl et al., 2015).”

10) Line 113- besides Lin et al. 2014, Liu et al. (2005) is also a valuable reference here in relation to ENSO and pollution transport from East Asia. Liu, J., D. L. Mauzerall, and L. W. Horowitz (2005), Analysis of seasonal and interannual variability in transpacific transport, *J. Geophys. Res.*, 110, D04302, doi:10.1029/2004JD005207.

Good suggestion. Liu et al. (2005) evaluated the meteorological component of the seasonal and interannual variability of transpacific transport. It is a valuable reference that relates the transpacific pollution transport to ENSO. Their analysis is mainly based on idealized tracer with constant emissions and chemical lifetimes. This finding has valuable implication for the ENSO effects on O₃ long-rang transport. We have discussed it in our revised manuscript (P5, L133-135).

“Liu et al. (2005) revealed that El Niño winters are associated with stronger transpacific pollutant transport, which also has implications for the long-range transport of O₃.”

11) Line 119- it would be useful to first discuss the surface ozone response for the specific ocean basin relative to the experiment and then discuss effects on surrounding continents. The four continental regions used in Fiore et al. (2009) and elsewhere should be defined here, as they are used throughout the text.

Good suggestion. We agree that it is beneficial to provide some discussion about the surface O₃ changes above ocean basins associated with regional SST anomalies. We have added some descriptions and explanations about those effects. The relevant table and figure are placed in the supplementary material. Please refer to our reply to major comment 3 for details. The major focus of this study is on the responses of surface O₃ over polluted continents to regional SST changes. The surface O₃ levels over these regions are much higher than remote oceans, which may negatively impacts human health and threatens food security. This SST-O₃ relationship over the populated continents may help air quality management. We have also clearly defined the four continental regions in the revised manuscript (P5, L140-144).

“To fill this gap, this study focuses on examining the sensitivity of O₃ evolution over four polluted continental regions in the Northern Hemisphere (i.e., North America (NA, 15°N–55 °N; 60°W–125°W), Europe (EU, 25°N–65 °N; 10°W–50 °E), East Asia (EA, 15 °N–50 °N; 95°E–160 °E) and South Asia (SA, 5 °N–35 °N; 50 °E–95°E), defined in Fiore et al. (2009)) with respect to nearby basin-scale SST changes.”

12) Line 157 typo- AEROCOM

Thanks for catching this typo. We have corrected it (P6, L178-180).

“...Anthropogenic emissions of chemical species are from the IPCC AR5 emission datasets (Lamarque et al., 2010), whose injection heights and particle size distributions follow the AEROCOM protocols (Dentener et al., 2006).”

13) Line 161 – “scientifically” is unnecessary.

We have removed this unnecessary description (P7, L184-185).

“...The performance of CESM in simulating tropospheric O₃ has been validated by comparing with ozonesondes and satellite observations (Tilmes et al., 2014).”

14) Line 251- “similar increases in VDIF” compared to?

We have clarified this in the revised manuscript (P11, L323-325).

“...In the “Atlantic-W” case, increases in VDIF are also observed over the upwind regions (i.e., North America) in JJA.”

15) Line 273- explain how net production rate in this section related to CHEM in the previous section.

Good question. The CHEM refers to the net cumulated contributions of the chemical production and loss of O₃ during a specific period. The net production rate is calculated by chemical production rate minus loss rate of O₃. Therefore, the CHEM and net-production rate are consistent with each other but indicate the O₃ change at different timescale. We have clearly defined these two variables in our revised manuscript.

In Section 2.3 (P8, L230-233):

“...Wet deposition and aqueous-phase chemistry are ignored here due to the low solubility and negligible chemical production of O₃ in water (Jacob, 1999). Therefore, CHEM represents the net production (production minus loss) rate of O₃ due to gas-phase photochemistry.”

In Section 4.2 (P12, L350-351):

“Changes in the net production rate (i.e., chemical production rate minus loss rate) of O₃ at the surface in JJA associated with basin-scale SST increases are shown in Figure 3.”

16) Line 305 – rephrase “jointly destructs O₃ production”.

We have rephrased this (P14, L389-391):

“...In addition, over South Asia, a warming of the North Indian Ocean decreases solar radiation and air temperature, and simultaneously increases air humidity, which jointly exert negative effects on O_3 production in that region.”

17) Lines 320-323, “Given that . . .)” This sentence contains a number of grammar errors. The following sentence starting line 323 seems to state that the pressure difference induced by warmer SSTs would be greater at lower latitude but notes this is not shown here in Figure 5. Please comment further on this or remove.

Thanks for pointing out this problem. We have revised this sentence to correct grammars errors. We also linked the warmer SST directly to the enhanced upward motion instead of the surface pressure changes (as showed in Figure 6). Please see the revised text in Section 4.3 (P14, L408-414) or below:

“...Previous studies have identified an SST threshold (approximately 26° – 28° C) to generating deep convection (Graham and Barnett, 1987; Johnson and Xie, 2010). Therefore, the sensitivity of deep convection to an SST anomaly is strongly dependent on the distribution of base SST. The enhanced upward motion in response to a uniform increase in basin-scale SST mainly occurs over regions with high climatological SST (Figure 6). Regions with a low climatological SST have little effects on the vertical movement of air masses.”

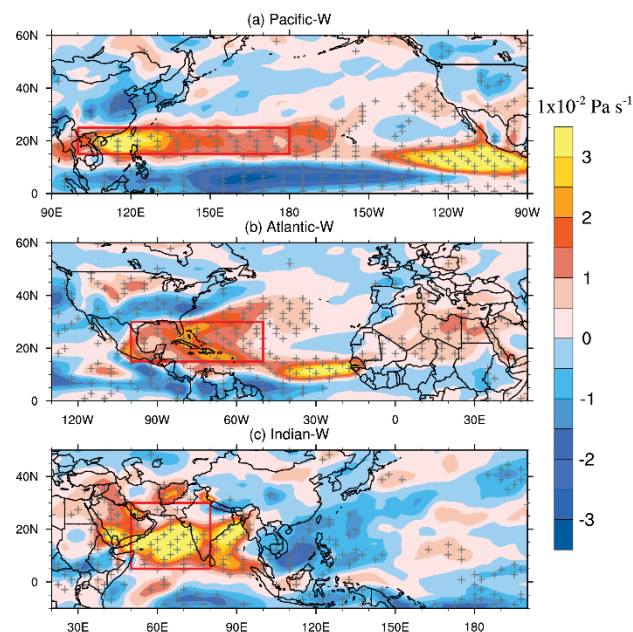


Figure 6. Spatial pattern of vertical velocity changes at 500 hPa (color contours, $1 \times 10^{-2} \text{ Pa s}^{-1}$) for (a) Pacific-W, (b) Atlantic-W, and (c) Indian-W relative to the CTRL in the boreal summer. Positive values indicate upward motion. Red polygons denote the regions where the surface pressure responses to SST anomalies are significant (see Figure 5 a-c). The + symbols indicate areas where

the results are significant at the 0.05 level, evaluated by Student's t-test using 20 years of data.

18) Line 363- Mediterranean?

As shown in Figure 5, the warming of the North Indian SST leads to a low-pressure anomaly that spreads to the Saudi Arabia and eastern Mediterranean. However, its effects on the Europe has proved to be insignificant (as shown in Table 1). To avoid confusion, we revised this sentence in Section 4.3 (P16, L452-453) and confined our analysis to the Indian Ocean and the Indian Subcontinent.

“The North Indian SST warming leads to a low-pressure anomalies centered over the Arabian Sea (Figure 5c).”

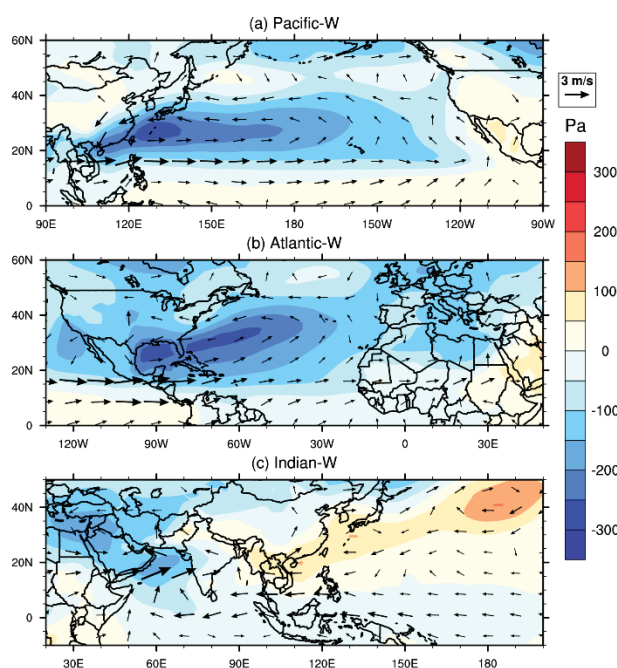


Figure 5. Changes in the surface pressure (color contours, Pa) and 850-hPa wind (arrows, m s^{-1}) for (a) Pacific-W, (b) Atlantic-W, and (c) Indian-W relative to the CTRL in the boreal summer.

19) Line 367-“Downward diffusion from the upper troposphere”- please clarify what is meant here as this is not a region of STE.

According to the IPR analysis, we find that the surface O_3 increase over the Indian Ocean associated with North Indian warming is mainly attributed to the enhanced vertical transport of O_3 to the surface through deep convection and vertical diffusion processes (Figure S11). It is not

related to the STE. We have clarified this in Section 4.3 of our revised manuscript (P16, L456-459).

“...According to the IPR analysis, the surface O_3 increase over the Indian Ocean is mainly caused by the enhanced vertical transport of O_3 to the surface through deep convection and vertical diffusion processes (Figure S11).”

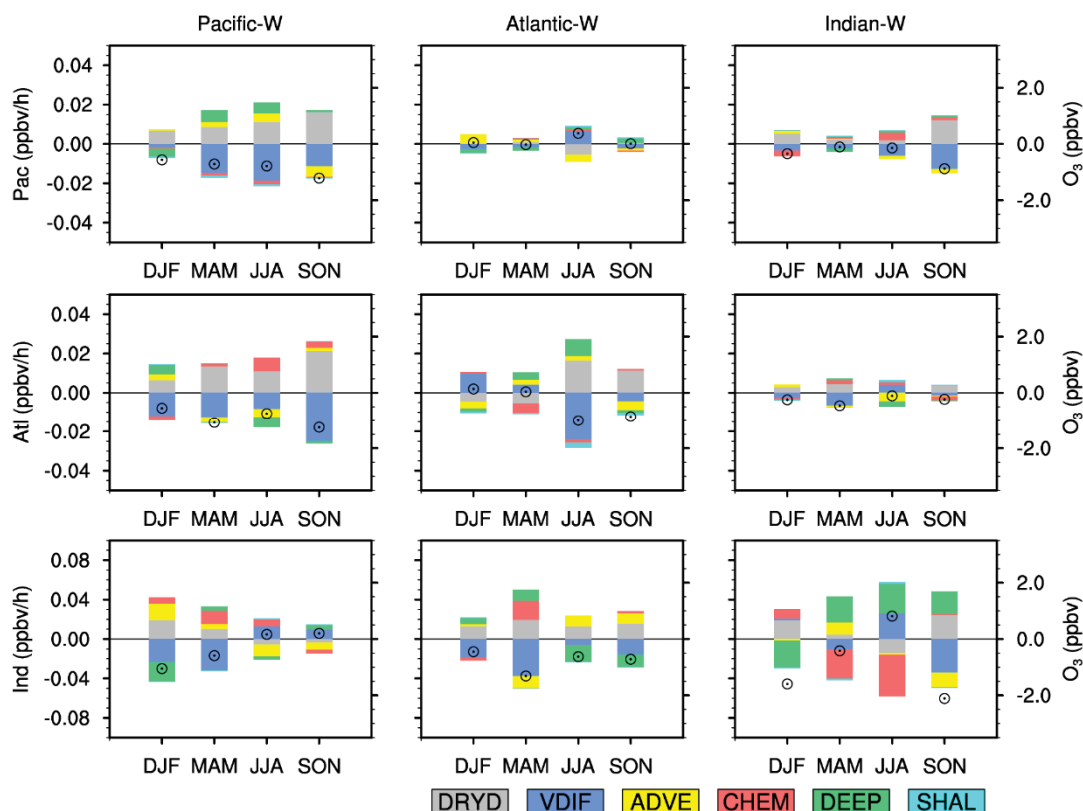


Figure S11. Seasonally averaged changes in IPR contributions (bars, ppbv h^{-1} , left scale) and surface O_3 concentrations (hollow circles, ppbv, right scale) for Pacific-W (left), Atlantic-W (middle) and Indian-W (right) relative to the CTRL. Values are regionally averaged over North Pacific (demoted as Pac, first row), North Atlantic (demoted as Atl, second row) and North Indian Ocean (demoted as Ind, third row) defined in our study, respectively. IPR contributions from six processes (i.e., CHEM, ADVE, VDIF, DRYD, SHAL and DEEP) are represented by different colors.

20) Line 374- why only at mid-latitudes? Figure S3 shows large temperature increases in temperature above all 3 basins.

Good question. As we have discussed in Section 4.3, the SST warming over a specific ocean basin tends to enhance the deep convection over tropical oceans. Strengthened deep convection further trigger large-scale subsidence over other areas through modulating large-scale circulations, which may suppress air convective movement there (Lau et al., 1997;Roxy et al., 2015;Ueda et al., 2015). As depicted in Figure S23, decreases of upward vertical velocity are significant over mid-latitudes and other oceans. As shown in Figure S16 (i.e., the Figure S3 in old version), the warming of air temperature are more significant over free troposphere at mid-latitudes, which leads to a remarkable decrease in the vertical air temperature gradient. This weakens vertical movement of air pollution.

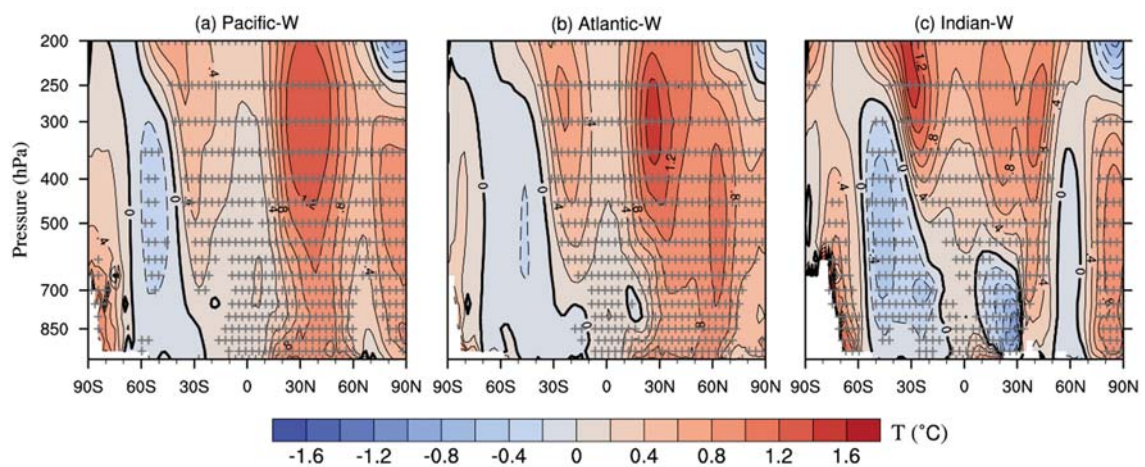


Figure S16. Vertical-meridional distributions of changes in the air temperature (contours, °C) for (a) Pacific_W (zonal averaged from 100°E-90°W), (b) Atlantic_W (zonal averaged from 100°W-180°W) and (c) Indian_W (zonal averaged from 30°E-100°E) relative to the CTRL in boreal summer. Black solid and dashed lines in the contours indicate positive and negative air temperature anomalies, respectively (contour interval: 0.2 °C). The + symbol denotes areas where the changes of air temperature are significant at the 0.05 level, evaluated by Student's t-test using 20 years of data.

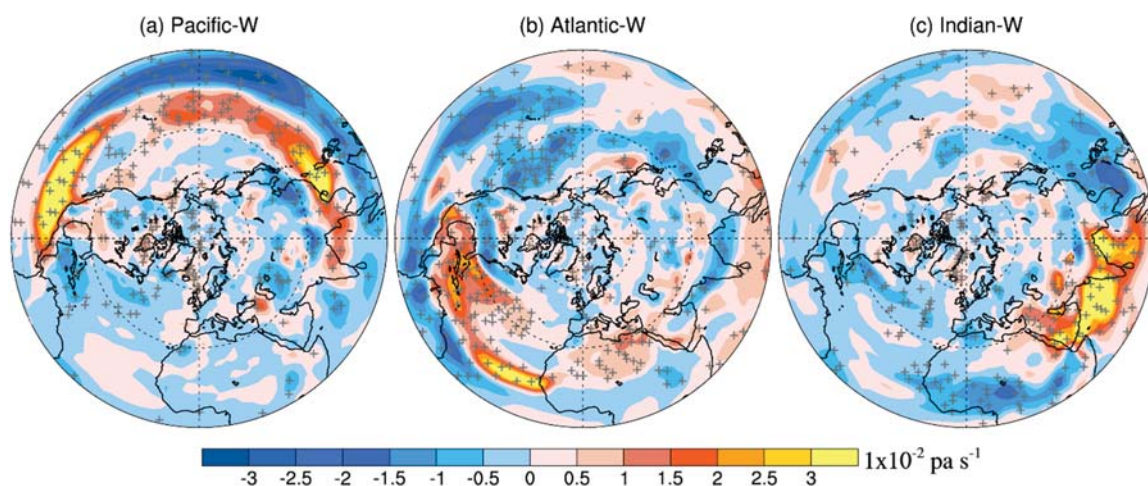


Figure S23. Spatial pattern of vertical velocity changes at 500 hPa (color contours, 1×10^{-2} Pa s⁻¹) for (a) Pacific-W, (b) Atlantic-W, and (c) Indian-W relative to the CTRL in the boreal summer. Positive values indicate upward motion. The + symbols indicate areas where results are significant at the 0.05 level, evaluated by Student’s t-test using 20 years of data.

21) Line 439/line 440 – rephrase “increasing influence on surface O₃ concentrations” as this is confusing e.g. regional surface ozone over SA decreases under the Indian W simulation.

We have rephrased this sentence in Section 6 (P19, L545-547).

“...Decreases in the convective transport of O₃ to the surface associated with North Indian warming are significant over South Asia and exert a negative impact on surface O₃ concentrations.”

22) Line 465 – natural variability is not discussed in this paper (although used for significance testing so it is odd to mention here).

The natural variability mentioned here is referred to the variability existed in the SST. As we have discussed in the Introduction section, regional SST exhibits natural periodic or irregular oscillations with timescales ranging from months to decades. In this study, we used idealized SST anomalies to generally compare the role of SST over different oceans in modulating the surface O₃ distributions. Our results highlight the sensitivity of the surface O₃ distribution to basin-wide SST changes. To provide a more realistically understanding of this SST-O₃ relationship, further studies are necessary and realistic SST variability should be taken into account. We have rephrased the relevant sentences in our summary section for clarification (P20, L569-574).

“Overall, our study highlights the sensitivity of O₃ evolution to basin-wide SST changes in the Northern Hemisphere and identifies the key chemical or dynamical factors that control this

evolution. However, to provide a more comprehensive understanding of the SST-O₃ relationship, further studies using realistic SST variability are necessary. This study may aid in the management of O₃ pollution by considering the influence of specific SST variability.”

23) Figure 6 refers to Figure 7 re surface pressure- should the reference be to Figure 5?

Thanks for pointing out this mistake. We have corrected the caption of Figure 6.

“Figure 6. *Spatial pattern of vertical velocity changes at 500 hPa (color contours, 1×10^{-2} Pa s⁻¹) for (a) Pacific-W, (b) Atlantic-W, and (c) Indian-W relative to the CTRL in the boreal summer. Positive values indicate upward motion. Red polygons denote the regions where the surface pressure responses to SST anomalies are significant (see Figure 5 a-c). The + symbols indicate areas where the results are significant at the 0.05 level, evaluated by Student’s t-test using 20 years of data.”*

24) Figure 7 – swap panels b) and c) to be consistent with text.

We have corrected this in the Figure 7.

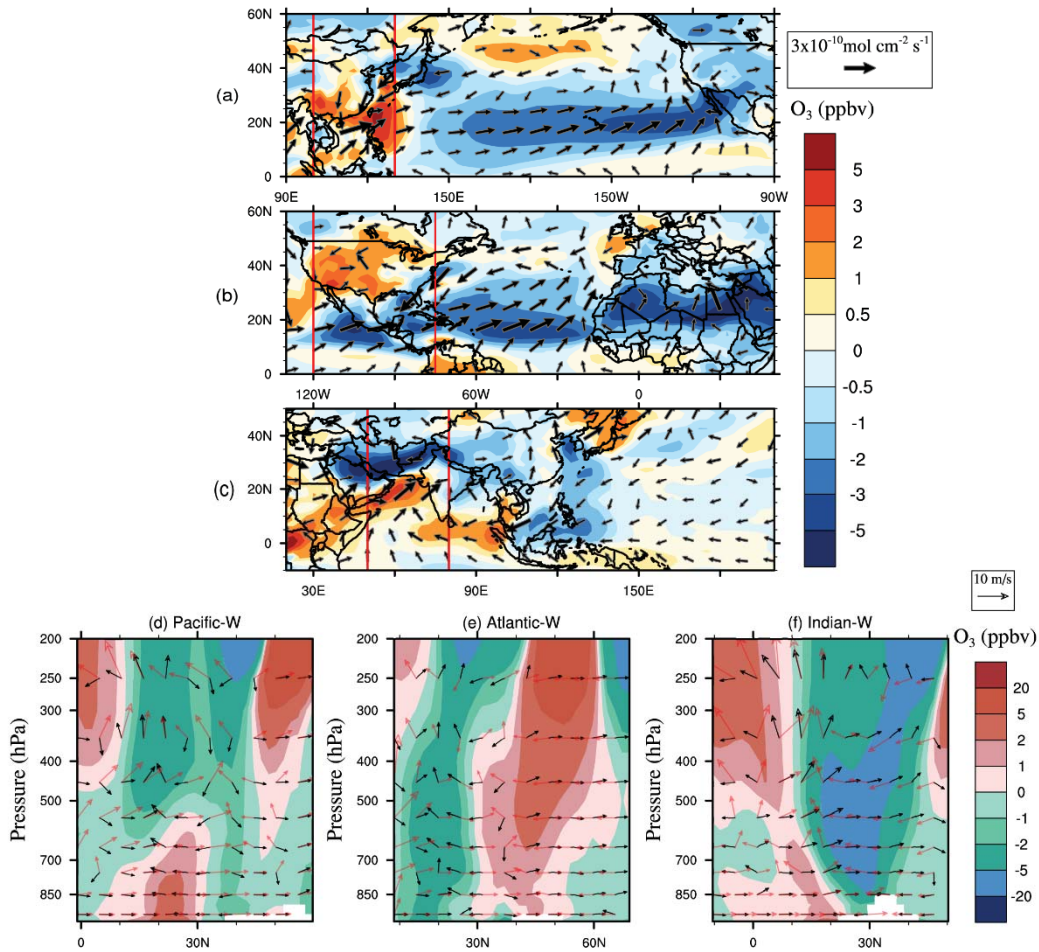


Figure 7. Top three rows: Changes in O₃ concentrations (color contours, ppbv) and horizontal fluxes (arrows, mol cm⁻² s⁻¹) at the surface level for (a) Pacific-W, (b) Atlantic-W, (c) Indian-W relative to the CTRL in the boreal summer. Last row: zonal average of the tropospheric O₃ changes (color contours, ppbv), wind fluxes in CTRL (red arrows, m s⁻¹) and the wind flux perturbation (black arrows, m s⁻¹) in (d) Pacific-W, (e) Atlantic-W, (f) Indian-W relative to the CTRL in the boreal summer. The red rectangles in (a), (b) and (c) denote the longitudinal range used for the zonal averages in (d), (e) and (f), respectively. The vertical wind velocity is amplified 1000 times to make it comparable to the horizontal wind velocity.

25) Figures 8, 9, S3: the season is omitted from the figure caption.

Thanks for pointing out these errors. These figures are all referring to boreal summers. We have revised the captions of these figures and clarified the relevant season:

“Figure 8. Left-hand panel: Difference in the surface concentration (ppbv) of a CO-like tracer

emitted from (a) East Asia for Pacific-W, (c) North America for Atlantic-W and (e) the South Asia for Indian-W relative to the CTRL in the boreal summer. Right-hand panel: the percentage changes in the surface concentration of a CO-like tracer emitted from (b) East Asia for Pacific-W, (d) North America for Atlantic-W and (f) South Asia for Indian-W relative to the CTRL in the boreal summer. Red polygons denote the region where the CO-like tracer is emitted from. The + symbol denotes areas where the results are significant at the 0.05 level, evaluated by Student's t-test using 20 years of data.”

“**Figure 9.** Zonally averaged changes in zonal wind (color contour, m/s) and geopotential height (contour, m) for (a) Pacific-W, (b) Atlantic-W and (c) Indian-W relative to the CTRL in the boreal summer. Black solid and dashed lines in the contours indicate positive and negative geopotential height anomalies, respectively (contour interval: 5 m). The + symbol denotes areas where the zonal wind changes are significant at the 0.05 level, evaluated by Student's t-test using 20 years of data.”

“**Figure S16.** Vertical-meridional distributions of changes in the air temperature (contours, °C) for (a) Pacific_W (zonal averaged from 100°E-90°W), (b) Atlantic_W (zonal averaged from 100°W-180°W) and (c) Indian_W (zonal averaged from 30°E-100°E) relative to the CTRL in boreal summer. Black solid and dashed lines in the contours indicate positive and negative air temperature anomalies, respectively (contour interval: 0.2 °C). The + symbol denotes areas where the changes of air temperature are significant at the 0.05 level, evaluated by Student's t-test using 20 years of data.”

References:

- Auvray, M., and Bey, I.: Long - range transport to Europe: Seasonal variations and implications for the European ozone budget, *Journal of Geophysical Research: Atmospheres* (1984–2012), 110, 2005.
- Barnes, E. A., and Fiore, A. M.: Surface ozone variability and the jet position: Implications for projecting future air quality, *Geophys Res Lett*, 40, 2839-2844, 2013.
- Bloomer, B. J., Stehr, J. W., Piety, C. A., Salawitch, R. J., and Dickerson, R. R.: Observed relationships of ozone air pollution with temperature and emissions, *Geophys Res Lett*, 36, 2009.
- Bronnimann, S., Luterbacher, J., Schmutz, C., Wanner, H., and Staehelin, J.: Variability of total ozone at Arosa, Switzerland, since 1931 related to atmospheric circulation indices, *Geophys*

- Res Lett, 27, 2213-2216, 2000.
- Brown, J., and Bowman, C.: Integrated Science Assessment for Ozone and Related Photochemical Oxidants, EPA 600/R-10, 2013.
- Chaudhari, H. S., Pokhrel, S., Kulkarni, A., Hazra, A., and Saha, S. K.: Clouds–SST relationship and interannual variability modes of Indian summer monsoon in the context of clouds and SSTs: observational and modelling aspects, *Int J Climatol*, 36, 4723-4740, 2016.
- Christoudias, T., Pozzer, A., and Lelieveld, J.: Influence of the North Atlantic Oscillation on air pollution transport, *Atmos Chem Phys*, 12, 869-877, 2012.
- Chuwah, C., van Noije, T., van Vuuren, D. P., Stehfest, E., and Hazeleger, W.: Global impacts of surface ozone changes on crop yields and land use, *Atmos Environ*, 106, 11-23, 10.1016/j.atmosenv.2015.01.062, 2015.
- Creilson, J., Fishman, J., and Wozniak, A.: Intercontinental transport of tropospheric ozone: a study of its seasonal variability across the North Atlantic utilizing tropospheric ozone residuals and its relationship to the North Atlantic Oscillation, *Atmos Chem Phys*, 3, 2053-2066, 2003.
- Dentener, F., Kinne, S., Bond, T., Boucher, O., Cofala, J., Generoso, S., Ginoux, P., Gong, S., Hoelzemann, J., and Ito, A.: Emissions of primary aerosol and precursor gases in the years 2000 and 1750 prescribed data-sets for AeroCom, *Atmos Chem Phys*, 6, 4321-4344, 2006.
- Ding, Y., Carton, J. A., Chepurin, G. A., Stenchikov, G., Robock, A., Sentman, L. T., and Krasting, J. P.: Ocean response to volcanic eruptions in Coupled Model Intercomparison Project 5 simulations, *Journal of Geophysical Research: Oceans*, 119, 5622-5637, 2014.
- Fan, M., and Schneider, E. K.: Observed decadal North Atlantic tripole SST variability. Part I: weather noise forcing and coupled response, *J Atmos Sci*, 69, 35-50, 2012.
- Fiore, A., Dentener, F., Wild, O., Cuvelier, C., Schultz, M., Hess, P., Textor, C., Schulz, M., Doherty, R., and Horowitz, L.: Multimodel estimates of intercontinental source - receptor relationships for ozone pollution, *Journal of Geophysical Research: Atmospheres* (1984–2012), 114, 2009.
- Graham, N., and Barnett, T.: Sea surface temperature, surface wind divergence, and convection over tropical oceans, *Science*, 238, 657-659, 1987.
- Hartmann, D. L.: Pacific sea surface temperature and the winter of 2014, *Geophys Res Lett*, 42, 1894-1902, 2015.
- Hess, P., and Mahowald, N.: Interannual variability in hindcasts of atmospheric chemistry: the role of meteorology, *Atmos. Chem. Phys*, 9, 5261-5280, 2009.
- Hsieh, W. C., Collins, W. D., Liu, Y., Chiang, J. C. H., Shie, C. L., Caldeira, K., and Cao, L.: Climate response due to carbonaceous aerosols and aerosol-induced SST effects in NCAR community atmospheric model CAM3.5, *Atmos Chem Phys*, 13, 7489-7510, DOI 10.5194/acp-13-7489-2013, 2013.
- Jacob, D.: Introduction to atmospheric chemistry, Princeton University Press, 1999.
- Jiang, Z., Miyazaki, K., Worden, J. R., Liu, J. J., Jones, D., and Henze, D. K.: Impacts of anthropogenic and natural sources on free tropospheric ozone over the Middle East, *Atmos Chem Phys*, 16, 6537-6546, 2016.
- Johnson, N. C., and Xie, S.-P.: Changes in the sea surface temperature threshold for tropical convection, *Nat Geosci*, 3, 842-845, 2010.
- Knowland, K., Doherty, R., and Hodges, K. I.: The effects of springtime mid-latitude storms on trace gas composition determined from the MACC reanalysis, *Atmos Chem Phys*, 15, 3605-3628, 2015.

- Kushnir, Y.: Interdecadal variations in North Atlantic sea surface temperature and associated atmospheric conditions, *J Climate*, 7, 141-157, 1994.
- Lamarque, J.-F., Bond, T. C., Eyring, V., Granier, C., Heil, A., Klimont, Z., Lee, D., Liousse, C., Mieville, A., and Owen, B.: Historical (1850–2000) gridded anthropogenic and biomass burning emissions of reactive gases and aerosols: methodology and application, *Atmos Chem Phys*, 10, 7017-7039, 2010.
- Lamarque, J. F., and Hess, P. G.: Arctic Oscillation modulation of the Northern Hemisphere spring tropospheric ozone, *Geophys Res Lett*, 31, 2004.
- Lau, K., Wu, H., and Bony, S.: The role of large-scale atmospheric circulation in the relationship between tropical convection and sea surface temperature, *J Climate*, 10, 381-392, 1997.
- Lau, N.-C., and Nath, M. J.: A modeling study of the relative roles of tropical and extratropical SST anomalies in the variability of the global atmosphere-ocean system, *J Climate*, 7, 1184-1207, 1994.
- Lau, N.-C.: Interactions between global SST anomalies and the midlatitude atmospheric circulation, *B Am Meteorol Soc*, 78, 21-33, 1997.
- Li, L., Chen, C., Huang, C., Huang, H., Zhang, G., Wang, Y., Wang, H., Lou, S., Qiao, L., and Zhou, M.: Process analysis of regional ozone formation over the Yangtze River Delta, China using the Community Multi-scale Air Quality modeling system, *Atmos Chem Phys*, 12, 10971-10987, 2012.
- Liu, J., Mauzerall, D. L., and Horowitz, L. W.: Analysis of seasonal and interannual variability in transpacific transport, *Journal of Geophysical Research: Atmospheres*, 110, 2005.
- Meehl, G. A., Teng, H., Maher, N., and England, M. H.: Effects of the Mount Pinatubo eruption on decadal climate prediction skill of Pacific sea surface temperatures, *Geophys Res Lett*, 42, 2015.
- Organization, W. H.: Review of evidence on health aspects of air pollution—REVIHAAP Project, World Health Organization, Copenhagen, Denmark, 2013.
- Pausata, F. S., Pozzoli, L., Vignati, E., and Dentener, F. J.: North Atlantic Oscillation and tropospheric ozone variability in Europe: model analysis and measurements intercomparison, *Atmos Chem Phys*, 12, 6357-6376, 2012.
- Pusede, S. E., Steiner, A. L., and Cohen, R. C.: Temperature and recent trends in the chemistry of continental surface ozone, *Chem Rev*, 115, 3898-3918, 2015.
- Rotstayn, L. D., and Lohmann, U.: Tropical rainfall trends and the indirect aerosol effect, *J Climate*, 15, 2103-2116, 2002.
- Roxy, M.: Sensitivity of precipitation to sea surface temperature over the tropical summer monsoon region—and its quantification, *Clim Dynam*, 43, 1159-1169, 2014.
- Roxy, M. K., Ritika, K., Terray, P., Murtugudde, R., Ashok, K., and Goswami, B.: Drying of Indian subcontinent by rapid Indian Ocean warming and a weakening land-sea thermal gradient, *Nat Commun*, 6, 2015.
- Sabeerali, C., Rao, S. A., Ajayamohan, R., and Murtugudde, R.: On the relationship between Indian summer monsoon withdrawal and Indo-Pacific SST anomalies before and after 1976/1977 climate shift, *Clim Dynam*, 39, 841-859, 2012.
- Simon, H., Reff, A., Wells, B., Xing, J., and Frank, N.: Ozone trends across the United States over a period of decreasing NO_x and VOC emissions, *Environ Sci Technol*, 49, 186-195, 2014.
- Stocker, T., Qin, D., Plattner, G., Tignor, M., Allen, S., Boschung, J., Nauels, A., Xia, Y., Bex, B., and Midgley, B.: IPCC, 2013: climate change 2013: the physical science basis. Contribution of

- working group I to the fifth assessment report of the intergovernmental panel on climate change, Cambridge University Press, 2013.
- Sutton, R. T., and Hodson, D. L.: Climate response to basin-scale warming and cooling of the North Atlantic Ocean, *J Climate*, 20, 891-907, 2007.
- Taboada, F. G., and Anadon, R.: Patterns of change in sea surface temperature in the North Atlantic during the last three decades: beyond mean trends, *Climatic Change*, 115, 419-431, 2012.
- Tao, W., Liu, J., Ban-Weiss, G., Hauglustaine, D., Zhang, L., Zhang, Q., Cheng, Y., Yu, Y., and Tao, S.: Effects of urban land expansion on the regional meteorology and air quality of eastern China, *Atmos Chem Phys*, 15, 8597-8614, 2015.
- Tilmes, S., Lamarque, J.-F., Emmons, L., Kinnison, D., Ma, P.-L., Liu, X., Ghan, S., Bardeen, C., Arnold, S., and Deeter, M.: Description and evaluation of tropospheric chemistry and aerosols in the Community Earth System Model (CESM1. 2), *Geoscientific Model Development Discussions*, 7, 8875-8940, 2014.
- Ueda, H., Kamae, Y., Hayasaki, M., Kitoh, A., Watanabe, S., Miki, Y., and Kumai, A.: Combined effects of recent Pacific cooling and Indian Ocean warming on the Asian monsoon, *Nat Commun*, 6, 2015.
- Vingarzan, R.: A review of surface ozone background levels and trends, *Atmos Environ*, 38, 3431-3442, 2004.
- Wang, X., Zhang, Y., Hu, Y., Zhou, W., Lu, K., Zhong, L., Zeng, L., Shao, M., Hu, M., and Russell, A.: Process analysis and sensitivity study of regional ozone formation over the Pearl River Delta, China, during the PRIDE-PRD2004 campaign using the Community Multiscale Air Quality modeling system, *Atmos Chem Phys*, 10, 4423-4437, 2010.
- Webster, P. J.: Mechanisms determining the atmospheric response to sea surface temperature anomalies, *J Atmos Sci*, 38, 554-571, 1981.
- Wu, L., and Liu, Z.: North Atlantic Decadal Variability: Air-Sea Coupling, Oceanic Memory, and Potential Northern Hemisphere Resonance*, *J Climate*, 18, 331-349, 2005.
- Wu, R. G., and Kinter, J. L.: Shortwave radiation-SST relationship over the mid-latitude North Pacific during boreal summer in climate models, *Clim Dynam*, 36, 2251-2264, DOI 10.1007/s00382-010-0775-5, 2011.
- Wu, S., Mickley, L. J., Leibensperger, E. M., Jacob, D. J., Rind, D., and Streets, D. G.: Effects of 2000–2050 global change on ozone air quality in the United States, *Journal of Geophysical Research: Atmospheres*, 113, 2008.
- Xi, J., Zhou, L., Murtugudde, R., and Jiang, L.: Impacts of intraseasonal sst anomalies on precipitation during Indian summer monsoon, *J Climate*, 28, 4561-4575, 2015.
- Zeng, G., Pyle, J., and Young, P.: Impact of climate change on tropospheric ozone and its global budgets, *Atmos Chem Phys*, 8, 369-387, 2008.
- Zhang, Y., and Wu, S.-Y.: Understanding of the Fate of Atmospheric Pollutants Using a Process Analysis Tool in a 3-D Regional Air Quality Model at a Fine Grid Scale, *Atmospheric and Climate Sciences*, 3, 18, 2013.

Response to Dr. Meiyun Lin

(Note: Reviewer comments are listed in grey, and responses to reviewer comments are in black. Pasted text from the new version of the paper is in italics.)

1. The manuscript is missing an importance reference on the connection among ENSO, intercontinental pollution transport, and ozone variability.

Meiyun Lin, L.W. Horowitz, S. J. Oltmans, A. M. Fiore, Songmiao Fan (2014): Tropospheric ozone trends at Manna Loa Observatory tied to decadal climate variability, *Nature Geoscience*, 7, 136-143, doi:10.1038/NGEO2066.

This paper used observations at Mauna Loa Observatory in Hawaii, multi-decadal model hindcasts (including those driven by observed SSTs) and idealized CO-like tracers to show that the eastward extension and equatorward shift of the subtropical jet stream during El Nino enhances long-range transport of Asian pollution towards the eastern North Pacific, raising free tropospheric ozone over the subtropical North Pacific region. La Nina manifests in an opposite way. They also found that long-range transport of Asian pollution has weakened in the 2000s due to more frequent La Nina-like conditions (the negative phase of the Pacific Decadal Oscillation).

It seems like that the ozone response to Pacific cooling shown in your Figure 1 resembles the response to El Nino discussed in the above paper. Their findings should be summarized in the Introduction and discussed in Section 5.

Thanks Meiyun for your thoughtful and valuable comments. Your paper presented an excellent work regarding the interactions among ENSO, SST anomaly, pollution transport and ozone variability, and fits well the scope of this study. We have summarized your key conclusions in the Introduction (see *P5, L131-133* in our revised manuscript or below). In our study, we also find that SST increase in North Pacific tends to weaken the zonal westerly wind at lower-middle latitudes (25°N - 45 °N) in the Northern Hemisphere while strengthen it at higher latitudes (Figure 9, see the revised manuscript or below), which further influence the O₃ long-range transport. The corresponding cooling in North Pacific, on the other hand, may exert an opposite effect. Since our analysis mainly focus on the surface O₃ changes in boreal summers while your findings are more relevant to O₃ changes in spring and autumn, we will do more analysis about these seasons and compare directly with your work in the follow-up studies.

“...The La Niña-like decadal cooling of the eastern equatorial Pacific Ocean in the 2000s weakened the long range transport of O₃-rich air from Eurasia towards Hawaii during spring (Lin et al., 2014).”

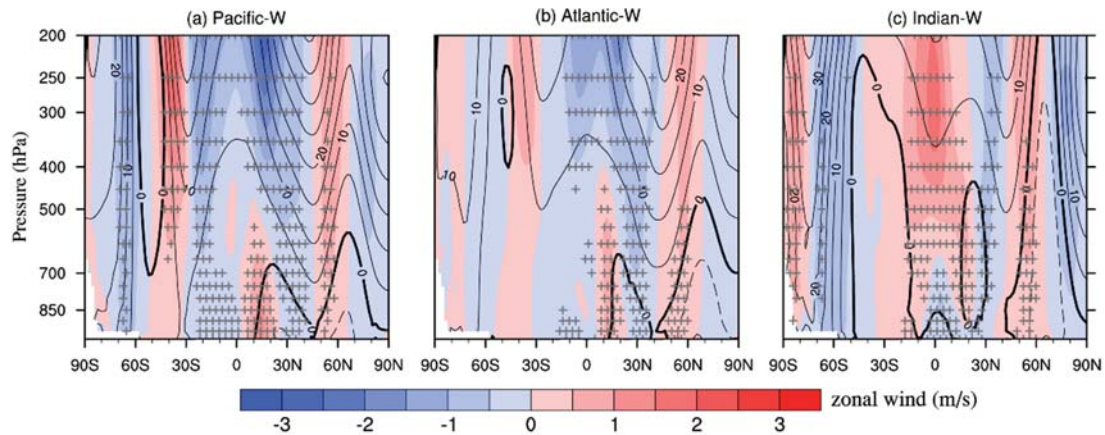


Figure 9. Zonally averaged changes in zonal wind (color contour, m/s) and geopotential height (contour, m) for (a) Pacific-W, (b) Atlantic-W and (c) Indian-W relative to the CTRL in the boreal summer. Black solid and dashed lines in the contours indicate positive and negative geopotential height anomalies, respectively (contour interval: 5 m). The + symbol denotes areas where the zonal wind changes are significant at the 0.05 level, evaluated by Student’s t-test using 20 years of data.

2. Lines 113-115 (Page 4), the description for the findings of Lin et al. (2015, Nature Communications) is not quite accurate. You stated "Lin et al. (2015) had found that more frequent deep stratospheric intrusions appear during ENSO springs". By "ENSO springs", it is not clear which phase of the ENSO. Please change that to "during strong La Nina springs".

Thanks for mentioning this. We have clarified the relevant text (see P5, L128-131) based on your suggestions:

“...Lin et al. (2015) found that more frequent deep stratospheric intrusions appear over the western US during strong La Niña springs because of the meandering of the polar jet towards this region. This process can remarkably increase surface O₃ levels in the western US.”

References:

Lin, M., Horowitz, L. W., Oltmans, S. J., Fiore, A. M., and Fan, S.: Tropospheric ozone trends at Mauna Loa Observatory tied to decadal climate variability, *Nat Geosci*, 7, 136-143, 2014.
 Lin, M., Fiore, A. M., Horowitz, L. W., Langford, A. O., Oltmans, S. J., Tarasick, D., and Rieder, H. E.: Climate variability modulates western US ozone air quality in spring via deep stratospheric intrusions, *Nat Commun*, 6, 2015.

1 **Response of the Global Surface Ozone Distribution to**
2 **Northern Hemisphere ie Sea Surface Temperature Changes:**
3 **Implications s for Long-Range Transport**
4

5 **Kan Yi¹, Junfeng Liu¹, George Ban-Weiss², Jiachen Zhang²,**
6 **Wei Tao¹, Shu Tao¹**
7

8 [1] Laboratory for Earth Surface Processes, College of Urban and Environmental
9 Sciences, Peking University, Beijing, China

10
11 [2] Sonny Astani Department of Civil and Environmental Engineering, University of
12 Southern California, U.S.A.

13
14 Correspondence to: Junfeng Liu (E-mail: jfliu@pku.edu.cn)
15
16
17

18 **Abstract**

19 The response of surface ozone (O_3) concentrations to basin-scale warming and cooling
20 of Northern ~~Hemispheric~~Hemisphere oceans is investigated using the Community
21 Earth System Model (CESM). Idealized, spatially uniform sea surface temperature
22 (SST) anomalies of +/- 1^o °C are individually superimposed onto the North Pacific,
23 North Atlantic, and North Indian ~~oceans,~~individually.Oceans. Our simulations suggest
24 large seasonal and regional variability of surface O_3 in response to SST anomalies,
25 especially in the boreal summer. The responses of surface O_3 associated with basin-
26 scale SST warming and cooling have similar magnitude but are opposite in sign.
27 Increasing ~~(decreasing)~~the SST by 1 °C in one of the ~~regions of focus induces~~oceans
28 generally decreases ~~(increases)~~inthe surface O_3 concentrations, ~~ranging~~ from 1 to 5
29 ppbv. With fixed emissions, SST increases ~~o~~in a specific ocean basin in the Northern
30 Hemisphere tend to increase the summertime surface O_3 concentrations over upwind
31 ~~continents~~regions, accompanied ~~with~~by a widespread reduction over downwind
32 ~~regions~~continents. We implement the integrated process rate (IPR) analysis ~~(IPR)~~ in

33 CESM and find that meteorological O₃ transport in response to SST changes is the key
34 process causing surface O₃ perturbations in most cases. During the boreal summer,
35 basin-scale SST warming facilitates the vertical transport of O₃ to the surface over
36 upwind regions while significantly reducing the vertical transport over downwind
37 ~~continents that are downwind.~~ This process, as confirmed by tagged CO-like tracers,
38 ~~implicates~~indicates a considerable suppression of ~~O₃~~-intercontinental O₃ transport due
39 to increased ~~stagnation~~tropospheric stability at lower mid-latitudes induced by SST
40 ~~increases. Changes in O₃ changes. On the other hand, the responses of~~ chemical O₃
41 production ~~associated with~~to regional SST ~~increases, on the other hand, warming~~ can
42 ~~increase~~exert positive effects on surface O₃ levels over highly polluted continents,
43 except ~~for~~ South Asia. ~~In South Asia,~~ where intensified cloud loading in response to
44 North Indian SST warming depresses both the surface air temperature and solar
45 radiation, and thus photochemical O₃ production ~~of O₃~~. Our findings indicate a robust
46 linkage between basin-scale SST variability and continental surface O₃ pollution, which
47 should be ~~taken into account for~~considered in regional air quality management.

48
49 **Keywords:** SST anomaly, Surface O₃, Process analysis, Transport, CESM

52 1. Introduction

53 ~~Ground level ozone (O₃) adversely impacts human health (WHO., 2006) and threatens~~
54 ~~food security (Chuwah et al., 2015). Considering its eco-toxicity, it is of great~~
55 ~~importance to understand the physical and chemical mechanisms that control~~
56 ~~atmospheric ozone concentrations.~~High ground-level ozone (O₃) concentrations
57 adversely impact human health by inducing respiratory diseases and threaten food
58 security by lowering crop yields (Brown and Bowman, 2013; Organization,
59 2013; Chuwah et al., 2015). Considering the eco-toxicity of O₃, understanding the
60 physical and chemical mechanisms that control atmospheric O₃ concentrations is of
61 great importance. Surface O₃ is produced in the atmosphere via photochemical

62 processing of multiple precursors including volatile organic compounds (VOCs),
63 carbon monoxide (CO) and nitrogen oxides (NO, NO₂). These precursors originate from
64 both natural and anthropogenic sources ~~(Vingarzan, 2004).~~~~(Vingarzan, 2004;Simon et~~
65 ~~al., 2014;Jiang et al., 2016).~~ In addition to local production, transport of O₃ and its
66 precursors from upwind regions and the upper atmosphere can also influence surface
67 O₃ abundance. Stratospheric intrusion events, which lead to vertical down-mixing of
68 ozone-rich air, can significantly elevate surface O₃ during spring and summer ~~(Lin et~~
69 ~~al., 2012;Zhang et al., 2014;Grewé, 2006)~~~~(Grewé, 2006;Lin et al., 2012b;Zhang et al.,~~
70 ~~2014).~~ ~~Long~~The long-range transport of O₃ and its precursors ~~have~~~~has~~ been extensively
71 studied, and their inter-continental impacts have been evaluated ~~with~~~~using~~
72 measurements and model simulations ~~(Fiore et al., 2009;Brown-Steiner and Hess,~~
73 ~~2011)~~~~(Parrish et al., 1993;Fehsenfeld et al., 1996;Wild and Akimoto, 2001;Creilson et~~
74 ~~al., 2003;Simmonds et al., 2004;Fiore et al., 2009;Brown-Steiner and Hess, 2011;Lin~~
75 ~~et al., 2012a;Lin et al., 2014).~~

76
77 Both photochemistry and dynamic transport collectively affect surface O₃ levels.
78 Important meteorological factors that can impact both photochemistry and transport
79 include atmospheric circulations, solar radiation, ~~and relative humidity.~~ ~~Atmospheric~~
80 ~~circulations determine the timescale and pathway of O₃ transport~~ ~~(Auvray and Bey,~~
81 ~~2005;Barnes and Fiore, 2013).~~ ~~air temperature, and relative humidity.~~ ~~Atmospheric~~
82 ~~circulation considerably determines the timescale and pathway of O₃ transport~~
83 ~~(Bronnimann et al., 2000;Auvray and Bey, 2005;Hess and Mahowald, 2009).~~ The
84 ~~efficiency of O₃ transport varies coherently with atmospheric circulations on different~~
85 ~~scales. Knowland et al. (2015) demonstrated the important role of mid-latitude storms~~
86 ~~in redistributing O₃ concentrations during springtime. The North Atlantic Oscillation~~
87 ~~(NAO) significantly affects surface and tropospheric O₃ concentrations over most of~~
88 ~~Europe by influencing the intercontinental transport of air masses~~ ~~(Creilson et al.,~~
89 ~~2003;Christoudias et al., 2012;Pausata et al., 2012).~~ Lamarque and Hess (2004)
90 ~~indicated that the Arctic Oscillation (AO) can modulate springtime tropospheric O₃~~
91 ~~burdens over North America. The shift in the position of the jet stream associated with~~

92 climate change was found to strongly affect summertime surface O₃ variability over
93 eastern North America (Barnes and Fiore, 2013). Increases in solar radiation and air
94 temperature can increase the rate of the chemical production of O₃ and modulate the
95 biogenic emissions of O₃ precursors (Guenther, 1993;Sillman and Samson,
96 1995;Peñuelas and Llusà, 2001), especially over highly polluted regions (Ordóñez et
97 al., 2005;Rasmussen et al., 2012;Pusede et al., 2015). Increases in humidity can enhance
98 the chemical destruction of O₃ and shorten its atmospheric lifetime (Johnson et al.,
99 1999;Camalier et al., 2007). Therefore, changes in meteorological conditions on
100 various spatial and temporal scales play key roles in determining the surface O₃
101 distribution. Understanding the mechanisms and feedbacks of the interactions between
102 O₃ and climate has received increasing attention and will be essential for future surface
103 O₃ mitigation (Jacob and Winner, 2009;Doherty et al., 2013).

104
105 ~~Sea surface temperature (SST) is an indicator for both marine and terrestrial~~
106 ~~meteorology.~~ Sea surface temperature (SST) is an important indicator that characterizes
107 the state of the climate system. Its variations strongly perturb the mass and energy
108 exchange between the ocean and atmosphere (Small et al., 2008;Gulev et al., 2013),
109 which further influence atmospheric circulation, solar radiation, atmospheric
110 temperature and specific humidity (Sutton and Hodson, 2005;Frankignoul and
111 Sennéchaël, 2007;Li et al., 2008) from regional to global scales (Glantz et al.,
112 1991;Wang et al., 2000;Goswami et al., 2006). Numerous studies have shown that SST
113 changes over different oceans and at different latitudes lead to significantly different
114 meteorological sensitivities and climate responses (Webster, 1981;Lau and Nath,
115 1994;Lau, 1997;Sutton and Hodson, 2007;Sabeerali et al., 2012;Ueda et al., 2015).
116 Details on the SST-climate relationships over individual oceanic regions are
117 summarized in Kushnir et al. (2002).

118 ~~SSTs are generally increasing due to the impacts of anthropogenic global climate~~
119 ~~change (Paehauri et al., 2014).~~ SSTs are generally increasing due to the impacts of
120 anthropogenic forcings on global climate change (IPCC, 2013, Chapter 2). In addition,
121 regional SST exhibits natural periodic or irregular oscillations with timescales ranging

122 from months to decades. The El Niño/Southern Oscillation (ENSO) is the most
123 influential natural SST variability that originates in the tropical Pacific and has
124 worldwide climate impacts (Philander, 1983; Wang et al., 2012). The Pacific decadal
125 oscillation (PDO), defined by ocean temperature anomalies in the northeast and tropical
126 Pacific Ocean, is another long-lived, El Niño-like pattern that persists for several
127 decades (Mantua and Hare, 2002). Over the Indian Ocean, SST anomalies feature a
128 seesaw structure between the western and eastern equatorial regions, known as the
129 Indian Ocean Dipole (IOD) mode (Saji et al., 1999). The North Atlantic Ocean
130 pronounces various modes of low-frequency SST variability ~~according to observations~~
131 (Kushnir, 1994; Wu and Liu, 2005; Fan and Schneider, 2012; Taboada and Anadon,
132 2012). The mechanisms responsible for SST variability includes ocean circulation
133 variability, wind stress, and ocean-atmosphere feedbacks (Frankignoul, 1985; Deser
134 et al., 2010). ~~Emissions of aerosols and greenhouse gases (GHGs) from anthropogenic~~
135 ~~and natural sources further complicate regional SST variability because of their climate~~
136 ~~effects (Wu and Kinter, 2011; Hsieh et al., 2013; Rotstayn and Lohmann, 2002).~~
137 Aerosols and greenhouse gases (GHGs) emitted from anthropogenic and natural
138 sources also contribute to regional SST variability through modulation of the solar
139 radiation received by the ocean surface (Rotstayn and Lohmann, 2002; Wu and Kinter,
140 2011; Hsieh et al., 2013; Ding et al., 2014; Meehl et al., 2015).

141
142
143 ~~Considering the distinct roles of regional SST variability in modulating regional climate~~
144 ~~system, there is a need to explore the impact of regional SST change on surface O₃~~
145 ~~distribution. To date very few studies have been conducted to address the linkage~~
146 ~~between SST-O₃ interactions except for the ENSO impacts. For example, Lin et al.~~
147 ~~(2015) had found that more frequent deep stratospheric intrusions appear during ENSO~~
148 ~~springs, which increase western US surface O₃ levels remarkably. Considering the~~
149 distinct roles of regional SST variability in modulating regional climate systems, the
150 impact of regional SST changes on the surface O₃ distribution needs to be explored. Lin
151 et al. (2015) found that more frequent deep stratospheric intrusions appear over the

152 western US during strong La Niña springs because of the meandering of the polar jet
153 towards this region. This process can remarkably increase surface O₃ levels in the
154 western US. The La Niña-like decadal cooling of the eastern equatorial Pacific Ocean
155 in the 2000s weakened the long range transport of O₃-rich air from Eurasia towards
156 Hawaii during spring (Lin et al., 2014). Liu et al. (2005) revealed that El Niño winters
157 are associated with stronger transpacific pollutant transport, which also has
158 implications for the long-range transport of O₃. Except for the ENSO impacts, very few
159 studies to date have directly addressed the linkage between SST and O₃. Therefore, a
160 comprehensive understanding of the response of surface O₃ to SST changes in
161 individual ocean basins is lacking and necessary.

162
163 To fill this gap, this study focuses on examining the sensitivity of O₃ evolution over
164 four polluted continental regions in the Northern Hemisphere (i.e., North America (NA,
165 15°N–55 °N; 60°W–125°W), Europe (EU, 25°N–65 °N; 10°W–50 °E), East Asia (EA,
166 15 °N–50 °N; 95°E–160 °E) and South Asia (SA, 5 °N–35 °N; 50 °E–95°E), defined
167 in Fiore et al. (2009)), ~~and its response with respect~~ to nearby basin-scale SST changes.
168 We describe the design of numerical experiments and model configuration in Section
169 2. Surface O₃ responses to regional SST changes are given in Section 3. Relevant
170 mechanisms governing the SST-O₃ relationships are discussed in Section 4. The impact
171 of basin-scale SST changes on inter-continental transport of O₃ is described in Section
172 5. Conclusions are drawn in Section 6.

173 **2. Methodology**

174 **2.1 Model description and configuration**

175 The Community Earth System Model (CESM, v1.2.2) developed by the National
176 Center for Atmospheric Research (NCAR) is used in this study, configured with the
177 Community Atmosphere Model version 5.0 (CAM5) and the Community Land Model
178 version 4.0 (CLM4). The ocean and sea ice components are prescribed with
179 climatological SST and sea ice distributions. Moist turbulence is parameterized
180 following the Bretherton and Park (2009) scheme. Shallow convection is parameterized

181 using the Park and Bretherton (2009) scheme. The parameterization of deep convection
182 is based on Zhang and McFarlane (1995) with modifications following Richter and
183 Rasch (2008), Raymond and Blyth (1986), and Raymond and Blyth (1992). The cloud
184 microphysical parameterization is following a two-moment scheme described in
185 Morrison and Gettelman (2008) and Gettelman et al. (2008). The microphysical effect
186 of aerosols on clouds are simulated following Ghan et al. (2012). The parameterization
187 of cloud macrophysics follows Conley et al. (2012).

188

189 The chemistry coupled in the CAM5 (i.e., CAM5-chem) is primarily based on the
190 Model for O₃ and Related chemical Tracers, version 4 (MOZART-4), which resolves
191 85 gas-phase species, and 196 gas-phase reactions (Emmons et al., 2010; Lamarque et
192 al., 2012). A three-mode (i.e., Aitkin, accumulation and coarse) aerosol scheme for
193 black carbon (BC), primary organic matter (POM), second organic aerosol (SOA), sea
194 salt, dust and sulfate was used in our simulations following Liu and Ghan (2010). The
195 lightning parameterization is modified according to Price et al. (1997) and tropospheric
196 photolysis rates are calculated interactively following Tie et al. (2005). Gaseous dry
197 deposition is calculated using the resistance-based parameterization of Wesely (1989),
198 Walmsley and Wesely (1996), and Wesely and Hicks (2000). The parameterizations of
199 in-cloud scavenging and below-cloud washout for soluble species are described in
200 detail by Giorgi and Chameides (1985) and Brasseur et al. (1998), respectively.
201 Anthropogenic emissions of chemical species are from the IPCC AR5 emission datasets
202 (Lamarque et al., 2010), whose injection heights and particle size distributions follow
203 the AEROCOM protocols (Dentener et al., 2006). The emissions of natural aerosols
204 and precursor gases are prescribed from the MOZART-2 (Horowitz et al., 2003) and
205 MOZART-4 (Emmons et al., 2010) datasets. All emission datasets are available from
206 the CESM data inventory (<https://svn-ccsm-inputdata.cgd.ucar.edu/trunk/inputdata/>).
207 The performance of CESM in simulating tropospheric O₃ has been **scientifically**
208 validated by comparing with ozonesondes and satellite observations (Tilmes et al.,
209 2014). The deviations between model and observations are within the range of about
210 25%. In general, the model can capture the surface ozone distribution and variability

211 well, but may overestimate O₃ over the Eastern US and Western Europe in the summer
212 (Tilmes et al., 2014).

213

214 **2.2 Numerical ~~Experiments~~experiments**

215 We first conduct a control simulation, hereafter referred to as CTRL, with prescribed
216 climatological SSTs averaged from 1981 to 2010 (see Hurrell et al. (2008)). We then
217 conduct six perturbation simulations with monthly SSTs that are uniformly increased
218 or decreased by 1°C in three ocean basins in the Northern Hemisphere: the North
219 Pacific (15°N-65°N; 100°E-90°W), ~~the~~ North Atlantic ~~Ocean~~ (15°N-65°N; 100°W-
220 20°E) and ~~the~~ North Indian Oceans (5°N-30°N; 30°E-100°E); here 5°N is used to
221 attain a relatively larger domain size. The simulations are denoted as “Pacific-W”,
222 “Atlantic-W”; and “Indian-W” for the three warming cases and “Pacific-C”, “Atlantic-
223 C”; and “Indian-C” for the three cooling cases. We defined the latitudinal and
224 longitudinal ranges of these ocean basins mainly based on their geographical features.
225 The boundaries of the prescribed SST anomalies generally align with the edge of the
226 ocean basins, except along the southern side. In each perturbation simulation, ~~southern~~
227 ~~boundaries of these oceanic regions are~~ further linearly ~~smoothed to prevent large~~
228 ~~SST~~ smooth the southern boundaries of these SST anomalies towards the equator to
229 remove the sharp SST anomaly gradients; at the edge, following a previous approach
230 (e.g., Taschetto et al., 2016; Seager and Henderson, 2016). Air pollution emissions,
231 including biogenic emissions of VOCs, are ~~held~~ fixed to distinguish the impacts of SST
232 variation on O₃ transport and photochemistry. All simulations are run for ~~1221~~ years
233 with the first year used for model spin-up.

234

235 To explore the impacts of SST changes on inter-continental transport, an explicit
236 emission tagging technique is used in our simulations following previous studies
237 ~~(Doherty et al., 2013; Shindell et al., 2008)~~ (Shindell et al., 2008; Doherty et al., 2013).
238 Artificial CO-like tracers emitted from four continental regions, i.e., North America
239 (NA, 15°N–55 °N; 60°W–125°W), Europe (EU, 25°N–65 °N; 10°W–50 °E), East Asia
240 (EA, 15 °N–50 °N; 95°E–160 °E) and South Asia (SA, 5 °N–35 °N; 50 °E–95°E), are

241 tracked individually. These tracers are idealized with a first-order decay lifetime of 50
242 days, which is similar to O₃ (Doherty et al., 2013); and used to single out changes in O₃
243 transport induced by SST anomalies.

245 **2.3 Integrated process rate (IPR) analysis**

246 To provide a process-level explanation ~~on~~for the response of surface O₃ to regional SST
247 changes, ~~an integrated process rate (the~~ IPR) method is applied. This ~~technique~~method
248 calculates the accumulated contributions of individual processes ~~to model (e.g.,~~
249 ~~chemical production and loss, advection, vertical diffusion, dry deposition, etc.)~~ to O₃
250 predictions during ~~runtime, which the model simulation and~~ has been widely used for
251 air pollution diagnostics (~~Tao et al., 2015; Li et al., 2012; Zhang and Wu, 2013).~~(Li et al.,
252 ~~2012; Zhang and Wu, 2013; Tao et al., 2015).~~ In this study, we ~~add~~added the IPR scheme
253 to the CESM ~~modeling~~ framework to track ~~hourly contributions from 6~~the contribution
254 ~~of six physicochemical~~ processes, ~~including (i.e.,~~ gas-phase chemistry (CHEM),
255 advection (ADVE), vertical diffusion (VDIF), dry deposition (DRYD), shallow
256 convection (SHAL) and deep convection (DEEP). ~~The wet))~~ to O₃ concentrations in
257 ~~every grid box. Wet~~ deposition and aqueous-phase chemistry are ~~not considered~~ignored
258 here due to the ~~negligible~~low solubility and ~~negligible chemical~~ production-rate of O₃
259 in water (Jacob, 1999). ~~The performance of~~Therefore, CHEM represents the net
260 ~~production (production minus loss) rate of O₃ due to gas-phase photochemistry. DRYD~~
261 ~~represents the dry deposition fluxes of O₃, which is an important sink for O₃. The other~~
262 IPR ~~is verified through~~terms (i.e., ADVE, VDIF, SHAL and DEEP) represent
263 ~~contributions from different transport processes. The IPR scheme tracks and archives~~
264 ~~the O₃ flux in each grid from every process during each model time step. The sum of~~
265 ~~the O₃ fluxes from these six processes matches the change in the O₃ concentration. The~~
266 IPR performance is verified by comparing the predicted hourly O₃ changes with the
267 sum of ~~the~~ individual ~~burdens~~fluxes from the ~~6~~six processes ~~during runtime~~. As shown
268 in Figure S1, ~~the hourly~~ surface O₃ ~~abundance is~~changes are well represented by the
269 sum of these ~~processes~~fluxes in the model.

270

3. ~~The response~~Response of surface O₃ concentrations to SST changes

The responses of surface O₃ concentrations to basin-scale SST changes (i.e., $\pm 1^\circ\text{C}$) are investigated over four highly populated continental regions (Table 1). Seasonally and regionally averaged surface O₃ changes (i.e., DJF (December, January, February), MAM (March, April, May), JJA (June, July, August) and SON (September, October, November)) for each SST perturbation simulation are mostly within 3 ppbv relative to CTRL. Larger anomalies (i.e., up to 5ppbv) are simulated in locations including the east coast of China, the Indian subcontinent, and remote oceans (Figure 1 and Figure S2). This magnitude of O₃ change is comparable to intercontinental changes in ozone in response to 20% reductions in anthropogenic emissions within a continental region (Fiore et al., 2009).

Seasonally (i.e., DJF (December, January, February), MAM (March, April, May), JJA (June, July, August) and SON (September, October, November)) and regionally averaged surface O₃ changes in each SST perturbation simulation for the four highly populated continental regions and three ocean basins defined in our study are given in Tables 1 and S1, respectively. The responses of the surface O₃ concentrations to basin-scale SST changes (i.e., $\pm 1^\circ\text{C}$) are mainly below 3 ppbv in the Northern Hemisphere (Tables 1 and S1), though larger anomalies (i.e., up to 5 ppbv) are also observed over the eastern coast of China, the Indian subcontinent, and certain oceanic areas (Figures 1 and S3). This SST-O₃ sensitivity is comparable to previous findings. For instance, Bloomer et al. (2009) reported a positive O₃-temperature relationship of 2.2~3.2 ppbv/ $^\circ\text{C}$ across the rural eastern United States. Wu et al. (2008) found that summertime surface O₃ may increase by 2-5 ppbv over the northeastern United States in the 2050s. Additionally, Fiore et al. (2009) demonstrated an intercontinental decrease in surface O₃ of no more than 1 ppbv in response to 20 % reductions in anthropogenic emissions within a continental region. Our study indicates that basin-scale SST changes alone may exert significant effects on the surface O₃ above specific ocean basin and its surrounding continents.

300
301 As shown in Figure 1, ~~up to 5 ppbv~~ seasonal changes of up to 5 ppbv in the mean surface
302 O₃ concentration ~~changes~~ are found~~observed~~ during boreal summers, mainly in coastal
303 regions and remote oceans. ~~Over Southern China, increases in Northern Pacific SSTs~~
304 ~~lead to increases in surface O₃ of nearly 3 ppbv, accompanied by decreases in North~~
305 ~~America (~1 ppbv, shown in Table 1). In the “Atlantic W” case, ground level O₃~~
306 ~~increases by nearly 1 ppbv over North America, but decreases by 1–2 ppbv over Europe.~~
307 Positive (negative) Surface O₃ changes in response to positive and negative SST
308 anomalies generally pronounce a consistent spatial pattern but are opposite in the
309 Northern Indian Ocean lead to increases (decreases) insign, suggesting robust
310 relationships between surface O₃ over the Indian Ocean levels and Africa, but decreases
311 (increases) over South and East Asia (Table SST anomalies (Figure 1). Generally, we
312 find that an An increase (decrease) in summertime SST over a specific ocean basin tends
313 to increase (decrease)the surface O₃ concentrations in concentration over the upwind
314 regions but reduce (rise) that this concentration over downwind ~~or remote~~ continents.
315 ~~During boreal winters, For instance, a 1 °C warming over the North Pacific leads to a~~
316 ~~widespread decrease (increase) of surface O₃ is observed in surface O₃ over the North~~
317 Pacific, North America and the North Atlantic of approximately 1 ppbv (Table S1) but
318 may enhance the surface O₃ by nearly 3 ppbv over South China. Similarly, in the
319 “Atlantic-W” case, the surface O₃ levels decrease by 1~2 ppbv over the North Atlantic
320 and Europe but increase (~1 ppbv) over North America and the North Pacific. For the
321 North Indian Ocean, positive SST anomalies tend to increase the surface O₃ over the
322 Indian Ocean and Africa but decrease the surface O₃ over South and East Asia (Figure
323 1). During the boreal winter, a widespread decrease in surface O₃ associated with the
324 warming (cooling) of different oceans of different oceans is observed. Significant
325 changes (e.g., up to 5 ppbv) mainly occur over remote ocean areas. Over populated
326 continents, the response of the surface O₃ to basin-scale SST changes is typically
327 insignificant. Details are shown in Figure S2S3 in the supporting
328 informationsupplementary material.

329

Our simulations reveal that ~~changes in SSTs~~different oceans can ~~impact~~exert distinct region-specific ~~complex changes in~~effects on the O₃ distribution. We further conduct two sensitivity tests with 1 °C SST warming and 1 °C SST cooling superimposed onto all three ocean basins (i.e., the North Pacific, North Atlantic and North Indian Ocean) in the Northern Hemisphere, denoted as “All-W” and “All-C”, respectively. The effects of these combined warming and cooling cases on surface O₃ distributions, are respectively compared with the sum of the three individual warming cases (i.e., Pacific-W, Atlantic-W and Indian-W) and three individual cooling cases (i.e., Pacific-C, Atlantic-C and Indian-C). The responses of surface O₃ to a hemispheric SST anomaly generally resemble the sum of responses to different regional SST changes (see Figures S5 and S7 in the supplementary material). We now ~~focus on~~analyze the processes that impact the ~~dependency~~dependence of SST on ~~ozone distribution~~the O₃ distribution using ~~the~~ simulations that increase the SST.

4. Mechanism ~~for~~of SST-~~induced~~ surface O₃ changes.

4.1 Process-level response to SST changes

~~Figure 2 shows~~IPR analysis is used to evaluate the contribution of different physicochemical processes to O₃ evolution. This type of analysis has been widely used in air quality studies to examine the cause of pollution episodes (Wang et al., 2010; Li et al., 2012). When applied in climate sensitivity analysis (usually measuring the difference between two equilibriums), the net change of all IPRs approaches zero. Typically, the positive changes in IPRs are mainly responsible for the increase in surface O₃, which may further induce O₃ removal to balance this forcing in a new equilibrium. Therefore, here, the IPR analysis is used not to budget the SST-~~induced~~ O₃ concentration changes but rather to help examine the relative importance of different transport and chemical processes in driving the sensitivity of O₃ to SST forcing. In this study, the SST-induced, process-level O₃ changes are spatially averaged over ~~the~~ four populated continental regions ~~of interest~~ (i.e., NA, EU, EA and SA), Figure 2) and three ocean basins (i.e., the North Pacific, North Atlantic and North Indian Oceans, Figure S9). In most cases, ~~vertical diffusion~~ (VDIF) and ~~dry deposition~~ (DRYD) are the

key processes controlling the O₃ variation. ~~Since both processes are closely dependent on the atmospheric~~ The downward transport of O₃ through diffusion is an important source of surface O₃, while DRYD acts as a sink. Both processes are simultaneously determined by the strength of turbulence intensity. Here, we define ~~here~~ a new term TURB as the sum of ~~DRYFDRYD~~ and VDIF, which can ~~represent~~ capture the overall effect of turbulence intensity changes on surface O₃ variation. ~~Meanwhile~~ concentrations. In addition, we ~~also combine the shallow convection (merge SHAL)~~ and ~~deep convection (DEEP)~~ as CONV to represent the total contribution of convective ~~contribution~~ transport to surface O₃ (Figures 2 and S9). More detailed IPR results are shown in Figures S10 and S11 in the supplementary material.

In the “Pacific-W” case, a ~~SST anomaly of +1 °C~~ SST warming over the North Pacific increases VDIF ~~over eastern China~~ in JJA (Figure S12), which is insignificant if averaged over the whole East Asia ~~while significantly reducing it~~ region. Meanwhile, ~~this Pacific warming considerably reduces VDIF over North America. (Figure S10).~~ The corresponding decrease ~~of~~ TURB ~~in~~ over North America ~~accounts for nearly 80 % of~~ mainly determines the surface O₃ reduction ~~during~~ in JJA and SON, while ~~reductions of the reduction in~~ CONV ~~are responsible for the remainder.~~ exerts an additional negative impact (Figure 2). In the “Atlantic-W” ~~run, similar~~ case, increases in VDIF are ~~simulated~~ also observed over ~~the upwind regions (i.e., North America) in JJA.~~ However, ~~it is~~ these increases are accompanied by commensurate decreases in DRYD, resulting in an insignificant overall change in TURB. ~~The (Figure 2). Therefore, the~~ increase ~~of~~ in CHEM ~~therefore tends to dominate~~ is mainly responsible for the surface O₃ increase over North America. ~~Relatively, in JJA.~~ TURB is more ~~relatively~~ important over Europe (~~only in~~ JJA and SON ~~only~~), leading to reduced surface O₃ ~~abundances. For~~ abundance. ~~In the “Indian-W” case,~~ both CHEM and ~~DEEP~~ CONV are reduced over South Asia in JJA and SON. ~~This reduction, though partially balanced by increases in ADVE and SHAL,~~ leads, leading to overall reductions in surface O₃ over the Indian subcontinent (Figure 2). ~~The IPR analysis over the ocean basins shows that the warming of the North Pacific or North Atlantic induces reductions in VDIF and CHEM, which are responsible~~

389 ~~for the significant decrease in surface O₃ above these regions in JJA (Figure S11). The~~
390 ~~North Indian Ocean warming, on the other hand, enhances DEEP and VDIF, leading to~~
391 ~~a local increase in surface O₃ in JJA.~~

392
393 The IPR analysis indicates that, in general, ~~increases in SSTs~~ SST increase in the
394 North Pacific or North Atlantic ~~are~~ is more likely to ~~elevate~~ enhance the vertical
395 diffusion of O₃ over upwind regions (i.e., East Asia ~~and~~ or North America, respectively)
396 but suppress ~~it over remote~~ this diffusion over the ocean basin as well as downwind
397 ~~continents, especially in boreal summer.~~ JJA (Figure S12). These opposite changes in
398 VDIF over upwind and downwind regions lead to ~~inconsistent~~ distinct surface O₃
399 responses. Changes in ~~photochemistry usually~~ CHEM enhance surface O₃ formation
400 ~~except for~~ in most cases. An exception is in South Asia, where ~~advection~~ CHEM and
401 ~~convection~~ DEEP dominate the ~~feedbacks of~~ reduction in surface O₃ over the region in
402 JJA associated with the North Indian Ocean warming. In the following subsections, the
403 mechanisms ~~responsible of~~ the SST-O₃ relationship for the ~~effects of SST changes in~~
404 ~~different oceans on modulating relevant chemical and physical processes~~ four polluted
405 continents are further explored. ~~We will~~ Here we focus on boreal summers since ~~both~~ the
406 surface O₃ ~~levels and their~~ response to SST changes ~~are highest~~ is more robust during
407 this period than other seasons.

409 **4.2 Response of O₃-photochemical O₃ production to SST**

410 **increaseincreases**

411 ~~Figure 3 shows changes~~ Changes in the net- production rate (i.e., chemical production
412 rate minus loss rate) of O₃ at the surface in JJA associated with basin-scale SST
413 increases. ~~Peak are shown in Figure 3. The peak~~ changes are mainly confined to ~~the~~
414 ~~polluted~~ regions ~~owing to their high precursor emissions.~~ where O₃ precursors are
415 abundant (e.g., South and East Asia and North America). For example, ~~an increase in a~~
416 warmer North Pacific ~~SSTs~~ SST exerts a positive (negative) impact on net O₃ production
417 in the northern (southern) regions of East Asia. Similarly, the warming of the North

418 Atlantic promotes a dipole impact on the surface O₃ production over North America,
419 while the warming of the North Indian Ocean significantly decreases the net O₃ net-
420 production rate over South Asia.

421

422 As emissions are fixed in all simulations, the change in net O₃ production is driven by
423 SST induced meteorological changes (e.g., air temperature, air humidity, and solar
424 radiation). ~~Figure 4 illustrates that an~~ An increase in SST of 1° °C in any ocean basin
425 leads to a widespread enhancement of the surface air temperature (i.e., the air
426 temperature at 2m2 m) over most continental areas. ~~(Figure 4)~~. An exception is the
427 North Indian Ocean, where an increase in SST tends to cool the Indian subcontinent by
428 1-2° °C. This temperature decrease is not only limited to the surface, but also spreads
429 to ~~600hPa~~ 600 hPa (Figure ~~S3~~ S16). Associated with this temperature decrease, ~~there~~ is
430 a remarkable reduction ~~of~~ in the solar radiation received at the continent ~~beneath~~ below
431 (more than 15 W/m², Figure ~~S4~~ S17). ~~Previous studies have indicated that moist~~
432 ~~convection is more sensitive to the SST changes in the tropical oceans than in mid- or~~
433 ~~high- latitude oceans (Lau and Nath, 1994;Lau et al., 1997;Hartmann, 2015)~~. The SST
434 increase over the North Indian Ocean ~~is believed~~ tends to ~~facilitate~~ strengthen the moist
435 convection ~~and that eventually facilitates~~ cloud formation in the upper troposphere,
436 ~~blocking~~ (Roxy et al., 2015;Xi et al., 2015;Chaudhari et al., 2016). ~~The latent heat~~
437 ~~released from convective activities significantly warms the air temperature over the~~
438 ~~upper troposphere (Sabeerali et al., 2012;Xi et al., 2015)~~. ~~Meanwhile, the corresponding~~
439 ~~increase in cloud cover blocks the~~ solar radiation reaching the ~~earth~~ surface of the
440 Indian subcontinent and reduce the air temperature of lower troposphere in that region.
441 These processes lead to opposite air temperature changes between upper and lower
442 troposphere over South Asia in response to the North Indian warming (as shown in
443 Figure S16), which may further suppress the development of deep convection over the
444 Indian subcontinent. ~~This is consistent with previous findings that moist convection is~~
445 ~~more sensitive to the SST changes in the tropical oceans rather than mid- or high-~~
446 ~~latitude oceans (Lau et al., 1997;Lau and Nath, 1994).~~

447

A positive relationship between air temperature and O₃ chemical production has been well documented previously (Jacob and Winner, 2009; Rasmussen et al., 2012a), and thus the SST induced warming or cooling of air temperature is thought to be largely responsible for the change in net O₃ production rate (Figure 3). Previous studies have indicated that air temperature positively affects both O₃ production and destruction rates (Zeng et al., 2008; Pusede et al., 2015). As shown in Figure S19, changes in the net O₃ production rate are mainly dominated by O₃ production over continents but by O₃ destruction over oceans. An increase in SST leads to a widespread enhancement of the air temperature, resulting in a positive change in the net O₃ production over most continental regions (Figure 3). On the other hand, the SST increases also enhance evaporation of ocean water and increase humidity above the respective ocean and its coastal areas (Figure S5). However, a warmer SST also increases the air humidity (Figure S21), which enhances O₃ destruction over most coastal and oceanic areas. In addition, over South Asia, a warming of the North Indian Ocean decreases solar radiation and air temperature, and simultaneously increases air humidity, which jointly exert negative effects on O₃ production in that region.

4.3 Response of O₃-physical O₃ transport to SST increase

In Section 4.1, our IPR analysis highlights multiple important physical processes (i.e., vertical diffusion, convection and advection) that are important in modulating surface O₃ concentrations. However, the role and relative importance of each process exhibit large spatial heterogeneity. In this section, we explore the key factors controlling O₃-physical O₃ transport in response to basin-scale SST changes.

Figure 5 shows the surface pressure and wind pattern changes induced by a basin-wide SST increase. The changes in the surface pressure and wind pattern induced by a basin-wide SST increase are shown in Figure 5. Generally, a warming of any ocean basin will lead to a low-pressure anomaly centered to its west at low-latitudes, which is caused by SST-induced convective activity. Additionally, the warming of the Indian Ocean

477 induces an anticyclonic anomaly over the subtropical western Pacific, which has been
478 documented in previous studies (Yang et al., 2007;Li et al., 2008). As shown in Figure
479 6, the surface pressure reduction induced by SST warming in any ocean basin is closely
480 associated with enhanced upward motions, suggesting a substantial enhancement in
481 deep convection over tropical oceans. ~~Given that an SST threshold (about 26°–28°C)~~
482 ~~is required for deep convection to generate, tropical oceans where meet this threshold~~
483 ~~are pronounced large-scale deep convections and more sensitivity to SST anomalies~~
484 ~~(Johnson and Xie, 2010;Graham and Barnett, 1987).~~ Previous studies have identified
485 an SST threshold (approximately 26°–28°C) to generating deep convection (Graham
486 and Barnett, 1987;Johnson and Xie, 2010). ~~Therefore, this low-pressure anomaly~~
487 ~~mainly occurs at low-latitudes whereas the SST increase imposed at higher latitudes~~
488 ~~would have relatively less effect on surface pressure changes (not shown~~
489 ~~here).~~ Therefore, the sensitivity of deep convection to an SST anomaly is strongly
490 dependent on the distribution of base SST. The enhanced upward motion in response to
491 a uniform increase in basin-scale SST mainly occurs over regions with high
492 climatological SST (Figure 6). Regions with a low climatological SST have little effects
493 on the vertical movement of air masses.

494
495 Strengthened deep convection will trigger large-scale subsidence over ~~adjacent~~
496 ~~regions~~nearby regions through the modulation of large-scale circulation patterns, which
497 may suppress convective ~~air movement over nearby continents (Lau et al.,~~
498 ~~1997).~~transport (Lau et al., 1997;Roxy et al., 2015;Ueda et al., 2015). This effect is
499 ~~confirmed~~verified by the ~~widespread~~ decreases ~~of~~in upward ~~vertical~~ velocity at 500 hPa.
500 As depicted in Figure 6-, significant decreases in upward velocity occur over regions
501 adjacent to the strengthened deep convection. Similar effects are also observed over
502 higher latitudes or remote oceans (Figure S23). Meanwhile, ~~we also find that~~the air
503 temperature increase ~~associated with~~ in response to regional SST warming is more
504 significant ~~in~~above the ~~upper~~ ~~versus~~ lower troposphere, which leads to a decrease in the
505 vertical ~~air~~ temperature gradient (~~shown in~~ Figure ~~S3~~S16). These factors tend to
506 ~~enhance atmospheric stability and lead to a more stagnant climate at mid-latitudes that~~

507 ~~restrains~~restrain the vertical exchange of air pollutants. ~~The corresponding decrease in~~
508 ~~air ventilation contributes to the~~ at mid-latitudes, which facilitates surface O₃
509 accumulation over polluted continental regions in JJA, but may weaken the intrusion
510 of O₃ from the upper troposphere to the surface in most ~~clean regions. We believe this~~
511 ~~effect~~unpolluted areas. This process helps to be responsible for ~~explain~~ the ~~wide-~~
512 ~~spread~~widespread decrease ~~of~~ surface O₃ over unpolluted regions associated ~~in clean~~
513 ~~regions~~ with ~~an~~ SST increase, as described in Section 3, and can be further verified
514 by the wide-spread reduction in VDIF shown in Figure S12.

515
516 The surface pressure anomalies induced by SST changes can play a dominant role in
517 modulating surface O₃ transport at specific locations. For example, the low-pressure
518 anomaly centered over the ~~east coast of Asia~~subtropical northwestern Pacific in the
519 “Pacific-W” case ~~tends to weaken~~causes the ~~East Asian summer monsoon~~convergence
520 of wind in the lower troposphere (Figure 5a). Consequently, surface O₃ pollution is
521 enhanced in ~~Southern~~southern China due to an increase ~~of~~ O₃ transport from ~~the~~ more
522 polluted ~~Northern~~northern China (Figure 7a). ~~Figure 7a also shows the~~The vertical
523 distribution of the corresponding O₃ changes, ~~zonally averaged over 100°E–130°E. It~~
524 also shows that the increase ~~of~~ O₃ over ~~Southern~~southern China ~~is limited to~~occurs
525 below 700hPa, accompanied by ~~a noticeable decrease in the North and~~decreases above-
526 700hPa as well as over nearby northern China (Figure 7d). The IPR analysis also
527 indicates that the ~~increase~~increases in advective transport ~~accounts for nearly 40% of~~
528 ~~the surface O₃ increase in the South China, with the depressed and downward~~
529 ~~turbulent/convective transport being~~are mainly responsible for the ~~remainder.~~ surface
530 O₃ increase in southern China.

531
532 In the “Atlantic-W” ~~run~~case, the SST warming--induced surface pressure anomalies
533 lead to substantial O₃ redistribution, especially over the North Atlantic Ocean (Figure
534 7b). ~~Ozone over~~For North ~~American is simulated to have large~~America, the changes in
535 horizontal O₃ fluxes have no significant effect on the O₃ concentration increase. In
536 addition, O₃ changes are observed to be larger in the upper troposphere ~~and negligible~~

537 ~~changes than~~ at the surface. ~~Therefore, as (Figure 7e). As~~ demonstrated in Section 4.1,
538 the response of ~~ground-level/lower-altitude~~ O₃ over North America to the North Atlantic
539 warming is mainly caused by enhanced ~~photochemical/chemical~~ production, rather than
540 physical transport. –

541
542 ~~As shown in Figure 5c, the~~The North Indian SST warming leads to ~~two surface a low-~~
543 pressure ~~anomalies, with one anomaly~~ centered over the Arabian Sea ~~and the other~~
544 ~~centered over the Mediterranean.~~(Figure 5c). The warming of the North Indian Ocean
545 strengthens the upward motion of air at low-latitudes and further induces a convergence
546 of highly polluted air over the Indian Ocean. ~~Effects~~The effects of this process on O₃
547 concentrations are observed to be more significant in the upper troposphere (Figure
548 ~~7e7f~~). According to the IPR analysis, the surface O₃ increase over the Indian Ocean is
549 mainly caused by the ~~downward~~enhanced vertical transport of O₃ to the surface through
550 ~~deep convection and vertical~~ diffusion ~~of O₃ from upper troposphere processes (Figure~~
551 ~~S11)~~. However, over the nearby Indian subcontinent, the suppressed ~~deep~~ convection
552 ~~accounts for nearly 20% of~~tends to decrease surface O₃ ~~reduction there in that region~~
553 ~~(Figure 2)~~.

555 **5. ~~Implication~~Implications for O₃ long-range transport**

556 The above findings indicate that, in general, a basin-scale SST increase (~~decrease~~) in
557 the Northern Hemisphere is more likely to enhance (~~reduced~~) atmospheric stability at
558 mid-latitudes, which may suppress (~~promote~~) air pollutants from lofting to the free
559 troposphere. This process potentially has large effects on O₃ intercontinental transport.
560 ~~We follow~~Following previous work (e.g., (~~Doherty et al., 2013~~) and ~~Doherty et al., 2013~~ ;
561 (~~Fang et al., 2011~~) and ~~Fang et al., 2011~~), we use passive CO-like tracers to demonstrate
562 the potential effect of regional SST changes on long-range O₃ transport. ~~The surface~~
563 ~~changes of CO tracers originating from East Asia in the “Pacific-W” run, North~~
564 ~~America in the “Atlantic-W” run, and South Asia in the “Indian-W” run are displayed~~
565 ~~in Figure 8~~. A warming of North Pacific SSTs by 1°C tends to increase the East Asian

566 CO tracer concentrations by nearly 86% at the surface. ~~This (Figure 8b), which~~ is
567 accompanied ~~with~~by a significant reduction (~~>5%~~) ~~of (~4%)~~ in eastward transport to
568 North America ~~(Figure 8a)~~. Similarly, for the North American tracer, a warming of
569 North Atlantic SSTs by 1°C ~~slightly~~ increases (~~~2%~~) ~~1%~~ the concentrations in North
570 America but decreases (3-4 %) ~~the~~ concentrations over downwind Europe. ~~These~~
571 ~~results suggest that the warming (cooling) of SSTs tend to block (promote) trans-Pacific~~
572 ~~or trans-Atlantic transport. (Figure 8d)~~. The response of the ~~Indian~~South Asian CO
573 tracer to North Indian Ocean warming also shows a decreasing tendency over
574 downwind regions, but ~~the~~ patterns are more complicated over the source region in this
575 case (Figure ~~8e~~). ~~Because the CO-like tracers added in the simulation have a fixed~~
576 ~~decay lifetime, their concentration changes are completely caused by the SST-induced~~
577 ~~transport anomalies. The decrease in CO tracer concentrations over downwind regions~~
578 ~~suggests that the warming of basin-scale SST tends to suppress the long-range transport~~
579 ~~of air pollutants. Additionally, in the “Pacific-W” case, changes in the East Asian CO~~
580 ~~tracer (Figure 8a) generally resemble the changes in surface O₃ over East Asia (Figure~~
581 ~~7a), indicating the dominant effect of physical transport on the O₃ distribution over East~~
582 ~~Asia. Regarding the North American CO tracer in response to the North Atlantic~~
583 ~~warming or the South Asian CO tracer in response to the North Indian Ocean warming,~~
584 ~~their concentration changes are spatially inconsistent with those of O₃ (see Figures 7~~
585 ~~and 8). This further indicates the distinct roles that different basin-scale SSTs play in~~
586 ~~nearby air quality.~~

587
588 ~~The changes in upper tropospheric circulation generally shows that warming of SSTs~~
589 ~~in different oceans tend to increase the 500-hPa geopotential height at mid-latitudes and~~
590 ~~decrease it over polar areas (Figure 9). Additionally, the increase in North Indian SSTs~~
591 ~~lead to geopotential height reductions above the Arabian Sea. The spatial pattern of~~
592 ~~geopotential height anomalies at 500hPa is roughly consistent with that of air~~
593 ~~temperature changes (Figure 9). This nonuniform increase in air temperature (i.e., more~~
594 ~~significant at mid-latitudes) weakens the meridional temperature gradient, resulting in~~
595 ~~a reduction of thermal winds. Therefore, the decreases in CO tracer transport to remote~~

596 ~~regions can be well explained by both suppressed vertical ventilation and weakened~~
597 ~~westerlies at mid-latitudes. Further investigations of zonal wind suggest that an increase~~
598 ~~in SST over different oceans consistently decreases the westerly winds at lower mid-~~
599 ~~latitudes (25°N - 45 °N) in the Northern Hemisphere but increases these winds at higher~~
600 ~~latitudes (Figure 9). In general, increases in the geopotential height induced by basin-~~
601 ~~scale SST warming are more significant at mid-latitudes than at other latitudes, which~~
602 ~~is consistent with the air temperature changes. Consequently, the meridional~~
603 ~~geopotential height gradient is decreasing at lower latitudes but increasing at higher~~
604 ~~latitudes, leading to corresponding changes in the westerly winds. The latitude band at~~
605 ~~25°N - 45 °N covers many polluted regions (i.e., North America and East Asia). A~~
606 ~~weakened westerly wind may reduce long-rang O₃ transport. As demonstrated in~~
607 ~~Section 4.3, the basin-scale SST increases also exert negative effects on the upward~~
608 ~~transport of air masses at mid-latitudes. Therefore, the decreases in CO tracer~~
609 ~~concentrations over downwind regions (Figure 8a and 8c) can be explained by both~~
610 ~~suppressed vertical transport and weakened westerly winds. In the “Indian-W” case, the~~
611 ~~SST increase over North India leads to a low-pressure anomaly above the Arabian Sea~~
612 ~~due to the enhanced deep convection (as discussed in Section 4.3). The corresponding~~
613 ~~anomalous cyclone should be responsible for the dipole of the South Asian CO tracer~~
614 ~~changes over the source region depicted in Figure 8e.~~

615
616 In addition, we also find a hemispheric-scale decrease ~~of peroxyacetylnitrate in~~
617 ~~peroxyacetyl nitrate~~ (PAN), a reservoir of O₃ precursors (NO_x and HO_x) that facilitates
618 the long-range transport of O₃, during the warming of different oceans (Figure ~~S6S25~~).
619 This decrease is likely ~~to be~~ caused by the increase ~~of in~~ the thermal decomposition of
620 PAN ~~responding in response~~ to the air temperature ~~rise increase~~ (~~Doherty et al.,~~
621 ~~2013; Jacob and Winner, 2009~~)(Jacob and Winner, 2009;Doherty et al., 2013).

622
623 Thus, it is reasonable to infer ~~that,~~ in general ~~that,~~ the increased thermal decomposition
624 of PAN, ~~the~~ weakened mid-latitude westerlies, and ~~the~~ reduced vertical ~~ventilation-air~~
625 ~~transport~~ may exert a joint reducing effect on ~~the~~ intercontinental transport of O₃

626 ~~for~~during basin-scale SST increases.

627

628 6. Summary

629 In this paper, we investigate the responses of surface O₃ to basin-scale SST anomalies
630 in the Northern Hemisphere. The latest version of CESM (version 1.2.2) is used in our
631 simulation, forced with climatological and stationary SST anomalies (± 1 °C) in the
632 North Pacific, North Atlantic and North Indian ~~Ocean~~Oceans, respectively. The
633 responses of surface O₃ associated with these SST changes are evaluated. Results of
634 similar magnitude but opposite sign are observed for the SST warming versus cooling
635 simulations for each ocean basin, suggesting robust connections between the SST
636 anomalies and surface O₃ changes. The regionally and seasonally averaged surface O₃
637 changes over four continental regions (i.e., NA, EU, EA and SA) pronounce wide
638 seasonal and regional variability (varying from 1-to 3 ppbv). The warming of the North
639 Pacific leads to >nearly 3 ppbv increases in the surface O₃ over ~~Southern~~southern China
640 in summer, with corresponding decreases over North America (\sim -1 ppbv). Similarly,
641 the North Atlantic SST warming elevates the surface O₃ pollution over North America
642 while reducing the surface O₃ (nearly 1-2 ppbv) over Europe. Changes ~~to~~in the North
643 Indian ~~SSTs~~SST exert significant impacts (1-~~3~~ppbv3 ppbv) over South and East Asia
644 during the entire year.

645

646 Process analysis indicates that dry deposition and vertical diffusion are two major
647 processes governing the surface ~~ozone~~O₃ balance. The increase ~~of~~in SST in different
648 ocean basins ~~tend~~tends to increase the contributions of vertical diffusion to surface O₃
649 over upwind regions while greatly restraining that over ~~other~~~~remoted~~downwind
650 continents. These processes generally lead to ~~a~~-widespread ~~decrease~~~~of~~decreases in
651 surface O₃, which are partially offset by increases in air temperature-dependent
652 ~~photochemical~~chemical production rates. Specifically, the ~~photochemical~~chemical
653 production changes ~~account~~are mainly responsible for ~~~90%~~~~of~~the surface O₃
654 ~~increase~~increases over North America in response to the North Atlantic SST warming;

655 but exert a negative effect on South Asia in response to the North Indian SST warming.
656 ~~IncreasesDecreases~~ in ~~advective-andthe~~ convective transport of O₃ to the ~~ground-level~~
657 ~~are significant over South Asia surface~~ associated with North Indian warming, ~~which~~
658 ~~exerts an increasing influence are significant over South Asia and exert a negative~~
659 ~~impact~~ on surface O₃ concentrations. Advective transport ~~also exerts an increasing~~
660 ~~influencehas a positive effect~~ on surface O₃ in ~~Southern~~southern China in the “Pacific-
661 W” case. ———

662

663 We further ~~reveals~~show that air temperature is an important factor controlling ~~the~~ surface
664 O₃ responses to SST anomalies. Reductions in ~~the~~ surface O₃ ~~photochemical~~chemical
665 production in ~~Southern~~South Asia associated with North Indian SST warming can be
666 explained by the corresponding SST-induced decreases in ground-level air temperature
667 and solar radiation. Meanwhile, the widespread increase ~~of~~in air temperature associated
668 with basin-scale SST warming is more likely to promote O₃ production over other
669 highly polluted regions.

670

671 On the other hand, SST increases ~~over~~at low latitudes ~~of~~over different oceans enhance
672 deep convection in ~~the~~summer, which promotes convergence at the surface, as well as
673 upward ~~ventilation in the~~motions at low- latitudes. ~~Corresponding~~The corresponding
674 surface pressure anomalies centered over the east coast of ~~Eastern~~East Asia associated
675 with the North Pacific warming and over the Arabian Sea associated with the North
676 Indian warming tend to increase the surface O₃ above through ~~exchanging~~exchanges
677 with ~~the~~ surrounding highly polluted air. The basin-scale SST increases in the
678 ~~North~~Northern Hemisphere ~~promote a more stagnant climate~~reduce the tropospheric
679 ~~temperature gradient at mid-latitudes~~ that restrains vertical transport of O₃ over
680 ~~continental regions as well as weakened mid-latitude~~continents and weakens the
681 westerlies- ~~at lower mid-latitudes~~. The ~~response of the~~ CO-tracer ~~analysis~~also suggests
682 that these factors may ~~have joint~~jointly exert a negative ~~effect~~effect on ~~long-range~~the
683 ~~intercontinental~~ transport of ~~surface~~ O₃.

684

685 Overall, our study highlights the sensitivity of ~~the surface O₃ distribution~~O₃ evolution
686 to basin-wide SST changes ~~over different oceans~~ in the Northern Hemisphere ~~as well~~
687 ~~and identifies~~ the key chemical ~~and/or~~ dynamical factors that control it. ~~We~~
688 ~~recommend that regional air quality this evolution. However, to provide a more~~
689 comprehensive understanding of the SST-O₃ relationship, further studies using realistic
690 SST variability are necessary. This study may aid in the management of O₃ pollution
691 ~~should consider~~by considering the influence of ~~natural~~specific SST variability ~~and~~
692 ~~future increases in SSTs on ozone concentrations.~~_____.

694 Acknowledgements

695 This work was supported by funding from the National Natural Science Foundation of
696 China under awards 41671491, 41571130010, and 41390240, National Key Research
697 and Development Program of China 2016YFC0206202, and the 111 Project (B14001).
698 This work was also supported in part by the National Science Foundation under grant
699 CBET-1512429.

700 References

- 701 :
- 702 Auvray, M., and Bey, I.: Long - range transport to Europe: Seasonal variations and implications for the
703 European ozone budget, *Journal of Geophysical Research: Atmospheres* (1984 - 2012), 110, 2005.
- 704 Barnes, E. A., and Fiore, A. M.: Surface ozone variability and the jet position: Implications for projecting
705 future air quality, *Geophys Res Lett*, 40, 2839-2844, 10.1002/grl.50411, 2013.
- 706 Bloomer, B. J., Stehr, J. W., Piety, C. A., Salawitch, R. J., and Dickerson, R. R.: Observed relationships of
707 ozone air pollution with temperature and emissions, *Geophys Res Lett*, 36, 2009.
- 708 Brasseur, G., Hauglustaine, D., Walters, S., Rasch, P., Müller, J. F., Granier, C., and Tie, X.: MOZART, a
709 global chemical transport model for ozone and related chemical tracers: 1. Model description,
710 *Journal of Geophysical Research: Atmospheres*, 103, 28265-28289, 1998.
- 711 Bretherton, C. S., and Park, S.: A new moist turbulence parameterization in the Community Atmosphere
712 Model, *J Climate*, 22, 3422-3448, 2009.
- 713 Bronnimann, S., Luterbacher, J., Schmutz, C., Wanner, H., and Staehelin, J.: Variability of total ozone at
714 Arosa, Switzerland, since 1931 related to atmospheric circulation indices, *Geophys Res Lett*, 27,
715 2213-2216, 2000.
- 716 Brown-Steiner, B., and Hess, P.: Asian influence on surface ozone in the United States: A comparison of
717 chemistry, seasonality, and transport mechanisms, *J Geophys Res-Atmos*, 116, Artn
718 D1730910.1029/2011jd015846, 2011.

719 [Brown, J., and Bowman, C.: Integrated Science Assessment for Ozone and Related Photochemical](#)
720 [Oxidants, EPA 600/R-10, 2013.](#)

721

722 Camalier, L., Cox, W., and Dolwick, P.: The effects of meteorology on ozone in urban areas and their use
723 in assessing ozone trends, *Atmos Environ*, 41, 7127-7137, 2007.

724 [Chaudhari, H. S., Pokhrel, S., Kulkarni, A., Hazra, A., and Saha, S. K.: Clouds–SST relationship and](#)
725 [interannual variability modes of Indian summer monsoon in the context of clouds and SSTs:](#)
726 [observational and modelling aspects, *Int J Climatol*, 36, 4723-4740, 2016.](#)

727 [Christoudias, T., Pozzer, A., and Lelieveld, J.: Influence of the North Atlantic Oscillation on air pollution](#)
728 [transport, *Atmos Chem Phys*, 12, 869-877, 2012.](#)

729 Chuwah, C., van Noije, T., van Vuuren, D. P., Stehfest, E., and Hazeleger, W.: Global impacts of surface
730 ozone changes on crop yields and land use, *Atmos Environ*, 106, 11-23,
731 10.1016/j.atmosenv.2015.01.062, 2015.

732 Conley, A. J., Garcia, R., Kinnison, D., Lamarque, J.-F., Marsh, D., Mills, M., Smith, A. K., Tilmes, S., Vitt, F.,
733 and Morrison, H.: Description of the NCAR community atmosphere model (CAM 5.0), NCAR
734 technical note, 2012.

735 [Creilson, J., Fishman, J., and Wozniak, A.: Intercontinental transport of tropospheric ozone: a study of](#)
736 [its seasonal variability across the North Atlantic utilizing tropospheric ozone residuals and its](#)
737 [relationship to the North Atlantic Oscillation, *Atmos Chem Phys*, 3, 2053-2066, 2003.](#)

738 Dentener, F., Kinne, S., Bond, T., Boucher, O., Cofala, J., Generoso, S., Ginoux, P., Gong, S., Hoelzemann,
739 J., and Ito, A.: Emissions of primary aerosol and precursor gases in the years 2000 and 1750
740 prescribed data-sets for AeroCom, *Atmos Chem Phys*, 6, 4321-4344, 2006.

741 Deser, C., Alexander, M. A., Xie, S.-P., and Phillips, A. S.: Sea surface temperature variability: Patterns
742 and mechanisms, *Annual Review of Marine Science*, 2, 115-143, 2010.

743 [Ding, Y., Carton, J. A., Chepurin, G. A., Stenchikov, G., Robock, A., Sentman, L. T., and Krasting, J. P.: Ocean](#)
744 [response to volcanic eruptions in Coupled Model Intercomparison Project 5 simulations, *Journal*](#)
745 [of Geophysical Research: Oceans](#), 119, 5622-5637, 2014.

746 Doherty, R. M., Wild, O., Shindell, D. T., Zeng, G., MacKenzie, I. A., Collins, W. J., Fiore, A. M., Stevenson,
747 D. S., Dentener, F. J., Schultz, M. G., Hess, P., Derwent, R. G., and Keating, T. J.: Impacts of climate
748 change on surface ozone and intercontinental ozone pollution: A multi-model study, *J Geophys*
749 *Res-Atmos*, 118, 3744-3763, 10.1002/jgrd.50266, 2013.

750 Emmons, L., Walters, S., Hess, P., Lamarque, J.-F., Pfister, G., Fillmore, D., Granier, C., Guenther, A.,
751 Kinnison, D., and Laepple, T.: Description and evaluation of the Model for Ozone and Related
752 chemical Tracers, version 4 (MOZART-4), *Geoscientific Model Development*, 3, 43-67, 2010.

753 Fan, M., and Schneider, E. K.: Observed decadal North Atlantic tripole SST variability. Part I: weather
754 noise forcing and coupled response, *J Atmos Sci*, 69, 35-50, 2012.

755 Fang, Y., Fiore, A. M., Horowitz, L. W., Gnanadesikan, A., Held, I., Chen, G., Vecchi, G., and Levy, H.: The
756 impacts of changing transport and precipitation on pollutant distributions in a future climate,
757 *Journal of Geophysical Research: Atmospheres*, 116, 2011.

758 [Fehsenfeld, F., Daum, P., Leaitch, W., Trainer, M., Parrish, D., and Hübler, G.: Transport and processing of](#)
759 [O3 and O3 precursors over the North Atlantic: An overview of the 1993 North Atlantic Regional](#)
760 [Experiment \(NARE\) summer intensive, *Journal of Geophysical Research: Atmospheres*, 101,](#)
761 [28877-28891, 1996.](#)

762 Fiore, A., Dentener, F., Wild, O., Cuvelier, C., Schultz, M., Hess, P., Textor, C., Schulz, M., Doherty, R., and

763 Horowitz, L.: Multimodel estimates of intercontinental source - receptor relationships for ozone
764 pollution, *Journal of Geophysical Research: Atmospheres* (1984 - 2012), 114, 2009.

765 Frankignoul, C.: Sea surface temperature anomalies, planetary waves, and air - sea feedback in the
766 middle latitudes, *Reviews of geophysics*, 23, 357-390, 1985.

767 Frankignoul, C., and Sennéchaël, N.: Observed influence of North Pacific SST anomalies on the
768 atmospheric circulation, *J Climate*, 20, 592-606, 2007.

769 Gettelman, A., Morrison, H., and Ghan, S. J.: A new two-moment bulk stratiform cloud microphysics
770 scheme in the Community Atmosphere Model, version 3 (CAM3). Part II: Single-column and global
771 results, *J Climate*, 21, 3660-3679, 2008.

772 Ghan, S. J., Liu, X., Easter, R. C., Zaveri, R., Rasch, P. J., Yoon, J.-H., and Eaton, B.: Toward a minimal
773 representation of aerosols in climate models: Comparative decomposition of aerosol direct,
774 semidirect, and indirect radiative forcing, *J Climate*, 25, 6461-6476, 2012.

775 ~~Gill, A. E.: *Atmosphere-ocean dynamics*, Academic press, 1982.~~

776 Giorgi, F., and Chameides, W.: The rainout parameterization in a photochemical model, *Journal of*
777 *Geophysical Research: Atmospheres*, 90, 7872-7880, 1985.

778 Glantz, M. H., Katz, R. W., and Nicholls, N.: Teleconnections linking worldwide climate anomalies,
779 Cambridge University Press Cambridge, 1991.

780 Goswami, B., Madhusoodanan, M., Neema, C., and Sengupta, D.: A physical mechanism for North
781 Atlantic SST influence on the Indian summer monsoon, *Geophys Res Lett*, 33, 2006.

782 Graham, N., and Barnett, T.: Sea surface temperature, surface wind divergence, and convection over
783 tropical oceans, *Science*, 238, 657-659, 1987.

784 Grewe, V.: The origin of ozone, *Atmos Chem Phys*, 6, 1495-1511, 2006.

785 Guenther, R.: Isoprene and monoterpene emission rate variability: model evaluations and sensitivity
786 analyses, *J Geophys Res*, 98, 1993.

787 Gulev, S. K., Latif, M., Keenlyside, N., Park, W., and Koltermann, K. P.: North Atlantic Ocean control on
788 surface heat flux on multidecadal timescales, *Nature*, 499, 464-467, 2013.

789 ~~Hartmann, D. L.: *Pacific sea surface temperature and the winter of 2014*, *Geophys Res Lett*, 42, 1894-~~
790 ~~1902, 2015.~~

791 ~~Hess, P., and Mahowald, N.: *Interannual variability in hindcasts of atmospheric chemistry: the role of*~~
792 ~~*meteorology*, *Atmos. Chem. Phys*, 9, 5261-5280, 2009.~~

793 Horowitz, L. W., Walters, S., Mauzerall, D. L., Emmons, L. K., Rasch, P. J., Granier, C., Tie, X., Lamarque, J.
794 F., Schultz, M. G., and Tyndall, G. S.: A global simulation of tropospheric ozone and related tracers:
795 Description and evaluation of MOZART, version 2, *Journal of Geophysical Research: Atmospheres*
796 (1984-2012), 108, 2003.

797 Hsieh, W. C., Collins, W. D., Liu, Y., Chiang, J. C. H., Shie, C. L., Caldeira, K., and Cao, L.: Climate response
798 due to carbonaceous aerosols and aerosol-induced SST effects in NCAR community atmospheric
799 model CAM3.5, *Atmos Chem Phys*, 13, 7489-7510, DOI 10.5194/acp-13-7489-2013, 2013.

800 Hurrell, J. W., Hack, J. J., Shea, D., Caron, J. M., and Rosinski, J.: A new sea surface temperature and sea
801 ice boundary dataset for the Community Atmosphere Model, *J Climate*, 21, 5145-5153, 2008.

802 Jacob, D.: *Introduction to atmospheric chemistry*, Princeton University Press, 1999.

803 Jacob, D. J., and Winner, D. A.: Effect of climate change on air quality, *Atmos Environ*, 43, 51-63, 2009.

804 ~~Jiang, Z., Miyazaki, K., Worden, J. R., Liu, J. J., Jones, D., and Henze, D. K.: *Impacts of anthropogenic and*~~
805 ~~*natural sources on free tropospheric ozone over the Middle East*, *Atmos Chem Phys*, 16, 6537-~~
806 ~~6546, 2016.~~

807
808 Johnson, C., Collins, W., Stevenson, D., and Derwent, R.: Relative roles of climate and emissions changes
809 on future tropospheric oxidant concentrations, *Journal of Geophysical Research: Atmospheres*
810 (1984–2012), 104, 18631-18645, 1999.

811 Johnson, N. C., and Xie, S.-P.: Changes in the sea surface temperature threshold for tropical convection,
812 *Nat Geosci*, 3, 842-845, 2010.

813 Kushnir, Y.: Interdecadal variations in North Atlantic sea surface temperature and associated
814 atmospheric conditions, *J Climate*, 7, 141-157, 1994.

815 Kushnir, Y., Robinson, W., Bladé, I., Hall, N., Peng, S., and Sutton, R.: Atmospheric GCM response to
816 extratropical SST anomalies: Synthesis and evaluation*, *J Climate*, 15, 2233-2256, 2002.

817 Lamarque, J.-F., Bond, T. C., Eyring, V., Granier, C., Heil, A., Klimont, Z., Lee, D., Liousse, C., Mieville, A.,
818 and Owen, B.: Historical (1850–2000) gridded anthropogenic and biomass burning emissions of
819 reactive gases and aerosols: methodology and application, *Atmos Chem Phys*, 10, 7017-7039,
820 2010.

821 Lamarque, J., Emmons, L., Hess, P., Kinnison, D. E., Tilmes, S., Vitt, F., Heald, C., Holland, E. A., Lauritzen,
822 P., and Neu, J.: CAM-chem: Description and evaluation of interactive atmospheric chemistry in
823 the Community Earth System Model, *Geosci. Model Dev*, 5, 369-411, 2012.

824 Lau, K., Wu, H., and Bony, S.: The role of large-scale atmospheric circulation in the relationship between
825 tropical convection and sea surface temperature, *J Climate*, 10, 381-392, 1997.

826 Lau, N.-C., and Nath, M. J.: A modeling study of the relative roles of tropical and extratropical SST
827 anomalies in the variability of the global atmosphere-ocean system, *J Climate*, 7, 1184-1207, 1994.

828 Lau, N.-C.: Interactions between global SST anomalies and the midlatitude atmospheric circulation, *B*
829 *Am Meteorol Soc*, 78, 21-33, 1997.

830 Li, L., Chen, C., Huang, C., Huang, H., Zhang, G., Wang, Y., Wang, H., Lou, S., Qiao, L., and Zhou, M.:
831 Process analysis of regional ozone formation over the Yangtze River Delta, China using the
832 Community Multi-scale Air Quality modeling system, *Atmos Chem Phys*, 12, 10971-10987, 2012.

833 Li, S., Lu, J., Huang, G., and Hu, K.: Tropical Indian Ocean basin warming and East Asian summer monsoon:
834 A multiple AGCM study, *J Climate*, 21, 6080-6088, 2008.

835 [Lin, M., Fiore, A. M., Horowitz, L. W., Cooper, O. R., Naik, V., Holloway, J., Johnson, B. J., Middlebrook, A.](#)
836 [M., Oltmans, S. J., and Pollack, I. B.: Transport of Asian ozone pollution into surface air over the](#)
837 [western United States in spring, *Journal of Geophysical Research: Atmospheres*, 117, 2012a.](#)

838 [Lin, M., Horowitz, L. W., Oltmans, S. J., Fiore, A. M., and Fan, S.: Tropospheric ozone trends at Mauna](#)
839 [Loa Observatory tied to decadal climate variability, *Nat Geosci*, 7, 136-143, 2014.](#)

840 Lin, M., Fiore, A. M., Horowitz, L. W., Langford, A. O., Oltmans, S. J., Tarasick, D., and Rieder, H. E.: Climate
841 variability modulates western US ozone air quality in spring via deep stratospheric intrusions, *Nat*
842 *Commun*, 6, 2015.

843 Lin, M. Y., Fiore, A. M., Cooper, O. R., Horowitz, L. W., Langford, A. O., Levy, H., Johnson, B. J., Naik, V.,
844 Oltmans, S. J., and Senff, C. J.: Springtime high surface ozone events over the western United
845 States: Quantifying the role of stratospheric intrusions, *J Geophys Res-Atmos*, 117, Artn D00v22
846 10.1029/2012jd018151, 2012.

847 [Liu, J., Mauzerall, D. L., and Horowitz, L. W.: Analysis of seasonal and interannual variability in](#)
848 [transpacific transport, *Journal of Geophysical Research: Atmospheres*, 110, 2005.](#)

849 Liu, X., and Ghan, S.: A modal aerosol model implementation in the community atmosphere model,
850 version 5 (CAM5), *J. Atmos. Sci*, 2010.

851 Mantua, N. J., and Hare, S. R.: The Pacific decadal oscillation, *J Oceanogr*, 58, 35-44, 2002.

852 [Meehl, G. A., Teng, H., Maher, N., and England, M. H.: Effects of the Mount Pinatubo eruption on decadal](#)

853 [climate prediction skill of Pacific sea surface temperatures, *Geophys Res Lett*, 42, 2015.](#)

854 Morrison, H., and Gettelman, A.: A new two-moment bulk stratiform cloud microphysics scheme in the

855 Community Atmosphere Model, version 3 (CAM3). Part I: Description and numerical tests, *J*

856 *Climate*, 21, 3642-3659, 2008.

857 Ordóñez, C., Mathis, H., Furger, M., Henne, S., Hüglin, C., Staehelin, J., and Prévôt, A.: Changes of daily

858 surface ozone maxima in Switzerland in all seasons from 1992 to 2002 and discussion of summer

859 2003, *Atmos Chem Phys*, 5, 1187-1203, 2005.

860 [Organization, W. H.: Review of evidence on health aspects of air pollution–REVIHAAP Project, World](#)

861 [Health Organization, Copenhagen, Denmark, 2013.](#)

862 [Pachauri, R. K., Allen, M., Barros, V., Broome, J., Cramer, W., Christ, R., Church, J., Clarke, L., Dahe, Q.,](#)

863 [and Dasgupta, P.: Climate Change 2014: Synthesis Report. Contribution of Working Groups I, II](#)

864 [and III to the Fifth Assessment Report of the Intergovernmental Panel on Climate Change, 2014.](#)

865 Park, S., and Bretherton, C. S.: The University of Washington shallow convection and moist turbulence

866 schemes and their impact on climate simulations with the Community Atmosphere Model, *J*

867 *Climate*, 22, 3449-3469, 2009.

868 [Parrish, D. D., Holloway, J. S., Trainer, M., Murphy, P. C., Fehsenfeld, F. C., and Forbes, G. L.: Export of](#)

869 [North American ozone pollution to the north Atlantic Ocean, *Science*, 259, 1436-1439, 1993.](#)

870 [Pausata, F. S., Pozzoli, L., Vignati, E., and Dentener, F. J.: North Atlantic Oscillation and tropospheric](#)

871 [ozone variability in Europe: model analysis and measurements intercomparison, *Atmos Chem*](#)

872 [Phys](#), 12, 6357-6376, 2012.

873 Peñuelas, J., and Llusà, J.: The complexity of factors driving volatile organic compound emissions by

874 plants, *Biologia Plantarum*, 44, 481-487, 2001.

875 Philander, S. G. H.: El Niño southern oscillation phenomena, *Nature*, 302, 295-301, 1983.

876 Price, C., Penner, J., and Prather, M.: NO_x from lightning: 1. Global distribution based on lightning physics,

877 *Journal of Geophysical Research: Atmospheres* (1984–2012), 102, 5929-5941, 1997.

878 Pusede, S. E., Steiner, A. L., and Cohen, R. C.: Temperature and Recent Trends in the Chemistry of

879 Continental Surface Ozone, *Chem Rev*, 115, 3898-3918, 10.1021/cr5006815, 2015.

880 Rasmussen, D., Fiore, A., Naik, V., Horowitz, L., McGinnis, S., and Schultz, M.: Surface ozone-temperature

881 relationships in the eastern US: A monthly climatology for evaluating chemistry-climate models,

882 *Atmos Environ*, 47, 142-153, 2012a.

883 Rasmussen, D. J., Fiore, A. M., Naik, V., Horowitz, L. W., McGinnis, S. J., and Schultz, M. G.: Surface ozone-

884 temperature relationships in the eastern US: A monthly climatology for evaluating chemistry-

885 climate models, *Atmos Environ*, 47, 142-153, 10.1016/j.atmosenv.2011.11.021, 2012b.

886 Raymond, D., and Blyth, A.: Extension of the stochastic mixing model to cumulonimbus clouds, *J Atmos*

887 *Sci*, 49, 1968-1983, 1992.

888 Raymond, D. J., and Blyth, A. M.: A stochastic mixing model for nonprecipitating cumulus clouds, *J Atmos*

889 *Sci*, 43, 2708-2718, 1986.

890 Richter, J. H., and Rasch, P. J.: Effects of convective momentum transport on the atmospheric circulation

891 in the Community Atmosphere Model, version 3, *J Climate*, 21, 1487-1499, 2008.

892 Rotstayn, L. D., and Lohmann, U.: Tropical rainfall trends and the indirect aerosol effect, *J Climate*, 15,

893 2103-2116, 2002.

894 [Roxy, M. K., Ritika, K., Terray, P., Murtugudde, R., Ashok, K., and Goswami, B.: Drying of Indian](#)

895 [subcontinent by rapid Indian Ocean warming and a weakening land-sea thermal gradient, Nat](#)
896 [Commun, 6, 2015.](#)

897 [Sabeerali, C., Rao, S. A., Ajayamohan, R., and Murtugudde, R.: On the relationship between Indian](#)
898 [summer monsoon withdrawal and Indo-Pacific SST anomalies before and after 1976/1977](#)
899 [climate shift, Clim Dynam, 39, 841-859, 2012](#)

900 Saji, N., Goswami, B., Vinayachandran, P., and Yamagata, T.: A dipole mode in the tropical Indian Ocean,
901 Nature, 401, 360-363, 1999.

902 [Seager, R., and Henderson, N.: On the Role of Tropical Ocean Forcing of the Persistent North American](#)
903 [West Coast Ridge of Winter 2013/14 a, J Climate, 29, 8027-8049, 2016.](#)

904 Shindell, D., Chin, M., Dentener, F., Doherty, R., Faluvegi, G., Fiore, A. M., Hess, P., Koch, D., MacKenzie,
905 I., and Sanderson, M.: A multi-model assessment of pollution transport to the Arctic, Atmos Chem
906 Phys, 8, 5353-5372, 2008.

907 Sillman, S., and Samson, P. J.: Impact of temperature on oxidant photochemistry in urban, polluted rural
908 and remote environments, Journal of Geophysical Research: Atmospheres, 100, 11497-11508,
909 1995.

910 [Simmonds, P., Derwent, R., Manning, A., and Spain, G.: Significant growth in surface ozone at Mace](#)
911 [Head, Ireland, 1987–2003, Atmos Environ, 38, 4769-4778, 2004.](#)

912 [Simon, H., Reff, A., Wells, B., Xing, J., and Frank, N.: Ozone trends across the United States over a period](#)
913 [of decreasing NOx and VOC emissions, Environ Sci Technol, 49, 186-195, 2014.](#)

914 Small, R., Xie, S., O'Neill, L., Seo, H., Song, Q., Cornillon, P., Spall, M., and Minobe, S.: Air–sea interaction
915 over ocean fronts and eddies, Dynam Atmos Oceans, 45, 274-319, 2008.

916 Sutton, R. T., and Hodson, D. L.: Atlantic Ocean forcing of North American and European summer climate,
917 Science, 309, 115-118, 2005.

918 Sutton, R. T., and Hodson, D. L.: Climate response to basin-scale warming and cooling of the North
919 Atlantic Ocean, J Climate, 20, 891-907, 2007.

920 Taboada, F. G., and Anadon, R.: Patterns of change in sea surface temperature in the North Atlantic
921 during the last three decades: beyond mean trends, Climatic Change, 115, 419-431, 2012.

922 Tao, W., Liu, J., Ban-Weiss, G., Hauglustaine, D., Zhang, L., Zhang, Q., Cheng, Y., Yu, Y., and Tao, S.: Effects
923 of urban land expansion on the regional meteorology and air quality of eastern China, Atmos
924 Chem Phys, 15, 8597-8614, 2015.

925 [Taschetto, A., Rodrigues, R., Meehl, G., McGregor, S., and England, M.: How sensitive are the Pacific–](#)
926 [tropical North Atlantic teleconnections to the position and intensity of El Niño-related warming?,](#)
927 [Clim Dynam, 46, 1841-1860, 2016.](#)

928 Tie, X., Madronich, S., Walters, S., Edwards, D. P., Ginoux, P., Mahowald, N., Zhang, R., Lou, C., and
929 Brasseur, G.: Assessment of the global impact of aerosols on tropospheric oxidants, Journal of
930 Geophysical Research: Atmospheres, 110, 2005.

931 Tilmes, S., Lamarque, J.-F., Emmons, L., Kinnison, D., Ma, P.-L., Liu, X., Ghan, S., Bardeen, C., Arnold, S.,
932 and Deeter, M.: Description and evaluation of tropospheric chemistry and aerosols in the
933 Community Earth System Model (CESM1. 2), Geoscientific Model Development Discussions, 7,
934 8875-8940, 2014.

935 [Ueda, H., Kamae, Y., Hayasaki, M., Kitoh, A., Watanabe, S., Miki, Y., and Kumai, A.: Combined effects of](#)
936 [recent Pacific cooling and Indian Ocean warming on the Asian monsoon, Nat Commun, 6, 2015.](#)

937 Vingarzan, R.: A review of surface ozone background levels and trends, Atmos Environ, 38, 3431-3442,
938 2004.

939 Walmsley, J. L., and Wesely, M. L.: Modification of coded parametrizations of surface resistances to
940 gaseous dry deposition, *Atmos Environ*, 30, 1181-1188, 1996.

941 Wang, B., Wu, R., and Fu, X.: Pacific-East Asian teleconnection: how does ENSO affect East Asian climate?,
942 *J Climate*, 13, 1517-1536, 2000.

943 Wang, C., Deser, C., Yu, J.-Y., DiNezio, P., and Clement, A.: El Nino and southern oscillation (ENSO): a
944 review, *Coral Reefs of the Eastern Pacific*, 3-19, 2012.

945 [Wang, X., Zhang, Y., Hu, Y., Zhou, W., Lu, K., Zhong, L., Zeng, L., Shao, M., Hu, M., and Russell, A.: Process](#)
946 [analysis and sensitivity study of regional ozone formation over the Pearl River Delta, China,](#)
947 [during the PRIDE-PRD2004 campaign using the Community Multiscale Air Quality modeling](#)
948 [system, *Atmos Chem Phys*, 10, 4423-4437, 2010.](#)

949 Webster, P. J.: Mechanisms determining the atmospheric response to sea surface temperature
950 anomalies, *J Atmos Sci*, 38, 554-571, 1981.

951 Wesely, M.: Parameterization of surface resistances to gaseous dry deposition in regional-scale
952 numerical models, *Atmospheric Environment (1967)*, 23, 1293-1304, 1989.

953 Wesely, M., and Hicks, B.: A review of the current status of knowledge on dry deposition, *Atmos Environ*,
954 34, 2261-2282, 2000.

955 [Wild, O., and Akimoto, H.: Intercontinental transport of ozone and its precursors in a three-dimensional](#)
956 [global CTM, *Journal of Geophysical Research: Atmospheres*, 106, 27729-27744, 2001.](#)

957 ~~[WHO.: Air Quality Guidelines: Global Update 2005. Particulate Matter, Ozone, Nitrogen Dioxide and](#)~~
958 ~~[Sulfur Dioxide, World Health Organization, 2006.](#)~~

959 Wu, L., and Liu, Z.: North Atlantic Decadal Variability: Air-Sea Coupling, Oceanic Memory, and Potential
960 Northern Hemisphere Resonance*, *J Climate*, 18, 331-349, 2005.

961 Wu, R. G., and Kinter, J. L.: Shortwave radiation-SST relationship over the mid-latitude North Pacific
962 during boreal summer in climate models, *Clim Dynam*, 36, 2251-2264, DOI 10.1007/s00382-010-
963 0775-5, 2011.

964 [Wu, S., Mickley, L. J., Leibensperger, E. M., Jacob, D. J., Rind, D., and Streets, D. G.: Effects of 2000–2050](#)
965 [global change on ozone air quality in the United States, *Journal of Geophysical Research:*](#)
966 [*Atmospheres*, 113, 2008.](#)

967 [Xi, J., Zhou, L., Murtugudde, R., and Jiang, L.: Impacts of intraseasonal sst anomalies on precipitation](#)
968 [during Indian summer monsoon, *J Climate*, 28, 4561-4575, 2015.](#)

969 [Yang, J., Liu, Q., Xie, S. P., Liu, Z., and Wu, L.: Impact of the Indian Ocean SST basin mode on the Asian](#)
970 [summer monsoon, *Geophys Res Lett*, 34, 2007.](#)

971 [Zeng, G., Pyle, J., and Young, P.: Impact of climate change on tropospheric ozone and its global budgets,](#)
972 [*Atmos Chem Phys*, 8, 369-387, 2008.](#)

973 Zhang, G. J., and McFarlane, N. A.: Sensitivity of climate simulations to the parameterization of cumulus
974 convection in the Canadian Climate Centre general circulation model, *Atmos Ocean*, 33, 407-446,
975 1995.

976 Zhang, L., Jacob, D. J., Yue, X., Downey, N. V., Wood, D. A., and Blewitt, D.: Sources contributing to
977 background surface ozone in the US Intermountain West, *Atmos Chem Phys*, 14, 5295-5309,
978 10.5194/acp-14-5295-2014, 2014.

979 Zhang, Y., and Wu, S.-Y.: Understanding of the Fate of Atmospheric Pollutants Using a Process Analysis
980 Tool in a 3-D Regional Air Quality Model at a Fine Grid Scale, *Atmospheric and Climate Sciences*,
981 3, 18, 2013.

982

983

984

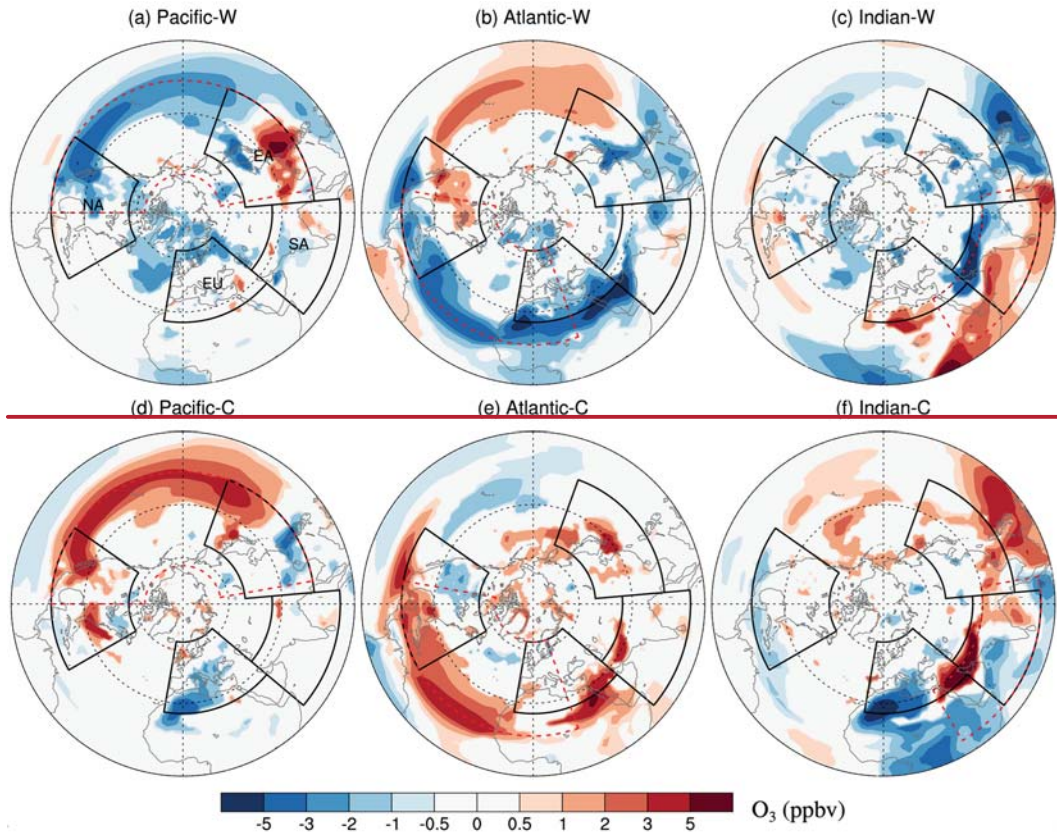
985 **Table 1.** Regionally and seasonally averaged (only land grid boxes are included)
 986 changes in surface O₃ concentrations (ppbv) for basin-scale SST perturbation cases
 987 relative to the control simulation. Positive (negative) changes ~~which that~~ are significant
 988 at the 0.105 level evaluated ~~with a by~~ Student's t-test are marked ~~by in~~ red (blue).

Ozone (ppbv)		DJF	MAM	JJA	SON	
North Pacific	+1° C	North America	-0.50^{**}27*	-0.78^{**}42*	-1.01^{**}0.92*	0.91^{**}1.03*
		Europe	-0.50^{**}	-0.71^{**}26	-0.2310	-0.4029
		East Asia	-0.96^{**}88*	-0.92^{**}71*	0.4520	0.0017
		South Asia	-1.37^{**}00*	0.2230	-0.6343	0.5843*
	-1° C	North America	0.58^{**}00	0.3857*	0.58^{**}55*	0.49^{**}82*
		Europe	0.40[*]19	0.3515	-0.86^{**}47*	0.4147*
		East Asia	0.50[*]30	-0.1817	-0.1222	-0.0067*
		South Asia	0.0204	-1.22[*]0.24	-0.0503	-0.5640
North Atlantic	+1° C	North America	-0.0703	0.2049	0.62^{**}50*	0.46^{**}53*
		Europe	0.3730*	0.0206	-1.77^{**}61*	-0.83^{**}89*
		East Asia	-0.50^{**}52*	-0.61^{**}68*	-0.2662*	-0.0625
		South Asia	-0.4120	-1.62^{**}46*	-0.96^{**}1.28*	-0.6082*
	-1° C	North America	-0.2707	-0.3210	-0.3510	-0.35[*]17
		Europe	-0.3300	0.2400	0.5207	-0.06
		East Asia	0.1116	-0.59^{**}08	0.6480*	-0.4160*
		South Asia	-0.0820	-0.5540	0.95[*]30	-0.2110
North India	+1° C	North America	-0.40[*]25	-0.3104	-0.1116	-0.0810
		Europe	-0.30	0.2908	-0.0712	0.4219
		East Asia	-0.67^{**}53*	-0.63^{**}77*	-0.57^{**}28	-1.56^{**}78*
		South Asia	-1.30^{**}00*	0.1214	-2.06^{**}1.67*	-2.33^{**}75*
	-1° C	North America	-0.0704	-0.1017	0.3104	-0.1225
		Europe	-0.2805	-0.0907	-0.5213	-0.2724
		East Asia	-0.2206	0.69^{**}15	0.2255*	1.60^{**}0.33
		South Asia	-0.0103	0.2157	1.94^{**}70*	1.70^{**}31*

989 *significant at the 0.1 level from Student t-test using 11 years model result

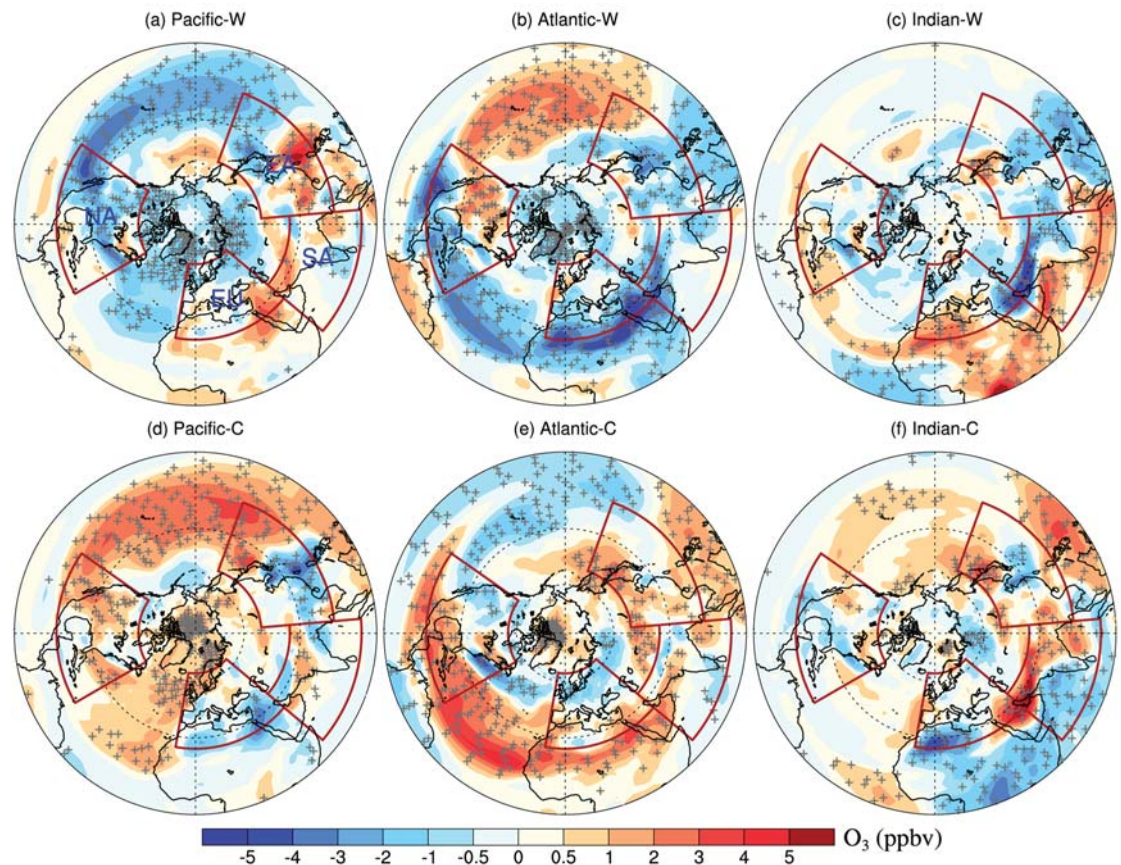
990 **significant at the 0.05 level from Student's t-test using 11 years of
 991 model results.

992



993

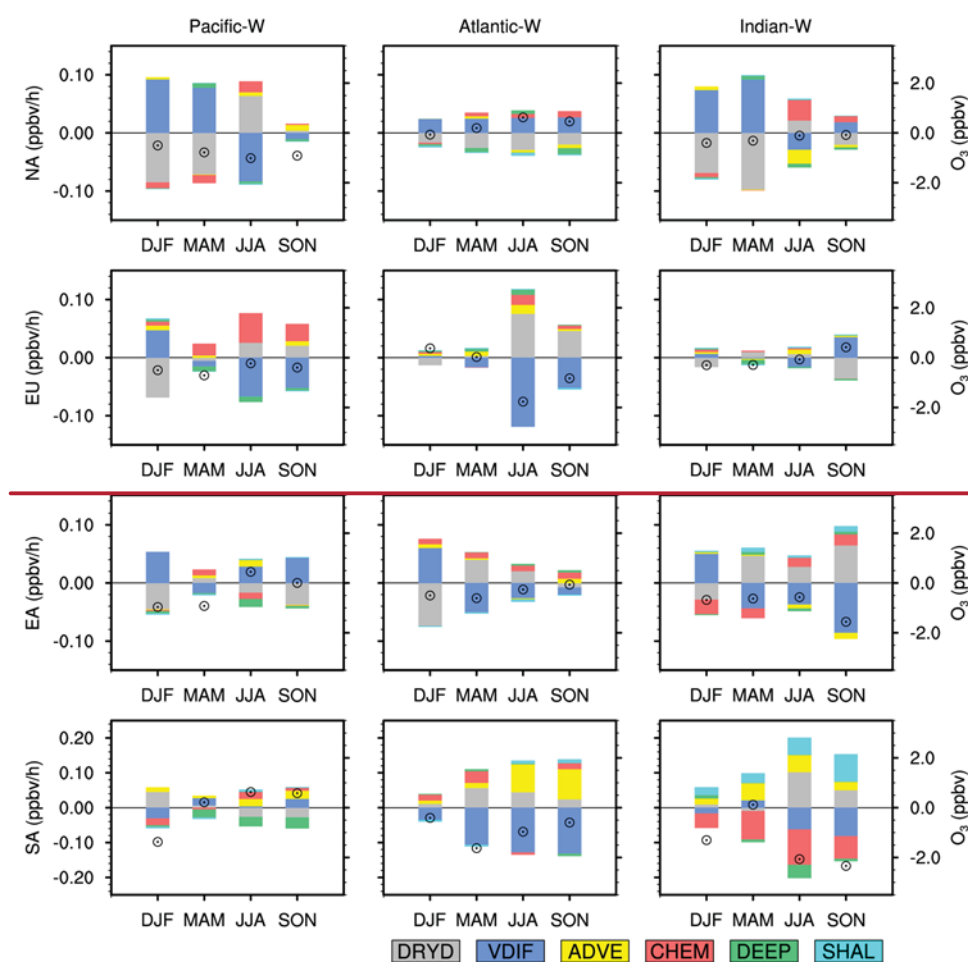
994



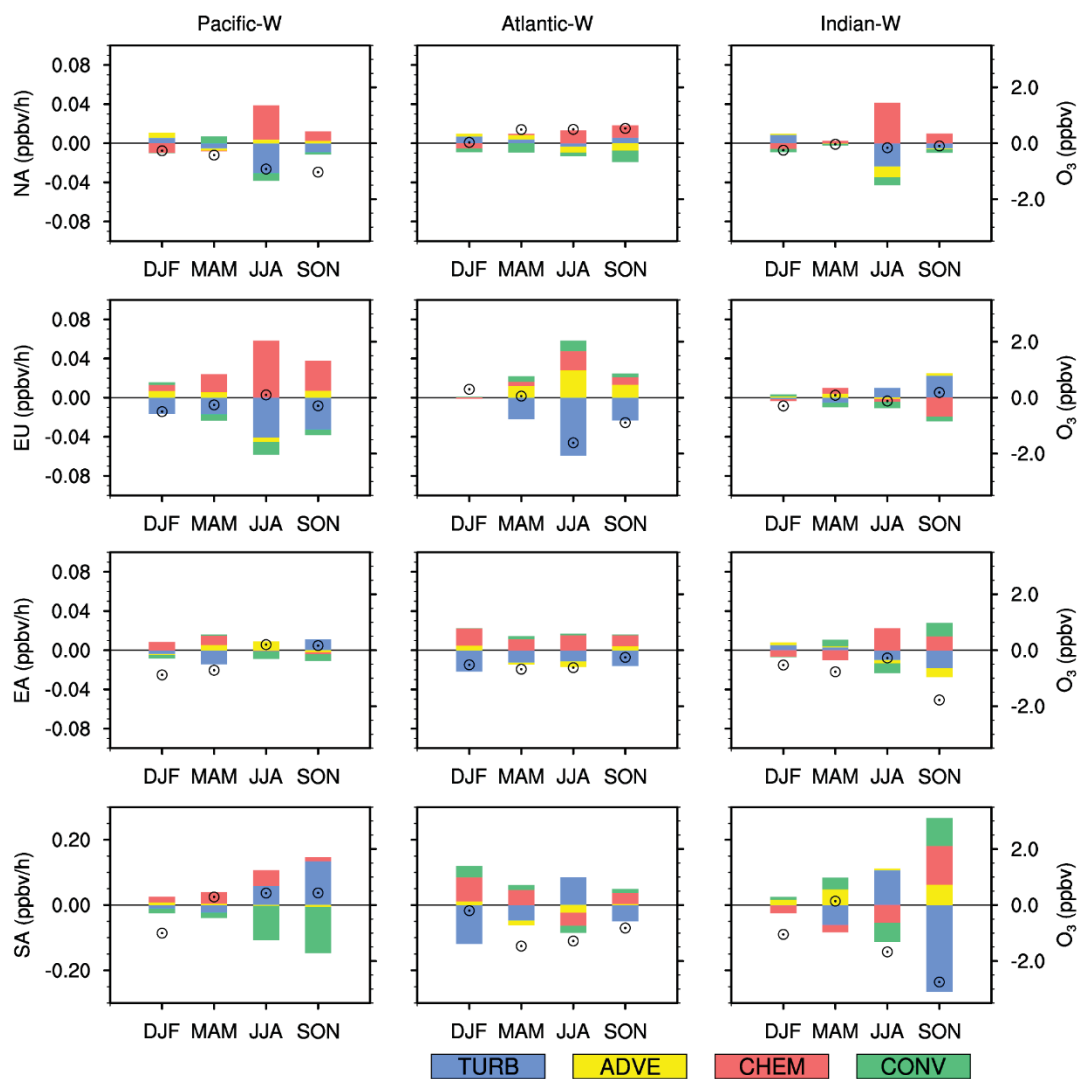
995

996 **Figure 1.** Changes in the summertime (June-August) surface ~~ozone~~ O_3 concentrations
 997 (ppbv) in the Northern Hemisphere induced by 1°C warming (top) and 1°C
 998 cooling (bottom) in the North Pacific Ocean (left), North Atlantic Ocean (center), and
 999 North Indian Ocean (right) relative to the CTRL. ~~Four~~The four major regions of interest
 1000 (i.e., NA (15°N–55 °N; 60°W–125°W), EU (25°N–65 °N; 10°W–50 °E), EA (15 °N–
 1001 50 °N; 95°E–160 °E) and SA (5 °N–35 °N; 50 °E–95°E)) are marked with ~~black~~red
 1002 polygons. ~~Only~~The + symbols denote areas where results are significant at the 0.105
 1003 level, evaluated with ~~aby~~ Student's t-test using 1120 years of data ~~are depicted.~~(plots
 1004 using the Mercator projection are shown in Figure S2 in the supplementary material).

1005

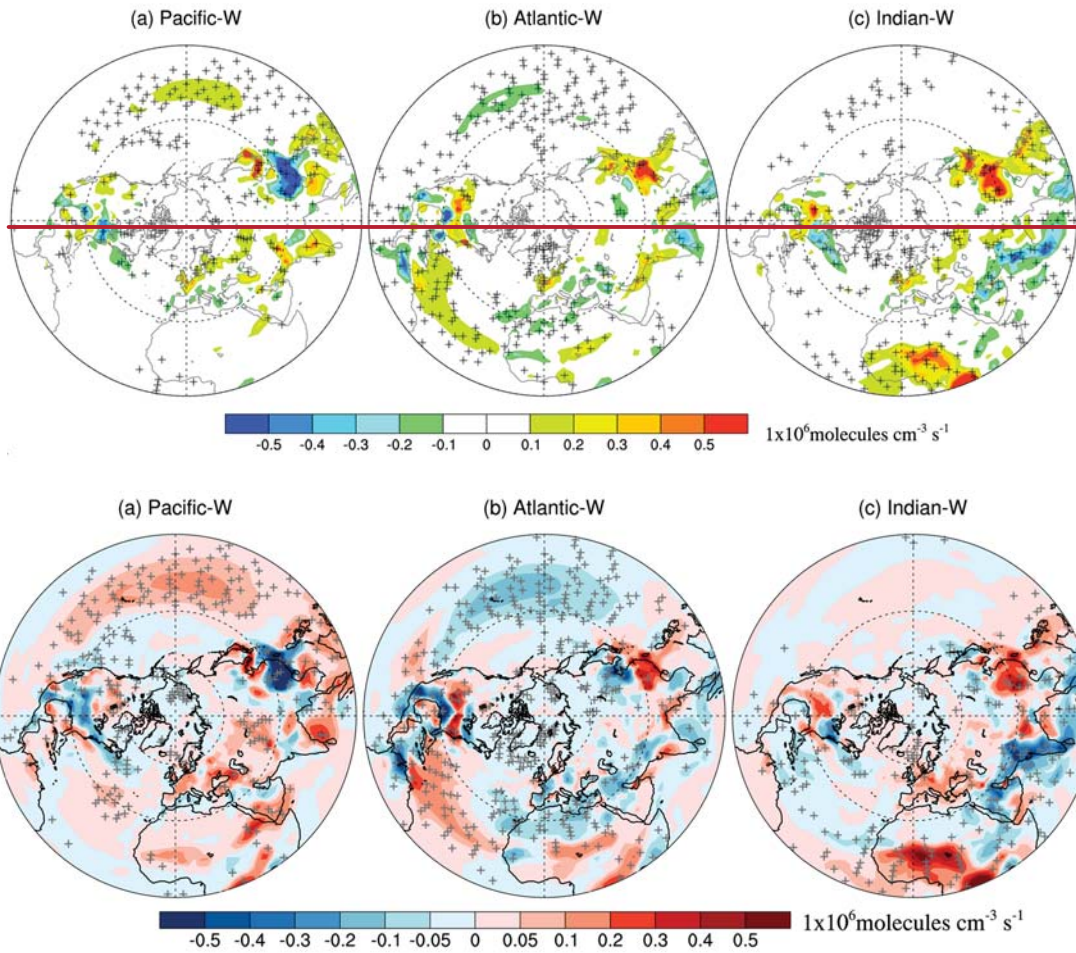


1006



1007
 1008
 1009
 1010
 1011
 1012
 1013
 1014
 1015
 1016
 1017
 1018

Figure 2. Seasonally averaged changes in the IPR contributions (bars, ppbv/h, left scale) and surface O₃ concentrations (hollow circles, ppbv, right scale) for Pacific-W (left), Atlantic-W (middle) and Indian-W (right) relative to the CTRL. Values are regionally averaged over NA (first row), EU (second row), EA (third row) and SA (last row); respectively). TURB is defined as the sum of VDIF and DRYD. CONV is the sum of DEEP and SHAL. IPR contributions from sixthe four processes (i.e., gas-phase chemistry (TURB, ADVE, CHEM), advection (ADVE), vertical diffusion (VDIF), dry deposition (DRYD), shallow convection (SHAL) and deep convection (DEEP) and CONV) are represented by different colors. A more detailed IPR result is shown in Figure S10 in the supplementary material.

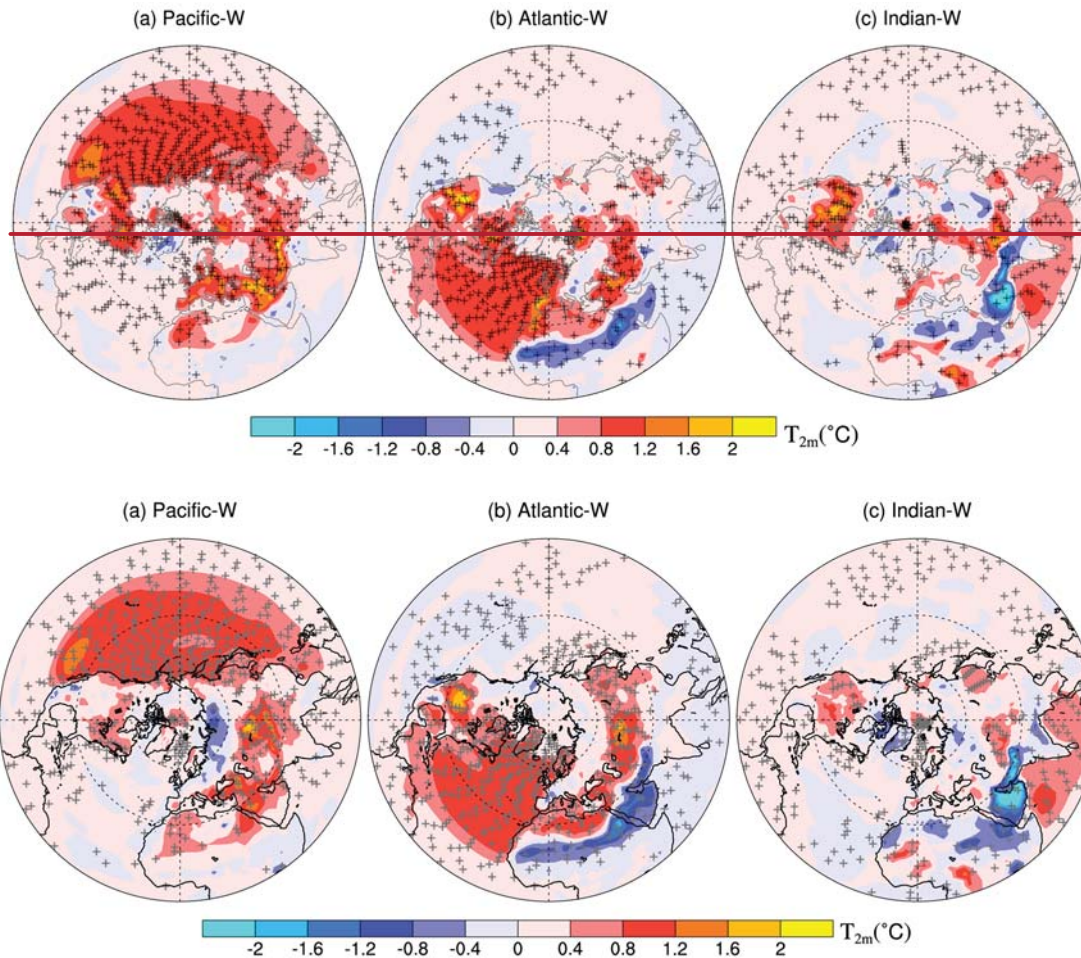


1019

1020

1021 **Figure 3.** Perturbations of the surface net O₃ net-production rate (1×10^6 molecules $\text{cm}^{-3} \text{s}^{-1}$) relative to CTRL for (a) Pacific-W, (b) Atlantic-W, and (c) Indian-W relative to
 1022 the CTRL in the boreal summer. The + symbols denote areas where the results are
 1023 significant at the 0.05 level-as, evaluated with-aby Student's t-test using 4420 years of
 1024 data- (plots using the Mercator projection are shown in Figure S14 in the supplementary
 1025 material).

1027



1028

1029

1030

1031

1032

1033

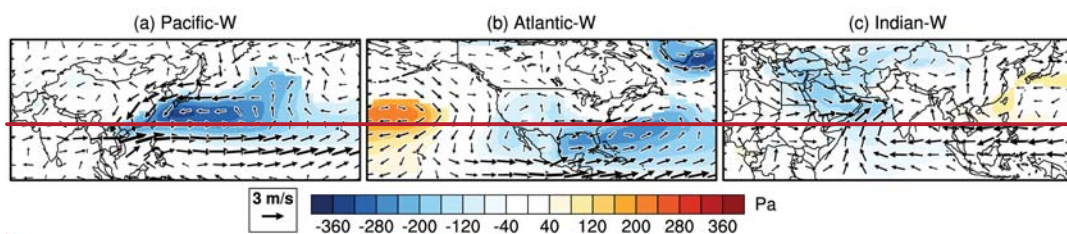
1034

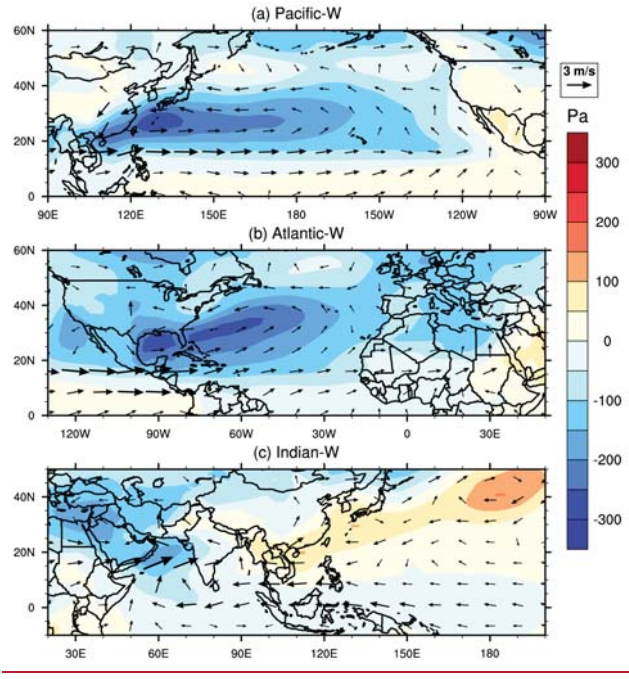
1035

Figure 4. ~~The difference~~Changes in the surface air temperature (~~°C~~°C) for (a) Pacific-W, (b) Atlantic-W, and (c) Indian-W relative to CTRL in the Northern Hemisphere in the boreal summer. The + symbols denote areas where the results are significant at the 0.05 level ~~as~~ evaluated ~~with~~ ~~aby~~ Student's t-test ~~using 20 years of data-~~ (plots using the Mercator projection are shown in Figure S15 in the supplementary material).

1036

1037



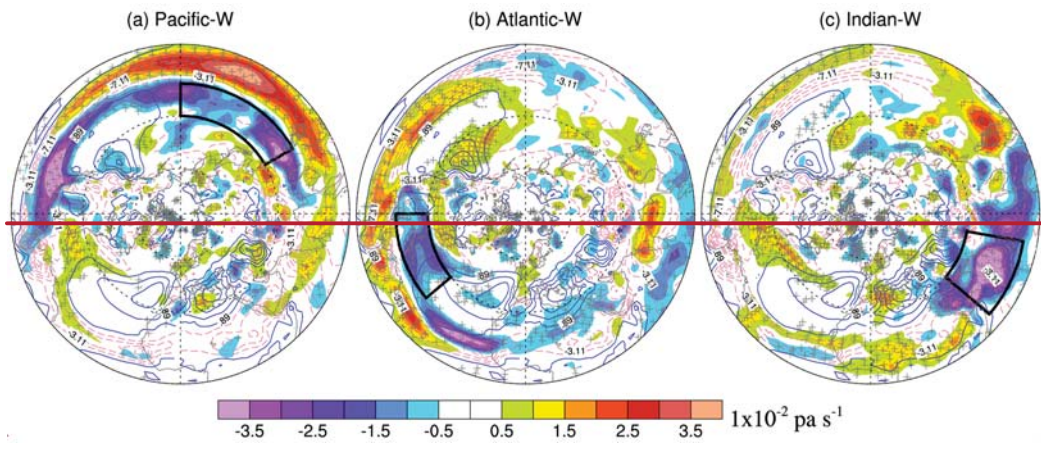


1038

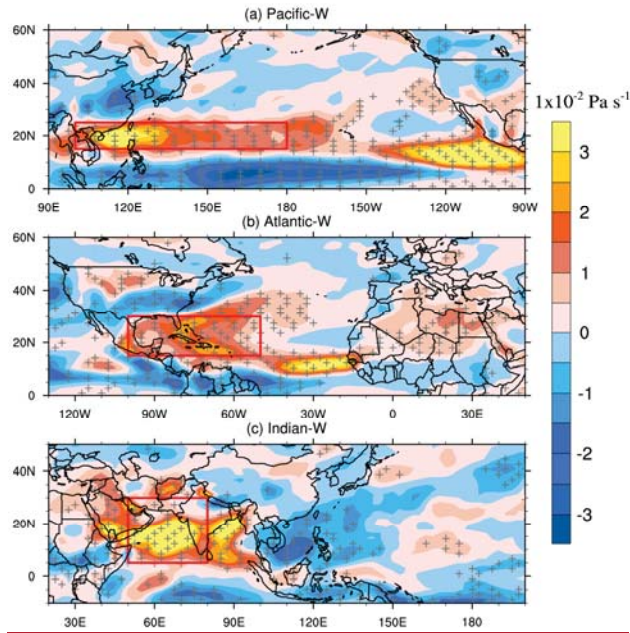
1039 **Figure 5.** –Changes in the surface pressure (color contours, Pa) and 850-hPa wind
 1040 pattern (arrows, m/s) for (a) Pacific-W, (b) Atlantic-W, and (c) Indian-W relative to
 1041 the CTRL in the boreal summer. ~~As for surface pressure changes, only results~~
 1042 ~~significant at the 0.05 level evaluated with a Student t test are depicted.~~

1043

1044



1045

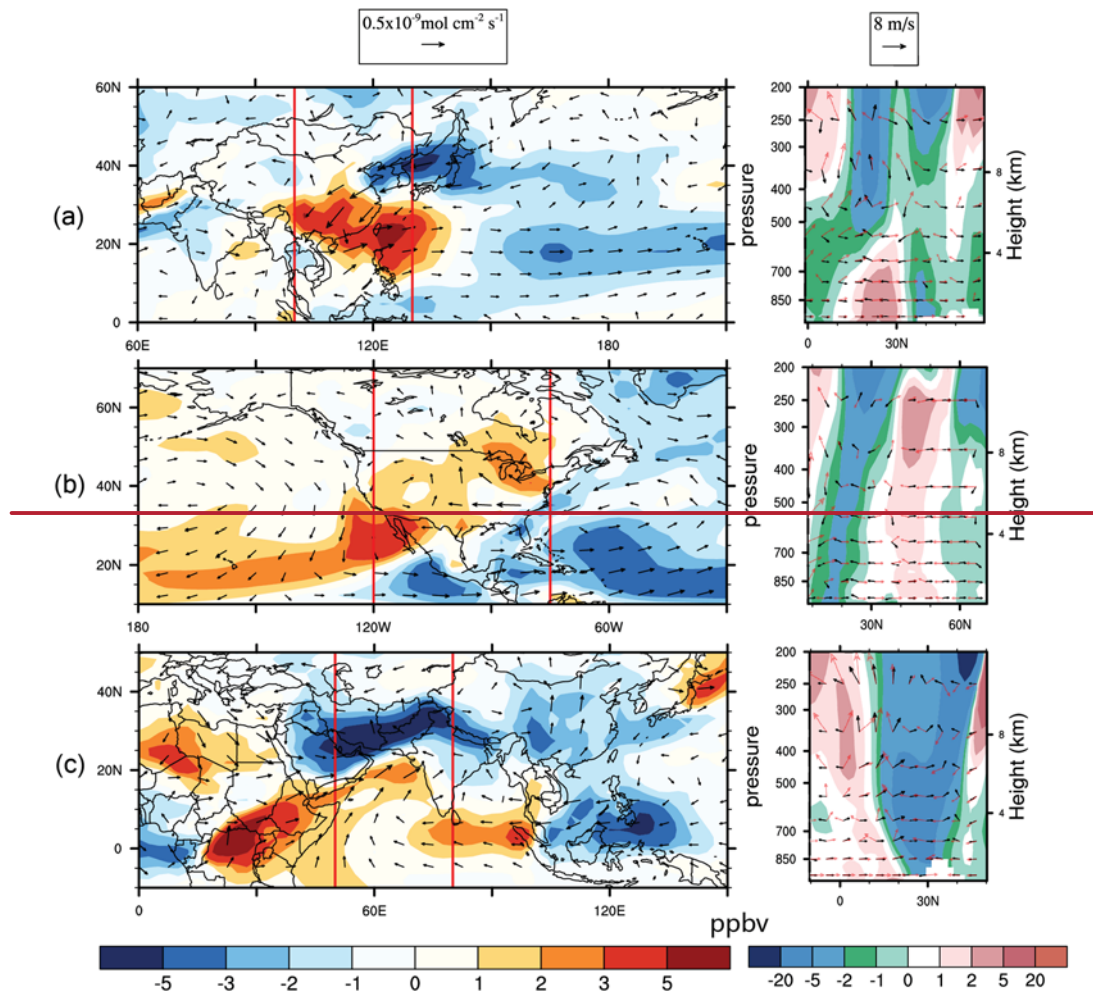


1046

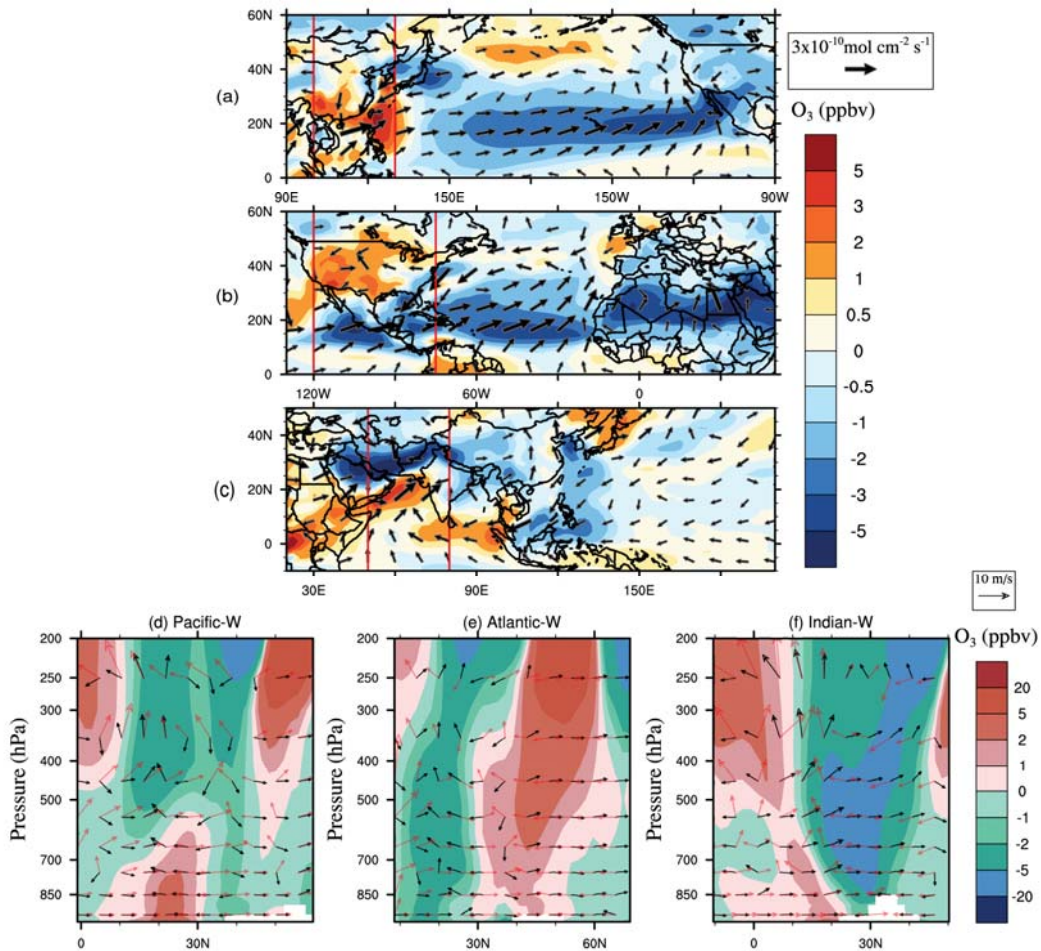
1047 **Figure 6.** ~~The spatial~~Spatial pattern of vertical velocity changes at 500 hPa (color
 1048 contours, $1 \times 10^{-2} \text{ Pa s}^{-1}$) for (a) Pacific-W, (b) Atlantic-W, and (c) Indian-W relative to
 1049 CTRL. ~~Contours with blue solid lines and red dashes indicate positive and negative~~
 1050 ~~downward vertical velocity in the control case, respectively (Contour interval: 2×10^{-2}~~
 1051 ~~Pa s^{-1}).~~Black the CTRL in the boreal summer. Positive values indicate upward motion.
 1052 Red polygons denote the regions where the surface pressure responses to SST
 1053 anomalies are significant (see Figure 75 a-c). The + symbols indicate areas where the
 1054 results are significant at the 0.05 level ~~as~~, evaluated ~~with~~by Student's t-test using ~~420~~
 1055 years of data.

1056

1057



1058

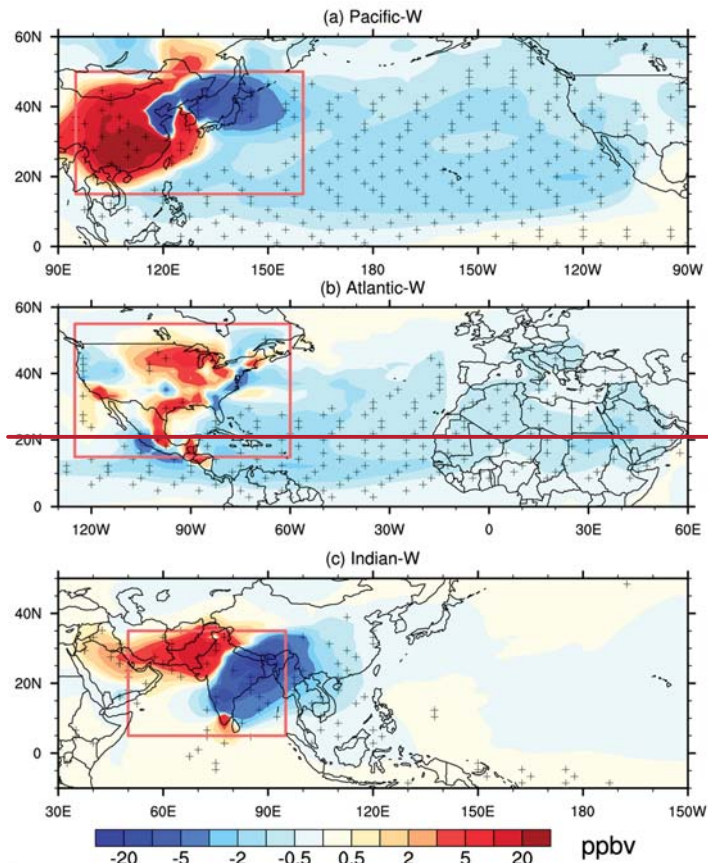


1059

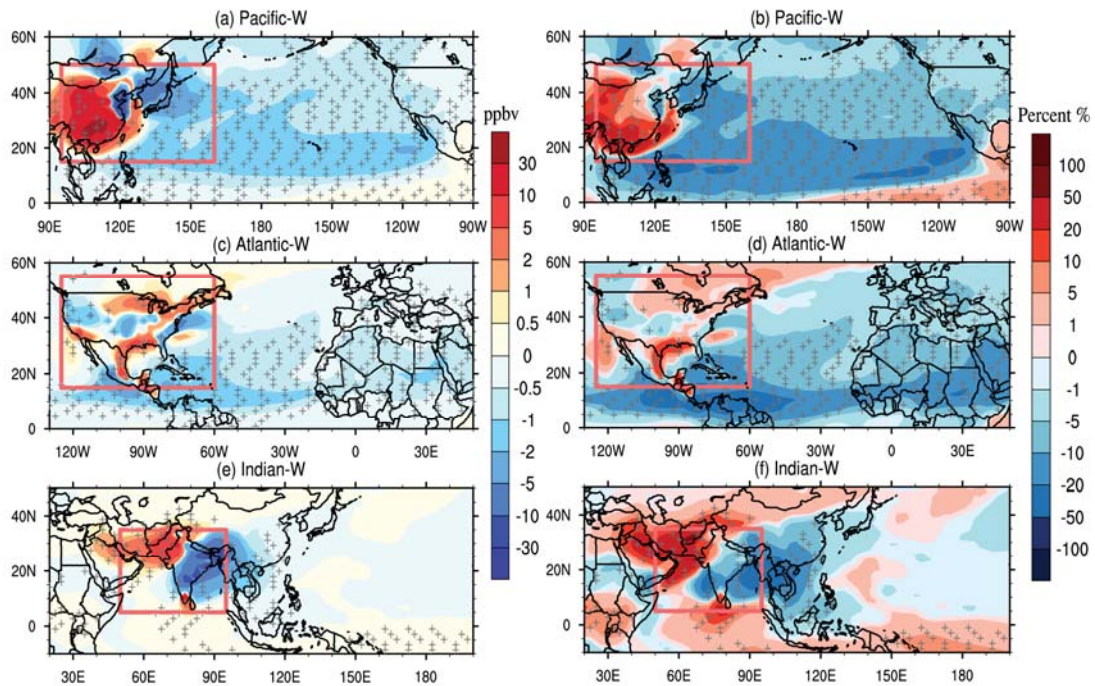
1060 **Figure 7.** ~~Left column~~ Top three rows: Changes in O₃ concentrations (color contours, ppbv) and horizontal fluxes (arrows, mol cm⁻² s⁻¹) at the surface level in boreal summer for (a) Pacific-W ~~(top)~~, (b) Atlantic-W ~~(middle)~~, (c) Indian-W ~~(bottom)~~ relative to the CTRL. ~~Right column:~~ Longitude averaged vertical and latitudinal distributions of in the boreal summer. ~~Last row:~~ zonal average of the tropospheric O₃ changes (color contours, ppbv) and wind velocity fluxes in CTRL (red arrows, m s⁻¹) and ~~is~~ the wind flux perturbation (black arrows, m s⁻¹) corresponding to the left. (d) Pacific-W, (e) Atlantic-W, (f) Indian-W relative to the CTRL in the boreal summer. The red rectangles in the left column (a), (b) and (c) denote the longitudinal range used for average the zonal averages in (d), (e) and (f), respectively. The vertical wind velocity is amplified 1000 times to be make it comparable with to the horizontal wind velocity and distinct in the panels.

1072

1073



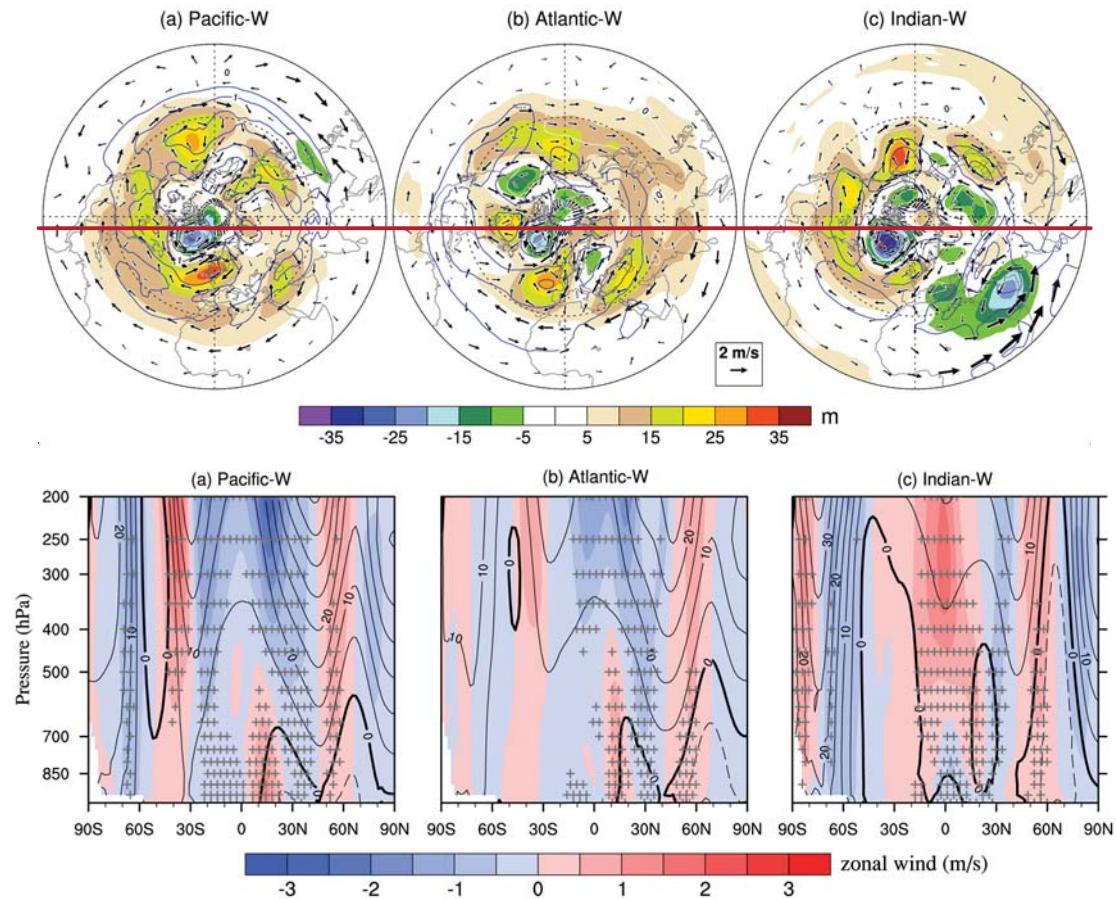
1074



1075

1076 **Figure 8.** ~~The difference in~~ Left-hand panel: Difference in the surface concentration
 1077 (ppbv) of a CO-like tracer emitted ~~in from~~ (a) ~~the~~ East Asia for Pacific-W, (b) ~~the~~ (c)
 1078 North America for Atlantic-W and (e) ~~the~~ (e) the ~~Indian~~ South Asia for Indian-W relative to
 1079 ~~CTRL~~ the CTRL in the boreal summer. ~~Right-hand panel: The percentage changes in~~

1080 the surface concentration of a CO-like tracer emitted from (b) East Asia for Pacific-W,
 1081 (d) North America for Atlantic-W and (f) South Asia for Indian-W relative to the CTRL
 1082 in the boreal summer. Red polygons denote the region where the CO-like tracer is
 1083 emitted from. The + symbol denotes areas where the results are significant at the 0.05
 1084 level, evaluated with aby Student's t-test using 20 years of data.



1087 **Figure 9.** Changes Zonally averaged changes in geopotential height zonal wind (color
 1088 contour, m), air temperature (/s) and geopotential height (contour, °C) and wind
 1089 pattern anomalies (arrows, m s⁻¹) at 500 hPa) for (a) Pacific-W, (b) Atlantic-W and (c)
 1090 Indian-W relative to CTRL. Blue the CTRL in the boreal summer. Black solid lines and
 1091 red dashed lines in the contours indicate positive and negative air
 1092 temperature geopotential height anomalies, respectively (Contour contour interval: 5 m).
 1093 The + symbol denotes areas where the zonal wind changes are significant at the 0.5-
 1094 0.05 level, evaluated by Student's t-test using 20 years of data.